THE UNIVERSITY
of EDINBURGH

Hypoxia, reactive oxygen species and glucose metabolism in the regulation of the innate immune system

Joseph Alexander Willson

Doctor of Philosophy with Integrated Study

Optical Medical Imaging with Healthcare Innovation and Entrepreneurship

The University of Edinburgh and The University of Strathclyde

2018

Declaration

1. I declare that this thesis has been composed solely by myself and that it has not been submitted, in whole or in part, in any previous application for a degree. Except where states otherwise by reference or acknowledgment, the work presented is entirely my own.

2. I confirm that this thesis presented for the degree of Doctor of Philosophy in Optical Medical Imaging, has

i) been composed entirely by myself

ii) been solely the result of my own work

iii) not been submitted for any other degree or professional qualification

3. I declare that this thesis was composed by myself, that the work contained herein is my own except where explicitly stated otherwise in the text, and that this work has not been submitted for any other degree or processional qualification except as specified.

Parts of this work have been published in Jones, McDonald, Willson *et al,* 2016 and Sadiku, Willson *et al* 2017.

Signed,

Joseph Alexander Willson

11th of March 2019

Acknowledgements

I would first like to express my sincere gratitude to my supervisors Professor Sarah Walmsley, Professor Moira Whyte and Dr Colin Campbell for their support and encouragement throughout these 4 years.

I would like to thank the members of the Walmsley/Whyte lab for their assistance and advice throughout the PhD, in particular Dr Pranvera Sadiku, Dr Patricia Coelho, Dr Emily Watts, Dr Rebecca Dickinson and Dr Fiona Murphy for their help, advice and encouragement throughout my time in the lab.

I would like to thank the directors of the OPTIMA CDT for Optical Medical Imaging, and Dr Jean O'Donoghue and Samantha Brown for their patience! I would also like to thank the students of the OPTIMA CDT, particularly Cat, Holly and Alisia for their invaluable support over the years.

For help with experimental work, I would like to thank Lauren Melrose for genotyping the murine colonies used in these studies, Catherine Doherty for assistance with growing bacteria for the infection models, Bart Ghesquiere and Pranvera Sadiku for running LC-MS samples, Peter Carmeliet and Max Mazzone for kind donation of the PHD3 LysMCre mouse strain and Roger Thompson for assistance and guidance with the murine model of *Staphylococcus aureus* skin infection. I would like to give special thanks to Shonna Johnston, Dr Will Ramsay and Dr Mari Pattison of the QMRI Cell Sorting and Flow Cytometry Facility for their help in setting up and running flow cytometry experiments.

I would like to thank my family for supporting me and being there to offer encouragement - my parents, Mark and Gill, my brother Ben and my sister Rachel.

Finally, I would like to thank my girlfriend Alice for her support and understanding, without which this thesis would not have been completed.

Abstract

Introduction - Neutrophils are the most abundant innate immune cells, essential for clearing pathogens from injured or infected sites and directing the ensuing inflammatory response. Sites of inflammation tend to be hypoxic due to rapid tissue volume expansion, loss of vascular integrity and oxygen consumption by infiltrating immune cells. Neutrophils are well suited to the hypoxic niche and have metabolic adaptations that enable them to exist in hypoxia, including a reliance on anaerobic respiration, despite possessing a mitochondrial network. The role of neutrophil mitochondria is unclear, and relatively few studies have examined what role the mitochondria play in regulating neutrophil apoptosis and function, and how hypoxia modulates anaerobic and aerobic neutrophil metabolism.

Methods - Neutrophils isolated from healthy volunteers were cultured in normoxia (21% O_2) and hypoxia (1% O_2) *in vitro* and neutrophil function and metabolic flux interrogated *ex vivo*. Functional consequences of hypoxic response pathway manipulation were investigated in infection models carried out in mice with myeloid specific PHD3 knockout.

Results – Neutrophil mitochondrial membrane potential and reactive oxygen species production are enhanced in hypoxia through a mechanism independent of oxidative phosphorylation. Neutrophil mitochondrial reactive oxygen species are capable of stabilising HIF-1α and enhancing hypoxic survival of neutrophils. Manipulation of the hypoxic response pathway and neutrophil metabolism through knockout of PHD3 enhances control of bacterial infection through changes in neutrophil metabolic flux.

Conclusion - We describe a signalling role for the neutrophil mitochondria in hypoxic conditions that is independent of oxidative phosphorylation activity. Neutrophil anaerobic metabolism is also linked closely to antioxidant production through the pentose phosphate pathway that compensates for mitochondrial oxidant signalling from the mitochondria. Regulation of glycolysis is therefore required for both reactive oxygen signalling and for managing oxidative stress in hypoxic conditions. These pathways are also regulated by the activity of PHD3, in a manner capable of modulating neutrophil bactericidal function.

Lay Summary

Our bodies need oxygen – we breathe oxygen into our lungs, which then enters into our bloodstream and is used by cells to produce energy. In sites of infection and inflammation, oxygen levels can be very low because inflamed tissue has huge numbers of cells using large amounts of oxygen. In order to adapt to these low oxygen sites, specific white blood cells called neutrophils, which can help kill bacteria, can not only function without oxygen, but actually live longer in these conditions. These cells are very unusual in this regard as oxygen is an absolute requirement in other cells.

Neutrophils have also been linked to a number of inflammatory diseases. The activity of neutrophils can cause damage to the body. Understanding the regulation of the lifespans of these cells in low oxygen will therefore be very important when looking for treatments for these chronic inflammatory conditions.

My research shows that in low oxygen, neutrophils use the mitochondria, the powerhouse of the cell and the source of energy from oxygen, in a slightly different way to other cells. The neutrophils use a byproduct of the energy producing process called reactive oxygen species to prolong their lifespan in low oxygen. The neutrophils do not use a lot of the same energy-producing pathways as other cells. This is part of what makes them specialized to low oxygen. Neutrophils also extend their lifespan in hypoxia through regulating the way they use glucose. Blocking part of the machinery that neutrophils use to adapt to hypoxic conditions can improve the way that neutrophils clear bacteria at the site of infection.

These findings shed some light on the activity of these cells and highlight two potential therapeutic targets that could be exploited in treating chronic inflammatory diseases. Further work will be needed to explore the consequences of targeting these pathways in disease.

Table of Contents

List of Figures

List of Tables

Abbreviations

2-DG: 2-Deoxyglucose

3-NP: 3-Nitropropionic acid

6-AN: 6-Aminonicotinamide

ABB: Annexin Binding Buffer

AML: Acute Myeloid Leukaemia

APS: Ammonium persulphate

BAL: Bronchoalveolar Lavage

BHI: Brain heart infusion

BMDM: Bone Marrow-derived Macrophages

CCCP: Carbonyl Cyanide M-Chlorophenyl Hydrazone

ccRCC: Clear Cell Renal Cell Carcinoma

CFSE: Carboxyfluorescein Succinimidyl Ester

CFU: Colony Forming Units

CGD: Chronic Granulomatous Disease

CODD: C-terminal Oxygen Degradation Domain

COPD: Chronic Obstructive Pulmonary Disease

DCF: Dichlorofluorescein

DFBS: Dialysed Foetal Bovine Serum

DMSO: Dimethyl Sulfoxide

DPBS: Dulbecco's Phosphate Buffered Saline

DTT: Dithiothreitol

FBS: Foetal Bovine Serum

FSC: Forward Scatter

FIH: Factor Inhibiting HIF

fMLP: N-formylmethionine Leucyl-Phenylalanine

G-CSF: Granulocyte-Colony Stimulating Factor

GM-CSF: Granulocyte-Macrophage Colony-Stimulating Factor

GSH: Reduced Glutathione **(GSSG:** Oxidised Glutathione)

HBSS: Hank's Balanced Salt Solution

HIF: Hypoxia Inducible Factor

MPO: Myeloperoxidase

mROS: Mitochondrial reactive oxygen species

MSucc: Methyl Succinate

NE: Neutrophil Elastase

NET: Neutrophil Extracellular Trap

NO: Nitric Oxide

NODD: N-terminal Oxygen Degradation Domain

O_2^-: Superoxide radical

$ONOO^-$: Peroxynitrite radical

PAMP: Pathogen-Associated Molecular Pattern

PBMC: Peripheral Blood Mononuclear Cells

PBS: Phosphate Buffered Saline

PHD: Prolyl Hydroxylase Domain

PMN: Polymorphonuclear

PMSF: Phenylmethanesulfonyl Fluoride

PVDF: Polyvinylidene fluoride

ROS: Reactive oxygen species

RPMI: Roswell Park Memorial Institute Media

SSC: Side Scatter

SDS: Sodium Dodecyl Sulphate

TCA Cycle: Tricarboxylic Acid Cycle

TEMED: Tetramethylethylenediamine

TMRM: Tetra Methyl Rhodamine, Methyl Ester

VHL: Von Hippel Lindau protein

1. Introduction

1.1. The role of the neutrophil in health and disease

1.1.1. Antimicrobial response

Neutrophils are the most abundant leukocyte in the mammalian circulation and are critical for the elimination of invading pathogens and mediation of the ensuing acute inflammatory response through the synthesis and release of inflammatory lipids and proteins (Kennedy and Deleo, 2009). Terminally differentiated, short-lived cells that are rapidly turned-over in the body, neutrophils have short lifespans, with estimates from human studies ranging from 8-12 hours in the circulation, which extends to 1-2 days after infiltrating tissue, to just over 5 days following release from the bone marrow (Dancey *et al.*, 1976)(Pillay *et al.*, 2010). The bone marrow releases neutrophils at a rate of 10^{11} cells per day, and as such they account for 50% to 70% of all circulating leukocytes (Luo and Loison, 2008).

The activity of neutrophils is essential for proper control of infection. Neutropoenia, a condition defined by low levels of circulating neutrophils, is associated with immunodeficiency and recurrent bacterial infections (Zeidler *et al.*, 2009). Neutrophils primarily clear bacteria through phagocytosis and subsequent digestion of pathogens in the phagolysosome, utilising toxic chemicals stored in specialized lysosomes known as granules. Neutrophils possess three types of granules; primary, or azurophilic, granules which contain anti-microbial proteins such as myeloperoxidase (MPO), lysozyme, neutrophil elastase (NE), defensins, proteinase-3 and cathepsin G. Secondary granules contain the antimicrobial peptides lactoferrin, lysozyme, hCAP-18, NGAL and Nramp-1. Tertiary granules contain metalloproteases including gelatinase (summarised in Pham, 2006). During phagocytosis of bacteria, these granules fuse with the phagosome to form the phagolysosome, exposing the engulfed pathogen to the toxic granule contents. Granule proteins exert antimicrobial effects through proteolysis (NE, cathepsin G, proteinase 3), compromise of the microbial cell membrane and cell wall (defensins, lysozyme) and sequestration of nutrients (chelators). Neutrophils can also release reactive oxygen species into the phagolysosome through assembly and activation of

NADPH oxidase. NADPH oxidase produces large amounts of superoxide in the phagolysosome, which can oxidise bacterial components directly, or be dismuted into H_2O_2, which can then be converted to hypochlorous acid by MPO and exert potent bactericidal effects (Thomas *et al.*, 2014).

Neutrophils may also release granule contents into the extracellular space through a process known as degranulation. Release of granule contents can kill extracellular pathogens, but also cause damage to host tissues. Activity of serine proteases on chemoattractants can also potentiate their activity and positively regulate the inflammatory response. NADPH oxidase present on the membrane can release reactive oxygen species (ROS) into the extracellular environment, which aids with antimicrobial control but also contributes to tissue damage (Pham, 2006).

Neutrophils may also release neutrophil extracellular traps (NETs) to clear bacteria. NETs are large, extracellular fibres released by neutrophils, and composed of cytoplasmic and granule proteins including NE, cathepsin G and MPO bound to networks of decondensed nuclear and mitochondrial chromatin (Thomas *et al.*, 2014). NETs immobilise and kill bacteria, fungi, viruses and parasites through providing a highly localised concentration of antimicrobial proteins to act on the bacteria (reviewed in Papayannopoulos, 2018). Release of NETs is thought to be mediated by ROS-mediated translocation of NE to the nucleus, which can disrupt histone proteins and allow unpacking and decondensing of DNA (Papayannopoulos *et al.*, 2010).

A summary of cytotoxic mechanisms in neutrophils is shown in Figure 1.1-1.

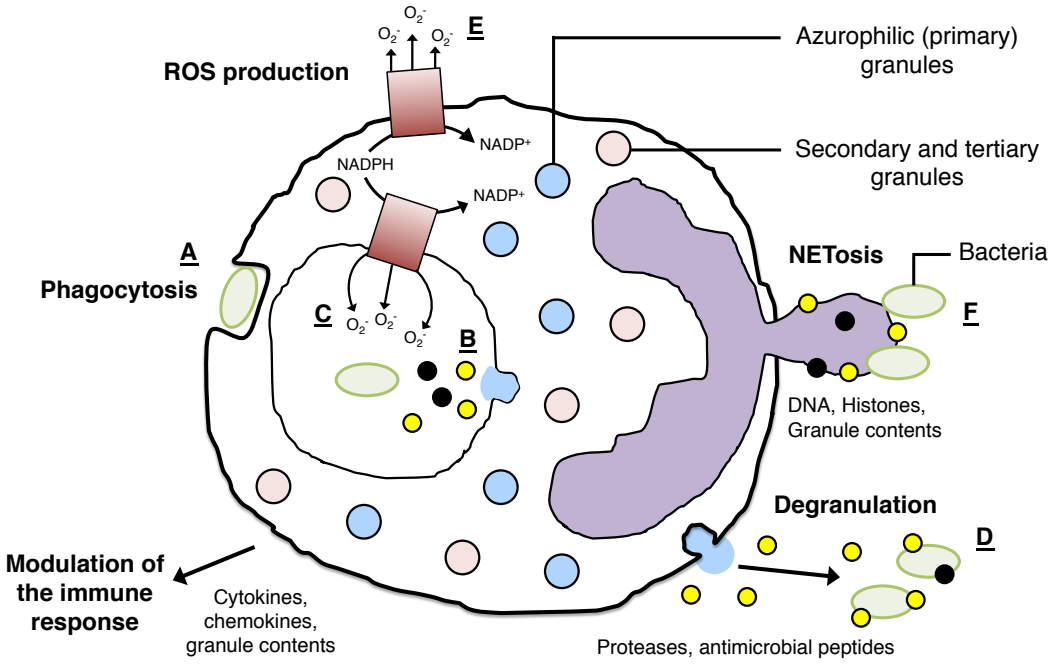

Figure 1.1-1: Cytotoxic functions of neutrophils. Neutrophils clear bacteria through phagocytosis (A) and then subsequent destruction of intracellular bacteria through the fusing of the phagolysosome with cytotoxic granules and exposure to serine proteases and antimicrobial peptides (B) and exposure to reactive oxygen species in the phagolysosome (C). Neutrophils can also kill extracellular bacteria through release of granule contents (D) and NADPH oxidase-derived reactive oxygen species (E) into the extracellular milieu. Neutrophils may also release their nuclear contents as neutrophil extracellular traps (F). Release of cytokines and chemokines can mediate the consequent immune response.

1.1.2. Recruitment

Neutrophil maturation and release from the bone marrow is predominantly driven through the activity of granulocyte colony-stimulating factor (G-CSF). G-CSF drives neutrophil release from the bone marrow in resting conditions, and can also drive enhanced neutrophil production and release from the bone marrow in infection. Endothelial cells respond to pathogen-associated molecular patterns (PAMPs) by releasing G-CSF, enhancing proliferation of haemopoietic stem cells in the bone marrow and skewing differentiation towards neutrophils (Boettcher *et al.*, 2014).

Following release from the bone marrow, circulating neutrophils are drawn to the site of infection and inflammation through the process of neutrophil recruitment. Recruitment is mediated through the activation of neutrophil receptors by ligands induced on the surface of the inflamed vascular endothelium. Endothelial cells react to stimuli such as TNFα, IL-1β and IL-17 generated during infection and express P- and E- selectins, as well as ICAMs and VCAMs on the luminal surface of the endothelium. Neutrophils bind these via PSGL-1 and L-selectin. The interactions between PSGL-1 and P- and E- selectins establish contact between the circulating neutrophils and the activated endothelial cell, and ESL-1 and E-selectin interactions mediate the deceleration of the circulating neutrophil and rolling along the endothelium. Rolling allows the cell to detect signals in the local microenvironment, including chemokines released by inflammatory cells in the site of inflammation. These secondary signals induce β1 and β2 surface integrins on the neutrophil membrane to unfold and interact with ICAM-1 and ICAM-2 ligands expressed on the inflamed endothelium. Integrin-ICAM interaction slows the rolling of the neutrophil along the endothelium and eventually arrests the cell. ICAM-2 congregates at the endothelial cell junctions and guides neutrophils to these sites. Neutrophils then transmigrate through the basement membrane into the tissue, mediated by JAMs, PECAMs, and CD99. Once through the membrane, neutrophils travel towards the insult (Summarised in Borregaard 2010).

1.1.3. Mediation of the inflammatory response

Although initially seen purely as obligate phagocytes, dedicated to clearance of invading pathogens, more recent studies have described a role for neutrophils as

critical regulators of the immune response, allowing fine regulation of inflammation through the release of pro- and anti-inflammatory cytokines in response to damage-associated molecular patterns (DAMPs), PAMPs and endothelial cell factors. In addition, neutrophils release an array of chemokines on activation which can recruit immune cells to the site of inflammation or infection (Zlotnik and Yoshie, 2012). Crucial neutrophil chemokines include potent neutrophil chemoattractants IL-8, CXCL1/KC and IL-1β that allow amplification of the initial immune response through an inflammatory "cascade", recruiting more neutrophils to the site of inflammation. Other innate immune cell chemoattractants are released by neutrophils, including MIP-1α and MIP-1β, allowing recruitment of monocytes, macrophages, natural killer (NK) cells and immature dendritic cells (Scapini *et al.*, 2000). Neutrophils also release chemokines including IP-10 and MIG, which induce B- and T-cell recruitment, mediating the adaptive immune response. *In vitro* experiments have shown CCL2, CCL20 and CXCL10 release from neutrophils can recruit IFNy- and IL-17-producing T lymphocytes (Codolo *et al.*, 2013). Tumour associated neutrophils can also release CCL17, a chemoattractant capable of recruiting Tregs, which is deleterious to the immune response to the tumour (Mishalian *et al.*, 2014).

Neutrophils are a source of both pro- and anti-inflammatory cytokines, including but not limited to IL-1, IL-6, IFNy, IL-17 and TNFα**.** TNFα can promote other cells to prime antiviral immune responses (Epaulard *et al.*, 2014) and cause microvascular leakage (Finsterbusch *et al.*, 2014). Neutrophils are also sources of other TNF superfamily members BAFF, APRIL and TRAIL. Expression of TRAIL also has antiviral properties and can mediate early bacterial killing in pneumonia (Stacey *et al.*, 2014)(Steinwede *et al.*, 2012).

1.1.4. Neutrophil apoptosis and inflammation resolution

As neutrophil activity can cause considerable damage to the host, rapid resolution of inflammation is essential. Resolution of inflammation is primarily mediated through a programme of constitutive neutrophil apoptosis and subsequent phagocytosis by macrophages (efferocytosis)(Perretti, Soehnlein and Ortega-Gómez, 2013). Apoptosis is a form of highly regulated programmed cell death that allows clearance

of cells without induction of pro-inflammatory pathways. Other forms of cell death, such as programmed pyroptosis and non-programmed necrosis, leads to loss of cell membrane integrity and subsequent release of toxic granule contents which can then cause further inflammation and tissue damage.

Neutrophils undergo apoptosis spontaneously through an as-unknown mechanism. However, rates of neutrophil apoptosis can be influenced by other external factors. Pro-inflammatory cytokines, such as IL-1β, TNFα, Granulocyte-Macrophage-Colony Stimulating Factor (GM-CSF), G-CSF and IFN-γ can all promote neutrophil survival (Colotta *et al.*, 1992). Exposure to pathogens and pathogen-derived products, such as lipopolysaccharide (LPS) and inactivated bacteria, can also promote survival (Fox *et al.*, 2010).

The apoptosis and subsequent engulfment of neutrophils by macrophages is in itself an anti-inflammatory process, suppressing the expression of pro-inflammatory cytokines TNFα, GM-CSF, IL-12, IL-1β and IL-18, and activating release of the anti-inflammatory cytokines IL-10, TGF-β and prostaglandin E_2 in *in vitro* studies (Fadok *et al.*, 1998). Further studies *in vivo* showed addition of apoptotic neutrophils can actually protect against LPS-induced shock (Ren *et al.*, 2008). Administration of apoptotic neutrophils reduced levels of pro-inflammatory cytokines IL-12, TNFα and IFN-γ in the blood of mice with LPS-induced sepsis, whereas levels of the anti-inflammatory cytokine IL-10 were elevated. Timely apoptosis of neutrophils is therefore essential for resolution of the inflammatory response.

Recruitment of neutrophils can also be regulated at least partially by the rate of apoptosis of neutrophils in the inflammatory tissue, as clearance of apoptotic neutrophils by macrophages and dendritic cells reduces IL-23 production, which in turn reduces the production of IL-17A by neutrophil regulatory T cells (Stark *et al.*, 2005). IL-17A is needed for the production of G-CSF; therefore, higher numbers of apoptotic neutrophils being phagocytosed in the tissue suppresses the production of neutrophils in the bone marrow (Stark *et al.*, 2005).

1.1.5. Pathologies associated with neutrophil functional deficiency

Defects in neutrophil phagocytosis and bacterial killing efficiency can lead to life-threatening immune diseases. Patients with conditions where neutrophil abundance or function are compromised are particularly susceptible to bacterial and fungal infections. Diseases caused by defects in NADPH oxidase function (Chronic granulatomous disease) and cytotoxic granule formation and function (Chediak-Higashi syndrome, neutrophil-specific granule deficiency) are all linked to more frequent bacterial infections (Lakshman and Finn, 2001). Chediak-Higashi syndrome is an autosomal recessive disorder also associated with a number of haematological and neurological symptoms, caused by a mutation in the lysosomal trafficking regulatory gene *LYST*, causing abnormal fusion of primary (azurophilic) granules with secondary (specific) granules. In this disease, an infection induces neutrophilia in the tissue, but the neutrophils lack elastase and cathepsin G and are unable to mount an effective response (Mackay and Rosen, 2000), with patients suffering recurrent *S. aureus* and *Streptococci* infections. Deficiencies in the capability of neutrophils to release NETs, for example in neutrophils isolated from neonates, can also lead to significant deficiencies in extracellular killing of *S. aureus* and *E. coli,* and can predispose the host to bacterial infections (Yost *et al.*, 2009).

1.1.6. Neutrophils and inflammatory disease

Normal activity of neutrophils can cause bystander damage to tissues due to the activity of toxic granule contents on host tissue, and neutrophil presence in the tissue and activity is also associated with a number of inflammatory diseases caused by tissue destruction, including Chronic Obstructive Pulmonary Disease (COPD) and rheumatoid arthritis. In COPD, the degree of airway neutrophilia in patients correlates with decline in lung function and is consequentially associated with the severity of disease symptoms (Stănescu *et al.*, 1996). The presence of neutrophils in chronic inflamed tissue is mediated in part by recruitment of neutrophils through release of pro-inflammatory cytokines IL-1, CCR1 and CXCR2 (Chou *et al.*, 2010), although the exact reason as to why the inflammatory response does not resolve in these conditions has not been elucidated.

Interestingly, patients with COPD have large numbers of infiltrating neutrophils in

the airways, but experience frequent bacterial infections known as exacerbations (Hoenderdos and Condliffe, 2013). Acute exacerbations are characterised by acutely enhanced inflammation of the peripheral airways, even greater neutrophil numbers in sputum and a profound deterioration in physiological wellbeing. Exacerbations are common despite enhanced neutrophil infiltration into the airway lumen, suggesting that neutrophils present in the lungs of COPD patients may also be functionally deficient. This is mirrored in cystic fibrosis patients, who experience frequent *S. aureus* and *H. influenzae* infections despite the observations that the airways of these patients have extremely high levels of neutrophils, neutrophil elastase and MPO, as well as enhanced oxidative stress as measured by glutathione concentration and redox ratios (Lyczak, Cannon and Pier, 2002)(Dickerhof *et al.*, 2017). Understanding the regulation of neutrophil apoptosis and function will therefore be essential in understanding how to treat these chronic inflammatory conditions.

1.2. Modulation of neutrophil lifespan and function by oxygen tension

1.2.1. Hypoxia

Oxygen is required by mammalian cells in order to produce ATP through oxidative phosphorylation. In the human body, arterial blood has an oxygen concentration of 11.3-13.3kPa, whereas venous blood is around 5.5-6kPa (Woerlee, 1988). Systemic hypoxia (hypoxaemia) can occur in cases of lung dysfunction such as COPD and cystic fibrosis, or in situations where oxygen is limiting such as at altitude, or during sleep apnoea (Barry and Pollard, 2003)(Lévy *et al.*, 2008)(Kent, Mitchell and McNicholas, 2011). Lower respiratory tract infections such as pneumonia are also associated with hypoxaemia; the degree of hypoxaemia is associated with adverse outcomes of infection in pneumonia patients (Majumdar *et al.*, 2011) and in children with lower respiratory tract infections (Lazzerini, Sonego and Pellegrin, 2015), and adverse outcomes in chronic lung diseases such as COPD (Kent, Mitchell and McNicholas, 2011).

Oxygen levels in the tissues are variable, and depend on metabolic rates of the specific tissue, between 1.7kPa in the liver to around 4.9kPa in the brain where

oxygen requirement is high. A number of particularly hypoxic niches exist in the body as part of normal function, including the bone marrow, the intestinal mucosa and the placenta (Campbell, Kao and Colgan, 2016)(Beerman *et al.*, 2017). These niches have adapted to low oxygen environments, and hypoxia is required for normal function of these tissues (Reviewed in Taylor & Colgan 2017).

Acute hypoxia also occurs in pathology, most commonly in cases of myocardial or cerebral ischaemia or in the tumour microenvironment (Kominsky, Campbell and Colgan, 2010)(Lin *et al.*, 2016). Hypoxia can occur at the site of infection or inflammation, where tissue oxygen demand is increased due to high concentrations of infiltrating immune cells. Oxygen concentrations at inflammatory sites, such as arthritic joints, can reach as low at 1kPa (Ng *et al.*, 2010). Lack of oxygen in the tissue can result in ATP depletion and cell death, but also can profoundly alter the immune response (Michiels, 2004).

1.2.2. The hypoxic response pathway

Mammalian cells regulate their response to oxygen concentration in order to maintain metabolic homeostasis. The main molecular mechanism for mounting this response is through the hypoxic response pathway, specifically through the transcription factors HIF-1α, HIF-2α, and the recently described HIF-3α. These transcription factors mount a profound transcriptional response in hypoxic conditions, modulating a host of cell responses. HIF-1α, the most well-characterised component of this pathway, is ubiquitously expressed and is a crucial regulator of homeostasis through modulating metabolism, apoptosis and tissue vascularization (Semenza, 1998). HIF-1α allows for adaptation to hypoxia; however, many cancers overexpress HIF-1α, and overexpression encourages proliferation and vascularisation of tumours (Semenza, 2002).

Regulation of HIF-1α and HIF-2α activity occurs at the level of transcription and protein stability. In normoxic conditions, HIF is transcribed and translated constitutively, then broken down through the activity of the prolyl hydroxylases PHD1, PHD2 and PHD3 (Schofield and Ratcliffe, 2004). PHD enzymes hydroxylate proline residues in HIF-α proteins (P402 and P564 in HIF-1α, P405 and P531 in

HIF-2α), promoting the interaction of the HIF-α subunit with Von-Hippel Lindau tumour suppressor protein (VHL)(Maxwell *et al.*, 1999)(Furlow *et al.*, 2009). VHL ubiquitinylates HIF-α, targeting it for rapid proteasomal degradation. Hydroxylation of HIFα by PHD enzymes requires molecular oxygen as a cofactor; therefore, in the absence of oxygen, the PHD enzymes are inactive and HIF-α remains stable and can go on to transcribe hypoxic response genes. This system allows a very rapid response to hypoxia. HIF activity is also regulated by another oxygen-dependent hydroxylase enzyme, Factor Inhibiting HIF (FIH), which blocks the transcriptional activity of HIF-1α subunits through hydroxylation of an asparagine residue, Asn803 in human HIF-1α. The activity of PHD enzymes and FIH therefore regulate HIFs through degradation and inhibition of transcription when oxygen is available. A simplified version of the pathway is shown in Figure 1.2.2-1.

HIF-1α and HIF-2α are both regulated by PHD proteins and have distinct transcriptional profiles. A list of HIF-1α and HIF-2α targets are shown in Table 1.2.2-1. HIF-3α is structurally related to HIF-1α and HIF-2α, but does not have transcriptional activity, and expression is not regulated by oxygen tension at a transcriptional level (Hara *et al.*, 2001). However, the alternative splicing of HIF-3α can produce a truncated form known as IPAS able to suppress HIF-1α and HIF-2α-mediated activity through forming inactivate heterodimers with them (Makino *et al.*, 2001). Unlike HIF-1α, HIF-2α and HIF-3α are expressed in a limited selection of tissues including endothelial cells, renal interstitial cells and myeloid cells (Majmundar, Wong and Simon, 2010).

In addition to molecular oxygen, PHD proteins also require free Fe^{2+} and the Krebs cycle intermediate 2-oxoglutarate (otherwise known as α-ketoglutarate, or α-KG). Metabolic flux can therefore regulate the activity of this pathway through modulating the efficiency of PHD in hydroxylating HIF targets (Schofield and Ratcliffe, 2004).

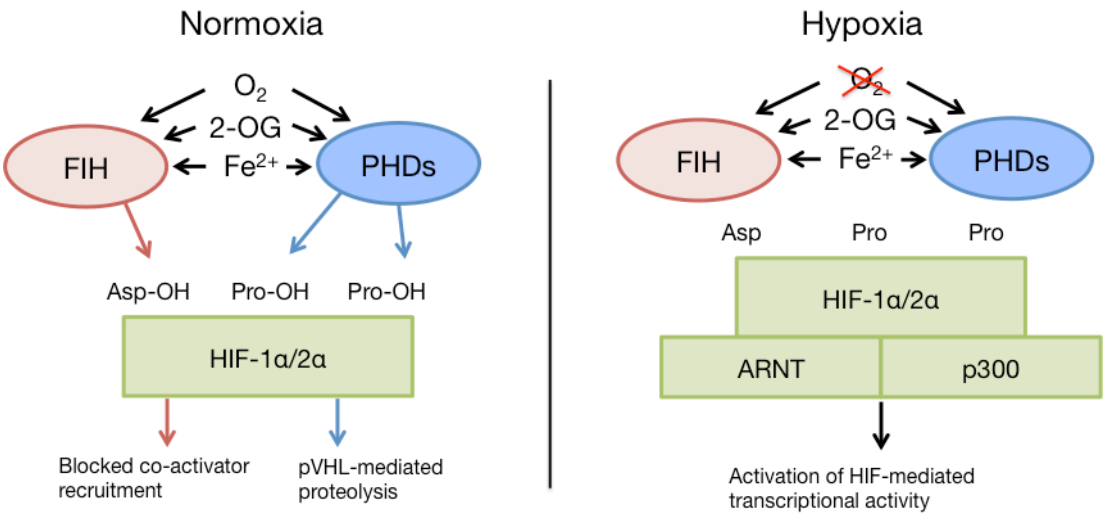

Figure 1.2.2-1: The hypoxic response pathway. Oxygen, 2-oxoglutarate and Fe^{2+} are essential cofactors for the activity of the prolyl hydroxylase domain enzymes PHD1, 2 and 3. These enzymes hydroxylate HIF and target it for degradation by VHL. Lack of oxygen, Fe^{2+} or 2-oxoglutarate prevents the activity of PHD enzymes and leaves HIF-1α stable and able to bind to hypoxic response elements of target genes and activate transcription.

Protein	Pathway	Regulation	Effectors
HIF-1α	Glucose transport	Upregulated	GLUT1, GLUT3
	Hypoxia response pathway	Positive feedback	EGLN1, EGLN3
	PDK	Upregulated	PDK
	Angiogenesis	Upregulated	VEGF
	Glycolysis	Upregulated	HK1, HK2, PFKFB1-4, ALDOA, ALDOC, TPI1, GAPDH, PGK1, PGM, ENO1, PKM2
	Pentose Phosphate Pathway	Upregulated	TKT, TKTL2
	Glycogen synthesis	Upregulated	GYS1
	Apoptosis	Upregulated	BNIP3, FAM162A, NOXA, P53, PUMA, BAX, MCL1, NPM
	Mitochondrial electron transport chain	Suppressed	TMEM70, CYCS, ISCU
	Citric acid cycle	Suppressed	FH, ALDH4A1
	Red blood cell differentiation	Upregulated	EPO
	Cell differentiation	Upregulated	NOTCH
	Solute transporters		MCT4, CA9, NHE1
HIF-2α	Red blood cell differentiation	Upregulated	EPO
	Endothelial cell proliferation	Upregulated	VEGF, TGF-α
	Angiogenesis	Upregulated	TGF-β1

Table 1.2.2-1: The hypoxic response pathway. A list of critical pathways regulated by the hypoxic response transcription factors HIF-1α and HIF-2α (Benita *et al.*, 2009)(Liu *et al.*, 2012)(Dengler, Galbraith and Espinosa, 2014)(Zhao *et al.,* 2015).

1.2.3. Modulation of neutrophil lifespan and function by oxygen tension

In a normal neutrophil-mediated inflammatory response, neutrophils migrate to the site of infection or inflammation and then phagocytose invading bacteria. Neutrophils are cleared from the site of infection through a programme of constitutive apoptosis and subsequent phagocytosis of the apoptotic neutrophils by other immune cells such as resident macrophages (Perretti, Soehnlein and Ortega-Gómez, 2013). In hypoxic conditions such as those found at sites of inflammation, constitutive neutrophil apoptosis and clearance are delayed (Hannah *et al.*, 1995). This hypoxic survival phenotype is thought to be important in allowing neutrophils to remain in inflamed tissue long enough to clear infection through degranulation and phagocytosis of invading pathogens. Indeed, hypoxia can positively regulate neutrophil degranulation and potential for tissue injury (Hoenderdos *et al.*, 2016). Inflammatory tissue tends to be hypoxic due to rapid tissue volume expansion increasing the distance between blood vessels and some areas of tissue, and the influx of large numbers of inflammatory cells, which then consume molecular oxygen. Neutrophils themselves can drive tissue hypoxia, through massive oxygen consumption after activation of NADPH oxidase activity, which acts as an inflammatory signal to nearby cells, as well as other neutrophils, through HIF-1α signalling (Colgan and Taylor, 2010)(Campbell *et al.*, 2014).

The exact mechanism of neutrophil persistence in chronic inflammatory conditions such as COPD is not known. However, dysregulation of this hypoxic survival phenotype and consequential lack of macrophage clearance may contribute to the accumulation of neutrophils in the airway lumen of COPD patients (Hoenderdos and Condliffe, 2013). Patients with moderate to severe COPD also experience alveolar hypoxia due to airway limitation and subsequently may develop hypoxaemia which can also influence the response of immune cells to infection (Kent, Mitchell and McNicholas, 2011). Pathways involved in the regulation of neutrophil hypoxic survival are associated with the modulation of intrinsic apoptosis and metabolic pathways, phagocytic capacity and redox potential, all of which may play a part in mediating neutrophil persistence and airway damage in inflammation (summarised in Thompson et al. 2013).

The neutrophil response to hypoxia is dependent on the activity of the transcription factors HIF-1α and HIF-2α. HIF-1α is critical for neutrophil hypoxic survival (Walmsley *et al.*, 2005) and for neutrophil infiltration and tissue destruction in models of inflammatory disease (Cramer *et al.*, 2003). HIF-1α regulates neutrophil survival through an NF-κB-mediated mechanism, although downstream effectors of this pathway are unclear and require further elucidation (Walmsley *et al.*, 2005). Macrophages isolated from HIF-1α-deficient mice were also shown to be functionally deficient, with aberrant bacterial killing, motility and ability to infiltrate into tissue (Cramer *et al.*, 2003), implicating HIF-1α as a master regulator of myeloid cell function in hypoxic conditions.

HIF-2α also regulates inflammation. Loss of HIF-2α is capable of suppressing neutrophilic inflammation and reducing the damage associated with lung injury induced by administration of LPS (Thompson *et al.*, 2014). In a model of sterile lung inflammation, the expression of HIF-1α and HIF-2α appear to be temporally distinct, with HIF-1α expression induced early in the inflammatory response, and HIF-2α expression induced from 24 hours following inflammatory insult. In contrast to HIF-1α knockouts, loss of HIF-2α was shown to accelerate constitutive neutrophil apoptosis even in normoxic conditions.

Unsurprisingly, regulation of the PHD enzymes also has knock-on effects on inflammation through modulating neutrophil function. Loss of PHD2 in neutrophils reduces rates of constitutive apoptosis through stabilisation of HIF-1α and causes an exaggerated response to *S. pneumonia* infection, with more neutrophils at the site of inflammation (Sadiku *et al.*, 2017). Conversely, loss of PHD3 in neutrophils causes loss of hypoxic survival and is beneficial for inflammation resolution (Walmsley *et al.*, 2011). Further analysis of this pathway will be essential for understanding how hypoxia and metabolism intersect to modulate neutrophil activity.

1.3. Function and significance of neutrophil mitochondria

1.3.1. Functions of neutrophil mitochondria

As predominantly glycolytic cells, there has been some debate as to the role mitochondria play in the neutrophil. Early electron microscopy studies showed a small number of mitochondria in the neutrophil which are small and possess poorly defined cristae (Hirsch and Fedorko, 1968). However, more recent studies using mitochondria-specific fluorescent antibodies have found neutrophils possess an extensive network of mitochondria (Fossati *et al.*, 2003), which has been confirmed by studies from our group (unpublished). These studies also found neutrophil mitochondria maintain mitochondrial membrane potential, suggesting they do undertake active electron transport (Fossati *et al.*, 2003)(van Raam *et al.*, 2008) although it is unclear whether this is used to generate ATP. Some studies suggest neutrophil mitochondria do not undergo oxidative metabolism; Maianski et al argue that neutrophil mitochondria do not participate in energy metabolism as inhibition of oxidative phosphorylation does not appear to significantly decrease the overall ATP found in the cell (Maianski *et al.*, 2004). In addition, neutrophil oxygen consumption is minimal (Kramer *et al.*, 2014) and neutrophil mitochondria seem to lack respiratory supercomplexes (van Raam *et al.*, 2008), suggesting neutrophil metabolism is predominantly glycolytic. However, studies by Bao *et al* implicate mitochondrially-produced ATP in autocrine purinergic signalling of the neutrophils, suggesting some degree of physiologically-relevant oxidative phosphorylation (Bao *et al.*, 2014).

Fossati et al outline a number of non-energy functions of neutrophil mitochondria through the use of inhibitors of the electron transport chain (Fossati *et al.*, 2003). Disruption of neutrophil mitochondrial membrane potential with the protonophore FCCP was found to have a profound effect on cell shape, respiratory burst capability and neutrophil chemotaxis. Furthermore, incubation with the ATP synthase inhibitor oligomycin was found to alter respiratory burst activation and chemotaxis of neutrophils with no effect on mitochondrial membrane potential and neutrophil apoptosis, indicating that while neutrophil mitochondria have limited respiratory activity, the electron transport chain itself may be intrinsic in other cellular

processes.

1.3.2. The role of neutrophil mitochondria in apoptosis

The involvement of mitochondria in the regulation of neutrophil apoptosis has been explored in a number of studies linking caspase activation and upstream regulators of caspases such as Bak, Bax, Bad and Mcl-1 to the regulation of the onset of constitutive neutrophil apoptosis. Neutrophils constitutively expressive pro-apoptotic Bcl-2 family proteins such as Bax, Bad, Bak, Bik and Bim, and also express anti-apoptotic proteins such as Mcl-1, Bcl-X_L and A1, but not Bcl-2 (reviewed in Milot & Filep 2011). Mcl-1 is known to be a profound survival signal as it antagonizes pro-apototic Bax protein, and is thought to be an important factor in regulating neutrophil survival. Neutrophils are unusual in that they do not express Bcl-2, an anti-apoptotic protein found in almost all other tissues as well as other innate immune cells known to be a critical regulator of apoptosis (Akgul, Moulding and Edwards, 2001)(Chipuk *et al.*, 2010). Neutrophils isolated from Mcl-1 conditional knockout mice were shown to have profoundly reduced survival when cultured *ex vivo* (Dzhagalov, St. John and He, 2007). Moreover, pro-survival stimuli such as GM-CSF, IL-1β, LPS and hypoxia increase Mcl-1 expression (Moulding *et al.*, 1998)(Dyugovskaya *et al.*, 2012), implicating Mcl-1 in a link between regulation of constitutive apoptosis and delay of apoptosis in inflammation..

Maianski *et al* show accumulation of Bax in and loss of cytochrome c from the neutrophil mitochondria during apoptosis and suggest constitutive neutrophil apoptosis is mediated by the intrinsic apoptosis pathway (Maianski *et al.*, 2004). This correlates with the profound survival effects of Mcl-1. A study by Scheel-Toellner *et al* suggests constitutive apoptosis is dependent on an extrinsic pathway involving the formation of lipid rafts which can localise death receptors such as CD95 and death-inducing signalling complexes (DISCs) (Scheel-Toellner *et al.*, 2004). They hypothesise that generation of ceramide allows clustering of CD95, DISCs and other TNFR1 homologues, which mediates apoptosis through caspase-8 activation and Bax insertion into the outer mitochondrial membrane. However, a study by Renshaw *et* al suggests blocking death receptors, in this case TRAIL-R2, does not alter constitutive neutrophil apoptosis, despite the potent pro-apoptotic

effects of TRAIL (Renshaw *et al.*, 2003). It is not entirely clear how the relative contribution of intrinsic and death receptor-mediated apoptotic pathways regulate constitutive neutrophil apoptosis or how these pathways are modulated in the hypoxic survival phenotype. Interestingly, treatment with desferoxamine, an inhibitor of hydroxyl radical production, was shown to reduce ceramide generation and CD95 clustering, and delay spontaneous neutrophil apoptosis, indicating ROS may be upstream regulators of this process and play an important role in the regulation of apoptosis.

1.3.3. Mitochondrial reactive oxygen species

It is well established that intact mitochondria produce reactive oxygen species. Production of mitochondrial reactive oxygen species (hereby referred to as mROS) is mediated through leak of electrons from the electron transport chain and subsequent reaction with molecular oxygen in the mitochondrial matrix or intracellular space to form superoxide, or O_2^- (Wulf, 2002). Superoxide can then be exported from the intracellular space to the cytoplasm, or rapidly dismutated to hydrogen peroxide (H_2O_2) which can freely diffuse across the mitochondria outer membrane and have far reaching effects in the cell (West, Shadel and Ghosh, 2011). Alternatively, superoxide can react with nitric oxide (NO) to produce peroxynitrite ($ONOO^-$), a powerful oxidant. H_2O_2 is detoxified by antioxidant enzymes such as catalase or glutathione peroxidase, or can be reduced by metal ions to form a hydroxyl radical, $^{\bullet}OH$ (Figure 1.3.3-1).

Traditionally, mROS have been thought of as an unwanted by-product of oxidative respiration, which can cause damage to the cell. Indeed, a wide range of pathologies are linked to enhanced oxidative stress, including rheumatoid arthritis and degenerative neurological disorders (Uttara *et al.*, 2009). However, a number of studies have found roles for mROS in the healthy cell and describe ROS such as hydrogen peroxide as intracellular signalling molecules capable of modulating the activity of phosphatase and kinase enzymes through oxidation of residues in the active site (Rhee *et al.*, 2000)(Banerjee *et al.*, 2010). Interestingly, there is also mounting evidence that HIF-1α stability in hypoxia is dependent on the production of reactive oxygen species by the mitochondria (Chandel *et al.*, 2000)(Guzy and

Schumacker, 2006). Inhibition and deletion of complexes I and III of the electron transport chain are sufficient to completely block HIF-1α stability (Guzy and Schumacker, 2006).

The mechanism for mROS-mediated HIF-1α is unclear, but it has been proposed this may be due to hydrogen peroxide radicals directly inhibiting PHD enzymes by oxidising non-heme-bound iron. Subsequent studies have suggested peroxide may also enhance HIF-1α stability through inhibition of the activity of FIH (Masson *et al.*, 2012).

There has been some prior investigation into the role of mROS in the context of neutrophil-mediated lung inflammation. Data suggests neutrophils have limited complex V activity, which may account for electron leak at other steps in electron transfer (Luo and Loison, 2008). Complex I is known to be a major source of electron leak and production of mROS (West, Shadel and Ghosh, 2011). In a study by Zmijewski, neutrophil complex I inhibition was shown to increase ROS production, inhibit NF-κB activation, and diminish pro-inflammatory cytokine production in neutrophils activated by LPS (Zmijewski *et al.*, 2008). The study went on to show inhibitors of complex I administered to mice with LPS-induced lung inflammation significantly decreased neutrophil counts in bronchoalveolar lavage (BAL) fluid and significantly lessened lung damage induced on addition of LPS. This correlates with studies suggesting HIF-1α requires ROS derived from complex I and III for stability (Guzy and Schumacker, 2006). Studies by van Raam have suggested neutrophil mitochondrial membrane potential and mROS production could be maintained by transfer of electrons to complex III via the glycerol 3-phosphate shuttle, suggesting the high level of glycolysis in the neutrophil can maintain mitochondrial membrane potential itself (van Raam *et al.*, 2008). These data therefore implicate neutrophil mROS as potential modulators of neutrophil function, and further investigation is required to understand how mROS may affect neutrophil apoptosis and function.

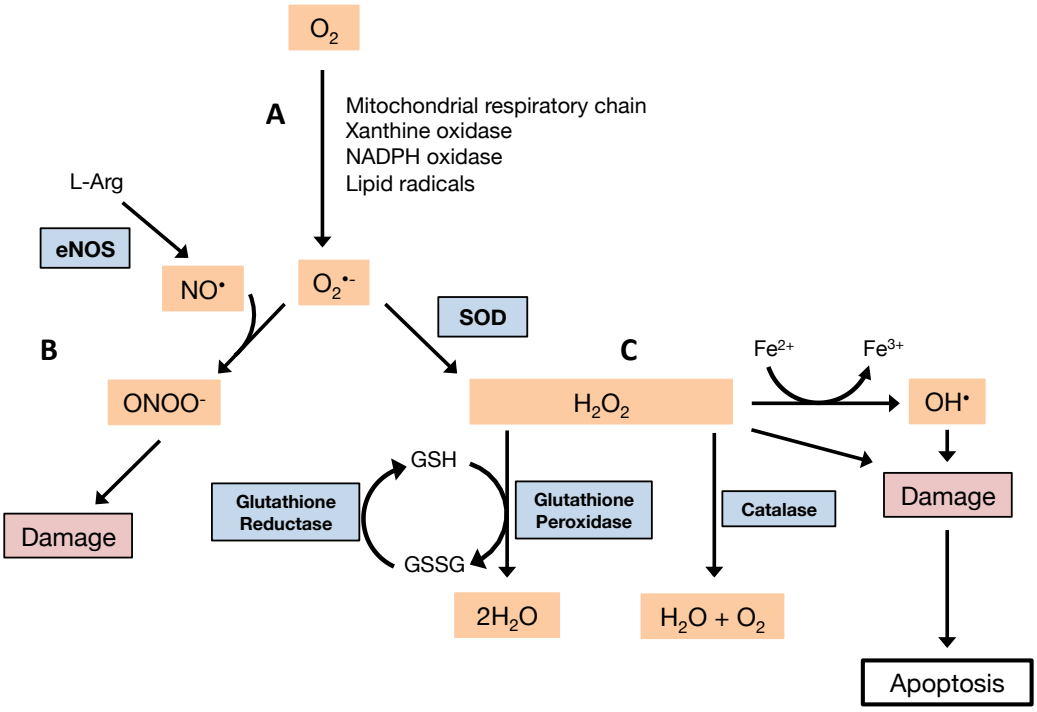

Figure 1.3.3-1: Reactive oxygen species in the cell. A schematic showing the various reactive oxygen and nitrogen species in the cell and cellular antioxidant mechanisms. A) Molecular oxygen is converted to superoxide through the activity of the mitochondrial respiratory chain complexes or through oxidase enzymes such as xanthine oxidase and NADPH oxidase. B) Reactive nitrogen species such as NO may react with superoxide to produce toxic radicals such as peroxynitrite that can cause cell damage. C) Superoxide may be dismutated by mitochondrial SOD into hydrogen peroxide. Hydrogen peroxide can freely diffuse out of the mitochondria and modulate mitochondrial and cytoplasmic signalling. It may be neutralised by the activity of antioxidant enzymes such as catalase or glutathione peroxidase. It may also cause cellular damage either directly or through it's oxidised intermediate, OH. Adapted from Redza-Dutordoir and Averill-Bates, 2016.

1.3.4. Neutrophil reactive oxygen species and apoptosis

The modulation of apoptotic pathways in hypoxic conditions or in patients with chronic lung disease has not been studied in much detail, especially in the context of ROS signalling. Mcl-1 has been under scrutiny as a downstream target of HIF-1α in other cell types. Studies have indicated Mcl-1 expression is closely linked with expression of HIF-1α at the transcriptional level (Liu *et al.*, 2006) but little information exists in the context of neutrophil apoptosis. Studies from our group have also implicated a HIF-1α-independent, PHD3-dependent hypoxic survival signal mediated via the balance between the pro-apoptotic protein Siva1 and the survival protein Bcl-X_L (Walmsley *et al.*, 2011).

Reactive oxygen species may be influential in driving neutrophil apoptosis, both constitutive and following phagocytosis of pathogens via a caspase-dependent pathway (Yamamoto *et al.*, 2002)(Sim *et al.*, 2005). Neutrophils from patients with Chronic Granulatomous Disease (CGD), a disease characterised by a defect in NADPH oxidase, were found to experience a profound delay in constitutive apoptosis when cultured *ex vivo* (Kasahara *et al.*, 1997). Sim *et al* posit that apoptosis is mediated through ROS interacting with the ERK1/2 signalling pathway, and from oxidative damage to the cell inducing caspase-dependent apoptosis. However, there is also evidence that indicates ROS may have a pro-survival role. ROS are thought to stabilise HIF-1α, and stabilisation of HIF-1α allows for a profound survival response (Walmsley *et al.*, 2005). Other studies have shown inhibition of NADPH oxidase can actually induce caspase-3 activity (Fadeel *et al.*, 1998).

.

1.4. Neutrophil metabolism and regulation of apoptosis and function

Glucose metabolism is closely linked with immune cell function both at the site of inflammation and infection. High glucose levels in the blood are known to be proinflammatory; chronic hyperglycemia associated with diabetes has been linked to increased levels of chronic inflammatory markers including IL-1β, IL-6 and TNF-α (Chang and Yang, 2016). Hyperglycaemia can also profoundly modulate neutrophil function and apoptosis. Neutrophils isolated from patients with type 1 diabetes have been shown to have functional defects in adhesion, migration, phagocytosis and survival (summarised Huang *et al.*, 2016).

The regulation of carbohydrate metabolism in innate immune cells has given rise to the field of Immunometabolism. Immune cell functions are closely related to their metabolic regulation and substrate use. Enhanced glycolytic flux is a hallmark of immune cell activation on ligation of TLR receptors, occurring during pro-inflammatory macrophage activation and dendritic cell activation, and activation of B and T cells (Krawczyk *et al.*, 2010)(Rodriguez-Prados *et al.*, 2010). Pro-inflammatory M1 classical macrophage activation with bacterial LPS is characterised by an increase in HIF-1α expression and glycolytic flux, whereas anti-inflammatory M2 macrophages activated with IL-4 and IL-13 instead rely on oxidative phosphorylation for energy production (Kelly and O'Neill, 2015). This upregulation of glycolysis is though to occur through LPS-induced activation of HIF-1α and NF-κB; similarly, hypoxia can acts as a potent pro-inflammatory stimulus through HIF-1α, and HIF-1α is essential for inflammatory macrophage activation (Kelly and O'Neill, 2015)(Wang *et al.*, 2017).

These data perhaps explain why fasting and administration of inhibitors of glycolysis have had some success *in vivo* as treatments against inflammatory diseases (Lee *et al.*, 1999)(Gasior, Rogawski and Hartman, 2006). A study by Wang *et al* elegantly showed that the glucose hexokinase inhibitor 2-deoxyglucose (2-DG) and fasting could actually reverse morbidity associated with *Listeria monocytogenes* infection or LPS-induced sepsis, whereas nutrient deprivation or inhibition of glucose utilisation was detrimental in models of viral infection using influenza virus A/WSN/33 or Poly

(I:C) (Wang *et al.*, 2016). Glucose supplementation was also detrimental in a model of LPS-induced sepsis – indicating glucose could fuel detrimental pro-inflammatory functions of the immune system. Similarly, hypoxia is capable of sensitizing cells to 2-DG due to an increase in glycolytic flux after exposure to hypoxia (Liu *et al.*, 2002)(Xintaropoulou *et al.*, 2015).

Metabolism can also regulate hypoxic signalling. The PHD enzymes require oxygen and the Krebs cycle metabolite α-KG to hydroxylate HIFs. Flux through the Krebs cycle can modulate HIF activity through the availability of α-KG (Majmundar, Wong and Simon, 2010). Recent studies have implicated other Krebs cycle metabolites as critical immune regulators. Succinate generated in the Krebs cycle can inhibit PHDs and mediate a pro-inflammatory, HIF-1α driven macrophage response (Tannahill *et al.*, 2013). Hypoxia itself can modulate Krebs cycle metabolism, with hypoxia causing the production of L-2-hydroxyglutarate, a Krebs cycle byproduct which can competitively inhibit PHD enzymes (Xu *et al.*, 2011)(Intlekofer *et al.*, 2015). Glycolytic flux also feeds back to HIF-1α expression, with lactate and pyruvate production stimulating the accumulation of HIF-1α even in aerobic conditions (Lu, Forbes and Verma, 2002). Pharmacological manipulation of these pathways can therefore modulate immune cell function; for example, suppression of CARKL, an enzyme that limits flux through the pentose phosphate pathway, is sufficient to push macrophages to an M1-like state by increasing glycolytic flux (Haschemi *et al.*, 2012).

As neutrophils have long been thought of as metabolically "simple" cells, mainly glycolytic with little capacity for aerobic respiration, there has been little focus on metabolism in mediating neutrophil function. Recent studies by Sadiku *et al* in neutrophils have shown an exaggerated inflammatory response caused by myeloid specific knockout of PHD2 is caused by enhanced glycolytic flux and can be rescued on treatment with 2-DG (Sadiku *et al.*, 2017). This parallels similar observations in macrophages that link glycolytic metabolism to function. Through giving C^{13}-labeled glutamine, Sadiku *et al* were able to show neutrophils are capable of both reductive Krebs cycle activity and gluconeogenesis, as labeled carbon was found to be present in the cellular glucose 6-phosphate pool; the capacity for gluconeogenesis

activity was profoundly increased in PHD2 knockout cells.

Hypoxia and the HIF-1α pathway can therefore profoundly modulate immune cell function through carbohydrate metabolism. However, there have been few studies investigating the role of metabolism in regulating neutrophil function and apoptosis specifically.

1.5. Aims of the thesis

Hypoxia has been shown to be a profound stimulus for neutrophil survival and persistence in tissues. Oxygen sensing mechanisms, including HIF-1α and HIF-2α, are essential for the adaptation of neutrophils to the hypoxic niche of inflamed sites. Modulation of HIF-1α expression is predominantly caused by the absence of oxygen substrate for PHD enzymes. However, alternative regulators of HIF activity can finely tune the hypoxic response of the cell. One of these regulators is mitochondrial ROS, which can be released in response to acute hypoxia. Direct targeting of HIF-1α is not a desirable approach for reducing inflammation in chronic inflammatory diseases for the reason that HIF-1α is required for many processes including motility, invasiveness and bacterial killing. However, attenuation of inappropriate HIF activity in the context of hypoxia may prevent over-exaggerated immune reactions. Therefore, targeting pathways that augment the HIF-1α transcriptional response, such as mROS, may be useful in limiting HIF-1α-mediated chronic inflammation. Previous studies using the mitochondrial inhibitors metformin and rotenone have both been shown to limit LPS-driven lung injury, indicating targeting neutrophil mitochondrial may be a potential treatment for neutrophil inflammation (Zmijewski *et al.*, 2008). The PHD enzymes are also profound regulators of the HIF proteins. PHD2 has been well characterized as able to modulate HIF-1α stability and glucose metabolism in neutrophils in a way which augments their function (Sadiku *et al.*, 2017). The contribution of other PHD enzymes to neutrophil function and apoptosis, especially in the inflammatory environment *in vivo*, is less well established.

My thesis therefore has two distinct questions regarding the regulation of reactive oxygen species in the neutrophil in both the mitochondrial compartment, and

cytosolic reactive oxygen species produced by NADPH oxidase. My hypotheses are:

1. That neutrophils mitochondrial function regulates neutrophil apoptosis not through generation of ATP, but via signaling through the production of mitochondrial ROS, which can stabilize HIF-1α and enhance neutrophil survival.
2. That the prolyl hydroxylase enzyme PHD3 is a metabolic regulator that can suppress reactive oxygen species production through regulating metabolism, and loss of this enzyme may be beneficial in resolving bacterial infection through enhancing production of reactive oxygen species and consequently, enhancing bacterial killing and encouraging rapid neutrophil apoptosis and clearance.

The aims of this thesis are therefore as follows:

1. To understand if, despite being predominantly glycolytic cells, neutrophils maintain a mitochondrial membrane potential and release mitochondrial ROS uaing fluorescent probes which can measure mitochondrial function in live cells.
2. To examine how hypoxia affects neutrophil mitochondrial function; in particular, whether neutrophil mitochondria release ROS in response to hypoxia, and whether ROS modulate the stability of HIF-1α with downstream effects on survival and function.
3. To interrogate the mechanism of hypoxic mROS release using neutrophils as a model of cells with little mitochondrial ATP production, using mass spectrometry to measure metabolic flux.
4. To use a model of PHD3 knockout to understand whether loss of PHD3 is beneficial for the resolution of bacterial infection as it is in models of sterile inflammation.
5. To measure how the metabolic profiles of neutrophils are altered by loss of PHD3 through measuring inflammatory neutrophil metabolism using mass spectrometry.

2. Methods

2.1. Ethical approval

2.1.1. Healthy volunteers

Phlebotomy of healthy volunteers was approved by the Lothian Local Research Ethics committee. Volunteers gave full informed consent to participate.

2.1.2. *SDHBx* patients

20 patients with rare heterogenous germ-line mutations in *SDHB (SDHBx)* were recruited. Individuals with loss-of-function frameshift, splice, missense or nonsense mutations were included in the study.

2.2. Human neutrophil isolation

Neutrophils were isolated from peripheral blood through dextran sedimentation followed by discontinuous Percoll centrifugation. This method yields >95% pure neutrophils with minimal activation (Haslett *et al.*, 1985).

6% w/v dextran stocks were made up from 3g of sterile 500kDa dextran (Sigma-Aldrich Company Ltd., UK) and 50ml 0.9% Baxter's saline. The dextran stock was then passed through a 0.22um filter and warmed to 37°C prior to use. Peripheral blood was drawn from healthy volunteers using a 21 gauge needle and aliquoted into a 50ml falcon tube containing 4.4ml 3.8% sodium citrate (Sigma-Aldrich Company Ltd., UK) as an anti-coagulant. Tubes were gently mixed, then centrifuged at 270g for 20 minutes. The plasma phase was aspirated and removed. To the remaining lower cell-rich layer, 6ml of 6% dextran was added and the tube topped up to 50ml with sterile 0.9% saline (Baxter Healthcare Ltd.). The tube was then mixed by gentle inverting and rolling, air bubbles removed using a sterile Pasteur pipette, then left to settle for 20-30 minutes at 37°C with the lid loosely fitted to allow red cell sedimentation to occur. The upper leukocyte-rich layer was transferred to sterile falcon tubes and spun at 185g for 6 minutes. Discontinuous plasma-Percoll gradients were prepared by overlaying 2ml of 68% Percoll/32% Dulbecco's Phosphate Buffered Saline (DPBS)(Gibco™, ThermoFisher Scientific, UK) onto 2ml of 81%

Percoll/19% DPBS in 15ml tubes (Percoll® from Sigma-Aldrich Company Ltd., UK). The upper fraction was run gently down the side of the tube to avoid mixing the two layers. Leukocytes from 40ml of whole blood (1 Percoll gradient per tube) were re-suspended in 2ml 51% Percoll/49% DPBS and overlaid on top of the gradient. These tubes were then centrifuged at 1200g for 30 minute, with acceleration 1 and no brake, producing three distinct layers of cells. Erythrocytes were pelleted at the bottom of the tube. Between the 81% and 68% Percoll fractions, a band containing polymorphonuclear (PMN) cells (neutrophils and eosinophils) formed. Between the 68% and 51% fractions, a band comprised of peripheral blood mononuclear cells (PBMCs) formed. The PBMC layer was removed using a Pasteur pipette with care taken not to transfer cells to the lower layer. The granulocytes were transferred to a fresh falcon tube and the tube made up to 40ml with 1x DPBS, centrifuged at 350g for 5 minutes to pellet the cells, then resuspended again in 40ml with 1x DPBS and counted via microscopy using C-Chip disposable haemocytometer slides (Cambridge Bioscience, UK). Neutrophil purity was assessed through examination of slides prepared by cytocentrifuge immediately following isolation and samples with >95% purity used for subsequent assays.

2.3. Human neutrophil culture

Neutrophils isolated from whole blood were resuspended at $5x10^6$ ml^{-1} in RPMI 1640 (Sigma-Aldrich Company Ltd., UK) supplemented with 1% 100x penicillin/streptomycin (Gibco™, ThermoFisher Scientific, UK) and 10% foetal bovine serum (FBS)(Gibco™, ThermoFisher Scientific, UK) and pre-warmed to 37°C and cultured on 96-well non-tissue culture treated polyvinylchloride plates (BD Falcon™, BD Biosciences, Becton Dickinson Ltd., Oxford, UK). Normoxic cell culture was carried out at 37°C in a humidified incubator with 5% supplemental CO_2 (Sanyo). Hypoxic cell culture was established by re-suspending cells in media which had been pre-equilibrated overnight at 1% O_2, 5% CO_2 in an Invivo2 400 hypoxic workstation (Ruskinn, Bridgend, UK).

2.4. Gas analysis of equilibrated culture media

The oxygen tension of re-equilibrated complete RPMI used for neutrophil culture was measured using a RAPIDLab® 348EX blood gas analyser. A 1ml aliquot was removed from RPMI equilibrated in either normoxia or hypoxia as described above into a 1ml syringe and the syringe capped. The sample was then fed into the blood gas analyser and pO2, pCO2 and pH of the media determined (Figure 2.4-1).

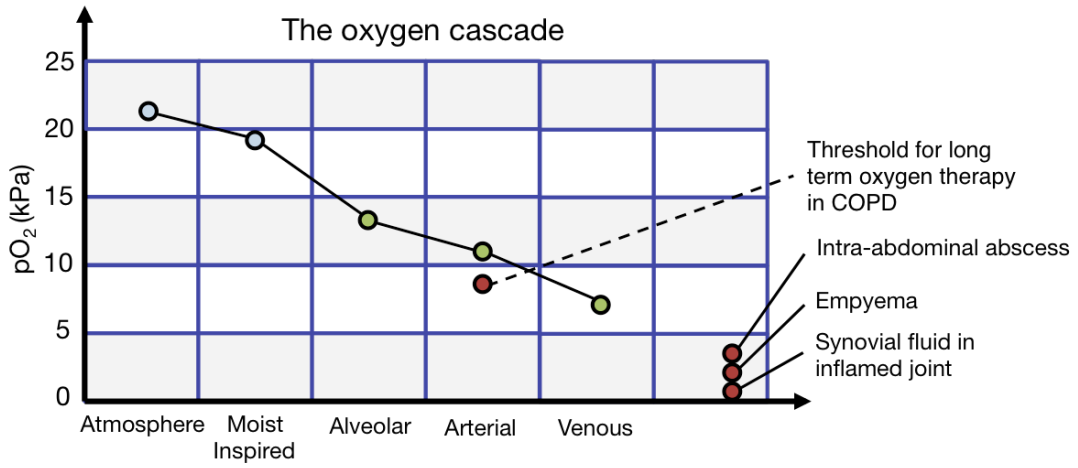

	Normoxia (n=4)	**Hypoxia (n=15)**
pO_2	18.5 (0.195)	4.082 (0.4916)
pCO_2	3.63 (0.2517)	4.329 (0.0572)
pH	7.43 (0.00673)	7.38 (0.0200)

Figure 2.4-1: Confirmation of hypoxic culture conditions. A: The oxygen cascade. Oxygen levels in the body range from 19kPa in inspired air to less that 5kPa in inflamed tisue. B: pO2, pCO2 and pH values of media equilibrated in normoxia and hypoxia. Gas values shown as mean (±SEM). Data from Law *et al,* 1999.

2.5. Assessment of apoptosis via morphology

Microscope slides (ThermoFisher Scientific, UK) were prepared through cytocentrifugation. 100µl of $5x10^6ml^{-1}$ neutrophil suspension was centrifuged onto a microscope slide using a Thermo Shandon Cytospin 3 (Harlow Scientific®) for 3 minutes at 300rpm. Slides were aired dried for 10 minutes, fixed with 100% methanol, then dipped in Diff-Quik staining solutions 1 and 2 for 30 seconds each to stain and then rinsed under the tap**.** Slides were left to dry for 1 hour before mounting. Coverslips were attached with DPX synthetic resin mountant (Sigma-Aldrich Company Ltd., UK). Slides were counted via oil-drop microscopy at 1000x magnification**.** Purity was assessed through counting visible eosinophils, monocytes and erythrocytes, and polymorphonuclear cell populations with <95% neutrophils excluded from further experiments. At least 300 neutrophils per slide were counted and apoptosis calculated as % of total counted neutrophils exhibiting nuclear condensation or condensation and fragmentation (Figure 2.5-1, A).

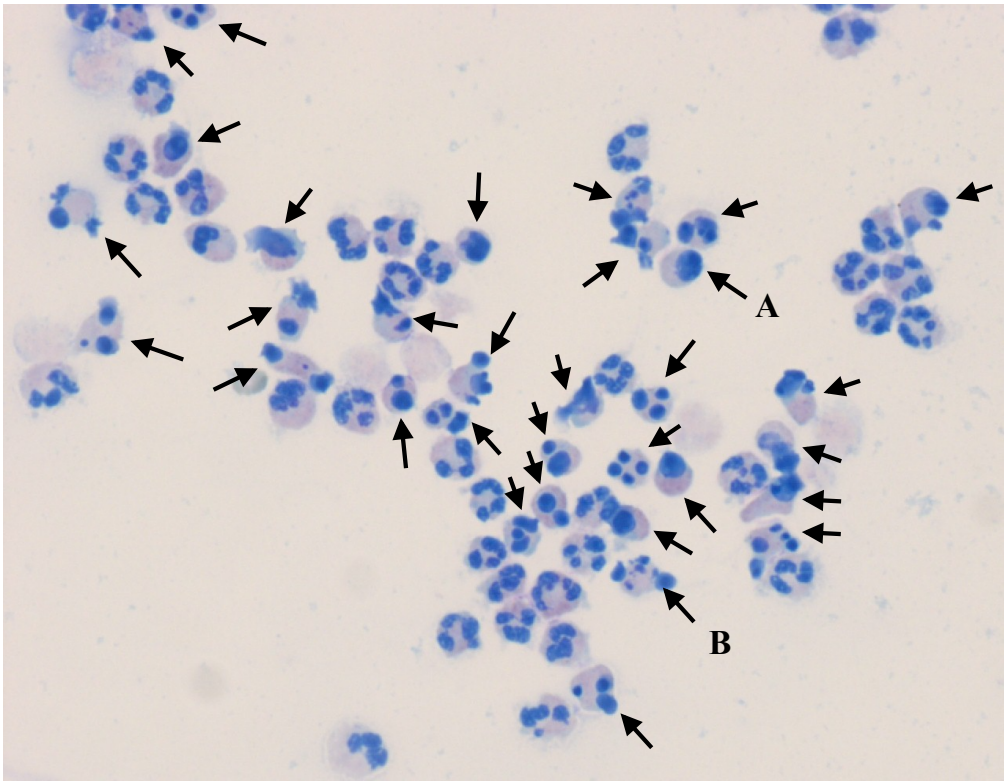

Figure 2.5-1: Identification of apoptotic cells via morphology. Apoptotic cells were identified through nuclear condensation and fragmentation. Apoptotic cells are indicated by black arrows. A: An apoptotic neutrophil with a single, highly condensed nucleus. B: An apoptotic neutrophil with a fragmented nucleus.

2.6. Flow cytometry

2.6.1. Assessment of apoptosis via Annexin V/TO-PRO-3 staining

Cultured neutrophils were removed from the culture plate and transferred to sterile 1.5ml eppendorffs, then centrifuged for 2 minutes at 350g at 4°C, resuspended in 1ml ice-cold 1xDPBS then centrifuged again. 1x Annexin Binding Buffer (ABB) was prepared from 1ml 10x ABB (Abcam®) and 9ml dH_2O. Neutrophils were resuspended in 95µl 1x ABB. 5µl Annexin V-PE (BD Biosciences) was added to 3 of the cell suspensions from each condition and incubated on ice in the dark for 10 minutes. 4 FACS tubes were prepared, 1 as a blank containing 100µl 1x ABB and 3 containing 100µl of a 1:20000 dilution of 1mM TO-PRO-3 (Invitrogen®) (5ml 1xABB, 1µl 1mM TO-PRO-3). Annexin stained cells were added to the 1:20000 TO-PRO-3 and unstained cells were added to the 1xABB as a negative control. Apoptosis was analysed using a BD FACSCalibur flow cytometer (Becton Dickinson®). Neutrophil populations were gated using side scatter (SSC) against forward scatter (FSC). Annexin V-PE binding was assessed through excitation with a 488nm laser filtered through a 585nm dichroic bandpass filter (FL2 channel). TO-PRO-3 binding was assessed through excitation with the 635nm laser and detection of fluorescence through a 661nm dichroic bandpass filter (FL4 channel). Apoptosis was determined as percentage of Annexin V-PE positive or Annexin V-PE/ TO-PRO-3 positive cells. Populations were gated using an unstained control.

2.6.2. Assessment of mitochondrial reactive oxygen species production using MitoSOX™ Red

Neutrophils were cultured in normoxia and hypoxia with and without 100µM MitoTEMPO (Sigma-Aldrich Company Ltd., UK), 10µM Rotenone (Sigma-Aldrich Company Ltd., UK), or 10µM Oligomycin (Sigma-Aldrich Company Ltd., UK), and 5 minutes from the end of incubation, normoxic and hypoxic cells were stimulated through the addition of 100nM N-Formlylmethionine-leucyl-phenylalanine (fMLP)(Sigma-Aldrich Company Ltd., UK) to cell suspension. MitoSOX™ Red (Life Technologies) stock solution was made up through dissolving one 50µg vial in 26µl in dimethyl sulfoxide (DMSO)(Sigma-Aldrich Company Ltd., UK). A working solution was then made through diluting stock by a factor of 10 in sterile 1xDPBS.

2µl of working solution was added to each well and plates loosely covered in tin foil and left to incubate for 30 minutes. Cells were then harvested, washed once in ice-cold PBS, and resuspended in 1x Hank's balanced salt solution (HBSS) ready for analysis. Cells were analysed via flow cytometry on the FACSCalibur using a 488nm laser filtered through a 585nm dichroic bandpass filter (FL2 channel)(Figure 2.6.2-1).

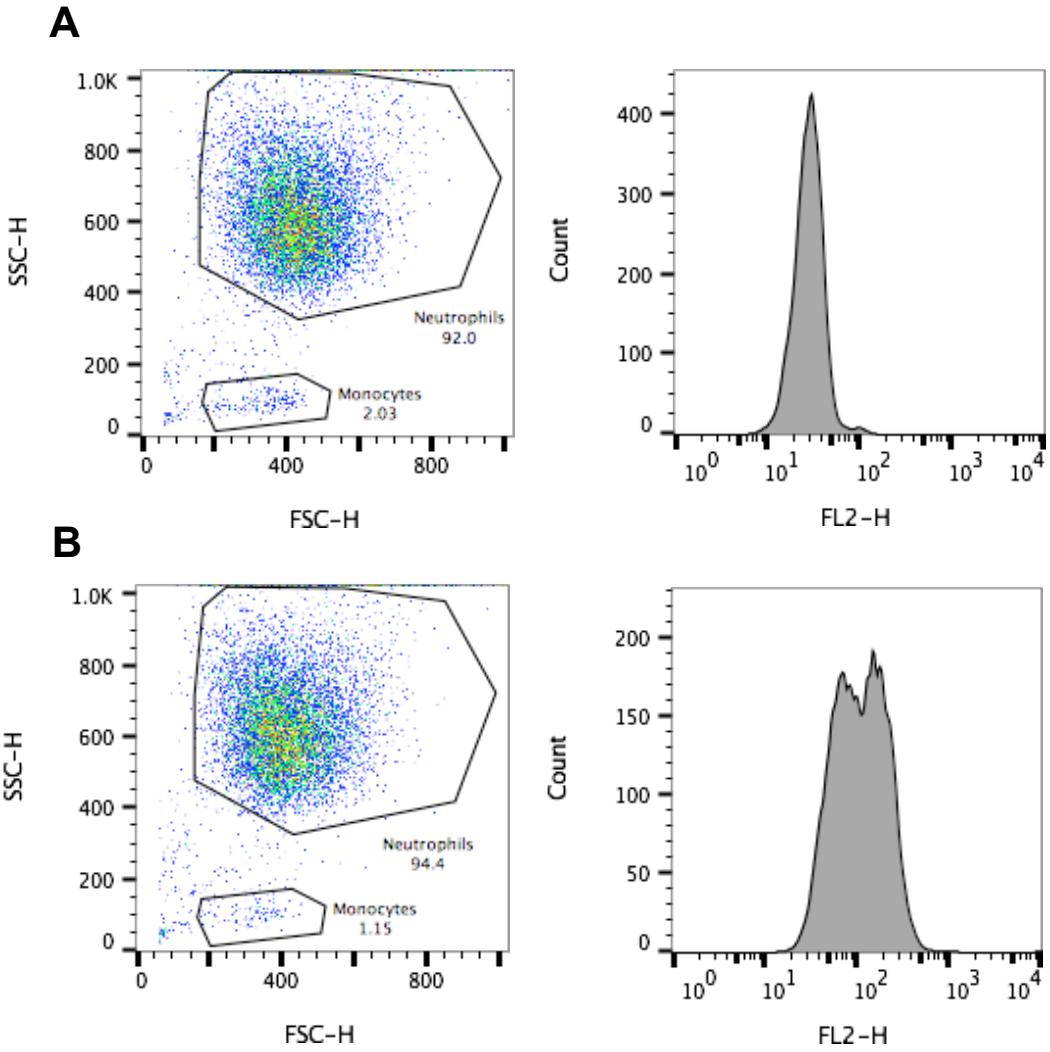

Figure 2.6.2-1: Assessment of mitochondrial reactive oxygen species production by MitoSOX™ Red staining. Neutrophils were gated based on forward-scatter (FSH-H) and side-scatter (SSC-H) and MitoSOX™ Red fluorescence assessed through the FL2-H channel. A: Unstained. B: Neutrophil population stained with MitoSOX™ Red.

2.6.3. Assessment of mitochondrial membrane potential using Tetra Methyl Rhodamine, Methyl Ester

Neutrophils were cultured in normoxia and hypoxia with and without 10μM carbonyl cyanide m-chlorophenyl hydrazone (CCCP)(Sigma-Aldrich Company Ltd., UK) and 100μM MitoTEMPO (Sigma-Aldrich Company Ltd., UK). After incubation, normoxic and hypoxic cells were harvested and transferred into 1.5ml eppendorffs. Cells were centrifuged for 2 minutes at 350g at 4°C. 10mM tetramethylrhodamine methyl ester (TMRM)(Sigma-Aldrich Company Ltd., UK) stock solution was diluted 1/1000 in 1x DPBS and then 3ul added to 1ml of 1x DPBS to make a working solution with a final concentration of 30nM. Cells were resuspended in TMRM working solution and incubated at room temperature for 30 minutes. Cells were analysed via flow cytometry on the FACSCalibur using a 488nm laser filtered through a 585nm dichroic bandpass filter (FL2 channel)(Figure 2.6.3-1).

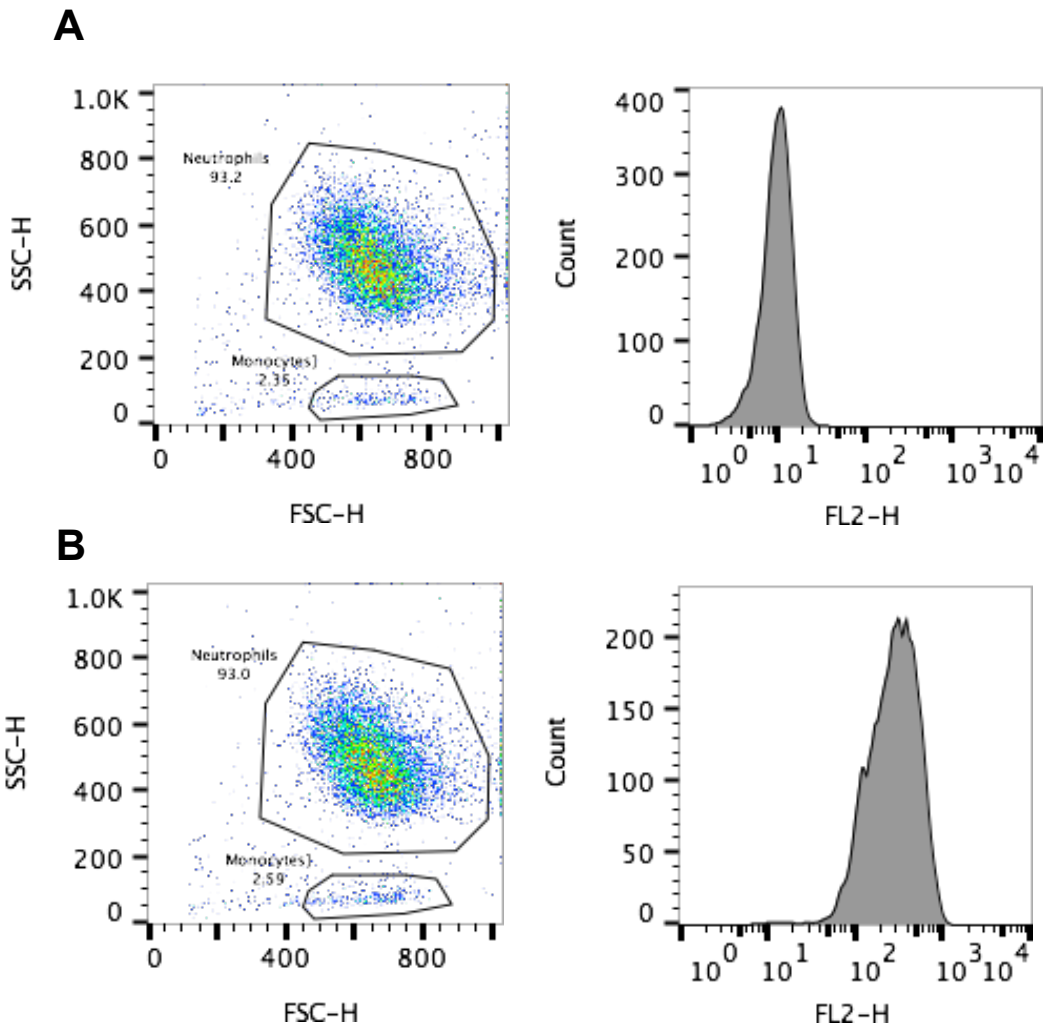

Figure 2.6.3-1: Assessment of mitochondrial membrane potential by TMRM staining. Neutrophils were gated based on forward-scatter (FSC-H) and side-scatter (SSC-H) and TMRM fluorescence assessed through the FL2-H channel. A: Unstained. B: Neutrophil population stained with TMRM.

2.6.4. Assessment of cellular reactive oxygen species production using CM-H2DCFDA

Neutrophils isolated from whole blood via dextran sedimentation and discontinuous percoll gradient were cultured in a 96-well plate for 30 minutes in complete RPMI in normoxia and hypoxia at $5x10^6$ cells/ml. CM-H2DCFDA (DCF)(Life Technologies) stock solution was made up through dissolving one vial in 5µl DMSO and a working solution made up through diluting stock by a factor of 100. 3µl of working solution was adding per well of cells and incubated for 30 minutes. Cells were incubated for a further 30 minutes with and without 100nM of fMLP (Sigma-Aldrich Company Ltd., UK) and analysed on an Attune NxT cytometer on the BL-1 channel (Figure 2.6.4-1).

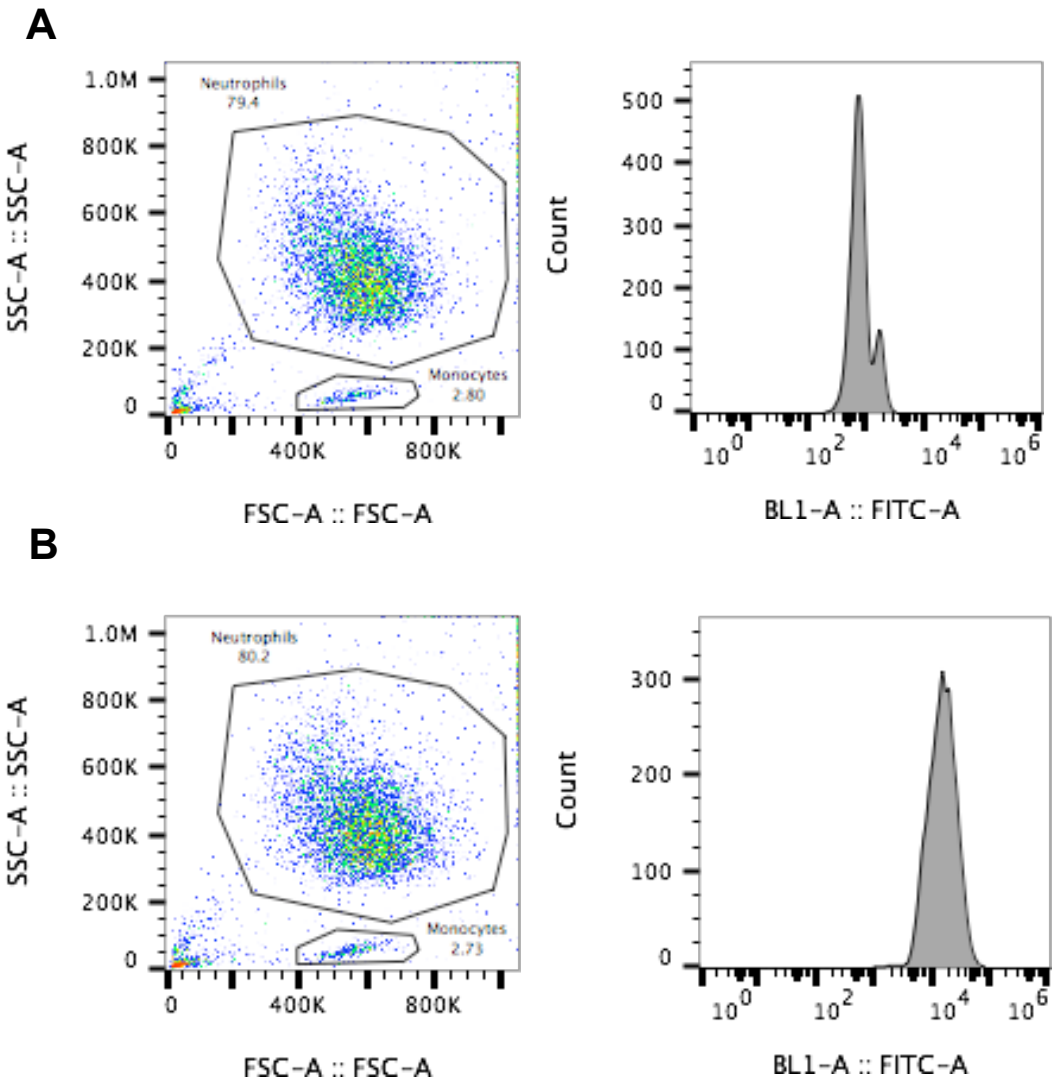

Figure 2.6.4-1: Assessment of neutrophil reactive oxygen species production through DCF staining. Neutrophils were gated based on forward-scatter (FSC-H) and side-scatter (SSC-H) and DCF fluorescence assessed through the BL-1A channel. A: Unstained. B: Neutrophil population stained with DCF.

2.7. Measurement of redox intermediates and redox ratios

Neutrophils were cultured in normoxia and hypoxia with and without 100nm LPS. Following incubation, cells were centrifuged for 2 minutes at 350g at 4°C and washed once in ice-cold 1xDPBS. Neutrophil pellet was lysed in 100µl Lysis Buffer (Abcam) and incubated for 15 minutes before assaying 25µl of lysate using a fluorimetric NAD^+/NADH Assay Kit (ab176723)(Abcam) or $NADP^+$/NADPH Assay Kit (ab176724)(Abcam). Fluorescence was read at 530/590nm using a TECAN infinite M1000 plate reader.

2.8. Assessment of protein expression via western blotting

2.8.1. Protein isolation from neutrophils

Whole cell lysates were prepared from neutrophils through sonication. Protease inhibitor cocktail was made up before harvest through dissolving a complete protease inhibitor tablet (Roche) in 1ml dH_2O. Neutrophils were harvested and $5x10^6$ cells (7 150µl wells) were pelleted at 350g for 2 minutes at 4°C, then resuspended in 500µl complete lysis buffer made up from a stock of 1.5ml sonication lysis buffer (100 mM Tris-HCl, pH 7.8, 1.5 mM EDTA, 10 mM KCl, 0.5mM dithiothreitol (DTT), 1 mM sodium orthovanadate, 2 mM levamisole) with 75µl protease inhibitor cocktail (Roche), 15ul EDTA-Free Protease inhibitor cocktail 3 (Merck Millipore) and 15µl phenylmethanesulfonylfluoride (PMSF)(Sigma-Aldrich Company Ltd., UK). Cells were spun again at 350g for 2 minutes at 4°C, resuspended in 50µl complete lysis buffer and placed on ice for 10 minutes. Cells were sonicated in a Bioruptor® Plus sonication device (Diagenode) in 30 second bursts for 10 minutes. Cells were centrifuged for 10 minutes at 12,000g at 4°C and the supernatant transferred to a clean eppendorff. 50µl 2x Sodium Dodecyl Sulphate (SDS)/Bromophenol blue solution was added to each aliquot and samples boiled for 5 minutes at 100°C before freezing at -80°C until use.

2.8.2. Western blotting

BioRad® Mini-PROTEAN Tetra-cell kits were used to set gels. 1.5mm 8% SDS gels were prepared in 50ml falcon tubes without ammonium persulphate (APS) and

tetramethylethlyenediamine (TEMED) (Appendix 7.1**).** BioRad® mini-PROTEAN 1.5mm separating plates and short plates, and BioRad® 1.5mm 10-well combs were cleaned with 70% IMS before use.

APS and TEMED were added immediately before the resolving gel was poured between two upright plates. The resolving gel was then overlaid with 0.5ml isopropanol and allowed to set. Once set, isopropanol was rinsed from the membrane with water and dried, and stacking gel overlaid onto the gel, a comb added, and the gel left to set.

Electrophoresis was carried out in a tank filled with 1x running buffer (recipes for western reagents in Appendix 7.2). Plates were submerged in running buffer and combs removed gently. Samples were heated to 100°C for 5 minutes before loading and 50µl of lysate loaded per lane. A lane was loaded with 15µl New England Biolabs® Colorplus™ broad range protein ladder (10-230kDa). Samples were run through the stacking gel at 100V, then through the resolving gel at 150V. Protein was not run off the gel as the proteins of interest were at the extreme of the protein ladder, at 15kDa. Instead, protein front was run approximately 1 inch from the end of the gel.

Gels were removed and transferred to a polyvinylidene fluoride (PVDF) membrane (Immobilon Transfer membrane, Millipore) via wet transfer.

1 square of PVDF membrane was cut per gel and soaked in 100% methanol for 5 minutes. Transfer cassettes were assembled in a bath of 1x transfer buffer (Appendix 7.2) with stacks of sponge, filter paper, gel and PVDF membrane. Cassettes were placed in a tank and submerged in 1x transfer buffer, and protein transferred at 100V for 70 minutes on ice. Membranes were then blocked in blocking buffer (Appendix 7.2) for 60 minutes. Membranes were incubated with primary antibody diluted in blocking buffer at an appropriate solution overnight at 4°C (See Appendix 7.8 for a summary of primary antibodies used). Membranes were washed 3 times in 10ml 1x TBS-Tween (Appendix 7.2) for 10 minutes per wash and incubated for 1 hour with Horseradish Peroxidase-coupled Goat Anti-Rabbit IgG (Dako) diluted 1:2000 in blocking buffer. Membranes were washed 3 times in 10ml TBS-Tween. Clarity™

Western ECL subtrates (Biorad®) were equilibrated for 5 minutes and membranes treated with ECL subtrates for 5 minutes before exposure to X-ray film and development in dark room.

2.8.3. Stripping and re-probing

After development, membranes were washed in water for 7 minutes, soaked in 0.2M NaOH for 15 minutes and washed again for 7 minutes in water before reprobing with Rabbit anti-p38 MAPK diluted 1:2000 in milk (Cell Signaling Technology) for 1 hour. Membranes were then washed, probed with secondary antibody and developed as described previously.

2.9. Murine study approval

Animal experiments were conducted in accordance with the UK Home Office Animals (Scientific Procedures) Act of 1986. All animal studies were approved by The University of Edinburgh Animal Welfare and Ethical Review Board.

2.10. Murine colonies

2.10.1. Wild-type animals

C57BL/6 mice were purchased from Harlan (Oxford, UK), aged 8 weeks. They were then rested in standard housing conditions for 1 week prior to experiments.

2.10.2. $PHD3^{flox/flox}$ $LysMCre^{+/-}$ colony

Breeding stocks were kindly donated by Peter Carmeliet and Max Mazzone, VIB-KU Leuven Centre for Cancer Biology. A myeloid cell lineage-specific Cre-loxP system was used to delete *PHD3*. Experimental animals were homozygous for the floxed *PHD3* allele targeted to myeloid cells via a lysozyme M-drived Cre recombinase ($LysMCre^{+/-}$ $PHD3^{flox/flox}$)(Clausen *et al.*, 1999)(Figure 2.10.2-1). All experiments were performed with sex and age-matched wild-type mice.

2.10.3. Genotyping

Genotyping was performed by Lauren Melrose (University of Edinburgh, UK).

100µl of sterile lysis buffer (5ml 1M NaCl, 5ml 10mM EDTA, 5ml 10% SDS, 500ul 1M Tris HCl pH 7.5, 10mg Proteinase K, 35ml sterile H_2O) was added to mouse ear clips and incubated for 50°C for 2 hours. After incubation, 200µl of phenol-chloroform was added, samples vortexed to mix and then centrifuged for 10 minutes at 11,000g. Supernatant was removed and stored at 4°C until used for PCR. Amplified cDNA was separated on a 2% agarose gel, run at 100V for 1 hour and read on a Gel Doc 2000 system (Biorad, UK). Primers used for genotyping are detailed in Appendix 7.3.

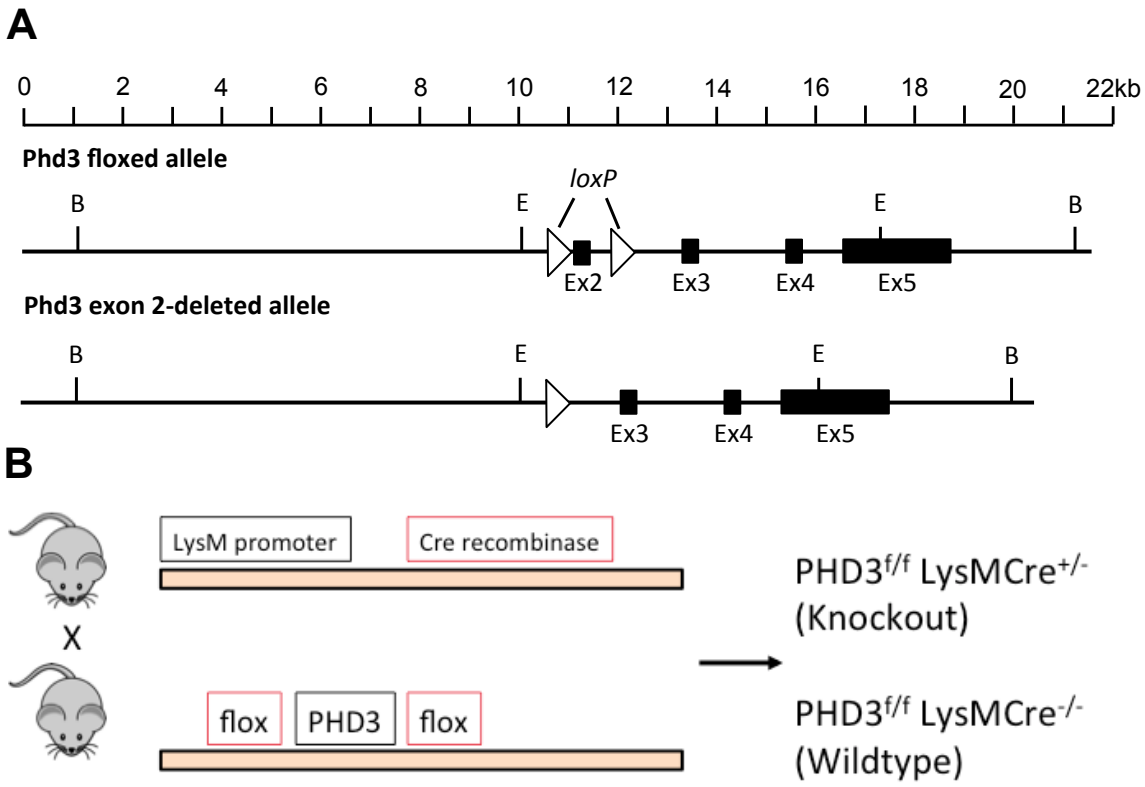

Figure 2.10.2-1: Schematic showing myeloid-specific knockout of PHD3 using the LysM promoter. A) Diagram showing location of flox sites within the Phd3 allele in *PHD3*$^{flox/flox}$ mice. B) *PHD3*$^{flox/flox}$ mice were crossed with heterozygous LysM Cre/Lox mice to generate PHD3$^{flox/flox}$ LysMCre$^{+/-}$ and PHD3$^{flox/flox}$ LysMCre$^{-/-}$ mice. PHD3 expression is controlled by expression of the LysM promoter, targeting knockout specifically to cells of the myeloid lineage. LysM is expressed in granulocytes and mature macrophages. Figure A adapted from Takeda *et al,* 2006. Mice kindly donated by the Carmeliet group.

2.11. Murine lung inflammation model

2.11.1. Induction of sterile lung injury

100mg of bacterial lipopolysaccharide from *Pseudomonas aeruginosa* (Sigma-Aldrich Company Ltd., UK) was dissolved in 10ml of 0.9% saline to make a 10mg/ml stock and stored at 4°C for up to 2 months before use. 300µl stock was diluted in 2.7ml sterile Baxter's saline to make a 1mg/ml solution. Mice were nebulised with 3ml 1mg/ml solution using a custom-made nebulisation rig and then housed in either room normoxia (21% O_2) or in a Coy™ Model 3 hypoxic chamber set at physiological hypoxia (10% O_2). The oxygen concentration in the hypoxic chamber was reduced gradually over the course of one hour to 10% oxygen/90% nitrogen using an oxygen sensing control unit (Coy Labs, Michigan, USA). Oxygen concentration was then steady at 10%. Carbon dioxide generated by animal respiration was removed using fresh soda lime placed in the chamber. At the indicated time points, mice were assessed for sickness and then culled via an overdose of pentobarbital administered interperitoneally.

2.11.2. Bronchoalveolar lavage

Inflammatory cells were harvested from the lung via bronchoalveolar lavage with 5 washes of 0.8ml ice-cold 0.9% saline. Cell counts per ml of BAL were determined using the Sartorius™ NucleoCounter™ NC-100™ Automatic Cell Counter. Total BAL cell counts were determined through cell counts per ml multiplied via total BAL volume returned. Cell purity and differential cell counts were performed through identifying the percentage abundance of each constituent cell on the slides.

2.11.3. Murine neutrophil isolation

Whole BAL was centrifuged at 300g for 10 minutes and supernatant removed and frozen at -80°C. Cells were washed once in 1ml ice-cold 1xDPBS before use.

2.11.4. Percoll purification of murine bronchoalveolar lavage neutrophils

Neutrophils isolated from mouse BAL were purified by discontinuous Percoll gradient to ensure ultra-purified cells for sensitive assays such as mass spectrometry.

Discontinuous Percoll gradients were prepared through adding 3ml 78% Percoll/22% 1xDPBS into a 15ml falcon tube and then carefully overlaying 3ml of 69% Percoll/31% 1xDPBS on top using a sterile Pasteur pipette, running the upper fractions gently down the side of the tube to avoid mixing. Neutrophils were resuspended in 3ml 52% Percoll/48% 1xDPBS, and then gently layered on top of the gradient. The gradient was centrifuged at 1200g for 30mins at acceleration 1, brake 0. The PBMC layer was carefully removed using a Pasteur pipette. The granulocytes were transferred to a fresh 15ml falcon tube, topped up to 15ml with 1x DPBS, and then centrifuged at 300g for 10 minutes. Cells were then resuspended in 1ml of PBS and transferred to a fresh eppendorff. 100µl of sample was removed and diluted in 100µl 2% FCS/PBS for haemocytometer counts and cytospins. Neutrophils were then centrifuged at 300g for 5 minutes and washed once in ice-cold 1xDPBS before use.

A

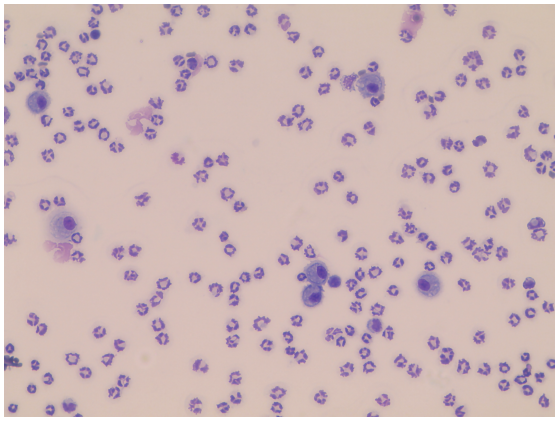

B

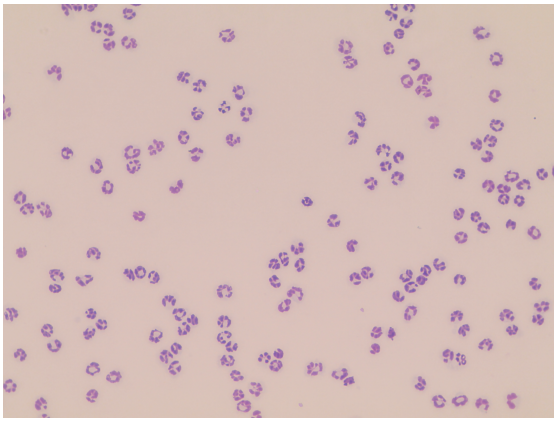

C

	Mean	SEM	Minimum	Maximum
Pre-gradient	93.7	0.398	85.8	97.6
Post-gradient	98.9	0.353	97.2	100

Figure 2.11.4-1: Increase in neutrophil purity following percoll density centrifugation. Neutrophils were isolated from mouse BAL 24 hours after mice were exposed to nebulized LPS and further purified via Percoll density centrifugation. A,B: Cytospins of neutrophils directly from the BAL (A) and post-Percoll density centrifugation (B). C: Purity counts from cytospins pre- and post-Percoll density centrifugation.

2.11.5. Murine neutrophil culture

Neutrophils isolated from mouse BAL were resuspended at $1x10^6$ ml^{-1} in RPMI 1640 (Sigma-Aldrich Company Ltd., UK) with 1% 100x penicillin/streptomycin (Gibco®) and 10% FBS pre-warmed to 37°C and cultured on 96-well non-tissue culture treated polyvinyl chloride plates (BD Falcon™, BD Biosciences, Becton Dickinson Ltd., Oxford, UK). Normoxic cell culture was carried out at 37°C in a humidified incubator with 5% supplemental CO_2 (Sanyo). Hypoxic cell culture was established by re-suspending cells in media which had been pre-equilibrated in 1% O_2, 5% CO_2 in an Invivo2 400 hypoxic workstation (Ruskinn, Bridgend, UK).

2.12. Analysis of cytokines in the bronchoalveolar fluid

Albumin levels in the bronchoalveolar lavage fluid were analysed via ELISA. Before analysis, mouse BAL was centrifuged at 300g for 5 minutes at 4°C to pellet cells and supernatant was transferred to a 15ml falcon tube and frozen at -80°C for up to 1 month before analysis. Before running these ELISAs, the sample was thawed at 4°C.

2.12.1. IgM ELISA

IgM levels in the bronchoalveolar lavage fluid were analysed via ELISA. 25µl of BAL supernatant was diluted in 25µl PBS for a 1:2 dilution and assayed via the Abcam® IgM Mouse ELISA Kit (ab133047). IgM BAL concentration was multiplied by total BAL volume for total IgM per BAL.

2.12.2. Albumin ELISA

10µl of BAL supernatant was added in 990µl 1xDPBS, and 2µl of this solution added to 798µl 1xDPS for a final dilution of 1:40000. 50µl was assayed via the Abcam® Albumin Mouse ELISA Kit (ab108792). Albumin BAL concentration was multiplied by total BAL volume for final albumin amount per BAL.

2.12.3. Elastase

Elastase levels in the bronchoalveolar lavage fluid were analysed via fluorimetric assay. 50µl of BAL supernatant was assayed via the EnzChek™ Elastase Assay (ThermoFisher Scientific). Elastase BAL concentration was multiplied by total BAL

volume for final elastase amount per BAL.

2.12.4. Myeloperoxidase

Myeloperoxidase (MPO) levels in the bronchoalveolar lavage fluid were analysed via fluorimetric assay. 50ul of BAL supernatant was assayed via the EnzChek™ MPO Assay (ThermoFisher Scientific). MPO concentration was multiplied by total BAL volume for final MPO amount per BAL.

2.13. Growth and storage of *Staphylococcus aureus* strain SH1000

2.13.1. Growth of SH1000 *S. aureus* from stock

SH1000, derived from the clinical isolate NCTC 8325, was used for subcutaneous infection models. Initial SH1000 master stocks were kindly donated by the David Dockrell group (University of Edinburgh Centre for Inflammation Research). Before use, vials of SH1000 bacteria were thawed for 10 minutes at room temperature. Bacteria were streaked onto ready-made Columbia horse blood agar plates (VWR). A single colony of SH1000 was inoculated into 30ml brain heart infusion (BHI) in a 50ml falcon tube for 15 hours at 37°C. The culture was centrifuged for 10 minutes at 500g and washed in 50mls of PBS, then centrifuged for 10 minutes at 500g and resuspended in 25ml PBS. 1ml PBS aliquots were frozen at -80°C for future use.

2.13.2. Determination of bacterial concentration

Stock concentrations were determined via Miles-Misra counts. 100µl of culture was serially diluted in 900ul PBS aliquots. 3 10µl aliquots of each dilution were pipetted onto Columbia horse blood agar plates (VWR) and incubated overnight. Aliquots of the stock solution were frozen at -80°C. Bacterial colonies were counted to determine CFU/ml (CFU = colony forming units) of the stock vial.

2.14. *In vivo* model of subcutaneous *Staphylococcus aureus* infection

2.14.1. 12 hour model of acute infection and hypoxia

Mice were shaved on the right flank and left to recover for 24 hours in standard housing conditions before the experiment. On the day of injection, stocks of SH1000 were defrosted for 10 minutes, centrifuged at 5000g for 5 minutes and made up with PBS into a $1x10^9$ CFU/ml solution. Mice were administered with 50ul $1x10^9$ CFU/ml ($5x10^7$) SH1000 subcutaneously into the right flank before being housed in either room normoxia (21% O_2) or in a Coy™ Model 3 hypoxic chamber set at physiological hypoxia (10% O_2) for 12 hours. The oxygen concentration in the hypoxic chamber was reduced gradually over the course of one hour to 10% oxygen/90% nitrogen using an oxygen sensing control unit (Coy Labs, Michigan, USA). Oxygen concentration was then steady at 10%. Carbon dioxide generated by animal respiration was removed using fresh soda lime placed in the chamber. Sickness scores, weight and temperature were assessed at 0 and 12 hours (see Appendix 7.4 for sickness scoring criteria). By 12 hours, a noticeable abscess had formed at the site of injection. Mice were culled via an overdose of pentobarbital administered intraperitoneally, and the abscess (overlying scab and pustule) was excised with a scalpel, weighed and snap frozen at -80°C.

2.14.2. 7 day model of prolonged inflammation

Mice were inoculated as above and then housed in room normoxia (21% O_2) for 7 days. Systemic effects of bacterial infection were measured. Mice were weighed every day. Temperatures were taken daily using a rectal probe (BAT-2, Physitemp Instruments Inc., USA) and photographs taken with a ruler for scale to calculate abscess size. Mice were scored on sickness based on gross external appearance, including assessment of fur ruffling, activity, perioptic exudate and dehydration. Following the 7 days, mice were culled via an overdose of pentobarbital administered intraperitoneally, and the abscess (overlying scab and pustule) excised with a scalpel and weighed. Abscesses were then dissected into 3 equal pieces, and the pieces weighed and either snap frozen at -80°C for bacterial counts and MPO assay or placed in 10% buffered formalin for histological analysis.

2.14.3. Measuring bacterial load at the site of infection

Abscess tissue was placed in a sterile dish and cut into small pieces with a sterile scalpel blade. Contents were placed into a sterile bijou and forceps and scalpel blade rinsed with 1ml PBS into the petri dish. The scalpel was used to remove any flesh stuck to the plate and the flesh added to the bijou. The plate was then washed with a further 1ml PBS and liquid transferred to bijou. The mixture was vortexed for 1 minute and left on ice for 1 hour to allow the scab to dissolve, before vortexing again for 1 minute. 1:10 serial dilutions were made on the homogenate and 3 10µl aliquots of each dilution plated onto Columbia Blood Agar plates (VWR). Plates were incubated at 37°C overnight before counting resultant colonies to determine colony forming units per lesion and per gram of lesion.

2.14.4. Measuring myeloperoxidase activity

The abscess was transferred to a sterile screw-cap tube with 6 homogenisation beads and 0.5ml cold HTAB buffer (Appendix 7.5) and the abscess homogenised in a bullet blender for 5 minutes. The homogenate was sonicated for 10 minutes in 30 second bursts in a Bioruptor® Plus sonicator (Diagenode Europe SA, Belgium) and then freeze-thawed on dry-ice once to ensure cell lysis. The solution was centrifuged at 14,000g for 10 minutes at 4°C and the supernatant transferred to a new sterile eppendorff tube. 100µl of supernatant was added to 1.9ml of O-dianisidine solution (0.167mg/ml O-dianisidine hydrochloride (Sigma-Aldrich Company Ltd., UK) and the change in absorbance at 450nm from 30 seconds to 90 seconds after addition of supernatant was read on a spectrophotometer (Jenway 6310, Barloworld Scientific, UK) to give relative MPO activity.

2.14.5. Abscess histology

Sections of abscess were excised and immediately fixed in 10% buffered formalin. Tissue was removed from the 10% buffered formalin and placed into a cassette. A Leica TP1020 processor (Leica Microsystems, UK) was used to place samples into wax and tissues then embedded into paraffin blocks before cutting with a microtome and mounting onto glass slides (Superfrost plus, ThermoFisher Scientific, UK). Slides were then dried overnight at 37°C. Before staining, slides were dewaxed in

xylene for 2 minutes, then rehydrated through submerging in 100% ethanol two times, then 95% ethanol and 75% ethanol for 2 minutes before rinsing in H_20 for one minute. Dewaxed and rehydrated slides were staining in Gill's haematoxylin for 2 minutes and then rinsed for 1 minute. Slides were then placed in Scott's tap water for 10 seconds and rinsed, before staining with eosin for 5 minutes and rinsing again. Slides were then dehydrated by dipping in 75%, then 95% and 100% ethanol three times each, mounted and then air dried. Sections were stained with Rabbit polyclonal anti-MPO antibody (ab9535, Abcam).

2.15. *In vivo* model of fulminant *Streptococcal* pneumonia

Pneumococci (*Streptococcus pneumonia* type 2, D39) were prepared to a concentration of $2x10^8$/ml in PBS. Mice were anesthetised with ketamine (76mg/kg, Willows Francis Veterinary, UK) and medetomidine (1mg/kg, Orion Pharma, UK) intraperitnoeally. While under anaesthetic, mice were suspended by the upper incisors and a blunt needle passed into the trachea orally. Mice were instilled with 50µl $2x10^8$/ml pneumococci ($1x10^7$/ml total). Twenty minutes after anaesthaesia, mice were administered with atipamezole (2mg/kg, Orion Pharma, UK) to reverse anaesthesia. Mice were recovered for 6 hours and housed for 12 hours in room oxygen.

2.16. Measurement of neutrophil phagocytic capacity

2.16.1. Growth of human D39 *Streptococcus Pneumoniae*

Before culture, stocks of D39 was removed from the -80°C freezer and defrosted at room temperature. Stocks were streaked onto Colombia Horse Blood Agar plates and incubated at 37°C overnight. The following day, 10 colonies of D39 from the blood agar plate were inoculated into 5ml BHI broth and mixed in an incubator at 37°C for 4.5 hours. Absorbance of the culture was read at 600nm. Culture was incubated until 0.5 OD600nm.

2.16.2. CFSE-labelling of D39 *Streptococcus Pneumoniae*

Aliquots of bacteria were centrifuged at 4000g for 5 minutes and then resuspended in 2ml of 10µM Carboxyfluorescein succinimidyl ester (CFSE). The cells were

incubated at room temperature for 1 hour in the dark while gently rocking to mix. After 1 hour, the culture was centrifuged at 4000g for 5 minutes and the pellet resuspended in 15ml PBS. Wash was repeated twice more. After the final wash, the pellet was resuspended in 5ml PBS and culture adjusted to OD600. Bacteria were heated at 65°C for 10 minutes to heat-kill and stored at 4°C for up to 1 month before use.

2.16.3. In-vitro phagocytosis assay

Heat-killed bacteria were vortexed (3x15 second burst at highest settings) to separate clumps. The suspension was diluted 100-fold and 10µl of diluted suspension added to a haemocytometer slide and examined using an inverted fluorescent microscope (EVOS FL Cell Imaging System)(ThermoFisher Scientific) on the GFP channel. If not a consistent single cell suspension, the cells were further vortexed and imaged again. This process was repeated until the bacteria were evenly dispersed. 50µl FBS was added to bacterial suspensions, vortexed and incubated at 37°C for 1 hour to opsonize, then washed twice with 1ml ice-cold 1xDPBS. Concentration of bacterial particles was determined through counting in a haemocytometer using an inverted fluorescent microscope and concentration of bacteria adjusted to $1x10^9$. Neutrophils were isolated from murine BAL and resuspended in RPMI +10% FBS at a concentration of $2x10^6ml^{-1}$ and 100µl suspension plated and incubated in either normoxia (21%) or hypoxia (1%) for 25 minutes. 10µM cytochalasin D was added to cells and incubated for a further 5 minutes. 2µl of $1x10^9$ $CFUml^{-1}$ bacterial suspension was then added to cells for an MOI of 10:1. Cells were incubated for a further 30 minutes at 37°C before being aspirated and transferred into 1.5ml eppendorffs, washed in ice-cold 1xDPBS once, and then resuspended in ice-cold 1xDPBS. Cells were analysed via flow cytometry on the Attune NxT cytometer (ThermoFisher Scientific) using a 405nm laser filtered through a 533/30nm dichroic bandpass filter (BL1 channel). Uptake was measured based on BL-1 positivity (Figure 2.16.3-1).

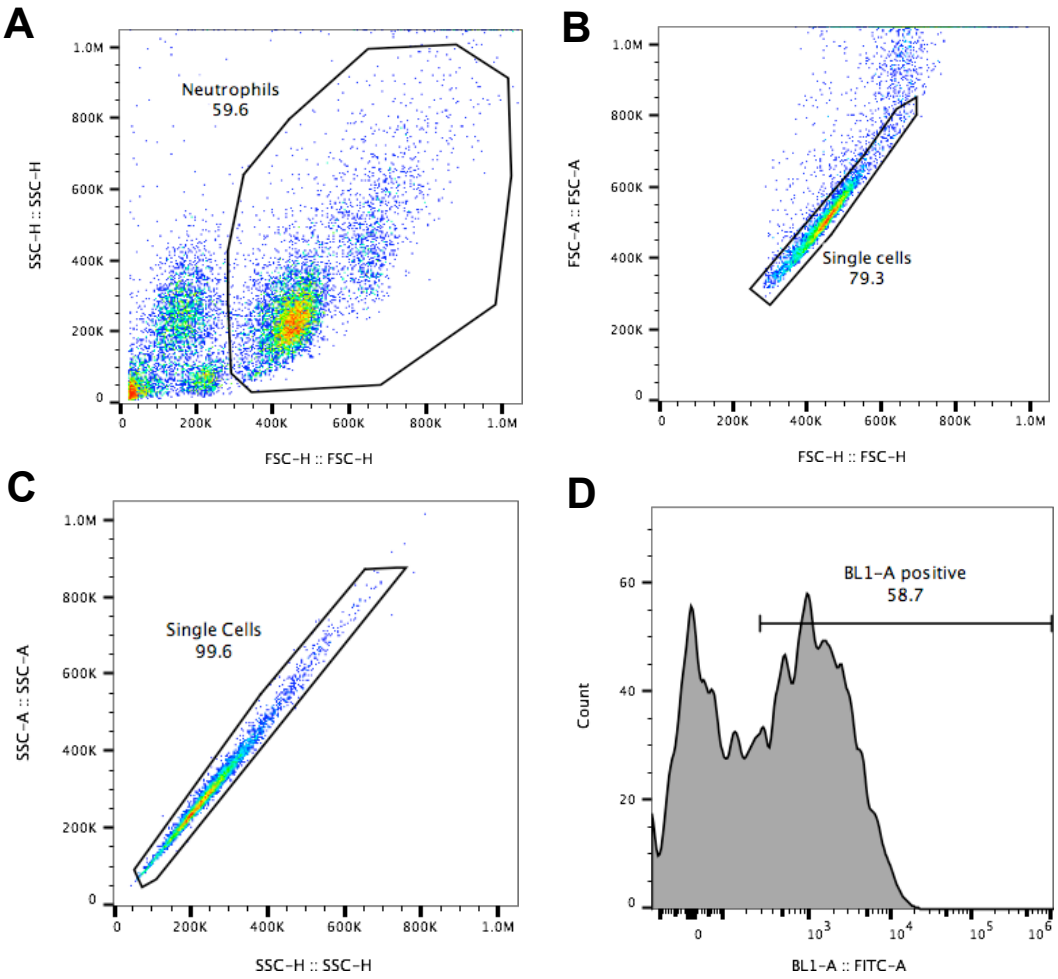

Figure 2.16.3-1: Gating strategy for murine phagocytosis assay. Neutrophils were gated out based on forward and side scatter (A) then single cells gated on through FCS-A/FCS-H (B) and SSC-A/SSC-H (C). Percentage uptake of cells was determined through gating against an unstained neutrophil population not cultured with bacteria. D: BL1-A plot showing two populations representing BL1-A-negative neutrophils (left) which have not taken up CFSE-labelled D39 *S. pneumonia* and a second BL1-A-positive population of neutrophils which have internalised heat-killed CFSE-labelled D39.

2.17. Liquid-chromatography/Mass Spectrometry analysis of intracellular metabolites in murine inflammatory neutrophils

2.17.1. Preparation of cells for Liquid Chromatography/Mass Spectrometry

Ultrapure BAL neutrophils were lysed in 100µl 80% methanol pre-cooled to -80°C and samples snap frozen at -80°C.

2.17.2. Protein quantification for normalisation

Samples were thawed and centrifuged at 10,000g for 5 minutes to pellet protein contents of the cell and supernatant removed for Liquid Chromatography-Mass Spectrometry analysis. Protein content of the pellets were analysed by Pierce™ BCA Protein Assay (ThermoFisher Scientific). The pellet was resuspended in 100µl of PBS and 25µl of sample and standards added to a 96-well microplate. 200µl of Pierce™ BCA Protein Assay working reagent was added to each well and mixed thoroughly on a plate shaker for 30 seconds. Plate was incubated at 37°C for 30 minutes, cooled to room temperature and absorbance measured at 562nm using a TECAN infinite M1000 plate reader.

2.17.3. Liquid-chromatography/Mass Spectrometry analysis

Measurements of relative levels of analyte abundance were carried out in collaboration with the Carmeliet lab (VIB Leuven, Belgium). Analysis was performed using a Dionex UltiMate 3000 LC System (ThermoFisher Scientific) coupled with a Q Exactive Orbitrap Mass Spectrometer (ThermoFisher Scientific) operated in negative mode (Figure 2.17.3-1). 25µl of sample was injected on a SeQuant ZIC/pHILIC Polymeric column (Merck Millipore). The gradient started with 10% solvent B (10mM NH_4-acetate in mqH_20, pH 9.3) and 90% solvent A (acetonitrile) and remained thus until 2 minutes following injection. Next, a linear gradient to 80% B was carried out until 29 minutes. At 38 minutes, the gradient returned to 40% B, followed by a decrease to 10% B at 42 minutes. The chromatography was stopped at 58 minutes. The flow was kept at 100µlmin^{-1}, and

the column kept at 25°C. The mass spectrometer operated in full scan-SIM mode using a spray voltage of 3.2kV, capillary temperature 320°C, sheath gas at 10.0, auxiliary gas at 5.0. AGC target was set at 1e6 using a resolution of 140,000, with a maximum IT of 500ms. Data collection and analysis were performed using Xcalibur Software (ThermoFisher Scientific) with a Genesis peak-picking algorithm identifying predicted peaks. Peaks were manually checked individually to ensure correct peak picking and manually corrected if needed (Figure 2.17.3-2).

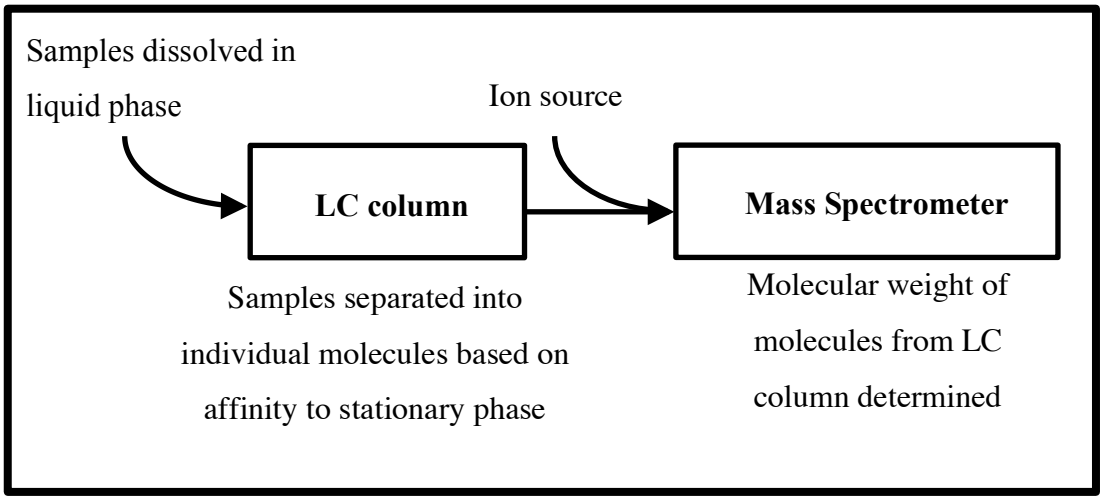

Figure 2.17.3-1: Analysing metabolite abundance via liquid-chromatography/mass-spectrometry. Neutrophil lysates dissolved in -80°C methanol were run through an LC-MS setup. The SeQuant® ZIC®-pHILIC HPLC column separates analytes based on the affinity of the analytes to the stationary phase of the column (hydrophobicity). The column is optimised for separation of polar hydrophilic compounds, including metabolites of anaerobic and oxidative respiration, through containing a polymeric stationary phase bonded to true zwitterionic functional groups. The mass spectrometer determines the size of analytes as they arrive from the Liquid Chromatography column.

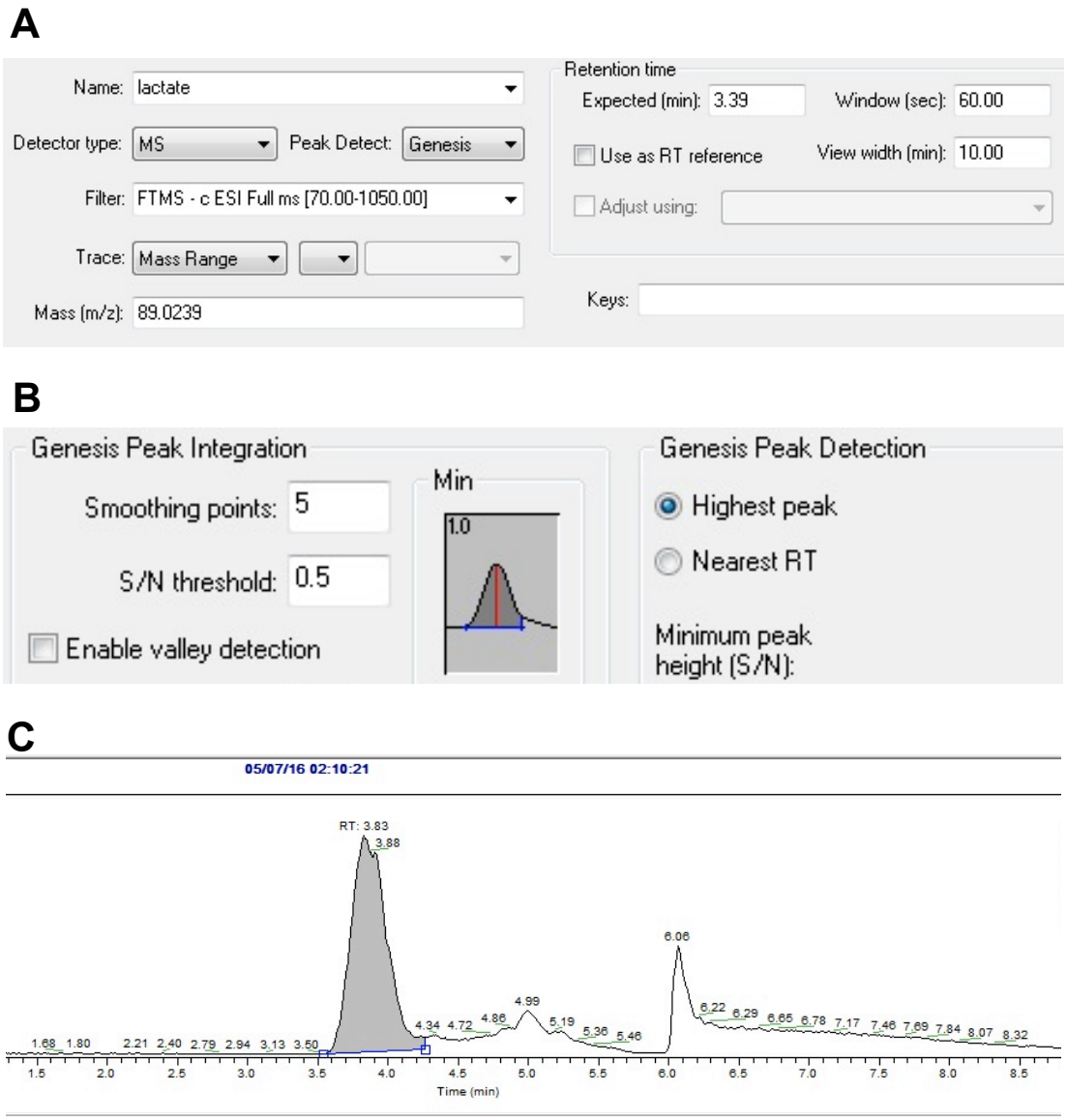

Figure 2.17.3-2: Analyte abundance determined using Xcalibur® software. A: Analytes of interest can be determined by their mass to charge ratio (m/z) and expected retention times determined by reference standards run through the set-up. **B:** Peaks were automatically determined using the Genesis peak integration software. Peaks were picked based on size due to small changes of measured retention time compared to reference analytes. **C:** Chromatogram showing the abundance of lactate (predicted RT 3.39). Abundance was measured as area under the peak. Each peak was manually corrected for consistency.

2.18. Real-time qPCR

2.18.1. RNA extraction

Inflammatory neutrophils isolated from mouse bronchoalveolar lavage were cultured for 4 hours in normoxia and hypoxia. Following culture, $1x10^6$ neutrophils were transferred to 1.5ml eppendorff tubes, centrifuged at 300g for 5 minutes and washed in 1ml 1xDPBS. Cells were then centrifuged at 300g for 5 minutes and lysed in 400µl *mir*VANA™ lysis/binding buffer (Invitrogen™, Waltham MA, US), pipetting up and down 5 times to aid lysis. Lysates were frozen for up to 3 months before further extraction. Before extraction, samples were thawed on ice and 40µl of miRNA Homogenate Additive added before vortexing for 30 seconds. Samples were incubated on ice for 10 minutes. 400µl of Acid-Phenol:Chloroform was added to the sample before vortexing for 30 seconds to mix, and the mixture centrifuged for 5 minutes at 10,000g at room temperature. The aqueous phase was removed from the sample and put in a sterile RNAse-free tube. A volume of 100% ethanol 1.25 times that of the extracted aqueous phase was then added. Lysates was added to a filter cartridge over a clean collection tube and centrifuged for 15 seconds at 10,000g. Flow-through was discarded and 700µl miRNA Wash Solution 1 was added to the filter and centrifuged for 30 seconds at 10,000g. Flow-through was discarded and 500µl Wash Solution 2/3 was added to the filter and centrifuged for 15 seconds at 10,000g. Flow through was discarded and a second wash was repeated using 500µl Wash Solution 2/3. Following the second wash, the filter and collection tube were centrifuged for 1 minute at 10,000g to remove residual fluid from the filter. The filter cartridge was transferred to a fresh collection tube and 40µl of pre-heated (95°C) RNAse-free H_20 added to the filter, and the assembly centrifuged for 30 seconds at 13,000g to recover RNA. Flow-through was run through the filter again for 30 seconds at 13,000g to ensure maximum recovery. RNA purity and abundance was measured using a NanoDrop Spectrophotometer (ThermoFisher Scientific). DNA and protein contamination was ascertained through ratio of absorbance at 260nm/280nm and 260nm/230nm, respectively. Samples were treated with 1µl TURBO™ DNAse (Invitrogen™) and incubated at 37°C in the heat block for 30 minutes. 2µl of DNAse inactivation reagent (Invitrogen™) was added and sample

centrifuged at 10,000g for 90 seconds at 4°C to pellet inactivation beads. Samples were then reanalysed with the NanoDrop for final RNA concentration.

2.18.2. cDNA preparation

At least 250ng of RNA from each sample was added to a PCR tube and made up to 12.4µl with RNase-free water. A mastermix was prepared based on number of samples for reverse transcription (Per sample: 16µl 10mM dNTPs (#U1240), 1.2µl RNasin (#N2115), 1.2µl random primers (#C1181), 1.2µl AMV (avian myeloblastosis virus) reverse transcriptase and 8µl 5x AMV buffer (both #M9004) (all Promega®)). 27.6µl mastermix was added to each sample and mixed by pipetting. Samples were then placed in a ^{3}Prime thermal cycler (Techne®) and cycled through 23°C for 5 minutes, 42°C for 2 hours and 99°C for 2 minutes, then held at 4°C. Resultant cDNA was then frozen at -80°C.

2.18.3. Taqman

cDNA were was thawed at 4°C. For each primer, a standard curve was prepared in 0.5ml PCR tubes from cDNA derived from pooled mouse BAL. cDNA was amplified in polymerase chain reactions using commercial primers (Appendix 7.6.2) and GoTaq Flexi DNA polymerase (Promega UK, UK). 19µl of mastermix (Appendix 7.6.1) was added to 1µl of cDNA and the plate was analysed using an ABI 7900HT Fast Real-Time PCR System (ThermoFisher Scientific). Cycling was set as 2 minutes at 50°C, 10 minutes at 95°C, then 40 cycles of 15 seconds at 95°C and 1 minute at 60°C before holding at 4°C. Data was analysed within the proprietary SDS software. All reads were normalised to the expression of β-actin in corresponding samples.

2.19. Apoptosis and functional assays: Statistics

Results are expressed as mean +/- SEM of the number (n) of independent experiments. In human studies, each independent experiment was performed from cells from separate donors and each experiment performed in triplicate. In murine studies, independent experiments were performed in separate mice or on cells pooled from two mice, and each experiment performed in triplicate. All figures and statistics

were performed using GraphPad Prism 7 for Mac (GraphPad Software Inc. USA). For comparing 2 groups, unpaired or paired Student's T-tests were used. For comparing the effects of two independent variables, 2-way ANOVA was performed with Sidak's post-hoc test for multiple comparisons. For comparing abscess size, linear regression analysis with ANCOVA was used. *P* values <0.05 were considered significant

3. The role of mitochondrial ROS in regulating neutrophil survival

3.1. Introduction

3.1.1. The role of mitochondrial reactive oxygen species as signalling molecules

Mitochondrial reactive oxygen species have long been known as toxic by-products of normal respiratory chain function, capable of inducing pathology through damage to cellular components including lipid peroxidation, oxidation of proteins thiols and oxidative damage to chromosomal DNA (Martínez-Cayuela, 1995). As such, mitochondrial free radicals have been implicated in the pathology of a number of disease states, with an extensive literature linking atherosclerosis (Napoli *et al.*, 2003), rheumatoid arthritis (Yoo *et al.*, 2016), ischaemia-reperfusion injury (Ambrosio *et al.*, 1993) and cancer (Sullivan and Chandel, 2014) to mROS production.

Despite the evident harmful nature of ROS, a growing body of literature has implicated reactive oxygen species as important signalling molecules in their own right, capable of modulating a host of cellular responses. Early studies showed that release of H_2O_2 by the mitochondria is essential for the proliferation of Balb/3T3 embryonic fibroblasts in response to platelet-derived growth factor *in vitro* and treatment of cells with exogenous catalase can prevent proliferation. This mechanism was shown to be due to the capacity of ROS to enhance PDGF- and EGF-induced tyrosine phosphorylation and subsequent MAPK activation (Sundaresan *et al.*, 1995)(Rhee *et al.*, 1997). Reactive oxygen species inhibit protein tyrosine phosphatase activity through oxidation of cysteine thiol residues, leading to enhanced phosphorylation of downstream effector proteins (Lee *et al.*, 1998). Key signal transduction pathways involved in proliferation and survival, including PI3K-AKT and RAS-MEK-ERK, are negatively regulated by protein tyrosine phosphatase activity, and as such ROS been implicated in the induction of these pathways. Subsequent studies have shown ROS mediates the activity of a number of proteins involved in promoting survival and proliferation through this mechanism, including

enhancing p53 DNA binding activity (Tishler *et al.*, 1993) and NF-κB signalling (Suzuki, Forman and Sevanian, 1996)(Lluis *et al.*, 2007), as well as positively regulating the activity of calcium channels voltage-dependent Ca^{2+} channels in the plasma membrane through oxidation of cysteine residues (Hudasek, Brown and Fearon, 2004).

3.1.2. Induction of mitochondrial ROS release in hypoxia

Studies from the Chandel group suggest that mitochondria act as cellular oxygen sensors and somewhat paradoxically, that oxidative stress can increase in cells in physiological (1.5% O_2) hypoxia (Chandel *et al.*, 1998). The study shows that hypoxia induces the production of ROS, which mediate the transcription of a number of hypoxic response genes in Hep3B cells such as EPO, VEGF and PGK1 (Chandel *et al.*, 1998). There have also been a number of *in vivo* studies that confirm hypoxia induces the release of ROS. Independent studies show mice exposed to chronic intermittent hypoxia have enhanced ROS levels in the cerebral cortex as measured by analysis of thiobarbituric acid reactive substances (Peng *et al.*, 2006) and DCF staining of cortical neuronal cells (Xu *et al.*, 2004).

The mechanism by which hypoxia causes the release of reactive oxygen species from the mitochondrion is unclear. In studies in isolated mitochondria, ROS production decreased as oxygen concentration was lowered to anoxia (Hoffman, Salter and Brookes, 2007), indicating that a decrease in oxygen itself does not cause the increase in superoxide directly by altering stability of the ubisemiquinone radical at complex III. It suggests that secondary effects must modulate mROS production. One possible model is that changes in the concentration of oxygen availability and NO abundance can modify the redox state of cytochrome *c* oxidase to favour the release of mROS (Palacios-Callender *et al.*, 2004). Hypoxic release of mROS has been implicated in the regulation of a host of cellular processes, including myocyte contraction (Duranteau *et al.*, 1998), p38 MAP kinase activation (Kulisz *et al.*, 2002), endocytosis of Na, K-ATPase by alveolar epithelial cells (Dada *et al.*, 2003) and adipocyte differentiation (Carrière *et al.*, 2004). The modulation of immune response has also been linked to hypoxic mROS release, including leukocyte adherence (Wood *et al.*, 2000) and the release of IL-6 by endothelial cells in hypoxia

(Pearlstein *et al.*, 2002).

3.1.3. Regulation of HIF-1α stability by mitochondrial ROS

Further studies from the Chandel group identify HIF-1α as a major mediator of ROS-dependent signalling pathways in hypoxia. Addition of exogenous H_2O_2 is sufficient to stabilise HIF-1α in normoxia, and the overexpression of catalase abolishes hypoxic response-element luciferase expression in hypoxic cells (Chandel *et al.*, 2000). Contemporaneous studies supported the involvement of the electron transport chain in HIF-1α stabilisation using *in vivo* experiments where the precursor to the potent complex I inhibitor MPP^+, MPTP, was administered to mice and HIF-1α levels measured in the mouse striatum and cortex. Addition of MPTP is sufficient to block HIF-1α accumulation in the mouse striatum, as well as HIF-1α stabilisation in neuronal CATH.a and PC12 cells exposed to hypoxia *in vitro* (Agani *et al.*, 2000).

The role of mROS in regulating HIF-1α was controversial for some time, following conflicting studies which suggest loss of a mitochondrial respiratory chain in p0 cell lines derived from a number of different tissues does not influence HIF-1α stability (Vaux *et al.*, 2001)(Srinivas *et al.*, 2001). However, more recent studies confirmed these findings using more advanced genetic and biochemical techniques. A study in 143B cells used a FRET-based sensor sensitive to redox conditions (Guzy *et al.*, 2005). Cells transfected with a plasmid expressing a redox-sensitive HSP-FRET probe and exposed to transient hypoxia (1% pO_2) have a profound increase in oxidative stress on exposure to hypoxia, which is attenuated in p0 cells lacking mitochondrial DNA and a functional respiratory chain. Subsequent studies have confirmed an induction of ROS release in hepatocellular carcinoma HepG2 cells, neuroblastoma SH-SY5Y, cells and adenocarcinoma DLD-1 cells through the use of the ROS-sensitive fluorescent probe DCF (Lluis *et al.*, 2007)..

Complex III has been identified as the site of mROS release in hypoxia. Addition of the complex III inhibitor stigmatellin blocks the release of mROS in hypoxia (Guzy *et al.*, 2005). Furthermore, cells containing a cytochrome b-deficient bc1 complex are unable to undergo oxidative respiration, but can generate mitochondrial ROS and stabilise HIF-1α. Pharmacological inhibition of the Q_0, but not Q_i site, attenuates

HIF-1α stability in hypoxia, indicating the Q_0 site of complex III specifically is the main source of hypoxia-induced mROS (Bell *et al.*, 2007). Complex III inhibition also reduces HIF-1α stabilisation, showing activity at complex III augments HIF-1α stability in hypoxia (Brunelle *et al.*, 2005)(Mansfield *et al.*, 2005). RNA interference against complex III, and cells transfected with SOD1 and SOD2-expressing adenoviruses have suppressed HIF-1α stabilisation in hypoxic conditions (Brunelle *et al.*, 2005). Moreover, loss of cytochrome c, which oxidises cytochrome c1 and keeps the Rieske iron sulphur protein subunit of complex III oxidised and capable of producing ROS, decreases ROS production and prevents stabilisation of HIF-1α in hypoxia (Mansfield *et al.*, 2005). Interestingly, anoxia (0% O_2) was sufficient to stabilize HIF-1α in cytochrome c-deficient cells, which emphasises the sensitivity of this response on the degree of hypoxia experienced by the cell.

These studies suggest a subtler model of HIF-1α stabilisation where mROS can augment HIF-1α stabilisation in hypoxia and modulate the hypoxic response in a mechanism complementary to oxygen availability for the hydroxylation of HIF-1α by PHD enzymes and FIH.

A number of studies have highlighted the paradoxical nature of mitochondrial reactive oxygen species, and shown that the degree of oxidant production can produce a spectrum of effects, with low levels of ROS capable of stabilising pro-survival proteins, but higher levels of ROS in cells depleted of mitochondrial antioxidant mGSH inducing sensitivity of cells to hypoxia (Lluis *et al.*, 2007)(Figure 3.1.3-1).

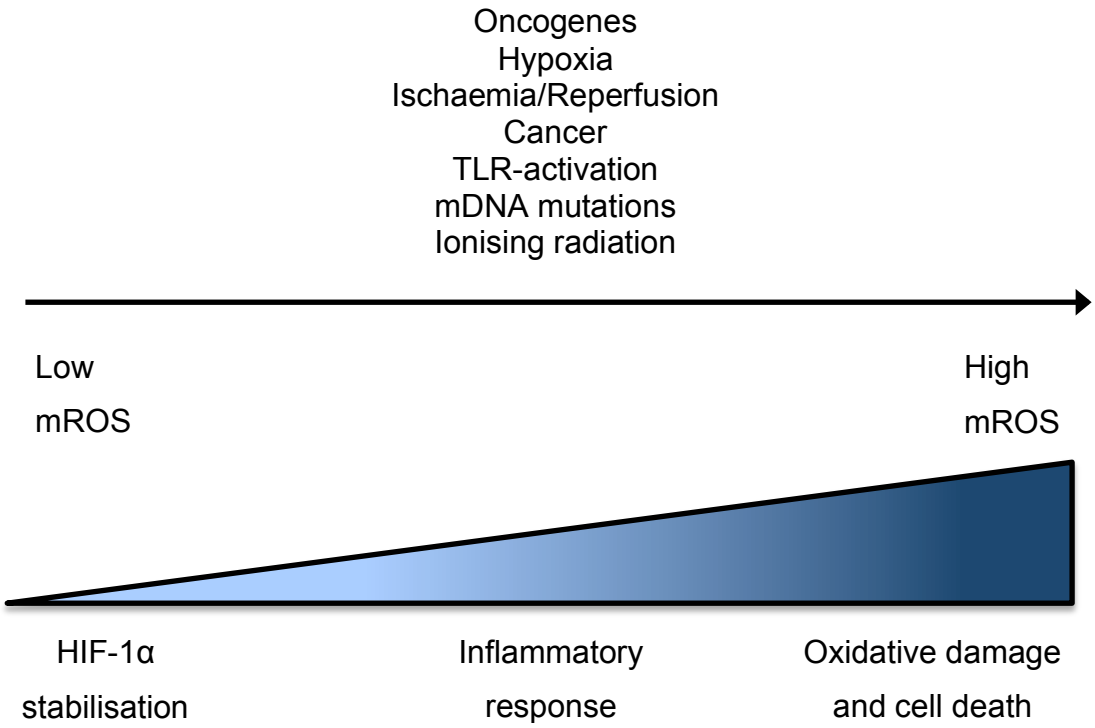

Figure 3.1.3-1: Balance of mitochondrial reactive oxygen species in the cell. Cells produce a low degree of mitochondrial ROS as part of normal electron chain function which are involved in signalling. Higher amounts of ROS, induced by cellular stress, can induce oxidative damage and cell death.

The mechanisms by which ROS stabilise HIF-1α are controversial. Early studies from Bell implicate the oxidation state of cytoplasmic iron as a modulator of HIF-1α through altering substrate availability for the PHD enzymes (Bell *et al.*, 2007). They suggest that cytosolic H_2O_2 may oxidise Fe^{2+} to Fe^{3+}, depleting the amount of available Fe^{2+} that PHDs can then use as a cofactor to hydroxylate and break down HIF-1α. This mechanism of PHD stabilisation was also seen in other studies in cells lacking the antioxidant *junD-/-* which have enhanced H_2O_2 production (Gerald *et al.*, 2004). Other studies have described the inhibition of PHD function on addition of *S*-nitroglutathione, a source of bioavailable NO, indicating NO may have a direct influence on inhibiting the PHD enzymes (Metzen *et al.*, 2003). Subsequent studies have implicated FIH as the main redox-sensitive regulator of HIF-1α activity (Masson *et al.*, 2012)., and an alternative model of HIF-1α stabilisation by ROS is proposed by Du *et al* where ROS mediates HIF-1α expression through Rac1 and activation of the PI3-ERM pathway (Du *et al.*, 2011). Secondary signalling via calcium release has also been implicated, as hypoxia and mROS can both stimulate calcium release, and HIF stabilisation is regulated by calcium signalling (Hui *et al.*, 2006).

It is unclear why HIF-1α stabilisation is specifically due to mitochondrial ROS as opposed to cytoplasmic ROS. Localisation of HIF-1α to the mitochondrial may explain why HIF-1α is more sensitive to mitochondrial ROS than other cellular sources of ROS. There have been studies suggesting HIF-1α localises to the mitochondria and therefore mitochondrial ROS may act as an extra signal to encourage stabilisation after translocation of the stable protein (Briston, Yang and Ashcroft, 2011). However, less than 5% of HIF-1α associates with the mitochondrial fraction of the cell, so alternative pathways may be intermediate between the release of ROS and their stabilisation of HIF-1α. Additional downstream targets of ROS which may regulate the hypoxic response pathway include NF-κB via the regulation sensitive activity of c-SRC (Bonello *et al.*, 2007)(Lluis *et al.*, 2007).

3.1.4. Innate immune cell regulation by mitochondria ROS

mROS have been implicated in the regulation of the innate immune system, specifically promoting pro-inflammatory activities.

Antibacterial responses are promoted by mROS through a number of different pathways, including through direct activation of NF-κB and MAPK signalling pathways, augmenting pro-inflammatory cytokine production. Endothelial cells can release IL-6 in response to hypoxia through mROS signalling to NF-κB (Pearlstein *et al.*, 2002). Recent studies have shown mROS can activate NLRP3 inflammasome activity and enhance the processing and activation of IL-1β and IL-18 precursors in bone-marrow derived macrophages (BMDMs) (Tschopp and Schroder, 2010)(Zhou *et al.*, 2011). Subsequent studies from Luke O'Neill's group have implicated mitochondrial membrane hyperpolarisation and subsequent increase in ROS production as essential mediators of pro-inflammatory activity of M1 macrophages (Tannahill *et al.*, 2013)(Mills *et al.*, 2016). Induction of mROS in pro-inflammatory macrophages is dependent on a more glycolytic phenotype, where mitochondrial metabolism is disrupted, whereas alternative polarisation of macrophages was characterised by a metabolic profile dependent on oxidative phosphorylation and normal Krebs cycle function.

Recent studies have also described how ionising radiation induces mROS, which is essential for induction of pro-inflammatory cytokines in BMDMs in the tumour microenvironment (Kim *et al.*, 2017). Blocking the production of mROS has been show to alleviate inflammatory symptoms through downregulating macrophage activation (Hall *et al.*, 2018).

Antiviral activities are also enhanced through mROS-mediated signalling through RIG-I-like receptor (RLR) mitochondrial antiviral signalling protein (MAVS) and downstream signalling to NF-κB and interferon regulatory factors IRF3 and IRF7(Tal *et al.*, 2009).

Neutrophil-derived mROS have been implicated in the control of pro-inflammatory neutrophil functions, such NADPH oxidase activation (Kröller-Schön *et al.*, 2014), degranulation (Vorobjeva *et al.*, 2017). A number of studies looking at the modulation of neutrophil function by neutrophil mitochondrial ROS have focused on metabolic diseases. Patients with diabetes and anorexia nervosa have defective neutrophil mitochondrial function as determined by reduced oxygen consumption and an increase in ROS formation and GSSG/GSH ratio (Hernandez-Mijares *et al.*,

2013)(Victor *et al.*, 2014). Therefore, close control of neutrophil mitochondrial function may be required for proper control of neutrophilic inflammation.

Recent studies have shown mitochondrial antioxidants are capable of treating inflammatory conditions. MitoQ has had some success in treating an experimental autoimmune encephalomyelitis (EAE) mouse model of multiple sclerosis. MS is typified by high numbers of activated microglia, causing unsheathing and demyelination in the cerebral cortex. Lipid and DNA oxidation correlates with inflammation in MS brain lesions, indicating mitochondrial ROS may play a role in MS pathology (Haider *et al.*, 2011). MitoQ reduced both neurological disability and physiological inflammatory effects of EAE such as inflammation of the spinal cord and TNF-α expression. MitoTEMPO has also been shown to reduce the severity of diabetic cardiomyopathy in mice (Ni *et al.*, 2016). MitoTEMPO has been shown as effective in reducing inflammation in models of periodontitis (Li *et al.*, 2016) and renal fibrosis (Liu *et al.*, 2018).

Conditions associated with hypoxia and mediated by release of reactive oxygen species, including ischaemia/reperfusion injury, have also been addressed using mitochondrial antioxidants. MitoQ has been showed to protect against mitochondrial DNA damage and subsequent loss of intestinal mucosa integrity in a mouse of ischaemia/reperfusion through suppression of mtDAMP release, partially through an Nrf2/ARE-dependent mechanism (Hu *et al.*, 2018).

MitoQ has been through a number of clinical trials in humans. Double-blind clinical studies of MitoQ as a potential therapy for Parkinson's disease have shown no benefit in slowing disease progression as measured by the Unified Parkinson's Disease Rating Scale (UPDRS). Moreover, doses of MitoQ up to 80mg were shown to induce nausea and vomiting in volunteers in a dose-dependent way (Snow *et al.*, 2010). Caution must be exercised, as off-target effects, including somewhat alarmingly acute swelling and depolarisation of mitochondria in cells in the kidney proximal tubule, have been described in recent studies (Gottwald *et al.*, 2018).

3.1.5. Measuring mitochondrial ROS

The induction of ROS in hypoxia is a controversial field due to conflicting reports in the literature and also because of the current limitations in studying mitochondrial ROS production. A review studying hypoxia-induced reactive oxygen species highlights that measurements of oxidative stress, especially *in vivo*, can be obfuscated by other factors such as oxygen consumption, acidity and shear stress, and that the degree of hypoxia may also not correlate linearly with reactive oxygen species release and redox stress (Clanton, 2007). Indeed, other studies have suggested that changes in the flux through the electron transport chain can change oxygen concentrations in the cytoplasm due to changes in the consumption of O_2 via oxidative phosphorylation, and this can have a knock-on effect on HIF stability, in this case HIF-2α in an adrenomedullary cell line (Brown and Nurse, 2008).

3.1.6. Regulation of ROS by anaerobic metabolism

Mitochondrial ROS production and function is closely linked with metabolism through a number of metabolic pathways, including the tricarboxylic acid cycle, the DHAP shuttle, and the action of antioxidant pathways including the pentose phosphate pathway (Liemburg-Apers *et al.*, 2015).

The primary link between energy metabolism and ROS is through the mitochondrial electron transport chain. Complexes I and III of the mitochondrial electron transport chain are major sources of mitochondrial reactive oxygen species (Figure 3.1.7-1), although complex II is also capable of producing mitochondrial ROS through the forward and reverse reactions from succinate and the QH_2 pool (Quinlan *et al.*, 2012) and modulation of complex II activity influences ROS release from other complexes (Dröse, Hanley and Brandt, 2009). Complex I and II both directly link the Krebs cycle to the mitochondrial respiratory chain. Complex I uses mitochondrial NADH as a substrate to transfer electrons to the Q pool. Complex II converts succinate to fumarate, transferring an electron to FAD in the SDHA subunit of complex II. Unsurprisingly, Krebs cycle activity is closely linked to mROS production. Increased TCA cycle flux can results in accumulation of oxidative phosphorylation substrates and elevated $NADH/NAD^+$ levels, which in turn can increased mROS production via complex I (Kussmaul and Hirst, 2006). Contrarily, addition of Krebs

cycle intermediates can reduce mitochondrial ROS production in cells (Sawa *et al.*, 2017). Similarly, a functional mitochondrial electron transport chain is needed for TCA cycle function (Martínez-reyes *et al.*, 2016). Krebs cycle activity can also influence HIF-1α activity in other ways; succinate can inhibit HIF-1α and *SDH* mutations are capable of stabilising HIF through the build-up of succinate (Selak *et al.*, 2005).

Increased glycolytic flux can also correlate with an increased flux into the mitochondrial respiratory chain via shuttling through glycerol 3-phosphate (Ishihara *et al.*, 1996). The glycerol 3-phosphate shuttle itself is an important site of ROS generation and is prone to electron leak (Mracek, Drahota and Hou, 2013). Therefore, glycolytic flux into the TCA cycle can influence mROS production. This mechanism has been observed in innate immune cells; in pro-inflammatory macrophages, glycolytic ATP production causes an increase in mitochondrial membrane potential, which in turn is needed for pro-inflammatory effects of LPS and also drives increased generation of mitochondrial ROS, driving the production of IL-1β (Mills *et al.*, 2016). Neutrophils can maintain mitochondrial membrane potential by oxidation of glycerol 3-phosphate (Figure 3.1.7-2), as isolated mitochondria from neutrophils treated with glycerol phosphate can recover a membrane potential as measured by TMRM, suggested that mGDP is present in neutrophil mitochondria and is functional (van Raam *et al.*, 2008). Inhibition of complex III correlates with increased lactate production, suggesting flux from glycolysis into the DHAP shuttle, and transfer of electrons to complex III from mGPDH, is occurring in the neutrophils in *in vitro* culture. However, whether this has functional consequences or is a physiologically relevant source of mROS in the neutrophil is unclear.

The pentose phosphate pathway can also modulate the activity of mROS through generation of antioxidants NADPH and GSH. Enhanced flux through the pentose phosphate pathway can protect against peroxide-induced cytotoxicity through an enhanced NADPH/$NADP^+$ ratio and regeneration of oxidised glutathione (GSSG) to reduced glutathione (GSH) (Le Goffe *et al.*, 2002). Skin fibroblasts with enhanced GLUT1 expression and glucose uptake have increased NADPH and GSH levels, and

preventing NADPH increase induced ROS production and subsequent cell death (Wu and Wei, 2012).

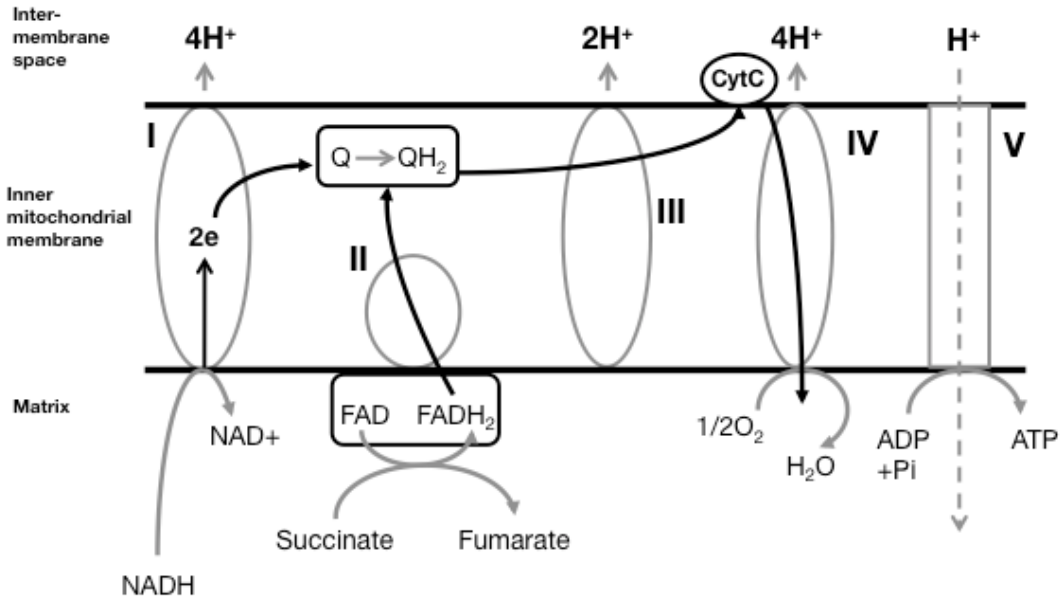

Figure 3.1.6-1: The electron transport chain. Electrons are passed from Krebs cycle products NADH (Complex I) or succinate (Complex II). Loss of electrons and formation of ROS can occur during normal function of electron transport complexes.

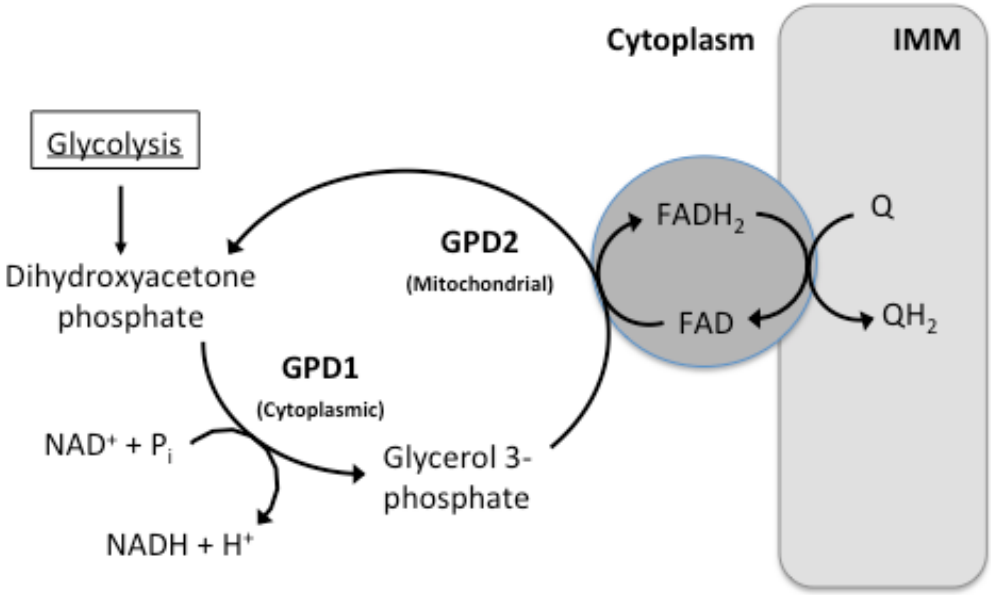

Figure 3.1.6-2: The DHAP shuttle. The DHAP shuttle acts as a way of transferring electrons into the electron transport chain directly from glycolysis. GPD2 is a significant source of mitochondrial ROS.

3.1.7. Aims of this chapter

Neutrophils are an interesting candidate for study of mitochondrial ROS signalling as they have a phenotype of delayed apoptosis in hypoxia, and the role of the neutrophil mitochondria is poorly understood, as neutrophils are predominantly glycolytic cells with little capacity for oxidative phosphorylation. As neutrophils do not use their mitochondria for ATP production, it is possible their mitochondria are used predominantly in a signalling role through release of reactive oxygen species. Given that HIF-1α profoundly regulates neutrophil apoptosis and function, it will be critical to understand whether there is an interaction between the neutrophil mitochondria and HIF-1α. In addition to understanding the basic biology of these non-proliferative cells, as neutrophils are implicated in a number of inflammatory diseases associated with localised and systemic hypoxia, understanding the regulation of the neutrophil hypoxic response pathway and ascertaining whether neutrophil mitochondria are capable of influencing neutrophil HIF-1α stability and survival may be essential in the study of potential treatments for chronic inflammatory diseases.

As stated in section 1.5., my hypothesis for this chapter is that:

> Neutrophils mitochondrial function regulates neutrophil apoptosis not through generation of ATP, but via signaling through the production of mitochondrial ROS, which can stabilize HIF-1α and enhance neutrophil survival.

The aims of this section are therefore as follows:

1. To understand if, despite being predominantly glycolytic cells, neutrophils maintain a mitochondrial membrane potential and release mitochondrial ROS uaing fluorescent probes which can measure mitochondrial function in live cells.
2. To examine how hypoxia affects neutrophil mitochondrial function; in particular, whether neutrophil mitochondria release ROS in response to hypoxia, and whether ROS modulate the stability of HIF-1α with downstream effects on survival and function.

3. To interrogate the mechanism of hypoxic mROS release using neutrophils as a model of cells with little mitochondrial ATP production, using mass spectrometry to measure metabolic flux.

3.2. Results

3.2.1. Confirmation of neutrophil hypoxic survival in *in vitro* culture conditions

As previously described, neutrophils experience delayed apoptosis *in vitro* when cultured in hypoxic conditions (Hannah *et al.*, 1995)(Sarah R Walmsley *et al.*, 2005). To confirm the effectiveness of our culture conditions, apoptosis of neutrophils isolated from healthy volunteers and cultured for 20 hours in normoxia (21% O_2) or hypoxia (1% O_2) was assessed through morphology and by staining with Annexin V and TO-PRO-3 and analysed by flow cytometry.

Culture in hypoxia significantly delays the constitutive apoptosis of neutrophils after 20 hours in culture as measured via morphology (mean (±SEM), N = 39.71 (10.45)%, H = 21.83 (16.13)%, n = 6, p*<0.05)(Figure 3.2.1-1, A-C) and Annexin V/TO-PRO-3 staining and analysis via flow cytometry (mean (±SEM), N = 47.1 (4.53)%, H = 29.5 (4.70)%, n = 6, p*<0.05)(Figure 3.2.1-2, A-C).

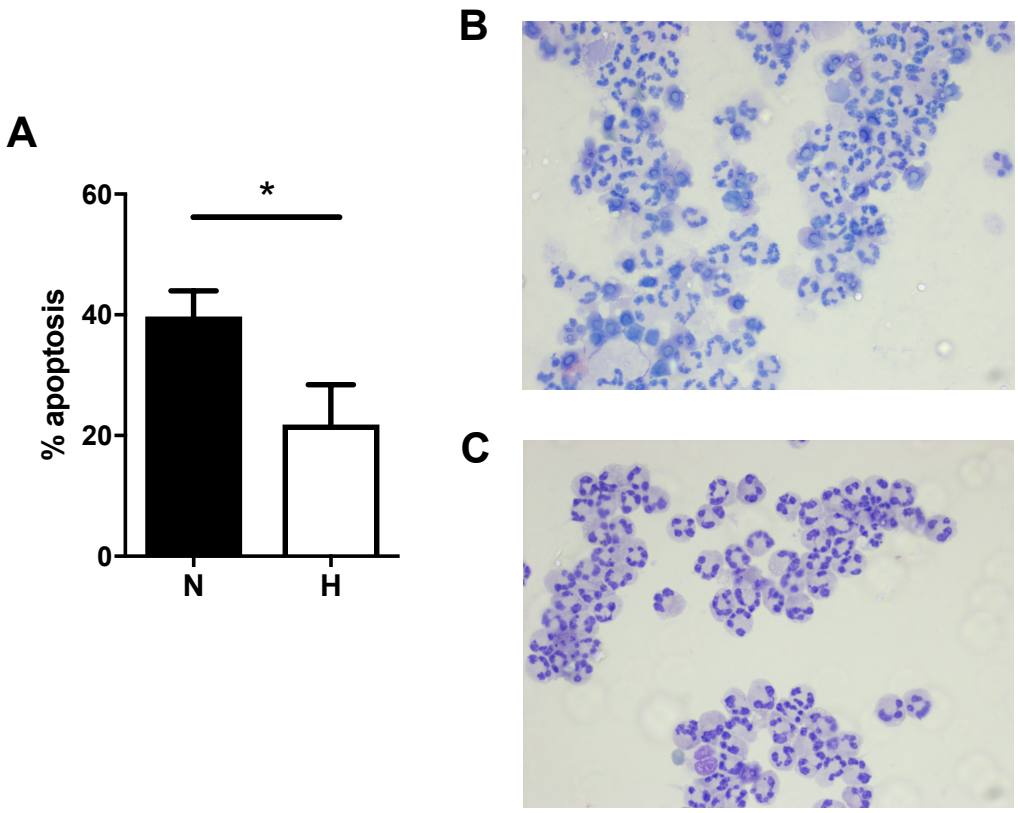

Figure 3.2.1-1: Hypoxia prolongs neutrophil survival as determined through morphological analysis of nuclear condensation and fragmentation *in vitro*. Neutrophils isolated from peripheral blood were cultured for 20 hours in normoxia (21% O_2) or hypoxia (1% O_2) and apoptosis assessed via morphology (A-C). B: Normoxic cells. C: Hypoxic cells. Data expressed as mean±SEM and analysed with paired two-tailed Student's T tests, n = 6, *$p<0.05$.

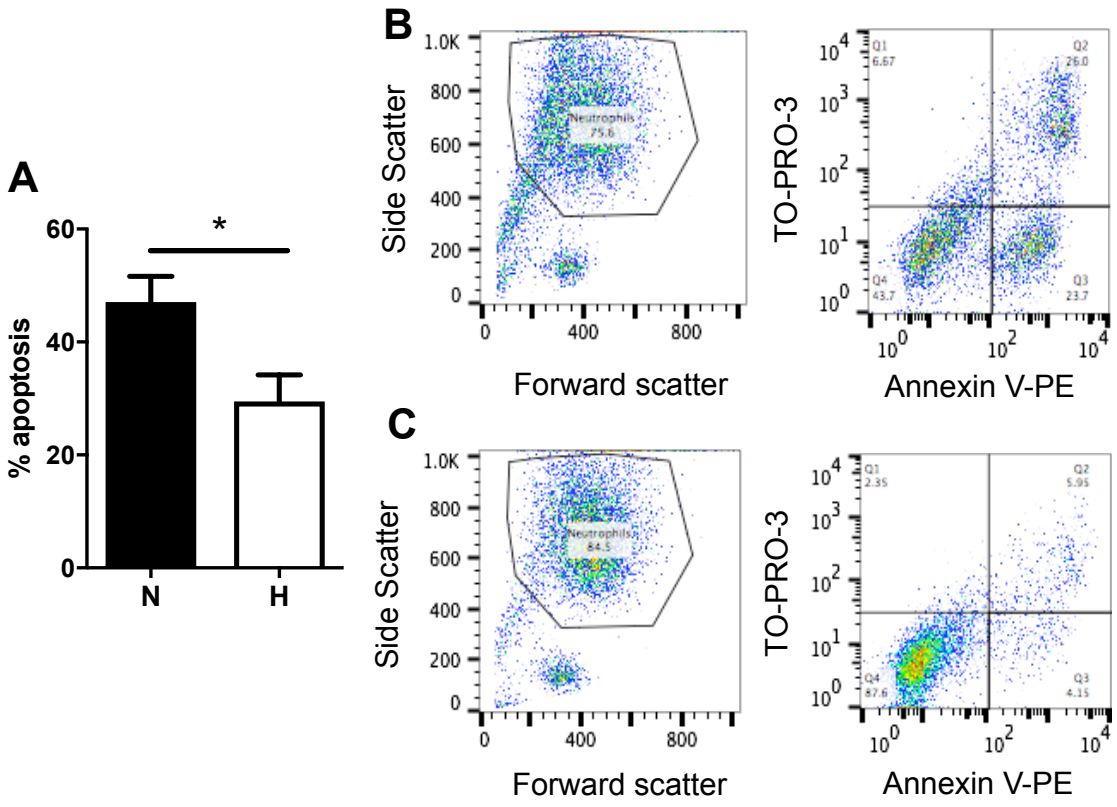

Figure 3.2.1-2: Hypoxia prolongs neutrophil survival as determined through Annexin V/TO-PRO-3 staining and analysis via flow cytometry. Neutrophils isolated from peripheral blood were cultured for 20 hours in normoxia (21% O_2) or hypoxia (1% O_2) and apoptosis assessed via Annexin V/TO-PRO-3 staining and flow cytometry (A-C). B: Normoxic cells. C: Hypoxic cells. Apoptosis was determined as % Annexin V +ve cells. Data expressed as mean±SEM and analysed with paired two-tailed Student's T tests, n = 6, *$p<0.05$.

3.2.2. Acute hypoxia stimulates production of neutrophil mitochondrial reactive oxygen species

To determine whether hypoxia induces release of mROS as it does in other cell types, neutrophil mROS production was measured using the mitochondria-targeted redox probe MitoSOX™ Red and fluorescence intensity measured via flow cytometry.

By 1 hour in hypoxic culture, neutrophils have significantly enhanced production of mROS as measured via MitoSOX™ Red staining (mean (±SEM), normoxia (black bar) 1 hour = 78.9 (10.2), hypoxia (white bar) 1 hour = 131 (41.0) gMFI, n = 7, p*<0.05)(Figure 3.2.2-1, A). Cells cultured for 4 hours in hypoxia still have elevated mROS production (normoxia (black bar) 4 hours = 71.8 (10.2), hypoxia (white bar) 4 hours = 145 (59.5) gMFI, p*<0.05, n = 7)(Figure 3.2.2-1, A). Mitochondrial ROS levels are at baseline levels in normoxic culture equivalent to freshly isolated neutrophils (mean (±SEM), 0 hours = 66.6 (17.0), normoxia (black bar) 1 hour = 78.9 (9.15), normoxia (black bar) 4 hours = 71.8 (10.2) gMFI, n = 7)(Figure 3.2.2-1, A). This indicates exposure to high glucose culture media does not induce production of mitochondrial ROS.

Treatment with the potent activation stimulus 100nM fMLP does not alter neutrophil mROS levels (mean (±SEM), normoxia (black bar) untreated 1 hour = 78.9 (9.15), normoxia (black bar) treated 1 hour = 81.7 (12.4), hypoxia (white bar) untreated 1 hour = 167 (41.0), hypoxia (white bar) treated 1 hour = 188 (50.9) gMFI)(Figure 3.2.2-1, B). However, fMLP does significantly induce the production of overall cellular ROS as measured by DCF fluorescence, enhancing the production of ROS by over a factor of 3 (mean (±SEM), untreated = $1.36x10^4$ ($1.52x10^3$), treated = $4.18x10^4$ ($5.8x10^3$) gMFI, n = 8. p***<0.001)(Figure 3.2.2-1, C). These data indicate the MitoSOX™ Red probe is specific for mitochondria-derived ROS and not sensitive to cytoplasmic or lysosomal ROS produced by NADPH oxidase, and the increase in MitoSOX™ Red fluorescence in hypoxia is induced by the induction of mROS specifically.

Treatment with the complex I inhibitor rotenone and the complex V/ATP synthase inhibitor oligomycin both induce the production of mROS (mean (±SEM), normoxia

(black bar) untreated = 74.7 (5.18), normoxia (black bar) rotenone = 97.3 (1.00), normoxia (black bar) oligomycin = 110 (19.0), hypoxia (white bar) untreated = 143 (23.4), hypoxia (white bar) rotenone = 178 (26.9), hypoxia (white bar) oligomycin = 215 (29.4) gMFI, n = 5, *$p<0.05$, **$p<0.01$)(Figure 3.2.2-1, D, E), indicating neutrophils possess a functional respiratory chain which can be blocked by mitochondrial inhibitors. However, inhibition in hypoxia does not produce a greater degree of mROS release in hypoxia, indicating flux through the electron transport chain is equivalent in normoxia and hypoxia (mean (±SEM), normoxia rotenone = 1.30 (0.134), hypoxia rotenone = 1.24 (0.188), normoxia oligomycin = 1.48 (0.254), hypoxia oligomycin = 1.5 (0.206), n = 5)(Figure 3.2.2-1, F). The data therefore show neutrophils have some respiratory chain activity and hypoxia, but not exposure to high glucose culture medium or activation via the fMLP receptor, is a potent stimulus for release of reactive oxygen species from the mitochondrial electron transport chain.

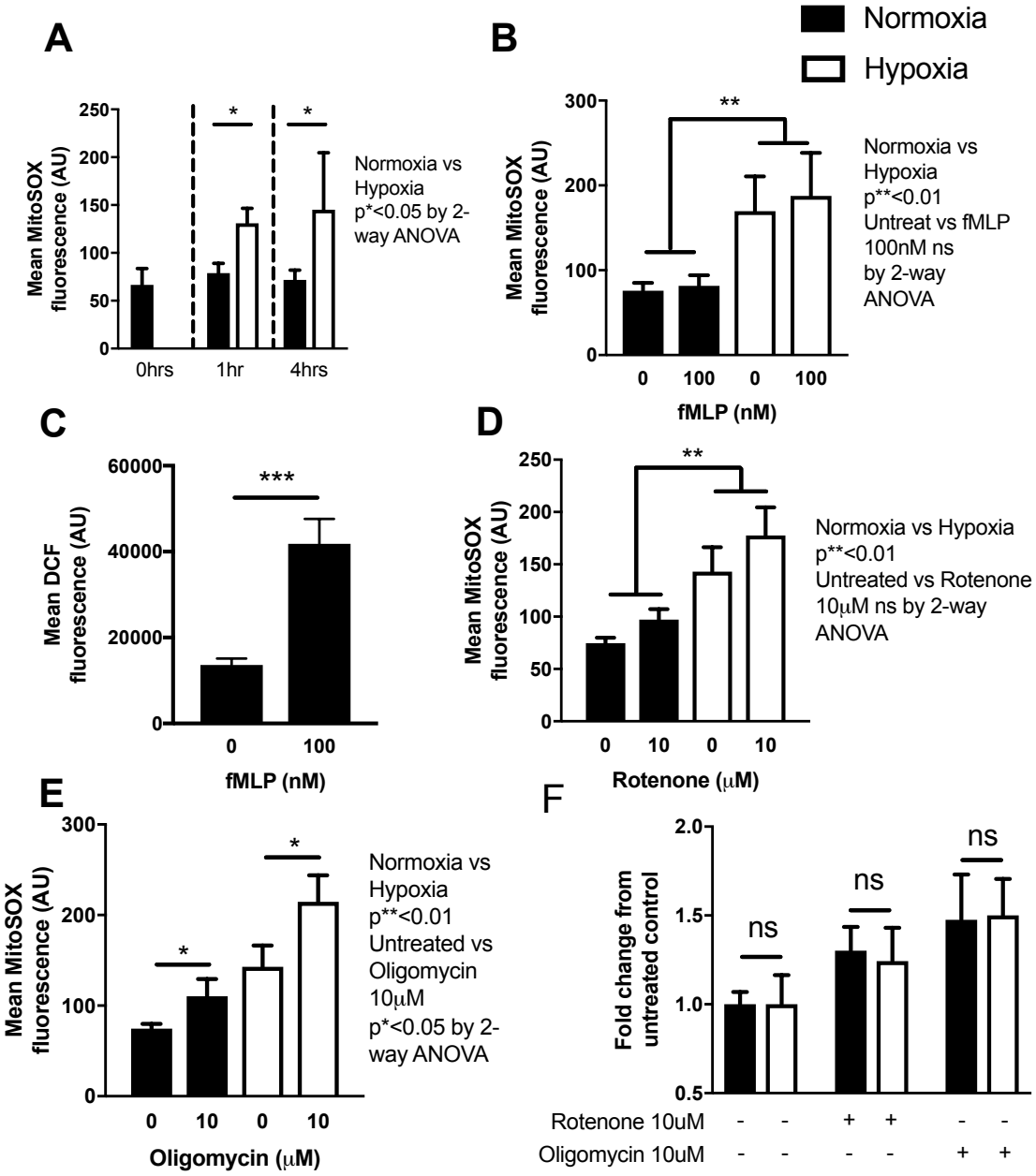

Figure 3.2.2-1: Hypoxia, but not neutrophil activation, induces production of mitochondrial ROS. Freshly isolated neutrophils or neutrophils cultured for 1 or 4 hours in normoxia or hypoxia were stained with the mitochondria-targeted redox probe MitoSOX™ Red to assess production of mitochondrial reactive oxygen species (A, B). Neutrophils were cultured with and without 100nM fMLP for 1 hour and stained with MitoSOX™ Red (B) or stained with DCF (C). Neutrophils were cultured for 1 hour with and without 10μM rotenone or 10μM oligomycin (D,E). fMLP = formyl Met-Leu-Phe peptide. DCF = dichlorofluorescein.. Data expressed as mean±SEM and analysed with paired two-tailed student's T tests (C, F) corrected for multiple comparisons with the Holm-Sidak method (F) or by 2-way ANOVA (A, B, D, E), n = 7 (A, B), n = 8 (C), n = 5 (D-E), *p<0.05.

3.2.3. Mitochondria-targeted antioxidants are pro-apoptotic to neutrophils and inhibit HIF-1α stabilisation

To determine the effects of mitochondrial ROS on neutrophil apoptosis, neutrophils were treated with 100μM MitoTEMPO, a mitochondria-targeted analogue of the antioxidant TEMPO (Figure 3.2.3-1, A). Mitochondrial ROS production measured via MitoSOX™ Red staining was significantly suppressed in neutrophils cultured for 1 hour in hypoxia (mean (±SEM), hypoxia untreated = 125 (10.2), hypoxia (white bar) MitoTEMPO = 105 (10.9) gMFI, n = 7, p*<0.05)(Figure 3.2.3-1, B). MitoTEMPO significantly increased the rate of apoptosis of neutrophils cultured for 20 hours as measured by morphology (mean (±SEM), normoxia (black bar) untreated = 45.3 (4.45), normoxia (black bar) MitoTEMPO = 56.9 (6.21), hypoxia (white bar) untreated = 27.1 (5.07), hypoxia (white bar) MitoTEMPO = 39.5 (7.38)%, n = 8, p*<0.05,)(Figure 3.2.3-1, C) and also increased apoptosis as measured by Annexin V/TO-PRO-3 staining and flow cytometry, although is result was not significant (mean (±SEM), normoxia (black bar) untreated = 53.4 (4.94), normoxia (black bar) MitoTEMPO = 58.7 (5.06), hypoxia (white bar) untreated = 36.4 (3.56), hypoxia (white bar) MitoTEMPO = 42.0 (4.62)%, n = 7, ns by 2-way ANOVA)(Figure 3.2.3-1, D).

To assess the effect of MitoTEMPO on HIF-1α stabilisation, neutrophils were cultured with MitoTEMPO for 4 hours and HIF-1α stability assessed by western blot and densitometry performed. MitoTEMPO modestly but significantly inhibited stabilisation of HIF-1α protein after co-incubation for 4 hours (mean (±SEM), normoxia (black bar) untreated = 0.145 (0.0593), normoxia (black bar) MitoTEMPO = 0.181 (0.0956), hypoxia (white bar) untreated = 3.08 (0.515), hypoxia (white bar) MitoTEMPO = 2.47 (0.161), n = 3, p**<0.01)(Figure 3.2.3-2, C). Neutrophils treated with the non-mitochondria targeted analogue TEMPOL for 4 hours have equivalent HIF-1α stabilisation in hypoxic conditions, indicating mitochondrial ROS specifically augment HIF-1α stabilisation in hypoxia (Figure 3.2.3-2, D).

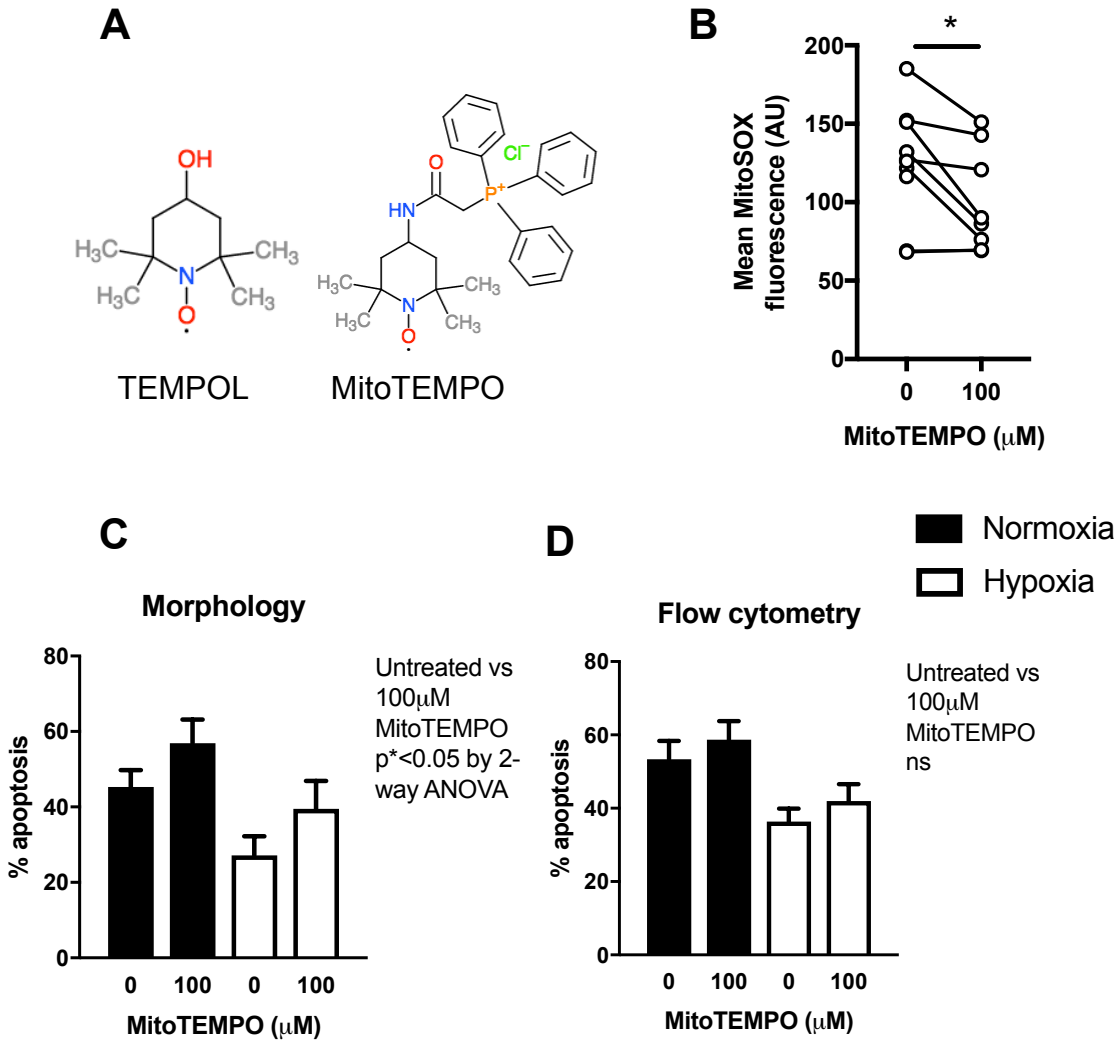

Figure 3.2.3-1: Addition of the mitochondria-targeted anti-oxidant MitoTEMPO blocks production of mitochondrial ROS and is pro-apoptotic. Neutrophils were cultured for 1 hour with and without 100μM MitoTEMPO (A) and stained with MitoSOX Red (B), or cultured for 20 hours and apoptosis measured via morphology (C) and Annexin V/TO-PRO-3 staining and flow cytometry (D). Data expressed as mean±SEM and analysed with paired two-tailed Student's T tests (B) and 2-way ANOVA (C, D), n = 7 p*<0.05.

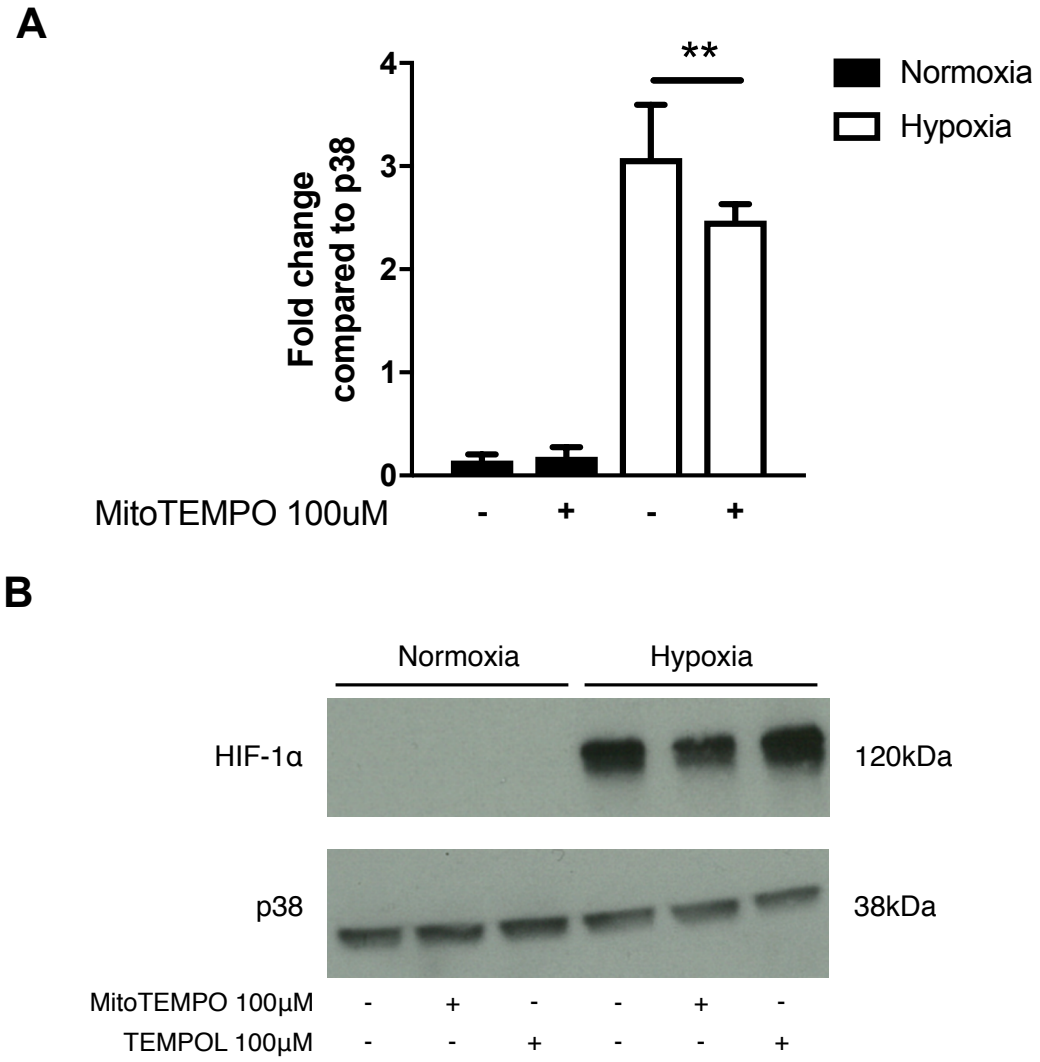

Figure 3.2.3-2: Addition of the mitochondria-targeted antioxidant MitoTEMPO inhibits HIF-1α stability in hypoxia. Neutrophils were cultured for 4 hours with and without 100μM MitoTEMPO, lysed in SDS lysis buffer and then lysates probed for HIF-1α expression via western blot (A,B). Data expressed as mean±SEM and analysed with paired two-tailed Student's T tests, n = 3, p**<0.01. Whole blot is shown in Appendix 7.7.

3.2.4. Acute hypoxia enhances neutrophil mitochondrial membrane potential through mechanism independent of enhanced Krebs cycle flux

To ascertain the mechanism of mitochondrial ROS release, we measured mitochondrial membrane potential ($\Delta\Psi m$) in cultured neutrophils. Mitochondrial membrane potential is closely linked to ROS production and is an indication of electron transport chain activity.

Neutrophils have significantly increased mitochondrial membrane potential when cultured in hypoxic conditions compared to normoxia (mean (±SEM), 0 hours = 214 (78.7), normoxia (black bar) 1 hour = 263 (33.1), hypoxia (white bar) 1 hour = 456 (89.9), normoxia (black bar) 4 hours = 327 (58.6), hypoxia (white bar) 4 hours = 569 (71.8) gMFI, n = 6, $p^*<0.05$)(Figure 3.2.4-1, A). Maintenance of mitochondrial membrane potential, however, is not required for survival, as collapse of mitochondrial membrane potential does not induce apoptosis. The protonophore CCCP significantly reduces mitochondrial membrane potential (mean (±SEM), normoxia (black bar) untreated = 263 (33.1), normoxia (black bar) treated = 227 (26.5), hypoxia (white bar) untreated = 456 (89.9), hypoxia (white bar) treated = 247 (32.9) gMFI, n = 6, $p^*<0.05$)(Figure 3.2.4-1, B) but does not affect neutrophil apoptosis (mean (±SEM), normoxia (black bar) untreated = 63.4 (4.41), normoxia (black bar) treated = 63.5 (4.50), hypoxia (white bar) untreated = 43.0 (5.01), hypoxia (white bar) treated = 39.1 (5.59) gMFI, n = 3, $p^*<0.05$)(Figure 3.2.4-1, C).

Neutrophil mitochondrial membrane potential increase in hypoxia is not dependent on an increase in Krebs cycle flux. Neutrophils have equivalent levels of Krebs cycle intermediates in normoxia and hypoxia as measured via Liquid Chromatography/Mass Spectrometry (LC-MS)(mean (±SEM), citrate normoxia = $5.39x10^8$ ($3.68x10^7$), citrate hypoxia = $5.82x10^8$ ($6.01x10^7$), αKG normoxia = $7.13x10^6$ ($1.75x10^6$), αKG hypoxia = $8.21x10^6$ ($8.73x10^5$), succinate normoxia = $1.51x10^7$ ($2.92x10^6$), succinate hypoxia = $1.78x10^7$ ($4.63x10^6$), fumarate normoxia = $2.91x10^6$ ($4.87x10^5$), fumarate hypoxia = $4.04x10^6$ ($1.63x10^6$), malate normoxia = $1.13x10^8$ ($1.56x10^7$), malate hypoxia = $1.53x10^8$ ($2.43x10^7$), oxaloacetate normoxia = $2.38x10^7$ ($4.71x10^6$), oxaloacetate hypoxia = $2.09x10^7$ ($4.86x10^6$), n = 4)(Figure

3.2.4-2, A). Neutrophil mitochondrial membrane potential increase in hypoxia is also not dependent on greater availability of NADH. Neutrophils have equivalent levels of total NAD^+/NADH in normoxia and hypoxia (mean (±SEM), normoxia = $1.58x10^8$ ($2.39x10^7$), hypoxia = $1.78x10^8$ ($3.54x10^7$), n = 4)(Figure 3.2.4-2,B) and have an equivalent NAD^+/NADH ratio (mean (±SEM), normoxia = 14.2 (2.20), hypoxia = 11.6 (1.38), n = 4)(Figure 3.2.4-2, C).

Addition of Krebs cycle intermediates can supplement the mitochondrial pool of substrate for the mitochondrial electron transport chain and has been shown to enhance mitochondrial activity (Hinke *et al.*, 2007). Addition of the complex I substrate malate and the membrane-permeable complex II substrate methyl succinate (MSucc) does not affect mitochondrial membrane potential, indicating minimal activity of complex I and II (mean (±SEM), normoxia untreated = 123 (37.6), normoxia CCCP = 49.2 (10.7), normoxia malate = 107 (28.8), normoxia MSucc = 118 (35.4), normoxia malate + MSucc = 106 (34.4), normoxia malate + MSucc + CCCP = 45.5 (9.45), hypoxia untreated = 217 (38.3), hypoxia CCCP = 60.2 (10.2), hypoxia malate = 186 (35.2), hypoxia MSucc = 202 (37.5), hypoxia malate + MSucc = 169 (40.0), hypoxia malate + MSucc + CCCP = 51.0 (6.35) gMFI, n = 4, $p^*<0.05$)(Figure 3.2.4-3, A).

These data show neutrophil mitochondrial electron chain activity is enhanced in hypoxia via a mechanism independent of mitochondrial glucose oxidation and oxidation of Krebs cycle substrates.

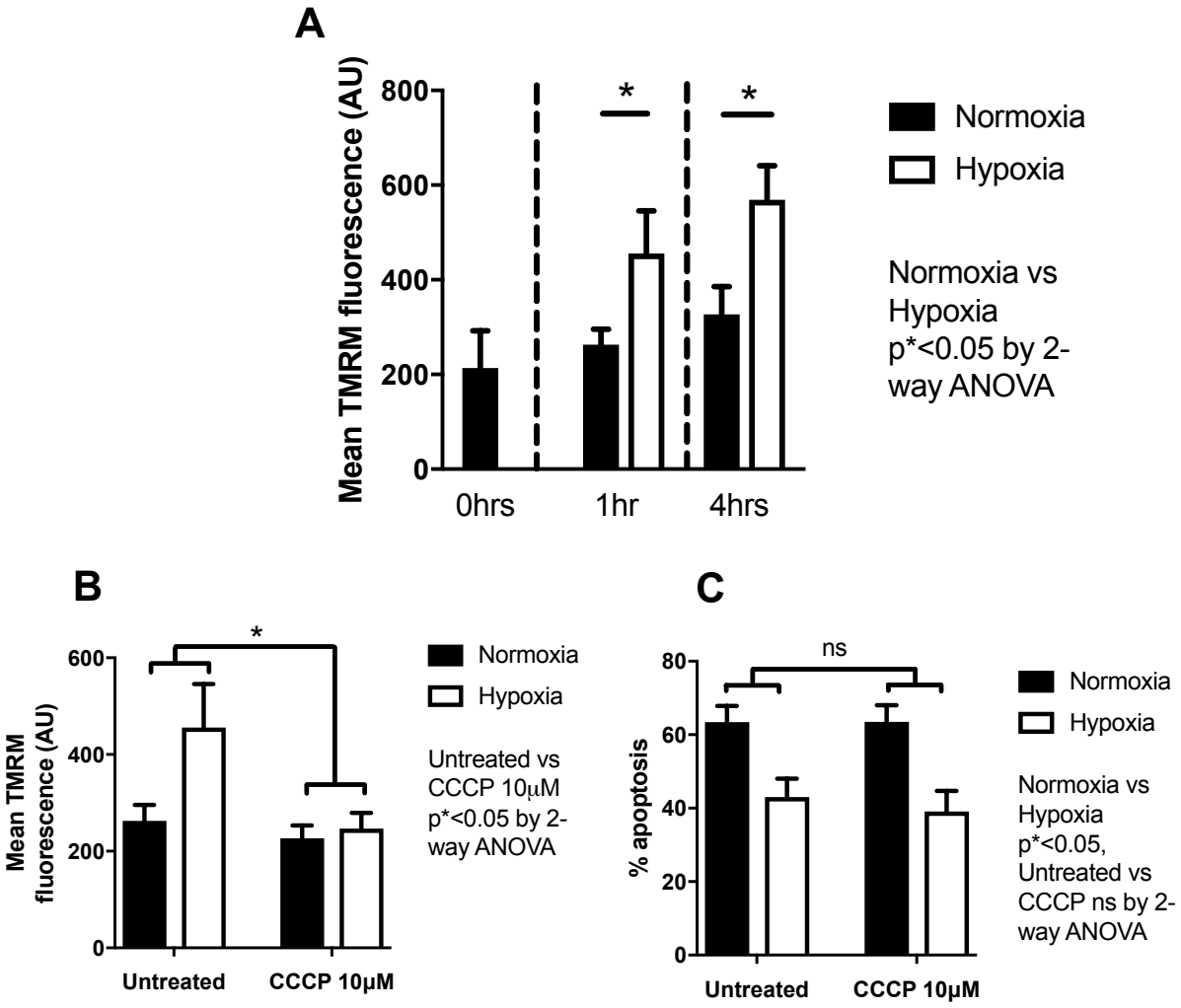

Figure 3.2.4-1: Neutrophils maintain a mitochondrial membrane potential that is enhanced in hypoxic conditions. Neutrophils were cultured for 1 and 4 hours in normoxia and hypoxia (A,B,) or 20 hours (C) with and without 10μM CCCP (B, C) and mitochondrial membrane potential determined via staining with TMRM dye (A,B) or apoptosis determined by staining with Annexin V and TO-PRO-3 (C) and analysis via flow cytometry. Apoptosis was determined as % Annexin V +ve cells. Data expressed as mean±SEM and analysed with 2-way ANOVA with Sidak's post hoc multiple corrections test (A-C), n = 6, *p<0.05.

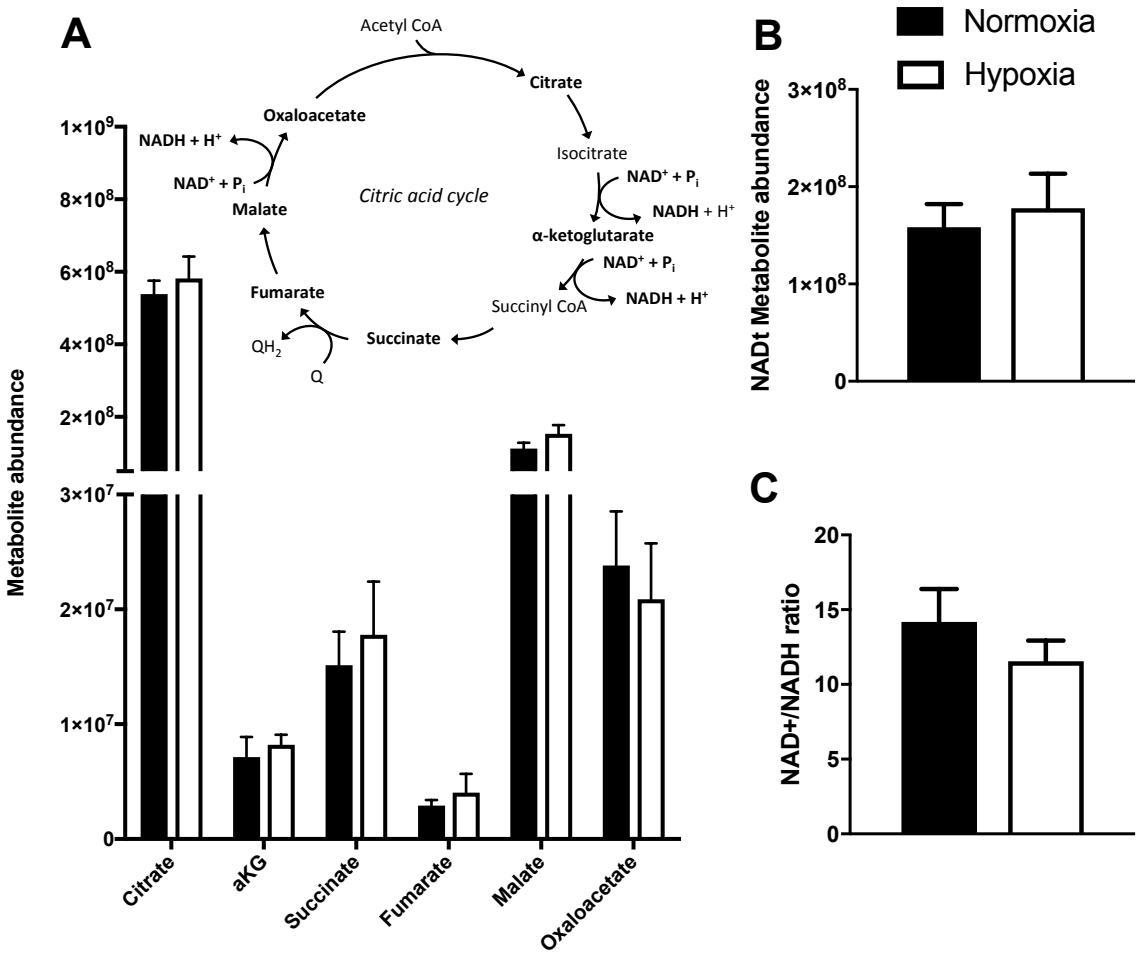

Figure 3.2.4-2: Neutrophils cultured in hypoxia have no change in Krebs cycle flux or NADH availability. Neutrophils were cultured for 4 hours in normoxia and hypoxia and lysed in methanol before LC-MS analysis. Relative abundance of tricarboxylic acid cycle intermediates (A) and total NADH and NAD^+ (B) in neutrophils cultured in normoxia and hypoxia C: NAD^+/NADH ratios of neutrophils cultured for 4 hours in normoxia and hypoxia. Data expressed as mean±SEM and analysed via two-way ANOVA (A) or Students two-tailed T tests (B,C), n = 4, ns).

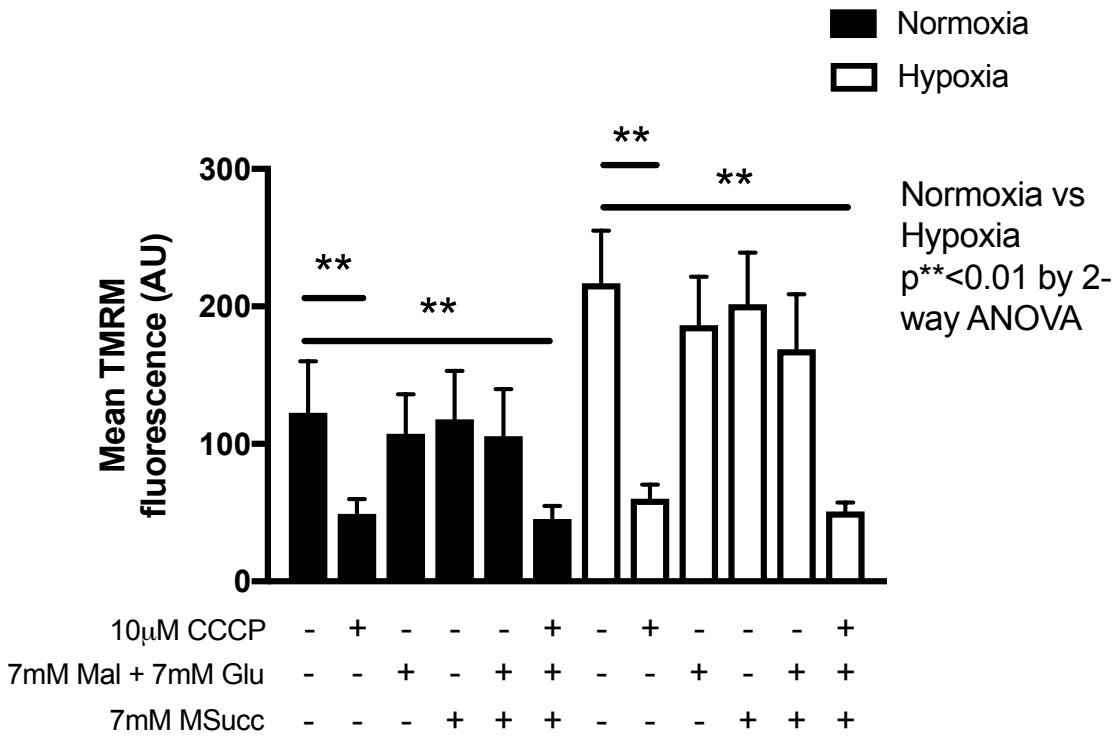

Figure 3.2.4-3: Addition of cell permeable Krebs cycle intermediates has no effect on mitochondrial membrane polarisation. Neutrophils were cultured for 1 hour in normoxia and with and without the krebs cycle intermediates malate, glutamate and methyl succinate, then stained with TMRM and analysed via flow cytometry. Data expressed as mean±SEM and analysed with 2-way ANOVA with Sidak's post hoc multiple corrections test , n = 4, p*<0.05).

3.2.5. Neutrophils cultured in hypoxia have reduced cellular ROS but equivalent capacity to mount a respiratory burst

To study whether this uplift in cellular ROS was specific to the mitochondria, we studied overall cell oxidant production in neutrophils using the cellular ROS probe dichlorofluorescein (DCF).

Neutrophils cultured in hypoxia have reduced baseline cellular ROS (mean (±SEM), normoxia = $1.36x10^4$ ($1.52x10^3$), hypoxia = $9.84x10^3$ ($1.27x10^3$) gMFI, n = 8, p**<0.01)(Figure 3.2.5-1, A). The majority of the ROS produced in stimulated neutrophils is mediated through the pentose phosphate pathway as determined through treatment with the OxPPP inhibitor 6AN. 6AN blocks cellular ROS production in fMLP-treated cells (Mean (±SEM), normoxia (black bar) untreated = $4.18x10^4$ ($5.80x10^3$), normoxia (black bar) 6AN = $2.85.10^4$ ($5.22x10^3$), hypoxia (white bar) untreated = $3.00x10^4$ ($7.02x10^3$), hypoxia (white bar) 6AN = $2.41x10^4$ ($3.35x10^3$) gMFI, n = 8, p=0.09)(Figure 3.2.5-1, B).

Hypoxia does not alter the capacity for neutrophils to mount a respiratory burst as measured by fold increase in DCF fluorescence following stimulation with fMLP (mean (±SEM), normoxia (black bar) untreated = 3.11 (0.377), normoxia (black bar) 6AN = 1.92 (0.148), hypoxia (white bar) untreated = 2.95 (0.418), hypoxia (white bar) 6AN = 2.32 (0.258) fold change from untreated control, n=8, p**<0.01)(Figure 3.2.5-1, C).

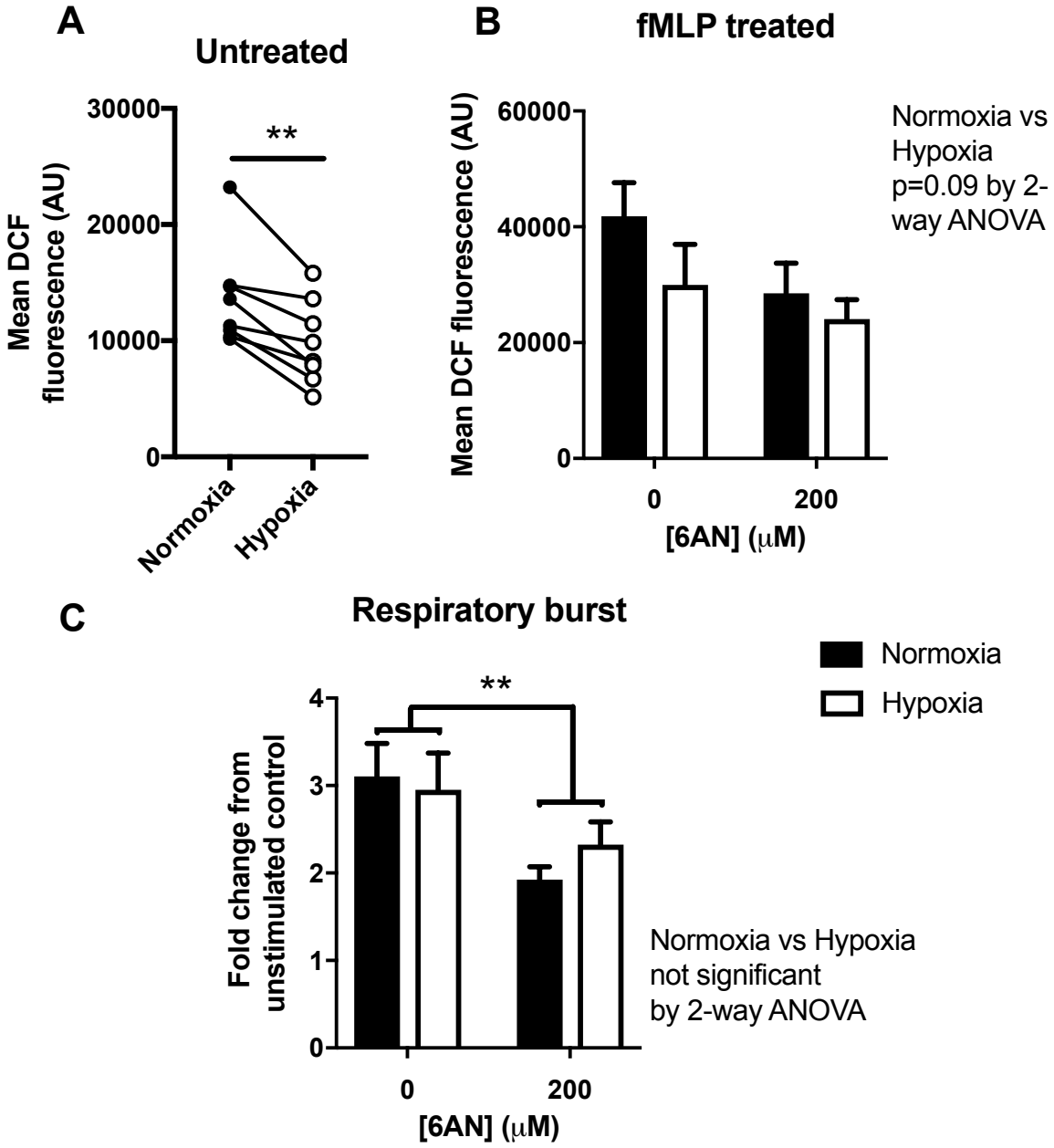

Figure 3.2.5-1: Neutrophils cultured in hypoxia have diminished ROS production but equivalent capability of mounting a respiratory burst. Neutrophils were cultured for 1 hour without (A) or with (B) 100nM fMLP and with or without the OxPPP inhibitor 6AN (B, C) and ROS production assessed through staining with the ROS-sensitive dye DCF (A, B, C). Respiratory burst was calculated as fold increase in DCF fluorescence after stimulation with 100nM fMLP (C). Data expressed as mean±SEM and analysed with paired two-tailed Student's T tests (A) or by two-way ANOVA (B, C), n = 8, p**<0.01).

3.2.6. A model of mitochondrial dysfunction: blockade of complex II

As a model of mitochondrial dysfunction, we had at our disposal a pool of patients with a rare deficiency in the mitochondrial protein succinate dehydrogenase. The patients have heterozygous loss-of-function mutations in *SDHB*. SDHB is a subunit of succinate dehydrogenase and is needed for transfer of electrons from $FADH_2$ to the Q pool (Figure 3.2.6-1). Neutrophils isolated from patients with mutations in *SDHB* have reduced succinate dehydrogenase activity and are functionally different to healthy control neutrophils in that they have diminished rates of constitutive apoptosis when cultured *in vivo* (Jones *et al.*, 2016). We examined whether loss of Kreb's cycle enzyme activity in this case had a significant effect on mitochondrial function, specifically mitochondrial membrane potential and release of mitochondrial reactive oxygen species.

Neutrophils isolated from patients with heterozygous *SDHB* mutations were found to have equivalent mROS levels to neutrophils isolated from healthy control blood directly after isolation (mean (±SEM), T0 HC = 98.0 (46.1), T0 HC MT = 49.5 (10.0), T0 SDH = 83.4 (28.7), T0 SDH MT = 46.4 (4.83) gMFI, n = 3, ns)(Figure 3.2.6-2, A). After culture in glutamine and glucose-rich media with and without LPS, mROS levels of neutrophils isolated from patients with heterozygous *SDHB* mutations were still equivalent (mean (±SEM), N6 HC = 97.7 (30.4), N6 HC MT = 60.4 (1.48), N6 SDH = 103 (31.3), N6 SDH MT = 53.7 (5.43), N6 HC LPS = 79.3 (41.7), N6 HC LPS MT = 46.9 (10.7), N6 SDH LPS = 56.2 (18.3), N6 SDH MT LPS = 48.4 (8.99) gMFI, n = 3, ns)(Figure 3.2.6-2, B-C). Likewise, freshly isolated neutrophils from patients with heterozygous *SDHB* mutations have equivalent mitochondrial membrane potential to neutrophils from healthy controls (mean (±SEM), T0 HC = 577 (71.7), T0 HC CCCP = 242 (38), T0 SDH = 557 (64.3), T0 SDH CCCP = 246 (28) gMFI, n = 3, ns)(Figure 3.2.6-2, D). The same is true for neutrophils cultured in media with and without LPS (mean (±SEM), N6 HC = 596 (20.0), N6 HC CCCP = 240 (1.32), N6 SDH = 566 (31.5), N6 SDH CCCP = 248 (5.36), N6 HC LPS = 491 (9.43), N6 HC CCCP LPS = 233 (5.06), N6 SDH LPS = 490 (14.4), N6 SDH CCCP LPS = 231 (13.5) gMFI, n = 3, ns)(Figure 3.2.6-2, E-F).

In contrast to these previous results which show no change in mitochondrial

respiratory chain function, neutrophils with heterozygous *SDHB* mutations do have a greater NAD^+/NADH ratio compared to healthy control neutrophils (mean (±SEM), T0 HC = 0.240 (0.178), T0 SDH = 1.05 (0.543), N6 HC = 0.183 (0.107), N6 SDH = 3.13 (1.32), N6 HC LPS = 0.624 (0.240), N6 SDH LPS = 1.36 (0.835), n = 4)(Figure 3.2.6-3, A) but equivalent total NADt (T0 HC = 0.0687 (0.0209), T0 SDH = 0.0816 (0.0250), N6 HC = 0.149 (0.0307), N6 SDH = 0.132 (0.00956), N6 HC LPS = 0.685 (0.144), N6 SDH LPS = 0.699 (0.0735), n = 4)(Figure 3.2.6-3, B).

Neutrophils with heterozygous *SDHB* mutations have an equal $NADP^+$/NADPH ratio compared to healthy control neutrophils (mean (±SEM), T0 HC = 1.11 (0.204), T0 SDH = 1.02 (0.0630), N6 HC = 0.887 (0.109), N6 SDH = 0.996 (0.0671), N6 HC LPS = 0.578 (0.100), N6 SDH LPS = 0.575 (0.0745), n = 3)(Figure 3.2.6-3, C) and an equivalent amount of total NADPt in all conditions (mean (±SEM), T0 HC = 0.0846 (0.0283), T0 SDH = 0.0726 (0.0237), N6 HC = 0.101 (0.0144), N6 SDH = 0.0942 (0.0178), N6 HC LPS = 0.217 (0.0271), N6 SDH LPS = 0.224 (0.0332), n = 3)(Figure 3.2.6-3, D).

Neutrophils cultured with the complex II inhibitor 3-NP have significantly reduced apoptosis consistent with *SDHB* patients (mean (±SEM), 0.5mM vehicle control = 64.5 (4.25), 0.5mM 3NP = 55.7 (1.46), 1mM vehicle control = 64.8 (2.85), 1mM 3NP = 49.8 (3.62), 2mM vehicle control = 65.0 (3.01), 2mM 3NP = 51.3 (5.67)%, n = 4, p*<0.05)(Figure 3.2.6-4, A). 3-NP significantly reverses apoptosis induced by rotenone inhibition, indicating anti-apoptotic effects of 3-NP are not due to inhibition of the electron transport chain. (mean (±SEM), untreated = 48 (2.52), rotenone = 73.7 (5.05), rotenone + 3NP = 56.5 (7.37), n = 3, p*0.05)(Figure 3.2.6-4, B).

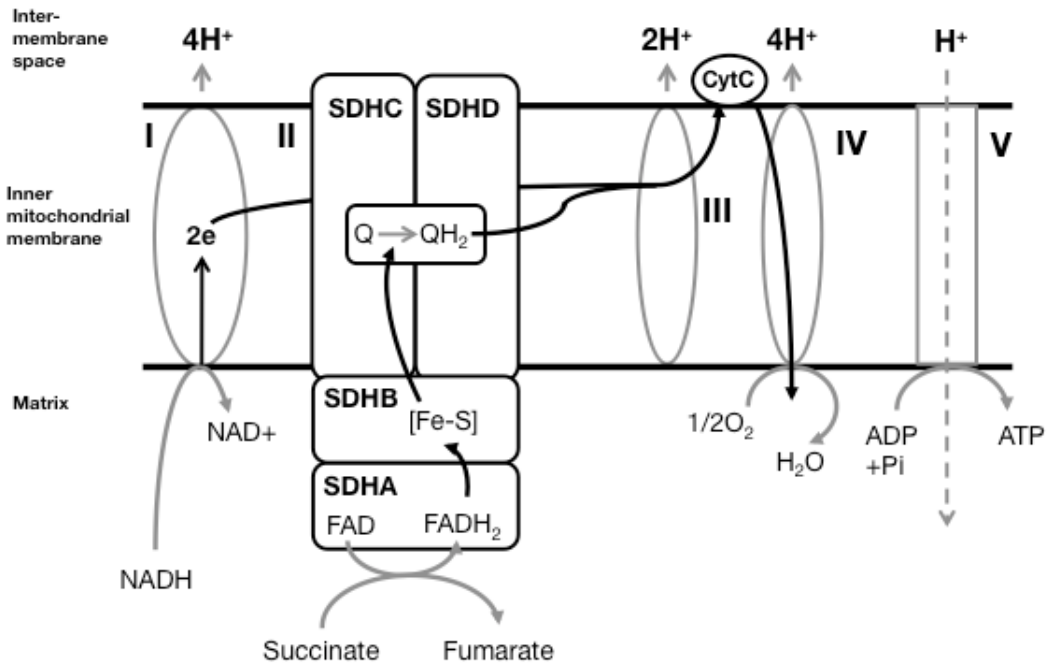

Figure 3.2.6-1: The role of SDHB in the tricarboxylic acid cycle and mitochondrial electron transport chain. SDHB is one of four subunits of the protein complex succinate hydrogenase (SDH). The SDHA subunit of succinate dehydrogenase catalyses the oxidation of succinate to fumarate, a key step in the krebs cycle. This reaction reduces FAD to $FADH_2$. Electrons from $FADH_2$ are transferred to the SDHB iron clusters, which in turn transfer these electrons to ubiquinone via SDHC/SDHD, reducing the ubiquinone to ubiquinol which can then pass electrons to complex III.

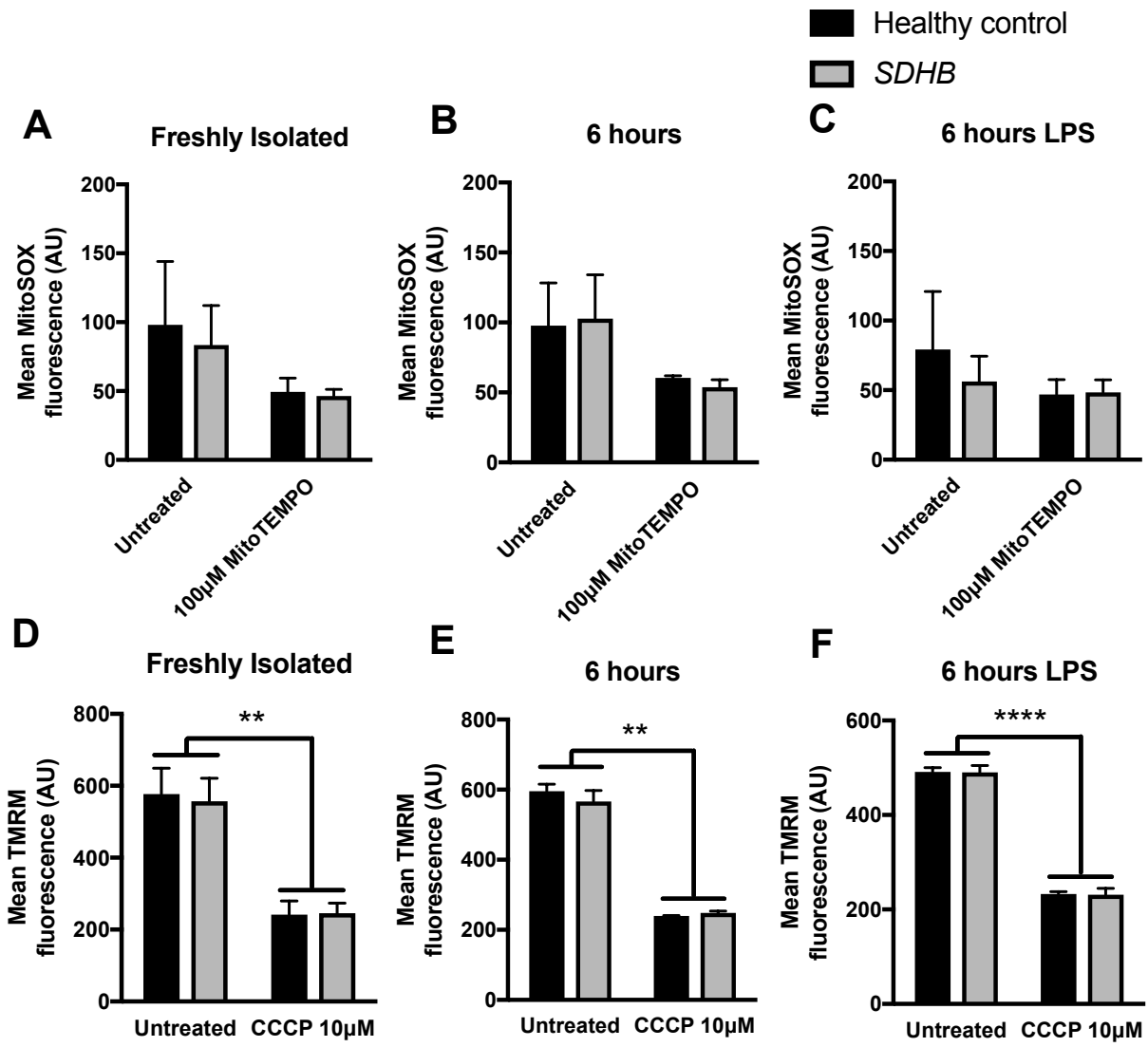

Figure 3.2.6-2: Neutrophils with succinate-dehydrogenase deficiency have equivalent mitochondrial ROS release and mitochondrial membrane potential. Neutrophils were isolated from healthy volunteers (black bars) or patients with germline mutations in *SDHB* (grey bars). Freshly isolated neutrophils ((A, D) and neutrophils cultured in normoxia for 6 hours with (B, E) and without (C, F) LPS were stained with MitoSOX™ Red (A-C) or TMRM (D-F) and fluorescence analysed via flow cytometry to assess production of mROS and mitochondrial membrane potential. Data expressed as mean±SEM and analysed with 2-way ANOVA, n = 3, p**<0.01, p****<0.0001.

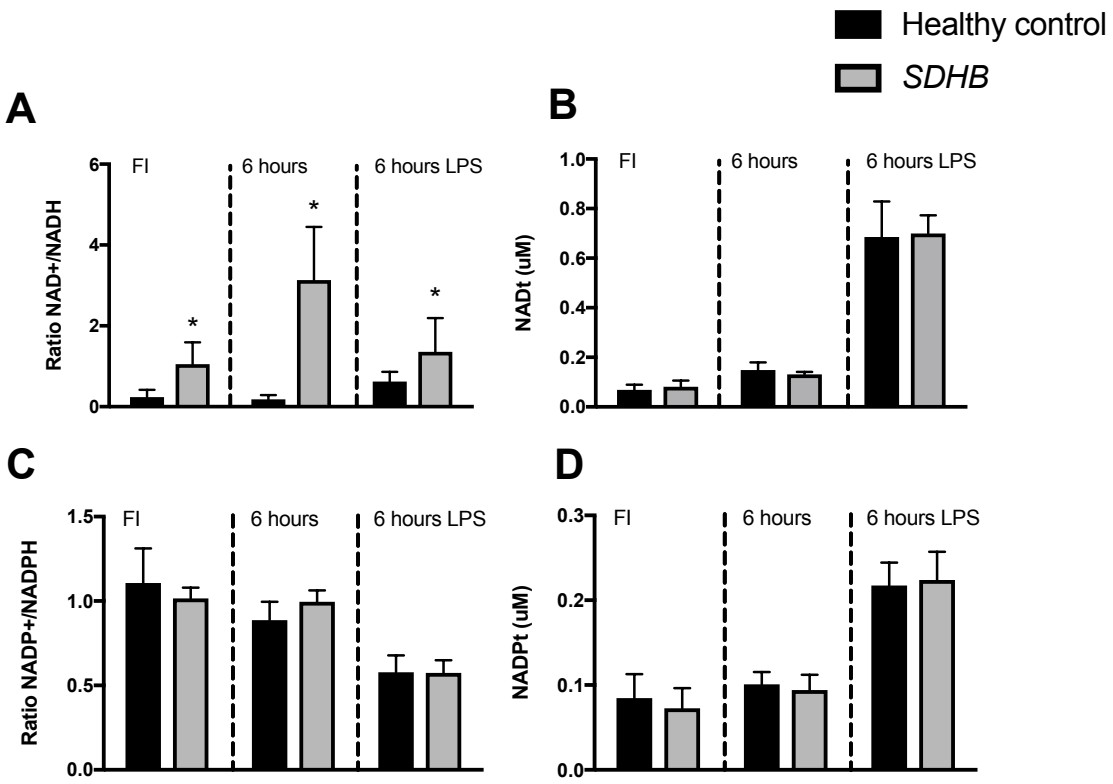

Figure 3.2.6-3: Neutrophils isolated from patients deficient in succinate-dehydrogenase B have higher NAD^+/NADH ratios but similar $NADP^+$/NADPH ratios. Neutrophils were isolated from healthy controls (black bars) and *SDHBx* patients (grey bars). Freshly isolated (FI) and neutrophils cultured for 6 hours with and without LPS were lysed and NAD^+/NADH (A,B) and $NADP^+$/NADPH (C,D) levels analysed via fluorimetric assay. NAD^+/NADH ratio (A), total NAD^+ and NADH (B), $NADP^+$/NADPH ratio (C) and total $NADP^+$ and NADPH (D) were calculated from observed values. Data expressed as mean±SEM and analysed via 2-way ANOVA, n = 4, p*<0.05.

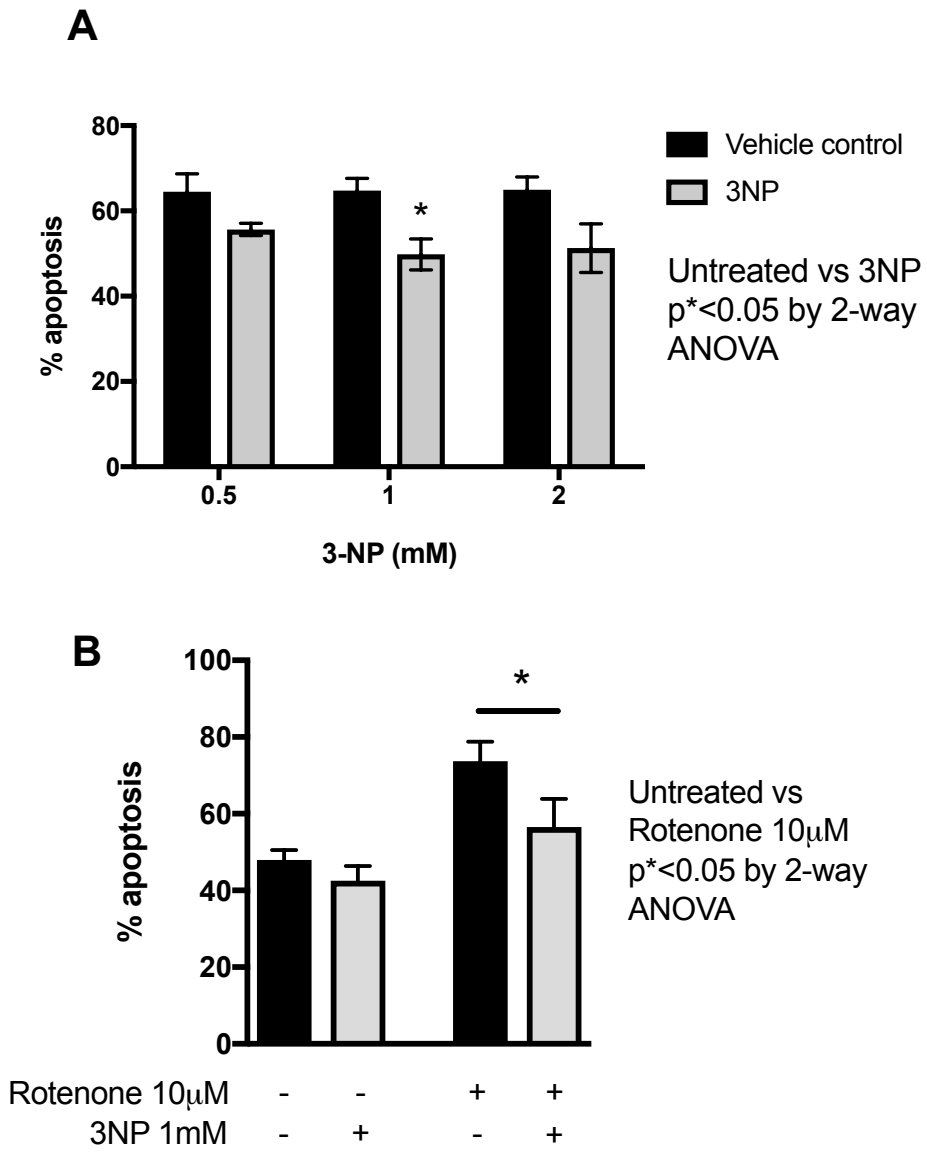

Figure 3.2.6-4: Inhibition of succinate dehydrogenase with 3-nitropropionic acid prolongs neutrophil lifespan and reverses rotenone-induced apoptosis. Neutrophils cultured for 20 hours were treated with 3NP (A) or 3NP and rotenone (B) and apoptosis assessed via morphology. Data expressed as mean±SEM and analysed by 2-way ANOVA with Sidak's post hoc multiple comparison test (A, B), n = 4 (A), n = 3 (B), p*<0.05.

3.2.7. Neutrophils cultured in hypoxia have significantly enhanced anaerobic respiration

Neutrophil metabolism is closely linked to mitochondrial electron chain function through the activity of the tricarboxylic cycle and availability of high-energy molecules such as ATP and NADH derived from glycolysis and the krebs cycle.

Neutrophils have significantly more ATP, ADP and AMP in hypoxia and a lower energy status (ATP/ADP), indicating a greater energy demand and use of ATP in hypoxic conditions. Neutrophils have more ATP after culture in hypoxia for 4 hours compared to normoxic controls (mean (±SEM), normoxia = $2.71x10^8$ ($3.21x10^7$), hypoxia = $4.11x10^8$ ($3.55x10^7$), n = 4, p*<0.05)(Figure 3.2.7-1, A). Other phosphorylation states are also upregulated in hypoxia. ADP levels are significantly higher in hypoxia (mean (±SEM), normoxia = $1.64x10^7$ ($3.01x10^6$), hypoxia = $3.13x10^7$ ($5.70x10^6$), n = 4, p*<0.05)(Figure 3.2.7-1, B). AMP is also upregulated in hypoxia (mean (±SEM), C, normoxia = $1.49x10^7$ ($6.08x10^5$), hypoxia = $2.38x10^7$ ($2.76x10^6$), n=4, p*<0.05)(Figure 3.2.7-1, C). Neutrophils have a lower energy status (ATP/ADP) in hypoxia (mean (±SEM), normoxia = 17.2 (1.87), hypoxia = 14.1 (2.12), n=4, p*<0.05)(Figure 3.2.7-1, D).

Glycolysis regenerates NAD^+ to NADH via glycolysis and can also make the mitochondrial-substrate DHAP (Figure 3.2.7-2, A). Neutrophils have significantly more flux through glycolysis in hypoxia (mean (±SEM), glucose 6-P normoxia = $5.31x10^7$ ($8.53x10^6$), glucose 6-P hypoxia = $1.20x10^8$ ($3.50x10^7$), fructose 1,6-BP normoxia = $1.19x10^7$ ($1.29x10^6$), fructose 1,6-BP hypoxia = $2.19x10^7$ ($3.34x10^6$), DHAP normoxia = $4.27x10^6$ ($9.51x10^5$), DHAP hypoxia = $7.47x10^6$ ($1.58x10^6$), GAP normoxia = $7.57x10^6$ ($2.75x10^6$), GAP hypoxia = $1.63x10^7$ ($3.13x10^6$), 2-PG normoxia = $1.07x10^7$ ($3.38x10^6$), 2-PG hypoxia = $1.98x10^7$ ($6.93x10^6$), pyruvate normoxia = $8.63x10^6$ ($5.66x10^5$), pyruvate hypoxia = $1.14x10^7$ ($5.34x10^5$), lactate normoxia = $6.66x10^8$ ($5.11x10^7$), lactate hypoxia = $7.91x10^8$ ($4.82x10^7$), n = 4, p*<0.05)(Figure 3.2.7-2, B).

Neutrophils require exogenous glucose for hypoxic survival. Neutrophils cultured without glucose in hypoxia lose hypoxic survival, whereas in normoxic conditions neutrophil survival is equivalent with or without exogenous glucose (mean (±SEM),

normoxia (black bar) FBS = 47.5 (3.07), normoxia (black bar) DFBS (dialysed FBS) = 53.4 (2.16), normoxia (black bar) DFBS-Gluc = 44.7 (2.83), hypoxia (white bar) FBS = 12.3 (2.53), hypoxia (white bar) DFBS = 36.0 (8.03), hypoxia (white bar) DFBS-Gluc = 93.4 (2.63), n = 8, p***<0.001)(Figure 3.2.7-3, A). Neutrophils cultured without glutamine have no change in apoptosis from DFBS controls, indicating glutamine is not necessary for maintaining neutrophil survival in hypoxia (mean (±SEM), normoxia (black bar) DFBS = 53.4 (2.16), normoxia (black bar) DFBS-Glut = 54.5 (3.13), hypoxia (white bar) DFBS = 36.0 (8.03), hypoxia (white bar) DFBS-Glut = 38.6 (6.06), n=8)(Figure 3.2.7-3, A). Neutrophils cultured with the hexokinase-inhibitor 2-deoxyglucose (2-DG) have accelerated apoptosis (mean (±SEM), normoxia (black bar) untreated = 52.8 (5.09), normoxia (black bar) 2-DG = 70.6 (10.3), hypoxia (white bar) untreated = 31.3 (8.75), hypoxia (white bar) 2-DG = 83.0 (3.31), n = 4, p*<0.05)(Figure 3.2.7-3, B). 2-DG-treated neutrophils cultured in hypoxia have a significantly greater degree of apoptosis compared to their untreated control than normoxic cells compared to their untreated control, indicating induction of hypoxic survival is dependent on the augmentation of glycolytic flux (mean (±SEM), C, normoxia = 1.34 (0.195), hypoxia = 2.65 (0.106), n=4, p*<0.05)(Figure 3.2.7-3, C).

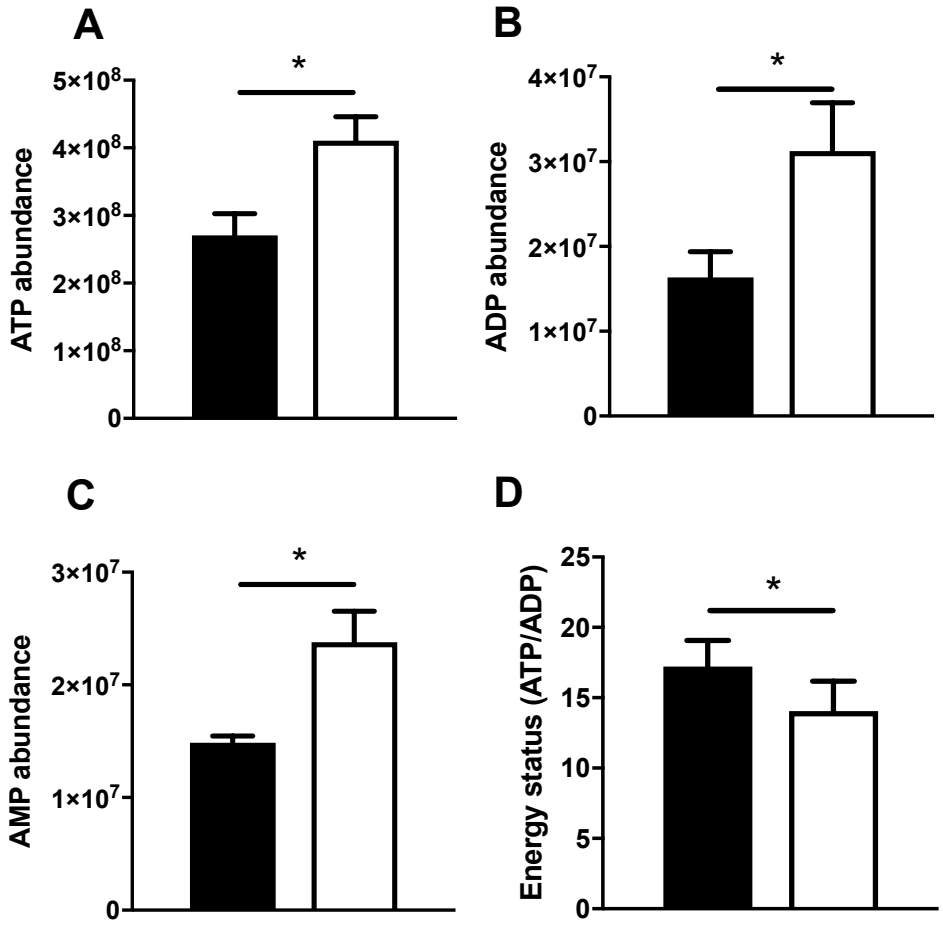

Figure 3.2.7-1: Neutrophils have significantly more ATP/ADP/AMP, but reduced energy status indicating higher energy requirement in hypoxia. Neutrophils were cultured for 4 hours in normoxia and hypoxia and ATP (A), ADP (B) and AMP (C) abundance measured via LC-MS. Energy status (ATP/ADP) (D) was calculated as a measure of energy demand in the cell. Data expressed as mean±SEM and analysed with paired two-tailed Student's T tests, n =4, p*<0.05.

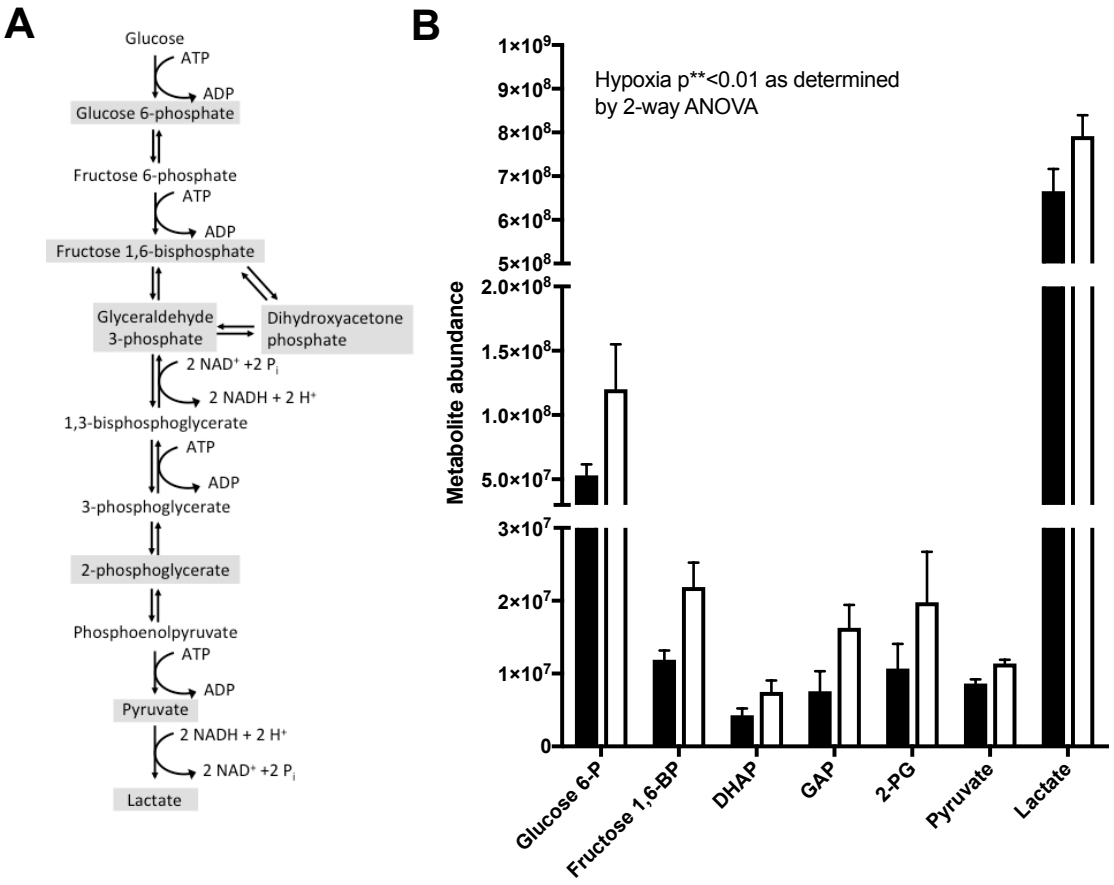

Figure 3.2.7-2: Neutrophils have significantly increased abundance of glycolytic intermediaries in hypoxic conditions. Neutrophils were cultured for 4 hours in normoxia and hypoxia and lysed in methanol before LC-MS analysis. **A:** Schematic showing anaerobic glycolysis. Measured metabolites are highlighted. **B:** Relative metabolite abundance in cells cultured in normoxia and hypoxia. Data expressed as mean±SEM and analysed via two-way ANOVA, n = 4, p**<0.01).

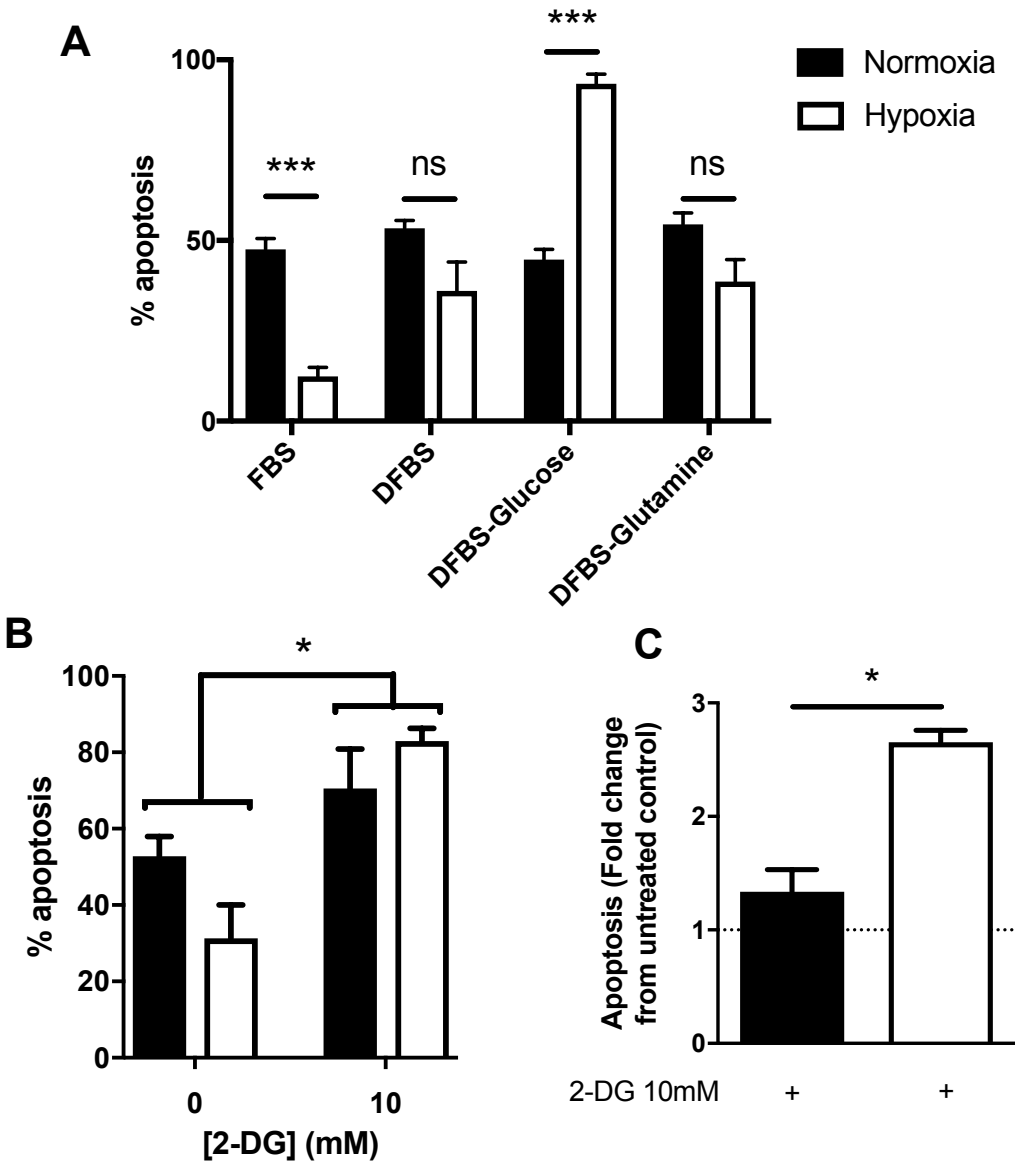

Figure 3.2.7-3: Hypoxic neutrophils require extracellular glucose for survival. Neutrophils were cultured for 20 hours in normoxia and hypoxia in either complete RPMI with 10% FBS, complete RPMI with 10% dialysed FBS, RPMI without glucose with 10% dialysed FBS, or RPMI without L-glutamine with 10% dialysed FBS (A), or with and without the glucose hexokinase-inhibitor 2-deoxy-D-glucose (B, C). Data expressed as mean±SEM and analysed by paired Student's two-tailed T tests (A, C) corrected for multiple comparisons with the Holm-Sidak method (A), and by two-way ANOVA (B), n = 8 (A), n = 4 (B, C), p*<0.05, p***<0.001).

3.2.8. Neutrophils cultured in hypoxia have significantly enhanced flux through the pentose phosphate pathway

Cellular antioxidant buffering capacity is primarily controlled through flux through the pentose phosphate pathway (Figure 3.2.8-1, A). We examined pentose phosphate pathway flux using LC-MS analysis in normoxia and hypoxic conditions. Neutrophils have significantly more flux through the pentose phosphate pathway in hypoxia (mean (±SEM). Ribulose 5-P normoxia = $6.27x10^5$ ($9.20x10^4$), Ribulose 5-P hypoxia = $1.22x10^6$ ($2.79x10^5$), Ribose 5-P normoxia = $3.06x10^6$ ($3.55x10^5$), Ribose 5-P hypoxia = $5.11x10^6$ ($7.78x10^5$), Sedoheptulose 7-P normoxia = $6.37x10^6$ ($8.85x10^5$), sedoheptulose 7-P hypoxia = $1.16x10^7$ ($2.18x10^6$), Erythrose 4-P normoxia = $7.06x10^4$ ($5.95x10^4$), erythrose 4-P hypoxia = $1.78x10^5$ ($8.28x10^4$), n = 4, p**<0.01 by 2-way ANOVA)(Figure 3.2.8-1, B).

Despite enhanced flux through the pentose phosphate pathway, neutrophils maintain an equivalent $NADP^+$/NADPH ratio and GSH/GSSG ratio. Total $NADP^+$ levels are equivalent between normoxic and hypoxic conditions. LPS was used as a control for NADPH oxidase activity and enhanced NADPt production (mean (±SEM), normoxia untreated = 0.154 (0.0305), hypoxia untreated = 0.177 (0.0142), normoxia LPS = 0.268 (0.0410), hypoxia LPS = 0.296 (0.0328), n = 3, p**<0.01)(Figure 3.2.8-2, A). $NADP^+$/NADPH levels are equivalent between normoxia and hypoxia (mean (±SEM), normoxia = 0.194 (0.0199), hypoxia = 0.241 (0.0359), normoxia LPS = 0.382 (0.0722), hypoxia LPS = 0.286 (0.0409), n = 3)(Figure 3.2.8-2, B). Total glutathione levels are equivalent between normoxia and hypoxia (mean (±SEM), normoxia = 2.25 (0.215), hypoxia = 2.32 (0.217), normoxia LPS = 2.07 (0.207), hypoxia LPS = 2.16 (0.316), n = 3)(Figure 3.2.8-2, C) as are glutathione redox ratios (mean (±SEM), normoxia = 17.3 (4.21), hypoxia = 17.22 (4.016), normoxia LPS = 21.2 (8.31), hypoxia LPS = 24 (1.97), n = 3)(Figure 3.2.8-2 D). This indicates an enhanced pentose phosphate flux is needed to maintain redox status. Consistent with these findings, blocking the pentose phosphate pathway with the G6PD inhibitor 6AN is pro-apoptotic to neutrophils cultured in normoxia or hypoxia (mean (±SEM), normoxia untreated = 55.8 (2.22), normoxia 6AN = 68.8 (0.454), normoxia LPS = 31.8 (6.23), normoxia LPS 6AN = 66.7 (4.00), hypoxia untreated = 35.6 (4.34), hypoxia 6AN = 50.1 (4.77), hypoxia LPS = 13.7 (2.24), hypoxia LPS 6AN = 48.3

(0.442)%, n = 3)(Figure 3.2.8-3, A), with stimulated cells and cells cultured in hypoxia having a significantly higher degree of apoptosis induced by 6AN than unstimulated, normoxic cells (mean (±SEM), normoxia = 1.24 (0.0648), hypoxia = 1.42 (0.0575), normoxia LPS = 2.59 (0.588), hypoxia LPS = 3.79 (0.781), n = 3)(Figure 3.2.8-3, B).

The addition of the antioxidant catalase significantly reduces apoptosis in both normoxia and hypoxia (mean (±SEM), normoxia untreated = 76.5 (1.25), normoxia catalase = 14.2 (3.31), hypoxia untreated = 35.4 (7.56), hypoxia catalase = 3.30 (1.01)%, n = 3)(Figure 3.2.8-4,A). Addition of catalase was also sufficient to reverse the apoptosis caused by culture in hypoxia without exogenous glucose (mean (±SEM), hypoxia untreated = 35.4 (7.56), hypoxia untreated –glucose = 82.7 (5.94), hypoxia catalase –glucose = 15.3 (9.23)%, n = 3)(Figure 3.2.8-4, A, B).

These data indicate that in hypoxia, oxidative stress is increased and glucose is needed to prevent oxidant-induced apoptosis in hypoxia through regeneration of antioxidant molecules via the pentose phosphate pathway.

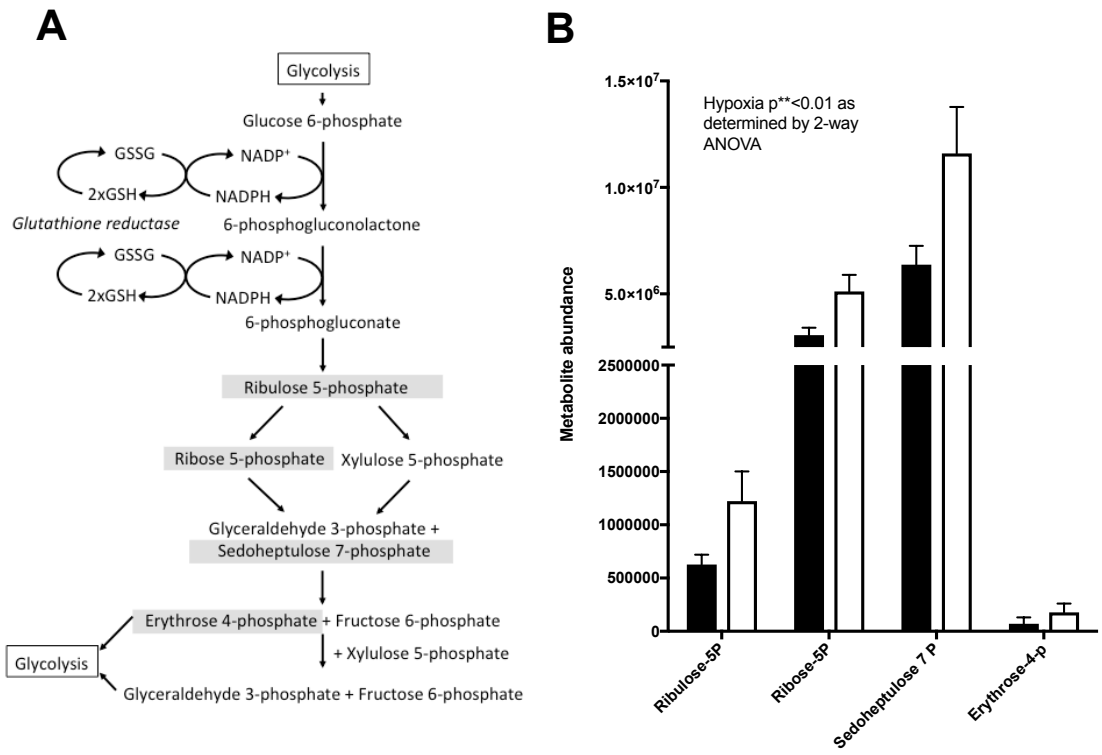

Figure 3.2.8-1: Neutrophils cultured in hypoxia have significantly higher levels of pentose phosphate pathway metabolites. Neutrophils were cultured for 4 hours in normoxia and hypoxia and lysed in methanol before LC-MS analysis. **A:** Schematic showing the oxidative pentose phosphate pathway. Measured metabolites are highlighted. **B:** Relative metabolite abundance in cells cultured in normoxia and hypoxia. Data expressed as mean±SEM and analysed via two-way ANOVA, n = 4, p**<0.01).

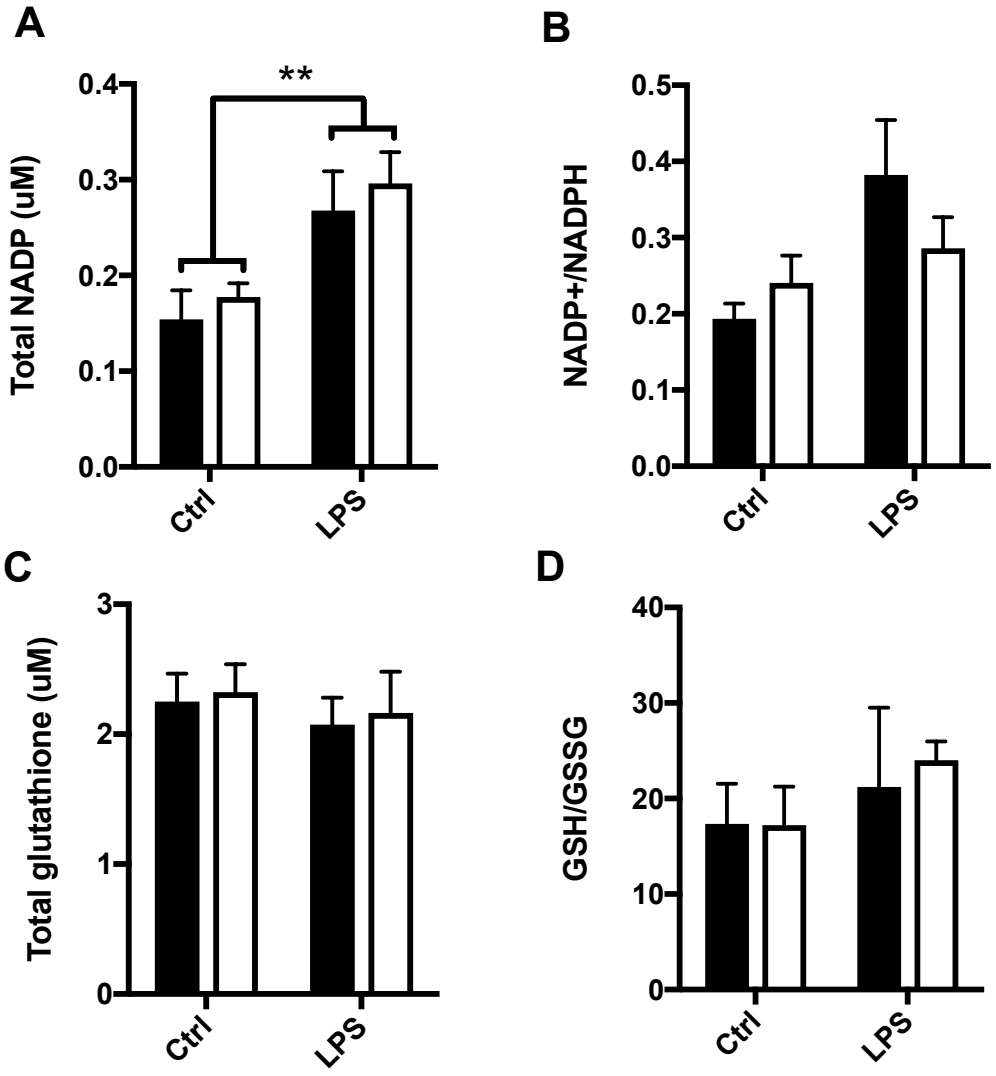

Figure 3.2.8-2: Neutrophils cultured in hypoxia have no difference in amounts or redox ratios of NADPH or glutathione. Neutrophils were culture for 4 hours in normoxia and hypoxia and lysed before glutathione and NADP levels measured via fluorimetric assay. **A:** Total $NADP^+$/NADPH **B:** $NADP^+$/NADPH ratio **C:** Total glutathione **D:** GSH/GSSG ratio. Data expressed as mean±SEM and analysed via two-way ANOVA, n = 4, p**<0.01).

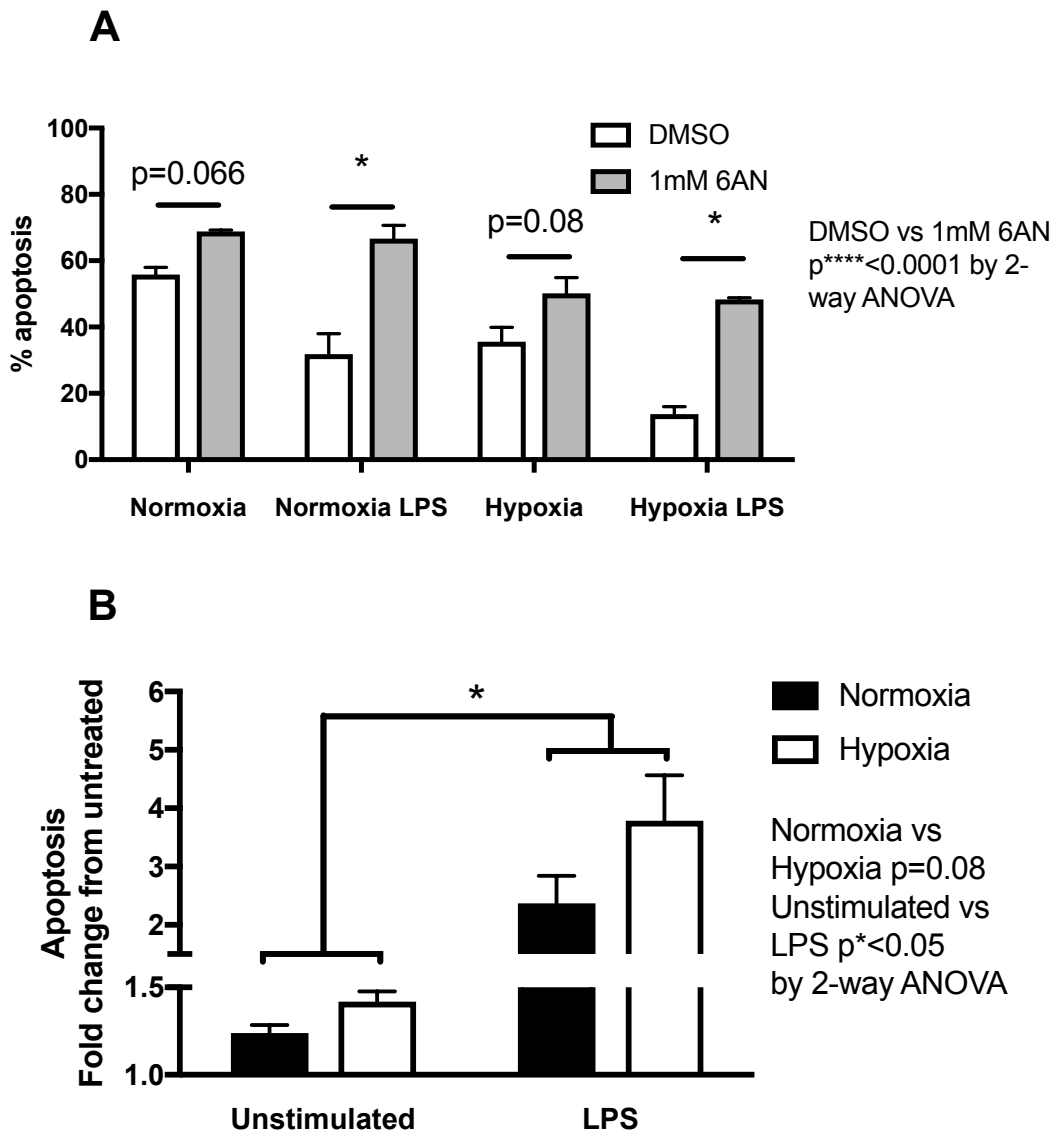

Figure 3.2.8-3: Blockade of the oxPPP is pro-apoptotic with a significantly greater effect on stimulated and hypoxic cells. Neutrophils were cultured with and without 1mM 6AN or 100ng/ml LPS and apoptosis assessed at 20 hours via morphology (A,B). Data expressed as mean±SEM and analysed via 2-way ANOVA (A, B) with Sidak's post-hoc multiple comparisons test (A), n = 3, p*<0.05.

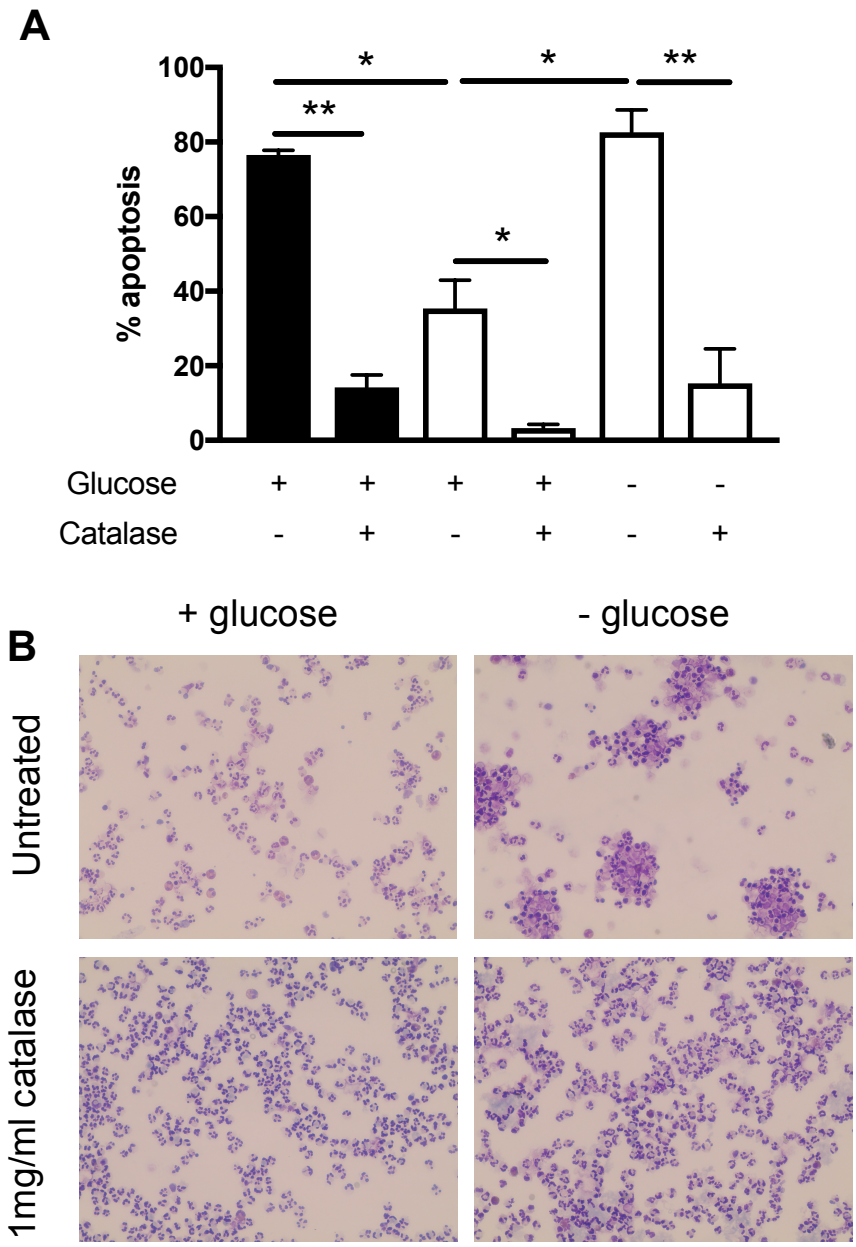

Figure 3.2.8-4: Catalase promotes neutrophil survival in both normoxia and hypoxia and the pro-apoptotic effects of glucose depletion in hypoxia can be reversed by exogenous addition of catalase. Neutrophils were cultured with and without 1mg/ml catalase in normoxia (A) and hypoxia (A,B) either in complete RPMI media or RPMI without glucose and apoptosis assessed at 20 hours via morphology. Data expressed as mean±SEM and analysed via paired two-tailed Student's T-tests, n = 3, p*<0.05, p**<0.01.

3.3. Discussion

3.3.1. Neutrophils use their mitochondria for signalling via mitochondrial ROS production

Neutrophils do not rely on electron transport chain function for ATP production, but still have extensive mitochondrial networks which maintain a mitochondrial membrane potential and can release ROS (Fossati *et al.*, 2003)(Maianski *et al.*, 2004). The role of mitochondria in the neutrophil is unclear. As neutrophils maintain a mitochondrial membrane potential, it seemed likely that the neutrophil respiratory chain is at least partly functional and may produce mitochondrial ROS in the absence of ATP production.

I investigated whether hypoxia induces the production of mitochondrial ROS in neutrophils as it does in other cell types. From the data it is clear that neutrophils do maintain a mitochondrial membrane potential (Figure 3.2.4-1, A-B) and produce mitochondrial ROS (Figure 3.2.2-2), and acute hypoxia, but not pro-inflammatory stimuli or exposure to high glucose culture media, is a potent inducer of mitochondrial ROS production (Figure 3.2.2-2).

The data also show the hypoxic release of mitochondrial ROS in neutrophils promotes survival and positively regulates the stability of HIF-1α as blockade of mROS production using mitochondrial inhibitors is pro-apoptotic (Figure 3.2.3-1) and inhibits HIF-1α stabilisation (Figure 3.2.3-2, A-B).

Interestingly, although the release of mROS is induced in hypoxia, overall cellular redox stress is reduced in hypoxic conditions (Figure 3.2.5-1, A), and non-mitochondrial antioxidants such as TEMPOL do not influence HIF-1α stability, suggesting HIF-1α stabilisation is mediated specifically by mROS release in hypoxia (Figure 3.2.3-2, B). The reason for this effect being specific to ROS produced in the mitochondria is unclear. ROS-induced HIF-1α stabilisation has been suggested to be dependent on AMPK signalling via JNK and JAK2 (Jung *et al.*, 2008). Cellular stress, including ROS, can cause JNK localisation to the mitochondria which can then amplify mROS production in a positive feedback loop (Chambers and LoGrasso, 2011). The involvement of this mitochondria-mediated JNK feedback

loop may explain why mROS specifically are capable of stabilising HIF-1α over NADPH-oxidase derived ROS. Indeed, these studies indicated inhibition of NADPH-oxidase activity with apocynin did not affect JNK-mediated upregulation of ROS production. Additional studies have suggested that a small percentage of cellular HIF-1α associates with the mitochondria (Briston, Yang and Ashcroft, 2011), which may explain why HIF-1α is more sensitive to mROS over cytoplasmic ROS. However, the precise mechanism remains unclear.

Further downstream functional effects of hypoxia-induced mROS have yet to be elucidated. Neutrophil mitochondrial function has been implicated in the regulation of chemotaxis induced by fMLP as treatment with the uncoupler CCCP can inhibit neutrophil chemotaxis (Fossati *et al.*, 2003) Recent studies have specifically implicated the release of neutrophil mROS in the regulation of neutrophil degranulation and extracellular ROS (Vorobjeva *et al.*, 2017). The addition of the mitochondrial antioxidant SkQ1 was shown to inhibit neutrophil degranulation in response to fMLP, and also induced apoptosis in fMLP-stimulated cells. Neutrophil degranulation is upregulated in hypoxic conditions through a HIF-1α-independent, PI3Kγ-dependent mechanism, and hypoxic supernatants produce a greater degree of injury on human tissues (Hoenderdos *et al.*, 2016). Whether hypoxic mROS release influences this regulation of degranulation is unknown, although as mROS is known to positively modulate PI3K pathways, it is possible mROS may play a role in enhanced degranulation in hypoxia (Sullivan and Chandel, 2014).

Neutrophil mROS have also been shown to be important for the calcium-dependent induction of NETosis through the activity of the mitochondrial channel SK3 (Douda *et al.*, 2015). Moreover, mROS have been implicated in the release of pro-inflammatory NETs comprised of oxidized mitochondrial DNA in patients with systemic lupus erythematous disease (SLE), with mitochondrial ROS scavengers capable of suppressing lupus-like disease *in vivo* (Lood *et al.*, 2016). NETosis is indeed modulated by hypoxia and HIF-1α stabilisation, with hypoxia limiting the capacity of neutrophils to undergo NETosis (Branitzki-Heinemann *et al.*, 2016).

Our data is therefore in agreement with studies in other cell types that suggest mROS can regulate HIF-1α stability, implicating neutrophil mitochondrial ROS as a

mediator of pro-inflammatory neutrophil activities. This parallels studies in pro-inflammatory macrophages implicating glycolysis and a subsequent increase in mitochondrial membrane potential as a mediator of pro-inflammatory macrophage functions such as IL-1β production (Mills *et al.*, 2016). Targeting neutrophil mitochondria may have potential for reducing neutrophilic inflammation in acute and chronic inflammatory disease. The increased importance of neutrophil mitochondrial ROS in hypoxia may suggest a way in which hypoxia can promote inflammation, which may be targeted by mitochondrial inhibitors or antioxidants.

3.3.2. Mechanism of hypoxia-induced mitochondrial ROS is independent of Krebs cycle flux, NADH availability and oxidative glucose metabolism

The mechanism for hypoxia-induced mROS release is not entirely clear, although our data show it is not due to changes in mitochondrial electron chain substrate availability via altered flux through the Krebs cycle (Figure 3.2.4-2, A), nor the enhanced availability of NADH or NADPH reducing intermediates (Figure 3.2.4-2, B-C) which can transfer electrons to the mitochondrial electron transport chain. Neutrophils lacking a functional complex II have changes in NAD^+/NADH ratio (Figure 3.2.6-3, A) yet maintain mROS production (Figure 3.2.6-2, A) and a mitochondrial membrane potential (Figure 3.2.6-2, B), indicating that either they make up for deficit through flux through complex I, or complex II in neutrophils does not contribute to electron transport chain flux. The latter hypothesis is likely as our data show loss of SdhB does not influence mROS production in neutrophils, whereas studies in Hep3B cells have shown pharmacological inhibition or genetic knockdown of SdhB enhances mROS production which stabilises HIF-1α (Guzy *et al.*, 2008). Furthermore, addition of cell-permeable complex II substrate methylsuccinate does not increase mitochondrial membrane potential, indicating minimal complex II activity (Figure 3.2.4-3, A).

It has been noted that maintenance of mitochondrial membrane potential by neutrophils is primarily caused by complex III; however, it is unclear whether this mechanism is the cause of this enhanced membrane potential in hypoxia (Guzy *et al.*, 2005)(van Raam *et al.*, 2008). The addition of mitochondrial inhibitors rotenone

and oligomycin did induce the production of mROS (Figure 3.2.2-2, D), indicating transit of electrons through the electron transport chain. However, the degree of mROS increase produced through treatment with these compounds was equivalent in normoxia and hypoxia (Figure 3.2.2-2, E), suggesting increased electron flux through these complexes of the electron transport chain was not the cause of this increased ROS production. Therefore, the mechanism of enhanced mROS and membrane potential may be due to either fundamental physiological changes to the mitochondria in hypoxia, or an increase in the use of alternative mitochondrial electron transport pathways that contribute to mitochondrial electron release which bypass complex I, such as the glycerol 3-phosphate shuttle. Electrons can be introduced into the electron transport chain at sites independent of complexes I and III, and then travel back to these complexes through reverse electron transport (RET), so an increase in mROS through complex I inhibition may reflect inhibition of reverse transit rather than acceptance of electrons from TCA cycle-derived NADH. Reverse electron transport allows cells to regenerate NADH through transfer of an electron to NAD^+ via complex I. Early studies showed isolated mitochondria can produce NADH from NAD^+ after supplementation with succinate, a complex II substrate (Chance and Hollunger, 1961). We have limited conclusive evidence for physiologically relevant RET in our model; however, it is interesting that neutrophils *in vitro* lacking complex II have a drastically higher NAD^+/NADH ratio (Figure 3.2.6-3, A), which may indicate this occurs in the neutrophil mitochondrial electron chain.

Regardless of direction of flow, electrons must be introduced into the respiratory chain through metabolic intermediates. As Krebs cycle activity is extremely limited and hypoxia does not change NAD^+/NADH ratio or Krebs cycle flux, it is unlikely hypoxic mROS upregulation is mediated through enhanced flux into the electron transport chain via complex I and II. One possible mechanism for entry of electrons into the electron transport chain is the glycerol 3-phosphate shuttle, which is a direct link between glycolysis and the electron transport chain. The shuttle is composed of a cytosolic glycerol 3-phosphate dehydrogenase enzyme, cGPDH, or GPD1, which converts the glycolytic intermediate DHAP to glycerol 3-phosphate, oxidising one molecule of NADH to NAD^+, and a mitochondrial glycerol 3-phosphate

dehydrogenase, mGPDH, or GPD2, which converts glycerol 3-phosphate back to DHAP, reducing a molecule of FAD to $FADH_2$ which can then reduce the mitochondrial Q pool. This allows the reducing power of cytosolic NADH to transfer to the mitochondrial electron transport chain. Glycerol 3-phosphate can also be dephosphorylated to produce glycerol by G3PP, a reaction which controls the rate of glycolysis and lipogenesis (Mugabo *et al.*, 2016).

As neutrophils have enhanced flux through glycolysis and more DHAP abundance, enhanced flux through this pathway may allow neutrophils to maintain a mitochondrial membrane potential for redox signalling without investing Krebs cycle intermediates into oxidative phosphorylation. This may also explain higher rates of mROS production as the mitochondrial GPD is a significant source of ROS, equivalent to Complex III during maximal electron flux (Vrbacký *et al.*, 2007). Other highly glycolytic cells use this pathway, such as some malignant cancers, have high rates of mROS release mediated by GPD2 (Mracek, Drahota and Hou, 2013) and GPD2 activity has been shown to be essential for survival of prostate cancer cells *in vitro* (Singh, 2014). There has been some evidence that neutrophil mitochondria primarily use this pathway, as mitochondria isolated from neutrophils can fully regenerate their mitochondrial membrane potential if treated with glycerol 3-phosphate (van Raam *et al.*, 2008). Addition of glycerol phosphate had a greater effect on regenerating mitochondrial membrane potential than complex I and II substrates malate and succinate, respectively. Other studies in neutrophils have shown glycerol metabolism is important in neutrophilic inflammation and survival (Moniaga *et al.*, 2015). Further study into whether this pathway is active in neutrophils and modulated by oxygen tensions is needed to ascertain whether this is indeed the mechanism behind enhanced neutrophil mROS production in hypoxia.

3.3.3. Neutrophil mitochondrial energy production is minimal and is not modulated by hypoxia

Concurrent with previous studies (Fossati *et al.*, 2003)(Maianski *et al.*, 2004), our data suggest neutrophil mitochondria are not required or needed for oxidative respiration and ATP production. We found that demand for ATP, and ATP production in general, is higher in neutrophils cultured in hypoxia (Figure 3.2.7-1).

Glycolytic flux is also upregulated in hypoxia (Figure 3.2.7-2), but not oxidative respiratory pathways such as the Krebs cycle (Figure 3.2.4-2). This suggests that the increase in ATP demand in hypoxia is not met through mitochondrial oxidative respiration, and instead up-regulation of glycolytic flux or regulation of alternative energy pathways is needed to satisfy increased hypoxic energy demand. In keeping with this concept, treatment of neutrophils with the mitochondrial inhibitor CCCP which collapses the membrane potential and capacity for ATP production through complex V of the respiratory chain, does not modulate neutrophil apoptosis either normoxic or hypoxic conditions (Figure 3.2.4-1), indicating neutrophils are not dependent on oxidative phosphorylation.

The reliance of neutrophils on glycolysis is paralleled by their metabolic response to hypoxia. The fact that ATP production and demand is enhanced in hypoxia in neutrophils *in vitro* is in stark contrast to a number of other studies in proliferative cells where hypoxia decreases ATP production as the cells lose respiratory chain function due to lack of available molecular oxygen (Heerlein *et al.*, 2005)(Kioka *et al.*, 2014). Perhaps consequently, lack of ATP availability in severe or chronic hypoxia in proliferative cells can induce apoptosis (Santore *et al.*, 2002)(Kioka *et al.*, 2014), whereas hypoxia or even a total lack of oxygen, is a potent survival stimulus to neutrophils (Figure 3.2.1-1, Figure 3.2.1-2)(Walmsley *et al.*, 2005). It is unclear whether this survival response is ATP-mediated. Previous studies have shown neutrophil apoptosis is inhibited by ATP in a way dependent on the activity of the $P2Y_{11}$ receptor (Vaughan *et al.*, 2007), although our data does not show if enhanced glycolytic flux and ATP production in the neutrophils directly translates to increased release of ATP into the extracellular milieu. Inhibition of glycolysis by 2-DG or culturing neutrophils in glucose-free culture medium is more pro-apoptotic in neutrophils cultured in hypoxia to the extent that normoxic neutrophils show no change in apoptosis after 20 hours in culture, whereas hypoxic neutrophils are completely non-viable at the same time-point (Figure 3.2.7-3). This indicates the pro-survival effect in hypoxia is dependent on glucose metabolism via glycolysis, although whether this is because of ATP availability or other downstream pathways is unclear.

3.3.4. The neutrophil antioxidant response is induced by hypoxia, mediated by flux through the pentose phosphate pathway and required for survival

Neutrophils can modulate mitochondrial reactive oxidant species levels not only through altering flux through the electron transport chain, but also through the expression of small molecules and proteins which act as antioxidants, removing reactive oxygen species from the cell.

Glutathione is a major antioxidant buffer and glutathione levels decrease in neutrophils over time while in culture, significantly declining within an hour of culture. This effect was reversed on addition of exogenous catalase to the culture medium (Ogino, Packer and Maguire, 1997). Ogino *et al* argue that ROS can irreversibly oxidise glutathione, potentially through the generation of chloramine by MPO, and that glutathione protects against the ROS produced by the neutrophils themselves. Glutathione is regenerated by the activity of the pentose phosphate pathway, which uses metabolites from glycolysis (Figure 3.2.8-1, A).

We measured glutathione levels after 2 hours in culture and found no difference in either glutathione levels or GSH/GSSG ratio (Figure 3.2.8-2, A-B), or NADPH levels or $NADP^+$/NADPH ratio. However, pentose phosphate activity was significantly enhanced in hypoxia (Figure 3.2.8-1, B), which suggests the neutrophils have to regenerate glutathione at a more rapid rate to compensate for an increase in redox stress in the cell. This indicates neutrophils maintain a steady overall redox ratio potentially through upregulating pentose phosphate activity in response to enhanced ROS production in hypoxia. Blocking hypoxic upregulation of pentose phosphate pathway activity using the GPD inhibitor 6-AN induces neutrophil apoptosis (Figure 3.2.8-3, A), and more so in hypoxic cells (Figure 3.2.8-3, B), suggesting neutrophils rely more on the pentose phosphate pathway in hypoxia. Addition of 6AN was sufficient to prevent the upregulation of ROS after administration of fMLP, indicating efficient inhibition of the pentose phosphate pathway (Figure 3.2.5-1, B-C), although interestingly in unstimulated cells, levels of reactive oxygen levels were unchanged. It is possible this is because residual glutathione levels are able to buffer ROS at this timepoint (Figure 3.2.5-1, D).

Similarly, blocking glucose availability or depriving neutrophils of glucose induces apoptosis as mentioned previously. This is either because neutrophil energy demand is higher in hypoxia so blocking the primary source of ATP induces apoptosis, or because glucose uptake is needed to induce upregulation of the pentose phosphate pathway and prevent oxidative damage in hypoxia. To ascertain which was the case, we added the antioxidant catalase to the culture medium to see if reducing oxidative stress of the neutrophils could prevent apoptosis caused by glucose starvation. Catalase is an antioxidant which is distributed throughout the cytoplasm of cells and is capable of converting H_2O_2 to H_2O and O_2 (Ballinger *et al.*, 1994). Previous work has shown catalase, but not superoxide dismutase, can reduce neutrophil apoptosis *in vitro* (Hannah *et al.*, 1995), and neutrophils actively transcribe and translate large amounts of endogenous catalase, in contrast to monocytes that express GPx in preference over catalase as their primary antioxidant defense mechanism (Pietarinen-Runtti *et al.*, 2000). Neutrophils also express MnSOD (Pietarinen-Runtti *et al.*, 2000). We found addition of catalase to the culture medium significantly prevents glucose-starved neutrophil cell death in hypoxia (Figure 3.2.8-4, A-B), indicating that upregulation of glucose metabolism is at least partially needed to protect against enhanced redox stress in hypoxia, and that protection against redox stress can prolong survival even in the absence of available energy substrates.

Hypoxia neutrophils also mount a transcriptional and translational antioxidant response to hypoxia. Neutrophils increase catalase expression in hypoxia *in vitro* (Thompson *et al.*, 2014) and also in response to apnoea (Sureda *et al.*, 2004). Apnoea was also shown to modulate the activity of thioredoxin reductase, an enzyme that is capable of reducing protein disulphides and therefore reversing the effect of oxidants on protein thiol residues.

Interestingly, even in hypoxic conditions, cells cultured with glucose also experienced a pro-survival effect on treatment with catalase. It is clear neutrophils employ a number of antioxidant defenses in response to hypoxia.

3.3.5. Summary

Our data describes a role for neutrophil mitochondria as a source of mitochondrial

ROS. In hypoxia, mitochondrial ROS production is increased in a way that augments hypoxic HIF-1α in hypoxia. Enhanced release of mitochondrial ROS in hypoxia is not due to enhanced Krebs cycle flux or oxidative phosphorylation. It is possible that glycolysis is moderating this release of ROS as we show glycolysis is profoundly upregulated in hypoxic conditions. Upregulation of glycolytic flux is also linked to enhanced pentose phosphate pathway flux essential for neutrophil survival. Antioxidants can completely rescue neutrophil survival in hypoxia following removal of glucose, indicating antioxidant molecules are essential for modulating neutrophil survival over energy production. Therefore, our data describe duel roles for mitochondrial and cellular ROS as both signalling molecules and critical regulators of neutrophil apoptosis that are modulated by hypoxia through modulation of metabolic flux and oxygen availability.

4. Regulation of neutrophil function and killing by PHD3

4.1. Introduction

4.1.1. Regulation of PHD3 in inflammation

Neutrophil metabolism and function is intrinsically linked by the hypoxic response pathway (Chapter 1.4). This pathway is composed of HIF proteins, and the PHD enzymes. These enzymes represent an intersection between hypoxia, inflammation, metabolism and cell function as they are sensitive to oxygen and Krebs cycle metabolite concentrations, and can also regulate both anaerobic and aerobic metabolism via the HIF proteins.

PHD3 is expressed by a number of cells involved in the innate immune response, and loss of PHD3 has been shown to have conflicting effects depending on the context of infection and oxygen tension. In a model of sepsis, loss of PHD3 has been shown exacerbate symptoms and contribute to an exaggerated inflammatory response. Whole-animal knockout of PHD3 ($PHD3^{-/-}$), but not PHD1 ($PHD1^{-/-}$) or PHD2 ($PHD2^{+/-}$) shortened the survival of mice subjected to abdominal sepsis because of an overwhelming innate immune response typified by Systemic Inflammatory Response Syndrome (SIRS)(Kiss *et al.*, 2012). Bone marrow transfer to wild-type mice from $PHD3^{-/-}$ mice induced this phenotype in the recipient mice, indicating PHD3 knockout in innate immune cells specifically exacerbates this inflammatory response. This correlates with an increase in HIF-1α expression, increased expression of pro-inflammatory cytokines IL-6 and IL-1β, enhanced migration, and enhanced phagocytosis of zymosan and apoptotic cells in BMDMs derived from PHD3-deficient bone marrow.

These data suggest that PHD3 suppresses immune cell activation and HIF-1α activity in a model of extreme inflammation. In contrast, in other models of inflammation not typified by immune dysfunction, PHD3 is highly expressed by proinflammatory M1 macrophages, implicating a pro-inflammatory role for PHD3 expression (Escribese *et al.*, 2012). Moreover, myeloid-specific knockout of PHD3

in BMDMs does not change HIF-1α-dependent target gene expression as it does in sepsis, but does protect BMDMs against apoptotic cell death after serum starvation (Swain *et al.*, 2014), stressing the inflammatory context is key in understanding PHD3 responses.

Neutrophils express PHD3 and transcription of PHD3 is upregulated in peripheral blood neutrophils isolated from rheumatoid arthritis patients (Walmsley *et al.*, 2011). Moreover, loss of PHD3 enhances the resolution of an LPS-induced lung injury model in hypoxic animals (Walmsley *et al.*, 2011) through increased neutrophil apoptosis. Subsequent studies have shown that myeloid-specific loss of PHD3 can also dampen the immune response in a model of hind-limb ischemia (Beneke *et al.*, 2017), indicating PHD3 activity can exacerbate immune responses in the context of hypoxia and PHD3 knockdown is beneficial for inflammation resolution. Therefore, data from models of non-septic inflammation identify PHD3 as an attractive target when examining the immune response to hypoxia and infection.

It is important to note that as loss of PHD3, but not PHD2, has been implicated in encouraging tumour growth (Henze *et al.*, 2014), studies must consider the potential side effects of PHD3 inhibition. Furthermore, COPD patients have been associated with an increased incidence in single-nucleotide polymorphisms in *PHD3,* suggesting *PHD3* deletion is involved in the pathogenesis of COPD (Fang *et al.*, 2017).

4.1.2. Regulation of PHD3 by oxygen tension

PHD3 transcription and protein expression is up-regulated in hypoxia in a number of cancer cell lines (Appelhoff *et al.*, 2004), and subsequent studies have shown hypoxia also up-regulates PHD3 in neutrophils (Walmsley *et al.*, 2011) and macrophages (Escribese *et al.*, 2012). Hypoxia induces PHD3 protein expression in cancer cells by over 30 fold, compared to a 3 fold induction of expression of PHD2 (Place and Domann, 2013), although in normoxia, PHD2 protein levels are far higher than that of PHD3. It is possible this is partially to compensate for a loss of activity, as hydroxylase activity of PHD3 is dependent on molecular oxygen being available to hydroxylate HIF-1α and HIF-2α. Indeed, studies by Stiehl *et al* indicate PHD2 and

PHD3 maintain some hydroxylase activity in hypoxia, even at oxygen concentrations as low as 0.2%, with PHD3 more capable of hydroxylation at low oxygen concentrations (Stiehl *et al.*, 2006). The regulation of PHD3 activity by oxygen tension is further complicated by recent findings describing novel non-HIF targets of PHD3 hydroxylation (Köditz *et al.*, 2007), as well as non-hydroxylase enzymatic activity of PHD3 that occurs independent of oxygen tension. Therefore, it is likely that PHD3 has multiple different roles depending on oxygen tension due to modulation of both expression and hydroxylase activity. Oxygen tension may also change the cellular localisation of PHD3, with oxygen inducing the aggregation of PHD3 in oxidative conditions in a p62-dependent manner (Rantanen *et al.*, 2007)(Rantanen *et al.*, 2013).

4.1.3. PHD3 and regulation of HIF-1α and HIF-2α

Traditionally, PHD3 has been thought to act through hydroxylation of HIF-1α (see chapter 1.1.3). However, a number of studies investigating PHD3 deletion have failed to show modulation of HIF-1α signalling on loss of PHD3. Recent work has instead implicated PHD3 in the regulation of HIF-2α. SiRNA gene silencing of PHD1, PHD2 and PHD3 in HeLa cells showed HIF-1α levels are regulated only by silencing of PHD2 and that PHD2 is the dominant regulator of HIF-1α expression (Berra *et al.*, 2003). Work from Chris Pugh's lab has shown HIF-2α, but not HIF-1α, is stabilised at protein level in normoxia in PHD3 knockdowns, with even higher levels in hypoxic knockdowns, suggesting HIF-2α is dominantly regulated by PHD3. In neutrophils, loss of PHD3 does not appear to regulate HIF-1α expression, as hypoxic upregulation of HIF target genes is not affected by *Phd3* deletion (Walmsley *et al.*, 2011). *In vivo* evidence also suggests control of HIF-1α stability by PHD3 is limited. Embryos of $PHD3^{-/-}$ mice do not show abnormalities in the placenta, which requires proper control of HIF-1α expression for normal development (Dunwoodie, 2009). This is echoed by the finding that $PHD2^{-/-}$ embryos have severe placental defects and die between 12.5 and 14.5 days of embryonic development (Takeda *et al.*, 2006).

Expression of PHD3 blocks HIF-1α and HIF-2α CODD-linked fusion protein GAL expression, whereas PHD3 had no effect whatsoever on HIF-1α and HIF-2α N-

terminal oxygen degradation domain (NODD). By contrast, PHD2 prefers the C-terminal oxygen degradation domain (CODD) over the NODD by a factor of 20 (Pektas and Knapp, 2013). This preference for CODD hydroxylation may account for the apparent specificity of PHD3 in controlling the stability of HIF-2α over HIF-1α.

PHD3 expression itself is positively regulated by the activity of HIF proteins. This is evident as deletion of VHL induces PHD3 at a transcriptional level in Hep3B cells Enhanced expression of HIF-2α specifically, but not HIF-1α, is enough to enhance PHD3 mRNA expression in Hep3B cells (Aprelikova *et al.*, 2004). However, enhanced expression of either HIF-1α or HIF-2α enhances PHD3 expression in U2OS cells, indicating that the regulation of this pathway is cell-type specific.

A further level of complexity is implied as PHD3 has been shown to bind to HIF-1α C-terminal activation domain (CTAD) and act as a co-activator for HIF-1α in hypoxia (Schoepflin *et al.*, 2017). Therefore, PHD3 hydroxylase activity appears to regulate HIF-2α through hydroxylation of the NODD, but can also augment HIF-1α gene transcription through acting as a co-activator. This adds a further level of complication to the regulation of the hypoxic response pathway in different oxygen tensions, but also stresses the importance of investigating each component of the hypoxic response pathway as a functionally distinct target for manipulating cellular responses to hypoxia.

HIF-2α is a critical mediator of innate immunity. HIF-2α were shown to have limited expression of IL-1β, CXCK8 and VEGF through an NF-κB-independent mechanism, indicating HIF-2α mediates a pro-inflammatory response to hypoxia (Fang *et al.*, 2009). Moreover, HIF-2α has been shown to be a critical regulator of neutrophil inflammation, with HIF-2α prolonging neutrophil lifespan and contributing to neutrophil persistence at the site of inflammation (Thompson *et al.*, 2014). Neutrophils from PHD3-deficient animals were shown not to influence HIF-2α target gene expression in neutrophils, indicating PHD3 does not regulate HIF-2α, although as this regulation is often context specific, this does not preclude the possibility of interactions with HIF-2α in other inflammatory and infective contexts.

4.1.4. Non-HIF PHD3 targets: Advances and controversy

Although the role of PHD3 has traditionally been confined to the hydroxylation of HIF proteins, recent studies have shown PHD3 can interact with a diverse array of proteins, both through oxygen and 2-oxoglutarate-dependent hydroxylation and through interactions where protein-protein signalling is not dependent on hydroxylase activity.

Initial studies showed PHD3 can hydroxylate and suppress the activity of the transcription factor ATF-4 (Köditz *et al.*, 2007). ATF-4 is the point where many stress response pathways converge, and is involved in the protection of the cell from oxidant stress following ER stress (Harding *et al.*, 2003). Contemporaneous studies by Nakayama *et al* suggest PHD3 can form complexes with other PHD isotypes and Siah2, and formation of these complexes is enriched in hypoxia (Nakayama *et al.*, 2007). These complexes were found to modulate the effectiveness of PHD3 to hydroxylate HIF-1α.

Following these studies, it was clear PHD3 had a very distinct role in regulating cell processes aside from the regulation of HIF proteins. There was growing interest in understanding how PHD3 can interact with target proteins. A number of studies described a non-hydroxylation role for PHD3 in negatively regulating the NF-κB pathway (Xue *et al.*, 2010)(Fu and Taubman, 2010)(Fu and Taubman, 2013). These studies have described a role for PHD3 as able to inhibit differentiation of C2C12 myoblasts in a HIF-independent manner through inhibition of the NF-κB pathway via inhibition of IKKγ (Fu and Taubman, 2010). A catalytic-inactive mutant of PHD3 was shown to be capable of inhibiting IKKγ, and PHD3 inhibition of IKK-NF-κB signalling requires interaction with IKKγ (Fu and Taubman, 2013). NF-κB controls a host of genes involved in inflammation and is upregulated in a host of inflammatory diseases (Lawrence, 2009).

Studies from Henze show PHD3 can inhibit hypoxic tumour growth in a hydroxylase-independent manner (Henze *et al.*, 2014). PHD3 was shown to be silenced in glioma progression, and loss of PHD3 enhanced tumour cell survival and proliferation. G55 tumour cells expressing PHD3 shRNA where PHD3 expression

was inhibited were transfected with a hydroxylase-deficient mutant PHD3-HI96A. Expression of the hydroxylase-deficient protein was sufficient to suppress tumour growth, indicating hydroxylase activity was not needed for the tumour suppression activity of PHD3. More recent studies have also described hydroxylation and stabilization of the tumour suppressor gene p53 by PHD3 (Rodriguez *et al.*, 2018).

An incomplete list of PHD3 binding proteins discovered so far is shown in Table 4.1.4-1.

The complexity of PHD3 activity and transcription activation may contribute to the context-specific and cell-specific effects on PHD3 deletion, and explain why loss of PHD3 does not mirror phenotypes of HIF-1α or HIF-2α deletion.

PHD3 target	Role	Hydroxylation/Non-hydroxylation	Interaction
ACC2 (German *et al.*, 2017)	Fatty Acid Oxidation	Hydroxylation	Suppression
PKM2 (Luo *et al.*, 2011)	Glycolysis	Hydroxylation	Enhancement
hCLK2 (Xie *et al.*, 2012)	Cell cycle	Hydroxylation	Enhancement
β2-AR (Xie *et al.*, 2009)	Adrenergic signalling	Hydroxylation	Suppression
hPRP19 (Sato, Sakota and Nakayama, 2010)	Apoptosis	Non-hydroxylation	Enhancement
IKK-β (Xue *et al.*, 2010)	Survival	Non-hydroxylation	Suppression
IKK-γ (Fu and Taubman, 2013)	Survival	Non-hydroxylation	Suppression
Morg1 (Hopfer *et al.*, 2006)	MAPK signalling	Non-hydroxylation	PHD3 enhancement
Bcl2 (Liu *et al.*, 2010)	Survival	Non-hydroxylation	Suppression
ATF-4 (Köditz *et al.*, 2007)	cAMP signalling	Unknown	Suppression
OS-9 (Baek *et al.*, 2005)	HIF-1a hydroxylation	Non-hydroxylation	Enhancement
MAGEA11 (Aprelikova *et al.*, 2009)	Androgen receptor	Unknown	Suppression
MAPK6 (Rodriguez *et al.*, 2016)	MAPK signalling	Hydroxylation	Enhancement
TRiC (Masson *et al.*, 2004)	Chaperonin	Unknown	Unknown
p53 (Rodriguez *et al.*, 2018)	Apoptosis	Hydroxylation	Enhancement
Siah2 (Nakayama *et al.*, 2007)	PHD3 degraded	Non-hydroxylation	PHD3 degradation
PHD1 (Nakayama *et al.*, 2007)	Hypoxic Response	Non-hydroxylation	Multimerization
PHD2 (Nakayama *et al.*, 2007)	Hypoxic Response	Non-hydroxylation	Multimerization
PHD3 (Nakayama *et al.*, 2007)	Hypoxic Response	Non-hydroxylation	Multimerization

Table 4.1.4-1: PHD3 binding partners. A list of binding partners that interact with PHD3, either through hydroxylation or non-hydroxylation Adapted and updated from Place and Domann, 2013.

4.1.5. PHD3 and metabolism

PHD3 can regulate metabolism both directly and through the stabilisation of HIF-2α. HIF-2α can moderate glucose metabolism through the activity of PPAR-α (Aragonés *et al.*, 2008), although studies in HIF-1α and HIF-2α over-expressing cells indicate PGK-1 and LDHA expression are not induced by overexpression of HIF-2α as they are by HIF-1α overexpression (Hu *et al.*, 2003). HIF-2α can also positively regulate the transcription of the mitochondrial cytochrome c oxidase (COX) subunit COX4I2 in hypoxia as part of the cell optimising aerobic metabolism machinery to hypoxic conditions (Fukuda *et al.*, 2007). Fatty acid metabolism is controlled by HIF-2α expression; a study in hepatocytes showed HIF-2α controlled adipose differentiation-related protein (*Adfp)* expression and β-oxidation, and that activation of HIF-2α was capable of suppressing fatty acid β-oxidation (Rankin *et al.*, 2009).

In addition to indirectly regulating glucose metabolism through HIF-2α, a number of studies have also confirmed the ability of PHD3 to regulate glycolysis directly. Two contemporaneous studies describe the interaction of PHD3 with the glycolytic enzyme PKM2 and the ability of PHD3 to modulate glucose metabolism (Chen *et al.*, 2011)(Luo *et al.*, 2011). Subsequent studies have shown silencing of PHD3 regulates the expression of a wide variety of metabolic genes involved in glucose metabolism, including glycolytic enzymes LDHA and GLUT1, the Krebs cycle enzyme MDH2, and G6PD, the critical rate-limiting enzyme of the pentose phosphate pathway (Miikkulainen *et al.*, 2017). Given that neutrophils are reliant on glycolysis, and PHD3 has been shown to inhibit neutrophil hypoxia survival, it will be important to investigate whether PHD3 expression regulates neutrophil metabolism and whether this affects neutrophil lifespan in hypoxia. Acute deletion of PHD3 has been investigated as a potential target for metabolic diseases such as diabetes, as PHD3 deletion improves sensitivity and reduces the severity of a model of diabetes in mice through stabilisation of HIF-2α, which increases Irs2 transcription and insulin-stimulated Akt activation (Taniguchi *et al.*, 2013).

4.1.6. PHD3 regulates neutrophil apoptosis

Loss of PHD3 has no effect on apoptosis in neutrophils cultured at room oxygen (21%) or neutrophils exposed to the inflammatory stimulus LPS. However, PHD3 is

a critical modulator of neutrophil apoptosis in hypoxic (1%) conditions (Walmsley *et al.*, 2011). This correlated with enhanced expression of Siva-1, an apoptosis-inducing gene, and abrogation of Bcl-X_L upregulation in hypoxia. Similarly, PHD3 knock out animals have fewer neutrophils at the site of inflammation after induction of a sterile lung inflammation with LPS, and neutrophils isolated from the airways were more apoptotic in hypoxia but not normoxia. In a model of hind-limb ischaemia, $PHD3^{-/-}$ animals have fewer Ly6G/CD11b-positive cells at the site of injury 3 days after surgery, indicating a dampened inflammatory response or more efficient clearance of neutrophils from the site of inflammation potentially through enhanced apoptosis (Beneke *et al.*, 2017). Whether or not enhanced apoptosis influences resolution of inflammation in a model of infection is unclear.

4.1.7. Neutrophil killing of *Staphylococcus aureus*

Staphylococcus aureus is a Gram-positive, commonly commensal pathogenic bacteria which can cause a range of pathologies including skin infections, septicaemia, endocarditis and necrotising pneumonia (Klevens *et al.*, 2007). Neutrophils are known to be essential for the control of *S. aureus* infection. Patients with conditions typified by compromised neutrophil numbers or function, such as severe congenital neutropenia, leukocyte adhesion deficiency, Chediak-Higashi syndrome and neutrophil-specific granule deficiency, present with frequent incidences of *S. aureus* infection (Lekstrom-Himes and Gallin, 2000). Moreover, in a model of *S. aureus* infection, repletion of neutrophils significantly compromises mouse survival (Gresham *et al.*, 2000). Neutrophils clear *S. aureus* through phagocytosis and then digestion with toxic granule contents including ROS and antimicrobial peptides. The induction of neutrophil respiratory burst is known to be essential for *S. aureus* killing as patients with chronic granulatomous disease, a disease characterised by a defect in NADPH oxidase and associated defects in ROS production, suffer recurrent bacterial infections including infections of *S. aureus* (Lekstrom-Himes and Gallin, 2000).

S. aureus have a number of mechanisms to evade killing, including inhibiting neutrophil recruitment, phagocytosis, and inducing neutrophil lysis following phagocytosis (McGuinness, Kobayashi and DeLeo, 2016). These can allow *S. aureus*

to exist in neutrophils, which can then act as a pool of infection and passage of bacteria into tissues. As such, neutrophil infiltration into the site of infection, although essential for control of *S. aureus* infection, can also negatively affect the resolution of infection. Limiting neutrophil migration into the site of infection through knockout of integrin-associated protein (CD47) expression can actually improve survival in response to an interperitoneal *S. aureus* infection (Gresham *et al.*, 2000). This is in contrast with other pathogens where CD47 deficiency can result in increased bacterial burden and mortality (Lindberg *et al.*, 1996).

4.1.8. Neutrophil killing of *Streptococcus pneumoniae*

Streptococcus pneumoniae is a pathogenic Gram-positive bacteria, the main cause of both pneumonia and meningitis in children and the elderly. *S. pneumoniae* is capable of inducing bacteraemia and sepsis (Christensen *et al.*, 2012). Killing of *S. pneumoniae* differs slightly from that of *S. aureus* in that it is thought to be mediated through the activity of serine proteases as opposed to reactive oxygen species. Inhibition of NADPH oxidase activity does not modulate the efficiency of *S. pneumonia* killing by isolated neutrophils (Standish and Weiser, 2009). Moreover, mice with deficiency in the $gp91^{phox}$ subunit of NADPH oxidase have been found to fare better in a model of fulminant pneumonia, with enhanced bacterial clearance and survival compared to wildtype controls (Marriott *et al.*, 2008).

4.1.9. Hypoxia and bacterial killing

Wound healing and bacterial clearance from the skin is impaired in hypoxia, and supplemental inspired oxygen has long been known to improve wound healing and control infection (Knighton, Halliday and Hunt, 1984). Studies by McGovern *et al* indicate that loss of respiratory burst function in hypoxia due to the absence of molecular oxygen reduces the capacity of neutrophils to kill *S. aureus in vitro* (McGovern *et al.*, 2011). Likewise, inhibition of neutrophils with the NADPH-oxidase inhibitor DPI significantly inhibitors killing of *S. aureus* (Standish and Weiser, 2009). Subsequent studies from our group show mice with either localised *S. aureus* or systemic *S. pneumonia* infection have enhanced sickness in hypoxia, which can be rescued by inhibition of HIF-1α (Thompson *et al.*, 2017), implicating the hypoxic response pathway in regulating the neutrophil response to *S. aureus* and

S. pneumoniae. That killing of both *S. aureus* and *S. pneumonia*e are compromised by hypoxia implicates a mechanism independent of reactive oxygen species production, although this has yet to be investigated. Modulation of other components of the hypoxic response pathway have been shown to alter the response of neutrophils to inflammation, but not to bacterial infection specifically; inhibition of either PHD3 and HIF-2α can inhibit neutrophilic inflammation (Walmsley *et al.*, 2011)(Thompson *et al.*, 2014), but whether manipulation of these components is advantageous in infective inflammation models is unclear. There has been little work investigating how PHD3 can modulate neutrophil bacterial killing and function.

4.1.10. Aims of this chapter

Work so far has identified PHD3 as an essential modulator of immune function in inflammatory disease and hypoxia-driven inflammation such as ischaemia reperfusion injury and acute injury. Other components of the hypoxic response pathway have been investigated and HIF-1α has been shown to exacerbate infection in the context of hypoxia.

My hypothesis is that:

PHD3 expression is associated with prolonged neutrophil inflammation in the context of infection and that inhibiting PHD3 expression can improve bacterial clearance and resolution of infection.

In this chapter I aim to:

1. Examine the effects of knocking out myeloid PHD3 expression in a model of localized skin infection to assess whether loss of PHD3 is beneficial in a model of infective inflammation to complement previous studies from the group in sterile inflammation models.
2. Investigate whether PHD3 influences the capacity of neutrophils to phagocytose and clear bacteria *in vitro.*
3. Interrogate the mechanism of enhanced inflammation resolution in PHD3-deficient animals.
4. Measure metabolic flux in PHD3-deficient neutrophils in the context of systemic hypoxia to parallel previous *in vitro* studies (Chapter 3).

4.2. Results

4.2.1. PHD3 is upregulated in hypoxia and loss of PHD3 has no systemic health effects in normoxic or hypoxic animals

Knockdown of *PHD3* was confirmed through qPCR of neutrophils isolated from mouse BAL. BAL cells were cultured in both normoxia and hypoxia and *PHD3* expression analysed via qPCR. Neutrophils isolated from *PHD3*$^{fl/fl}$ LysMCre$^{+/-}$ mice have significantly lower expression of *PHD3* transcript in both normoxia (Mean (±SEM), WT = 0.0754 (0.0200), KO = 0.00283 (0.000535), n = 4, p**<0.01)(Figure 4.2.1-1, A) and hypoxia (Mean (±SEM), WT = 2.45 (0.478), KO = 0.0378 (0.00960), n = 4, p***<0.001)(Figure 4.2.1-1, B). Low-level *PHD3* expression in neutrophils isolated from *PHD3*$^{fl/fl}$ LysMCre$^{+/-}$ may be due to a small number of contaminating lung epithelial cells in the BAL.

Rested mice with myeloid-specific *PHD3* deletion have no negative health consequences and equivalent weights (mean (±SEM), WT = 24.7 (0.651), KO = 24.0 (0.714) grams, n = 22)(Figure 4.2.1-1, A) and temperature (mean (±SEM), WT = 38.3 (0.127), KO = 38.2 (0.114) °C, n = 22)(Figure 4.2.1-1, B) at baseline.

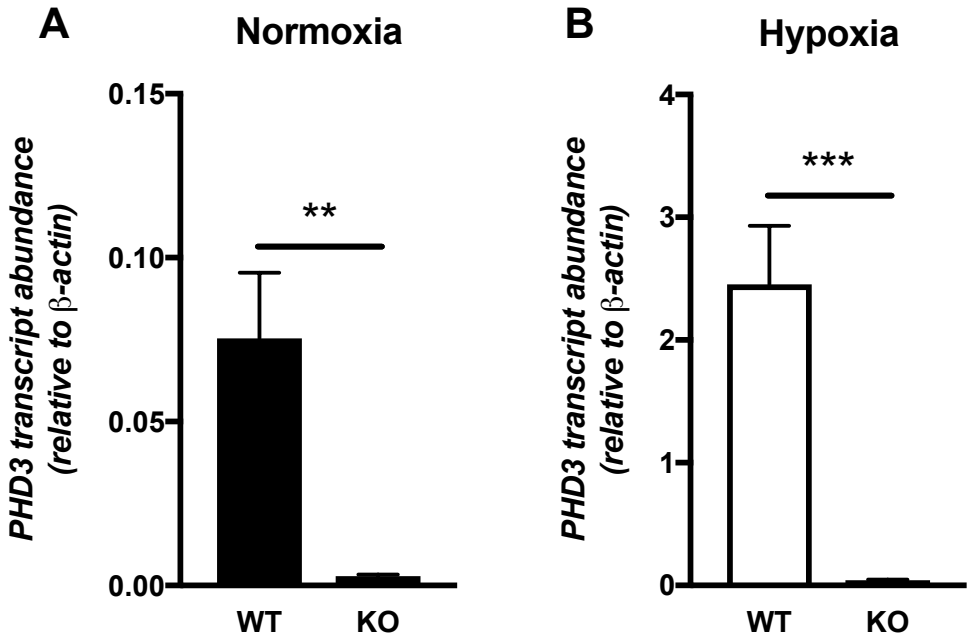

Figure 4.2.1-1. Successful knockout of *PHD3* expression in murine BAL neutrophils. *PHD3*$^{fl/fl}$ LysMCre$^{+/-}$ and littermate LysMCre$^{-/-}$ mice were nebulised with 1mg/ml LPS, housed for 24 hours and then neutrophils isolated via bronchoalveolar lavage. Isolated neutrophils were cultured in normoxia (21% O_2)(A) or hypoxia (1% O_2)(B) for 4 hours, RNA extracted and *PHD3* transcript levels measured via quantitative PCR and normalised to *β-actin* transcript levels. Data expressed as mean±SEM and analysed with unpaired two-tailed Student's T tests, p**<0.01, p***<0.001. WT = wildtype (*PHD3*$^{fl/fl}$ LysMCre$^{-/-}$) . KO = knockout (*PHD3*$^{fl/fl}$ LysMCre$^{+/-}$).

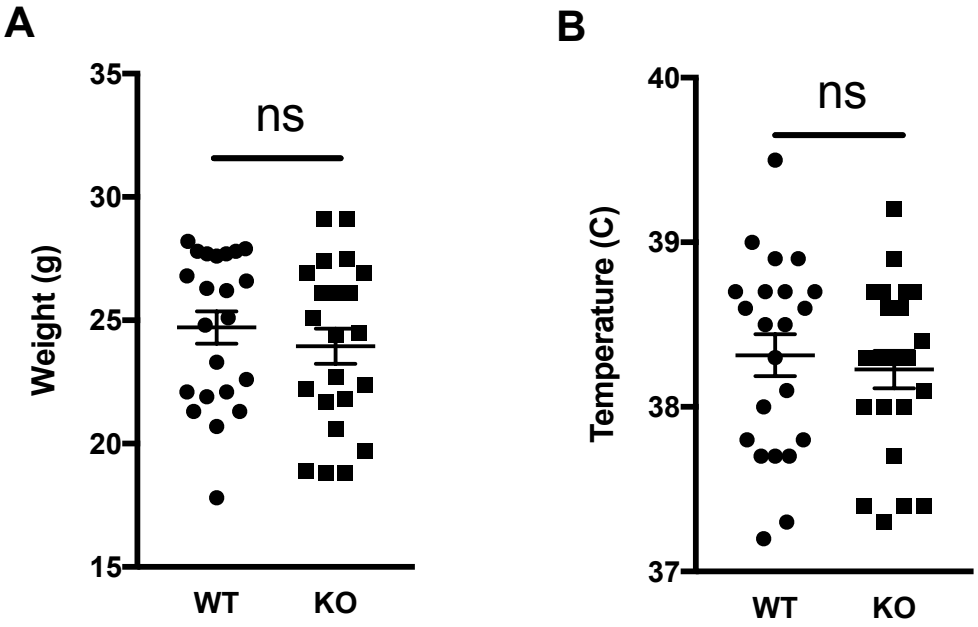

Figure 4.2.1-2. Unchallenged mice with myeloid-specific PHD3 knockout are phenotypically normal and display no signs of sickness. *PHD3*$^{fl/fl}$ LysMCre$^{+/-}$ and littermate *PHD3*$^{fl/fl}$ LysMCre$^{-/-}$ mice were weighed (A) and rectal temperatures taken (B) at baseline. Data expressed as mean±SEM and analysed with unpaired two-tailed Student's T tests, ns. WT = wildtype (*PHD3*$^{fl/fl}$ LysMCre$^{-/-}$), KO = knockout (*PHD3*$^{fl/fl}$ LysMCre$^{+/-}$).

4.2.2. Loss of PHD3 is beneficial for the resolution of a *S. aureus* skin abscess

To examine how PHD3 deletion influences the response of neutrophils to an infection, mice were injected with 50µl of $1x10^9$ CFU/ml SH1000 *S. aureus* into the right flank and rectal temperature, weight, abscess size and sickness scores taken every day to monitor the health of the animals and progression of infection.

Mice show no signs of gross sickness at any point during the experiment (mean (±SEM), WT = 0 (0), KO = 0 (0), n = 6)(Figure 4.2.2-1, B, C). Even mice with large abscesses extending to an area greater than $1cm^2$ exhibit no systemic symptoms of infection (Figure 4.2.2-1, A). Knockout and wild-type mice have equivalent rectal temperatures over the course of the 7 days of infection (mean (±SEM), WT day 0 = 38.2 (0.186), KO day 0 = 38.2 (0.317), WT day 1 = 38.0 (0.257), KO day 1 = 37.8 (0.105), WT day 7 = 37.9 (0.251), KO day 7 = 37.9 (0.304), n = 6)(Figure 4.2.2-2, A). Some mice experience a change in temperature the day following initial infection; however, the degree of this change is equivalent between WT and KO mice (mean (±SEM), WT = -0.207 (0.235), KO = 0.0786 (0.208), n= 14, ns)(Figure 4.2.2-2, B). Mice experience some weight loss in the first day of infection (mean (±SEM), WT day 0 = 23.85 (1.11), KO day 0 = 22.4 (1.07), WT day 1 = 22.4 (1.35), KO day 1 = 21.2 (1.05) grams, n = 6)(Figure 4.2.2-2, C), which then recovers completely by day 3 (mean (±SEM), WT day 3 = 23.0 (1.09), KO day 3 = 22.4 (0.908) grams, n = 6)(Figure 4.2.2-2, C). There is no difference in weight loss between WT and KO mice in the first 24 hours of infection (mean (±SEM), WT = -5.51 (0.687), KO = -4.32 (0.554) grams, n = 14)(Figure 4.2.2-2, D), indicating loss of PHD3 in the neutrophils has no significant impact on the systemic health of the mice in this model.

The progression of the localised bacterial infection is profoundly affected by the loss of PHD3. Mice with a myeloid-specific PHD3 deletion have macroscopically smaller abscesses over the course of the infection (Figure 4.2.2-3, A). Abscesses were significantly smaller at days 1 and 2 after inoculation (mean (±SEM), WT day 1 = 33.2 (9.75), KO day 1 = 8.67 (2.82), WT day 2 = 74.5 (11.3), KO day 2 = 42.7 (4.95), n = 6, $p^*<0.05$)(Figure 4.2.2-3, B). Abscesses from knockout mice were not

significantly smaller at later timepoints because of the large standard deviation in abscess sizes of wildtype mice at this point in the experiment. However, the progression of infection was significant different between Cre- and Cre+ mice by ANCOVA analysis.

Abscesses culled at 2, 4 and 7 days were homogenised and bacterial burden calculated as the number of viable CFUs per abscess. At 2 days after infection, when abscess size was significantly different, knockout mice have significantly less viable bacteria in the abscess compared to wildtype mice (mean (±SEM), WT day 2 = 4.49 $x10^6$ ($2.47x10^5$), KO day 2 = $1.98x10^6$ ($4.98\ x10^5$) CFU, n = 4, p*<0.05)(Figure 4.2.2-4, A). At later time-points, bacterial counts are not significantly lower in KO mice (mean (±SEM), WT day 4 = $1.35x10^7$ ($6.95x10^6$), KO day 4 = $4.83x10^6$ ($2.59x10^6$), WT day 7 = $2.21x10^7$ ($1.10x10^7$), KO day 7 = $1.15x10^7$ ($5.97x10^6$) CFU, n = 4, p*<0.05)(Figure 4.2.2-4, A). This is because of a high variation in abscess CFUs in the wildtype mice. Some abscesses have begun to resolve at this point in the infection, whereas others are continuing to grow, leading to a wide degree of variation within the experiment group.

The size of the abscesses is proportional to the concentration of bacteria in the tissue, indicating size of the abscess relates directly to the efficiency of bacterial control in the tissue (Slope mean (±SEM), WT = $4.61x10^6$ ($1.07x10^6$), KO = $9.17x10^6$ ($1.71\ x10^6$) (Figure 4.2.2-4, B). Larger abscesses in wildtype animals therefore reflect less efficient bacterial killing and clearance.

Abscesses were lysed and MPO activity measured. At 2, 4 and 7 days, MPO activity of the tissue is equivalent between wildtype and knockout mice (mean (±SEM), Day 2 Cre- = 0.241 (0.0941), Day 2 Cre+ = 0.395 (0.0471), Day 4 Cre- = 0.569 (0.183), Day 4 Cre+ = 0.474 (0.127), Day 7 Cre- = 0.206 (0.165), Day 7 Cre+ = 0.257 (0.252), n = 4)(Figure 4.2.2-5, A).

Abscess tissue from wildtype animals is heavily fibrotic, with a greater degree of destruction of the ultrastructure of the tissue than in knockout mice (Figure 4.2.2-6, A-B). Myeloperoxidase staining shows neutrophil infiltration into the adipose layer of the skin in wildtype abscess, whereas abscesses from knockout mice are typified

by neutrophils in the subcutaneous tissue, but little neutrophil activity in the skin (Figure 4.2.2-6, A).

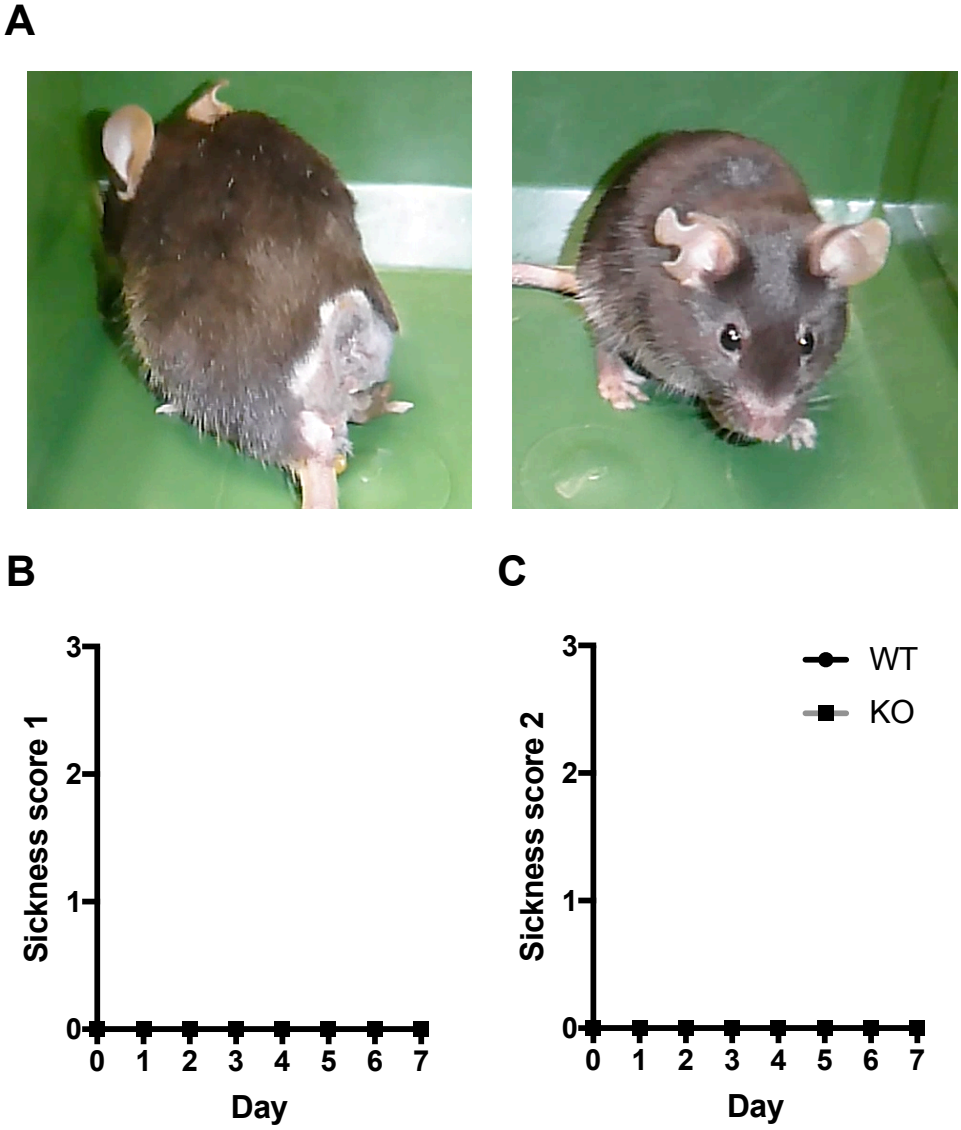

Figure 4.2.2-1: Mice with myeloid specific knockout of *PHD3* show no macroscopic signs of sickness following subcutaneous infection with *Staphylococcus aureus.* *PHD3*$^{fl/fl}$ LysMCre$^{+/-}$ and littermate *PHD3*$^{fl/fl}$ LysMCre$^{-/-}$ mice were inoculated with 5x10^{7} *S. aureus* in 50µl of PBS subcutaneously into the right flank and sickness assessed through mouse appearance and behaviour (A, B, C). Data expressed as mean±SEM and analysed with linear regression analysis followed by ANCOVA, n = 12, ns. WT = wildtype (*PHD3*$^{fl/fl}$ LysMCre$^{-/-}$), KO = knockout (*PHD3*$^{fl/fl}$ LysMCre$^{+/-}$).

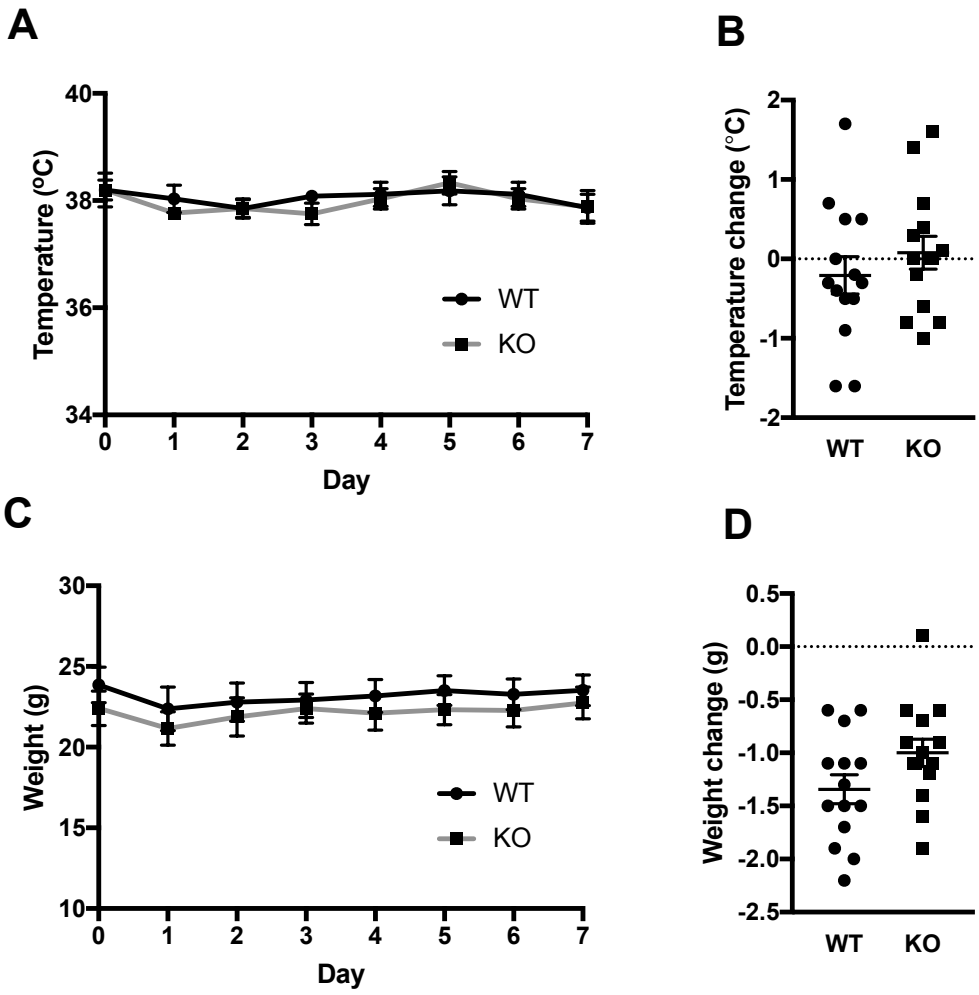

Figure 4.2.2-2: Mice with myeloid specific knockout of *PHD3* have equivalent weight loss and temperature change to wildtype mice following subcutaneous infection with *Staphylococcus aureus.* Mice were inoculated with $5x10^7$ *S. aureus* in 50µl PBS subcutaneously into the right flank and rectal temperature (A, B) taken and weight recorded (C,D) every day. Data expressed as mean±SEM and analysed with ANCOVA (A, C) or unpaired two-tailed Student's T tests (B, D), n = 14, ns. WT = wildtype (*PHD3*$^{fl/fl}$ LysMCre$^{-/-}$), KO = knockout (*PHD3*$^{fl/fl}$ LysMCre$^{+/-}$).

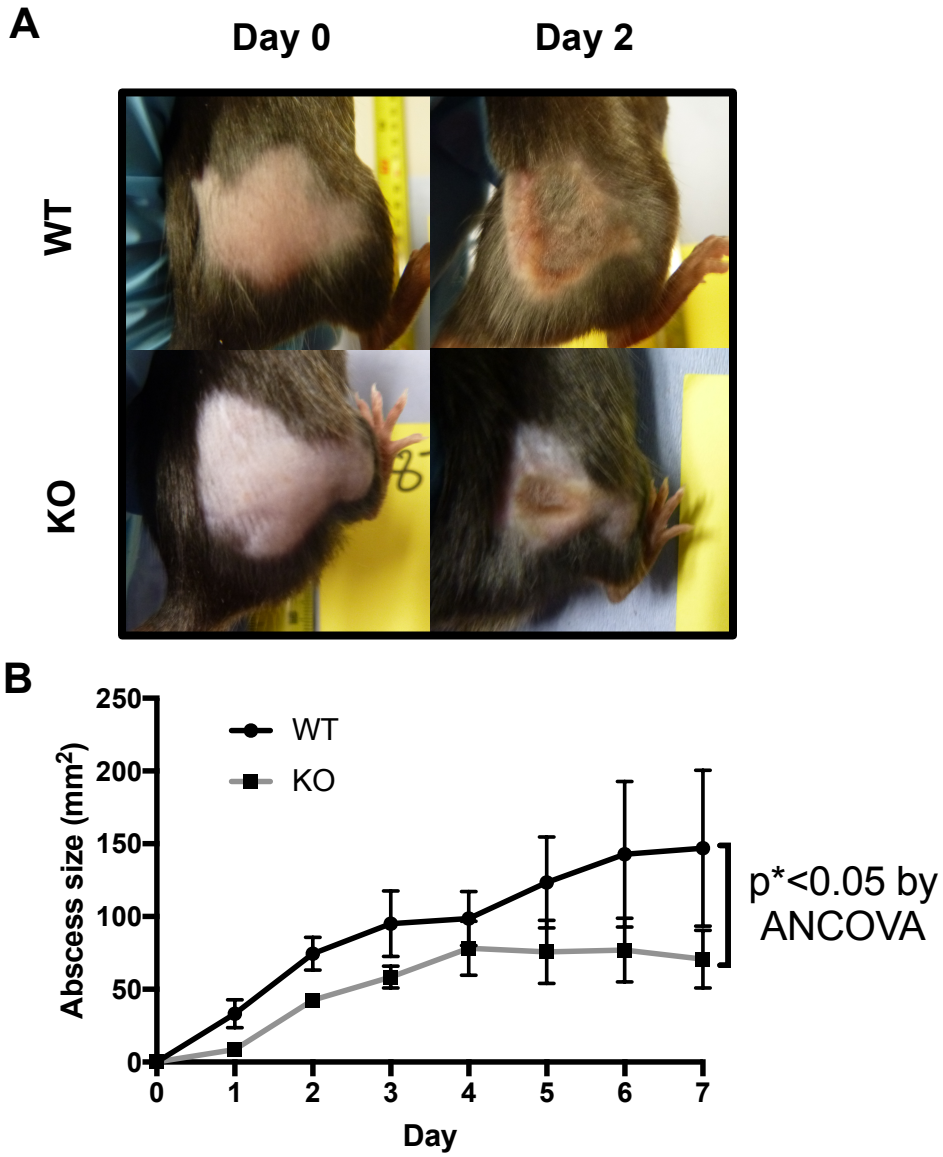

Figure **4.2.2-3: Myeloid specific knockout of PHD3 reduces localized skin inflammation in response to *Staphylococcus aureus* infection.** Mice were inoculated with $5x10^7$ *S. aureus* in 50µl PBS subcutaneously into the right flank and abscesses developed over the course of 7 days, with noticeable abscesses by day 2 (A, B). Abscess size was measured on a daily basis from photographs of the abscess (B). Data expressed as mean±SEM and slopes of WT and KO compared via ANCOVA, n = 12, p*<0.05. WT = wildtype (*PHD3*$^{fl/fl}$ LysMCre$^{-/-}$), KO = knockout (*PHD3*$^{fl/fl}$ LysMCre$^{+/-}$).

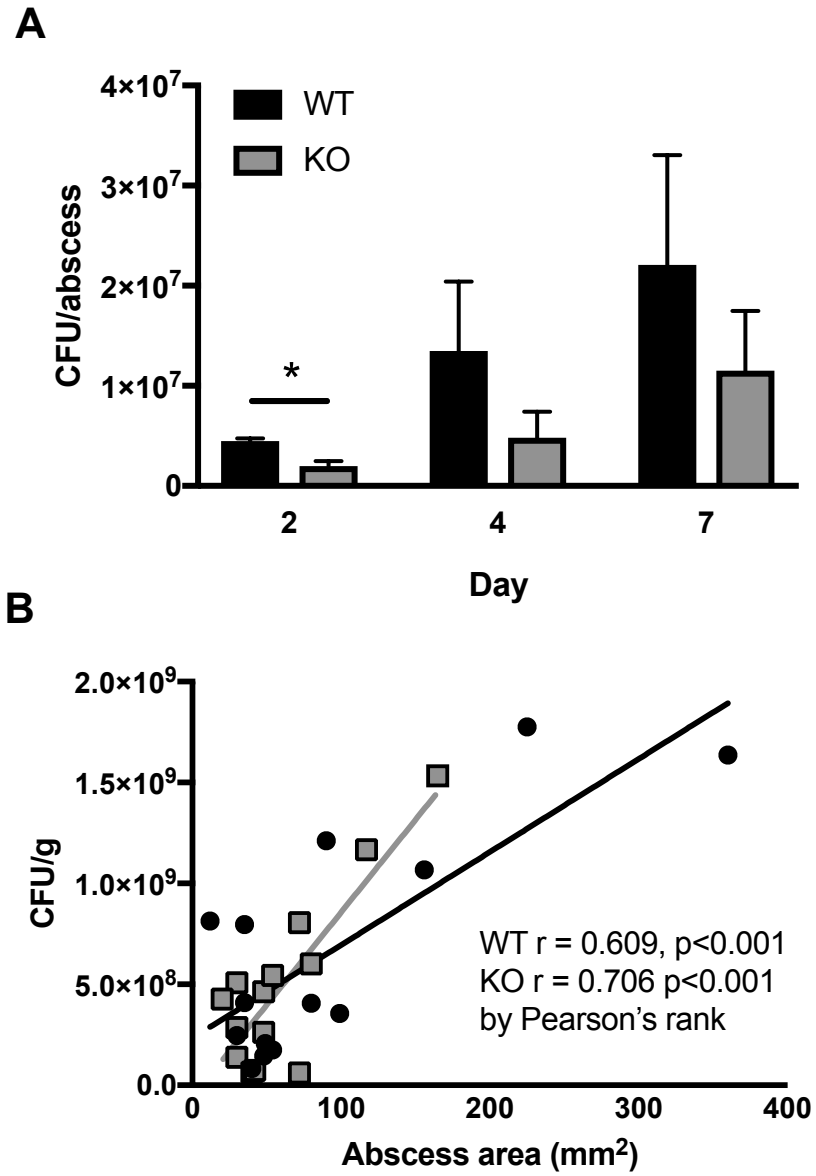

Figure 4.2.2-4: Myeloid specific knockout of PHD3 enhances bacterial control in a model of *Staphylococcus aureus* skin infection. Mice were inoculated with $5x10^7$ *S. aureus* in 50µl PBS subcutaneously into the right flank and abscesses developed over the course of 7 days. Mice were culled at day 2, 4 and 7 and abscesses homogenised and viable bacteria counted. Data expressed as mean±SEM and analysed with paired two-tailed Student's T tests, p*<0.05, n = 4 (A), or Pearson's rank coefficient and ANCOVA (B), n = 12. CFU/g and abscess area are significantly correlated, but WT and KO are not significant as determined by ANCOVA. WT = wildtype (*PHD3*$^{fl/fl}$ LysMCre$^{-/-}$), KO = knockout (*PHD3*$^{fl/fl}$ LysMCre$^{+/-}$).

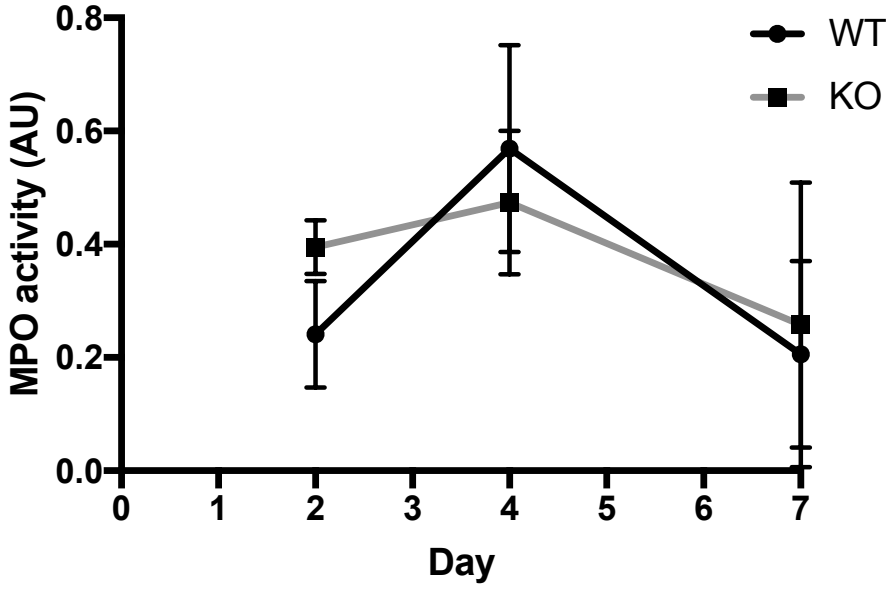

Figure 4.2.2-5: Myeloid specific knockout of PHD3 has no effect on MPO concentration at the site of infection. Mice were inoculated with $5x10^7$ *S. aureus* in 50µl PBS subcutaneously into the right flank and abscesses developed over the course of 7 days. Mice were culled at day 2, 4 and 7 and abscesses homogenised and MPO activity measured via fluorimetric assay. Data expressed as mean±SEM and analysed with paired two-tailed Student's T tests, n = 4. WT = wildtype (*PHD3*$^{fl/fl}$ LysMCre$^{-/-}$), KO = knockout (*PHD3*$^{fl/fl}$ LysMCre$^{+/-}$).

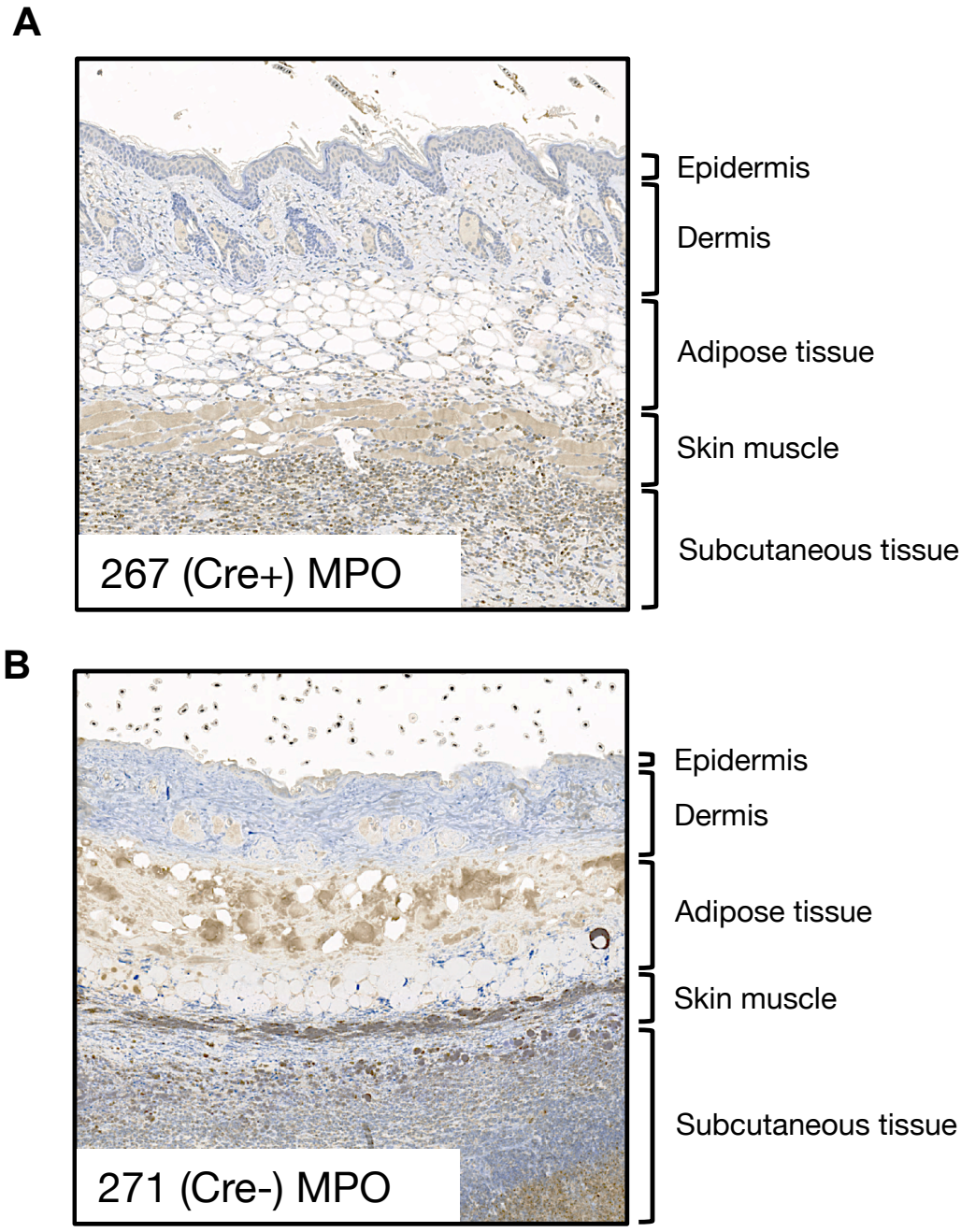

Figure 4.2.2-6: Tissue damage associated with a *Staphyloccocus aureus* abscess is diminished in mice with myeloid-specific PHD3 knockout. Mice were inoculated with $5x10^7$ *S. aureus* in 50µl PBS subcutaneously into the right flank and abscesses developed over the course of 7 days. Mice were culled at day 7 and abscesses preserved in 4% formaldehyde before processing and staining with anti-MPO antibody (A, B). Histology representative of n = 3.

4.2.3. Loss of PHD3 enhances resolution of infection in a model of Streptococcal pneumonia

To ascertain whether myeloid-specific knockout of PHD3 can adequately protect against bacterial infection in a more serious, fulminant model of infection, mice were inoculated with 50µl of $1x10^7$ $CFUml^{-1}$ mD39 *S. pneumonia* intratracheally and culled after 14 hours..

Knockout mice have significantly lower bacterial burden in the airways at 24 hours post inoculation compared to wildtype mice (mean (±SEM), WT = $2.23x10^5$ ($1.18x10^5$), KO = $4.23x10^3$ ($2.38x10^3$) CFU, n = 10, p*<0.05)(Figure 4.2.3-1, A). Mice with fulminant pneumonia have bacteria present in their blood. Knockout mice appear to have slightly reduced bacterial burden in the blood (mean (±SEM), WT = $1.66x10^7$ ($1.07x10^7$), KO = $2.41x10^5$ ($1.68x10^5$) CFU, n = 10, p=0.095)(Figure 4.2.3-1, B). Total numbers of infiltrating inflammatory cells in the airways are equivalent between wildtype and knockout mice (mean (±SEM), WT = $9.89x10^6$ ($1.18x10^6$), KO = $10.5x10^6$ ($1.21x10^6$), n = 10, ns)(Figure 4.2.3-1, C), as are neutrophil numbers (mean (±SEM), WT = $8.08x10^6$ ($9.22x10^5$), KO = $8.80x10^6$ ($8.59x10^5$), n = 10, ns(Figure 4.2.3-1, D). Airway IgM levels were also equivalent, indicating comparable vascular leak between genotypes (mean (±SEM), WT = 222 (28.2), KO = 204 (28.9) ng/ml, n = 10, ns)(Figure 4.2.3-1, E).

ELISA of BAL inflammatory cytokines shows no evidence that knockdown of PHD3 modulates the expression of inflammatory cytokines or chemokines. All neutrophil-derived chemokines measured were equivalent between wildtype and knockout mice, including the neutrophil chemoattractants CXCL1/KC (mean (±SEM), WT = 22.2 (7.11), KO = 18.6 (5.04) pg/ml, n = 10, ns)(Figure 4.2.3-2, A) and CCL4/MIP-1β (mean (±SEM), WT = 165 (32.1), KO = 122 (20.1), n = 10, ns)(Figure 4.2.3-2, A). Expression of neutrophil pro-inflammatory cytokines is unchanged by loss of PHD3, including IL-1α (mean (±SEM), WT = 12.7 (1.40), KO = 10.9 (1.15) pg/ml, n = 10, ns)(Figure 4.2.3-2, B), IL-1β (mean (±SEM), WT = 13.8 (1.69), KO = 12.5 (0.935) pg/ml, n = 10, ns)(Figure 4.2.3-2, B), IL-6 (mean (±SEM), WT = 277 (45.7), KO = 210 (42.3) pg/ml, n =10, ns), IL-12 (mean (±SEM), WT = 7.72 (1.59), KO = 7.66 (0.890) pg/ml, n = 10, ns) and TNF-α (mean (±SEM), WT =

167 (27.3), KO = 133 (21.5) pg/ml, n = 10, ns). Levels of the anti-inflammatory cytokine IL-10 were also unchanged (mean (±SEM), WT = 5.11 (1.03), KO = 5.70 (1.17) pg/ml, n = 10, ns).

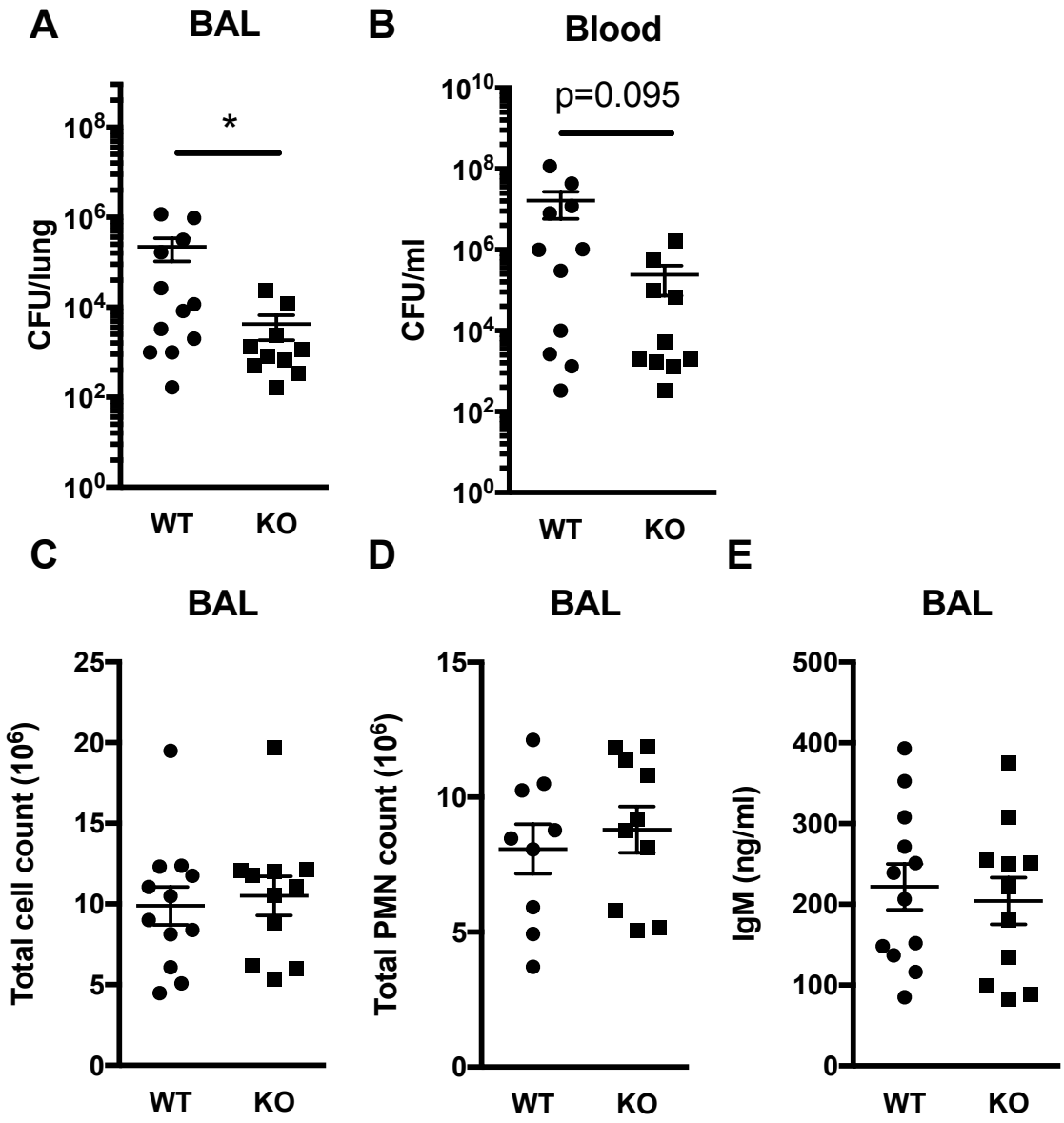

Figure 4.2.3-1: Mice with myeloid specific knockout of PHD3 are more efficient at bacterial clearance than wildtype controls in a model of fulminant *Streptococcus pneumoniae* lung infection. Mice were inoculated with $1x10^7$ *S. aureus* in 50µl PBS intratracheally and culled after 14 hours. Bacteria were grown from BAL (A) and blood (B) samples, and BAL cell counts (C), neutrophil differentials (D) and IgM concentration (E) calculated. Data expressed as mean±SEM and analysed with unpaired two-tailed Student's T tests, n = 11. WT = wildtype (*PHD3*$^{fl/fl}$ LysMCre$^{-/-}$), KO = knockout (*PHD3*$^{fl/fl}$ LysMCre$^{+/-}$). Experiments performed by Professor Sarah Walmsley.

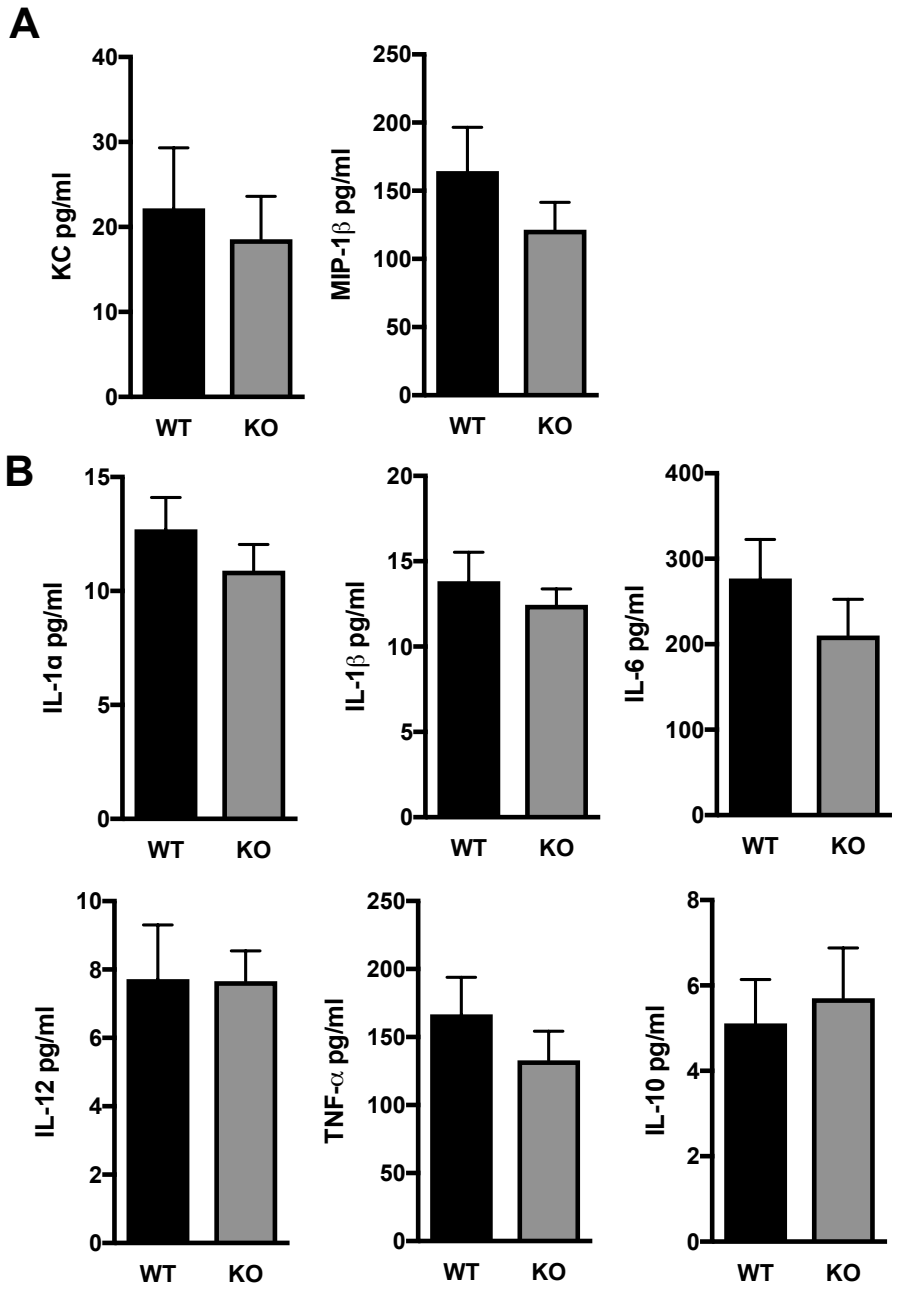

Figure 4.2.3-2: BAL cytokine and chemokine levels are equivalent in wildtype and knockout mice exposed to a fulminant *Streptococcus pneumoniae* lung infection. Mice were inoculated with $1x10^7$ *S. aureus* in 50µl PBS intertracheally and culled after 14 hours. BAL chemokines KC and MIP-1β **(A)** and cytokines IL-1α, IL-1β, IL-6, IL-12, TNF-α and IL-10 **(B)** concentrations were determined by ELISA. Data expressed as mean±SEM and analysed with paired two-tailed Student's T tests, n = 11. WT = wildtype (*PHD3*$^{fl/fl}$ LysMCre$^{-/-}$), KO = knockout (*PHD3*$^{fl/fl}$ LysMCre$^{+/-}$). Experiments performed by Professor Sarah Walmsley.

4.2.4. Loss of PHD3 does not influence systemic effects of infection in mice experiencing acute systemic hypoxia

To ascertain whether PHD3 influences response to infection in the context of systemic hypoxia, mice were inoculated with *S. aureus* subcutaneously into the right flank and then housed in either room oxygen (21% O_2) or hypoxia (10% O_2). Previous studies by A.A.R. Thompson have shown that mice inoculated with *S. aureus* and house in hypoxia become extremely ill by 24 hours after inoculation. We chose 14 hours as a timepoint for this reason.

Mice inoculated with *S. aureus* become ill after being housed in hypoxia for 14 hours. Mice housed in hypoxia have significantly higher sickness scores (mean (±SEM), WT N = 0 (0), WT H = 1.13 (0.350), KO N = 0 (0), KO H = 1.25 (0.164), n = 8, p**<0.01, p****<0.0001)(Figure 4.2.3-1, A)(mean (±SEM), WT N = 0 (0), WT H = 3.25 (1.01), KO N = 0 (0), KO H = 2.75 (0.773), n = 8, p**<0.01)(Figure4.2.3-1, B) and a significant degree of hypothermia (mean (±SEM), WT N = -0.225 (0.149), WT H = -2.53 (0.390), KO N = -0.45 (0.290), KO H = -3.08 (0.275)°C, n = 4, p**<0.01, p***<0.001)(Figure 4.2.3-1, C) and weight loss (mean (SEM), WT N = -0.475 (0.125), WT H = -1.85 (0.477), KO N = -0.8 (0.324), KO H = -2.08 (0.320) grams, n=4, p*<0.05)(Figure 4.2.3-1, D). There was no difference between wildtype and knockout animals in either normoxia or hypoxia in terms of systemic illness in the animals, indicating loss of PHD3, even in hypoxia in the context of infection, does not negatively influence the health of the mice.

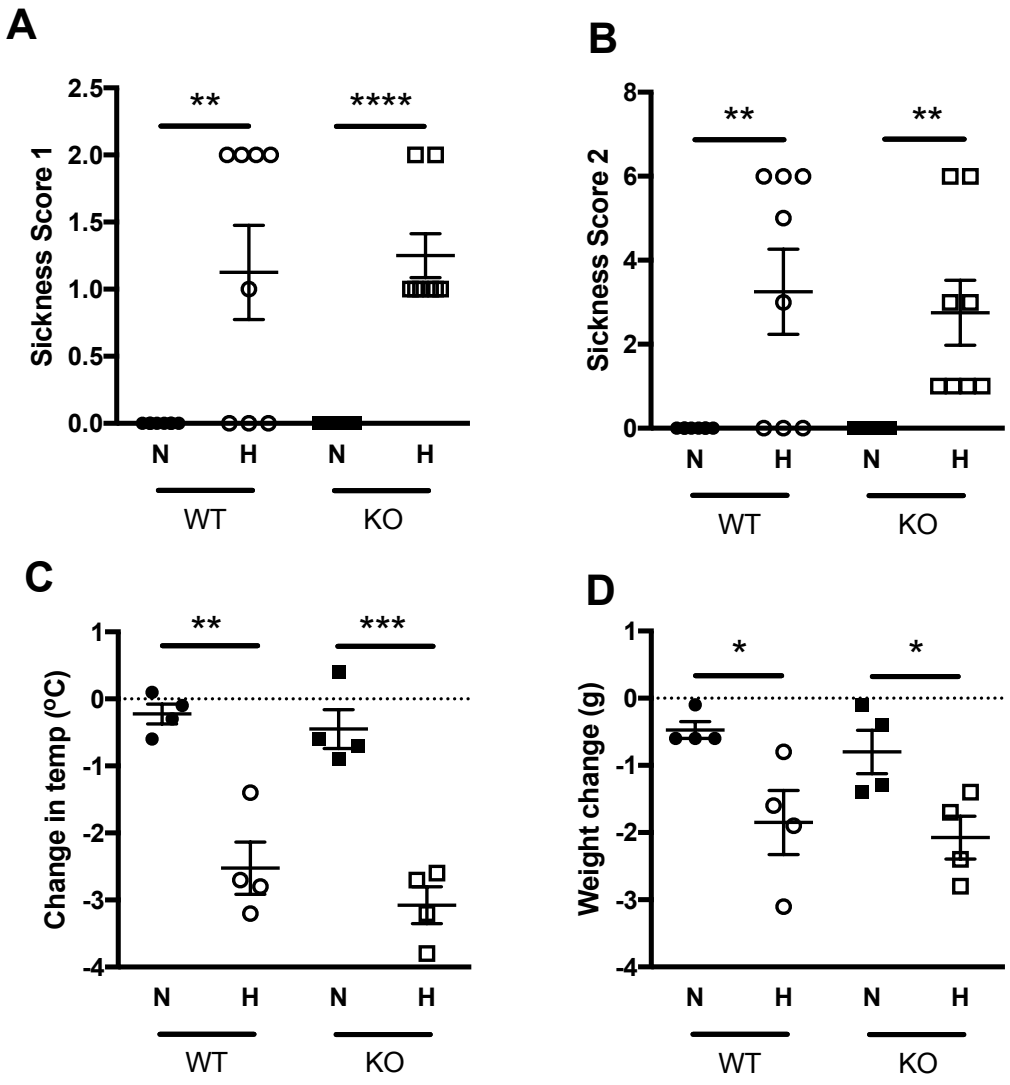

Figure 4.2.4-1: Myeloid specific knockout of PHD3 does not influence systemic effects of *Staphylococcus aureus* infection in mice experiencing systemic hypoxia. Mice infected with SH1000 *S. aureus* subcutaneously were assessed for signs of systemic illness via sickness scores (A, B), and change in rectal temperature (C) and weight (D) 14 hours following infection. Data expressed as mean±SEM and analysed with paired two-tailed Student's T tests, p*<0.05, p**<0.01, p***<0.001, n = 4. WT = wildtype (*PHD3*$^{fl/fl}$ LysMCre$^{-/-}$), KO = knockout (*PHD3*$^{fl/fl}$ LysMCre$^{+/-}$).

4.2.5. Myeloid-specific loss of PHD3 enhances resolution of sterile inflammation

Mice with whole-animal PHD3 knockout have been shown to possess a dampened immune response. To ascertain whether resolution of neutrophil inflammation is due to a loss of PHD3 in the myeloid cells specifically, we investigated this model of inflammation in the *PHD3*$^{fl/fl}$ LysMCre$^{+/-}$ animals. A model of sterile lung inflammation was induced through nebulisation of the mice with LPS and mice were housed for 24 hours in normoxia, and inflammatory neutrophils isolated via bronchoalveolar lavage.

Mice with myeloid-specific PHD3 knockout have significantly less inflammatory cells in the airways following nebulised LPS challenge (mean (±SEM), WT = 7.71x10^6 (9.65x10^5), KO = 4.99x10^6 (4.79x10^5), n = 8, p*<0.05)(Figure 4.2.4-1, A) and significantly less infiltrating neutrophils in the airway (mean (±SEM), WT = 7.28x10^6 (9.31x10^5), KO = 4.60x10^6 (4.49x10^5), n = 8, p**<0.01)(Figure 4.2.4-1, B). The abundance of macrophages in the BAL is equivalent between wild-type and knockout mice (mean (±SEM), WT = 0.425 (0.0708), KO = 0.391 (0.0544), n = 8, p**<0.01)(Figure 4.2.4-1, C). Myeloid-specific PHD3 deletion does appear to increase apoptosis in the knockout mice consistent with previous studies, although the result is not significant (mean (±SEM), WT = 0.962 (0.222), KO = 1.64 (0.328)%, n = 12, ns)(Figure 4.2.4-1, D). The levels of apoptosis are extremely low in the BAL, likely due to apoptotic neutrophils being cleared by alveolar macrophages.

Loss of PHD3 in myeloid cells reduces the IgM concentration in the airway 24 hours after inflammatory insult regardless of oxygen tension, indicating knockout animals experience less airway damage in this model, likely due to lower numbers of inflammatory cells in the airways (mean (±SEM), WT = 1170 (144), KO = 828 (149), n=9, p*<0.05)(Figure 4.2.4-3, A). When normalised to neutrophil number, IgM levels are equivalent between wildtype and knockout mice (mean (±SEM), WT = 153 (27.3), KO = 173 (29.9), n = 6, ns)(Figure 4.2.4-3, B). Loss of PHD3 in myeloid cells slightly reduces MPO concentration in the BAL, likely due to reduced neutrophil numbers in the airways (mean (±SEM), WT = 13.6 (3.29), KO = 12.3

(2.37), n = 12, ns)(Figure 4.2.4-3, C); however, when normalised to neutrophil number, MPO levels are slightly higher in the knockout mice, although this difference is not significant (mean (±SEM), WT = 2.00 (0.612(, KO = 2.83 (0.87), n = 9, ns)(Figure 4.2.4-3, D). Elastase concentration is also slightly lower in knockout mice, again likely due to less neutrophils in the airway (mean (±SEM), WT = 1.18 (0.359), KO = 0.652 (0.0904), n = 3)(Figure 4.2.4-3, E), with lower neutrophil elastase concentrations after normalisation to neutrophil number (mean (±SEM), WT = 0.196 (0.0409), KO = 0.137 (0.0395), n = 3)(Figure 4.2.4-3, F).

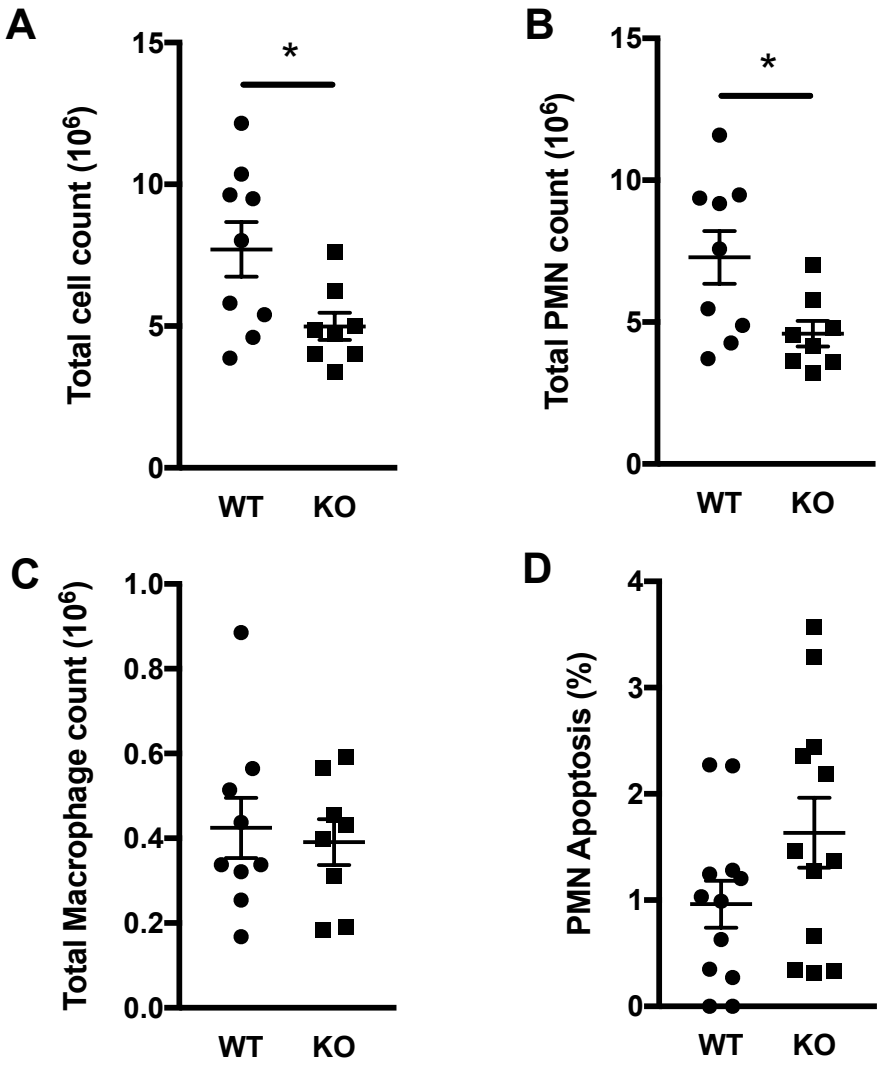

Figure 4.2.5-1: Myeloid specific loss of PHD3 enhances resolution of a sterile lung inflammation induced by LPS. Mice nebulised with 1mg/ml LPS were housed in normoxia (21% O_2) and culled after 24 hours and BAL taken. Cell counts were determined via haemocytometer (A) and differential counts and apoptosis calculated from cytospins (B, C, D). Data expressed as mean±SEM and analysed with unpaired two-tailed Student's T tests, p*<0.05, n = 9. WT = wildtype (*PHD3*$^{fl/fl}$ LysMCre$^{-/-}$), KO = knockout (*PHD3*$^{fl/fl}$ LysMCre$^{+/-}$).

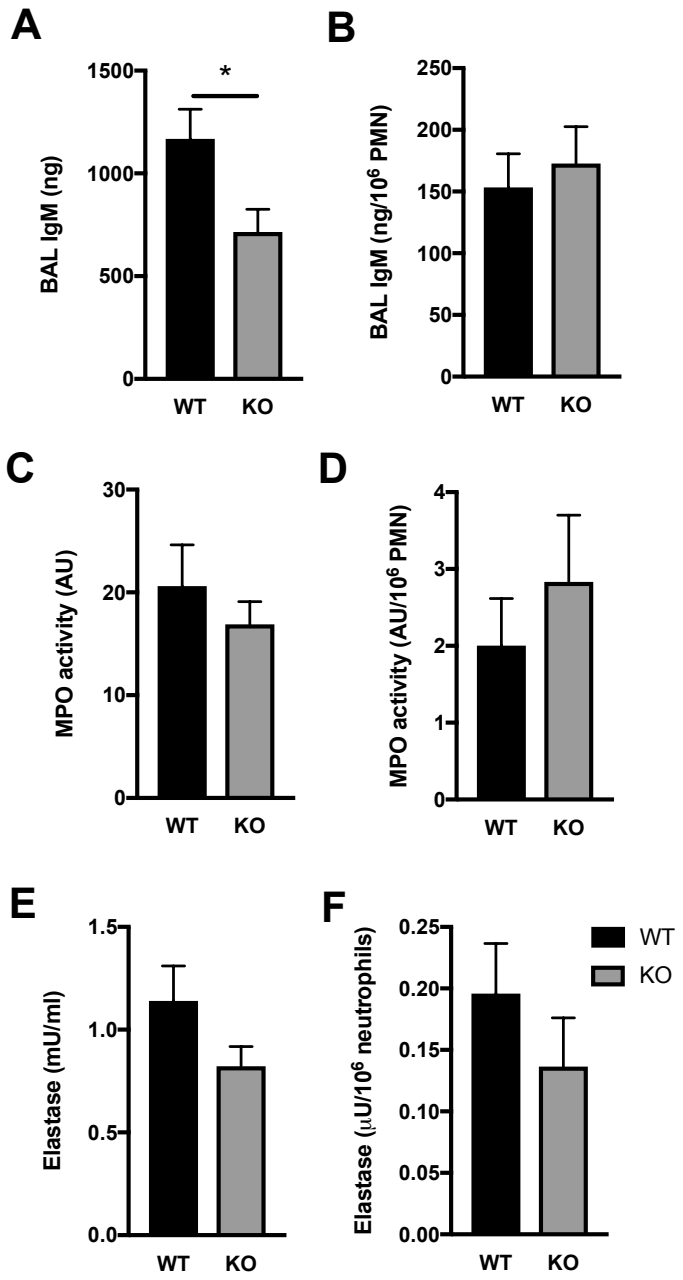

Figure 4.2.5-2: Mice with myeloid specific knockout of PHD3 have significantly less airway damage than wildtype littermate controls but equivalent levels of granule proteins. Mice nebulised with 1mg/ml LPS were housed in normoxia (N)(21% O_2) or hypoxia (H)(10% O_2) and culled after 24 hours and BAL taken. IgM (A, B), MPO (C, D) and Elastase (E, F) levels were analysed via ELISA. Data expressed as mean±SEM and analysed with unpaired two-tailed Student's T test, p*<0.05. WT = wildtype (*PHD3*$^{fl/fl}$ LysMCre$^{-/-}$), KO = knockout (*PHD3*$^{fl/fl}$ LysMCre$^{+/-}$).

4.2.6. Neutrophils have equivalent phagocytic capacity of *Staphylococcus aureus* and *Streptococcus pneumoniae*

To examine the phenotype of enhanced bacterial control in the model of *S. aureus* skin infection, we examined whether PHD3-deficient neutrophils were more capable of phagocytosing bacteria than wildtype controls. To do this, neutrophils isolated from LPS-nebulised wildtype and PHD3 knockout mouse BAL were co-incubated with FITC-labelled *S. aureus* bioparticles and CFSE-labelled D39 *S. pneumoniae* in either normoxia (21% O_2) or hypoxia (1% O_2).

By 1 hour of culture, neutrophils internalise fewer *S. aureus* bioparticles in hypoxia, but loss of PHD3 does not influence the phagocytic capacity of the neutrophils (mean (±SEM), WT N = 49.2 (3.46), KO N = 50.8 (5.81), WT H = 26.6 (0.609), KO H = 31.4 (5.95)%, n=3, p**<0.01)(Figure 4.2.5-1, A-B).

Neutrophils also internalise CFSE-labelled *S. pneumoniae* more slowly in hypoxia, but again loss of PHD3 does not influence phagocytic capacity of the neutrophils (mean (±SEM), WT N = 28.5 (3.93), KO N = 29.9 (2.52), WT H = 14.8 (1.81), KO H = 19.3 (4.74)%, n=3, p**<0.01)(Figure 4.2.5-2, A-B).

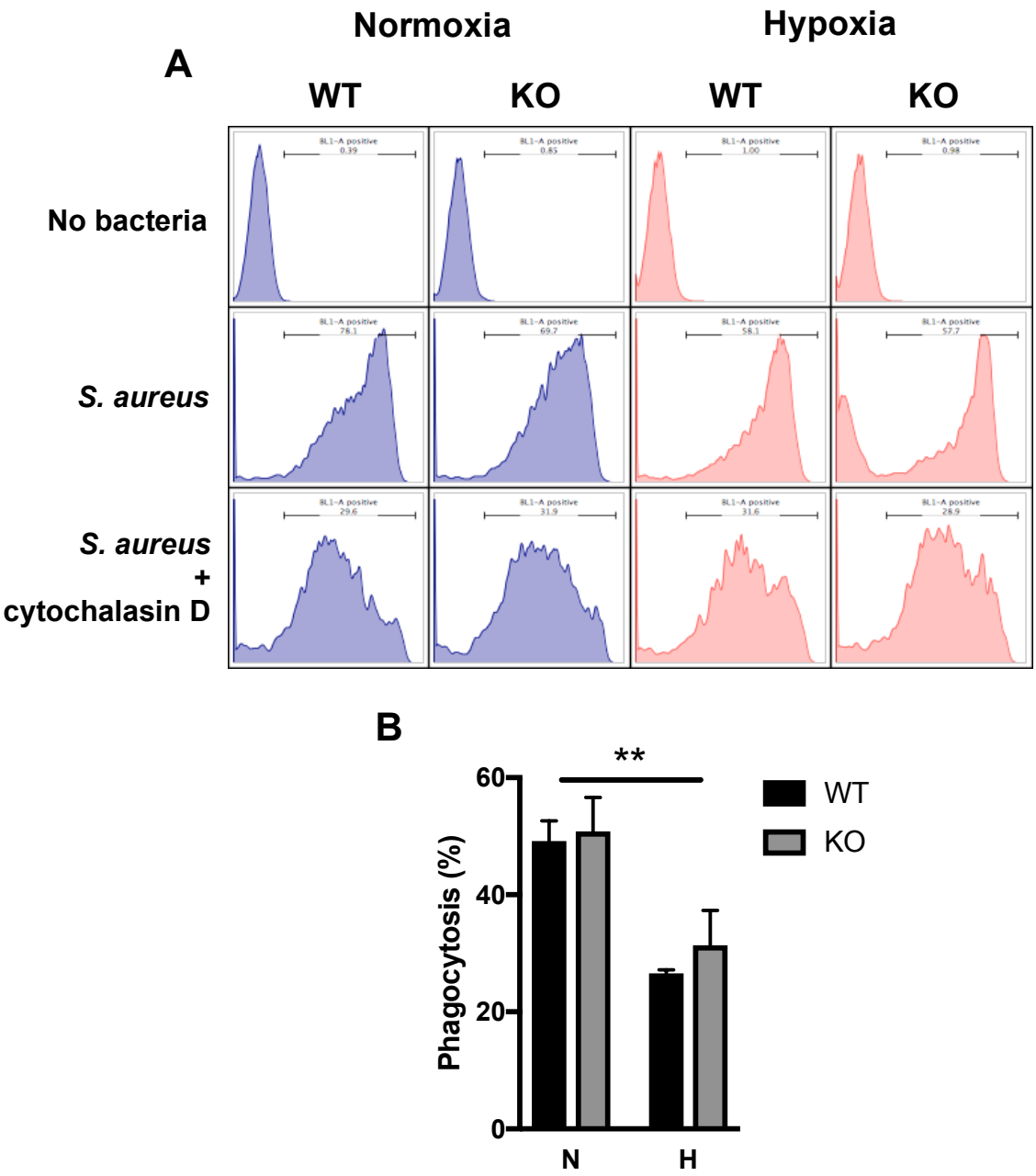

Figure 4.2.6-1: PHD3 knockout neutrophils have equivalent capacity for phagocytosis of *Staphylococcus aureus* bioparticles. Neutrophils were cultured for 1 hour with FITC-labelled *S. aureus* particles with and without cytochalasin D and fluorescence measured via flow cytometry. Phagocytosis (%) = % FITC-positive neutrophils - % FITC-positive cytochalasin D-treated neutrophils. Data expressed as mean±SEM and analysed with two-way ANOVA with Tukey's multiple comparisons, p**<0.01, n = 3. WT = wildtype (*PHD3*$^{fl/fl}$ LysMCre$^{-/-}$), KO = knockout (*PHD3*$^{fl/fl}$ LysMCre$^{+/-}$).

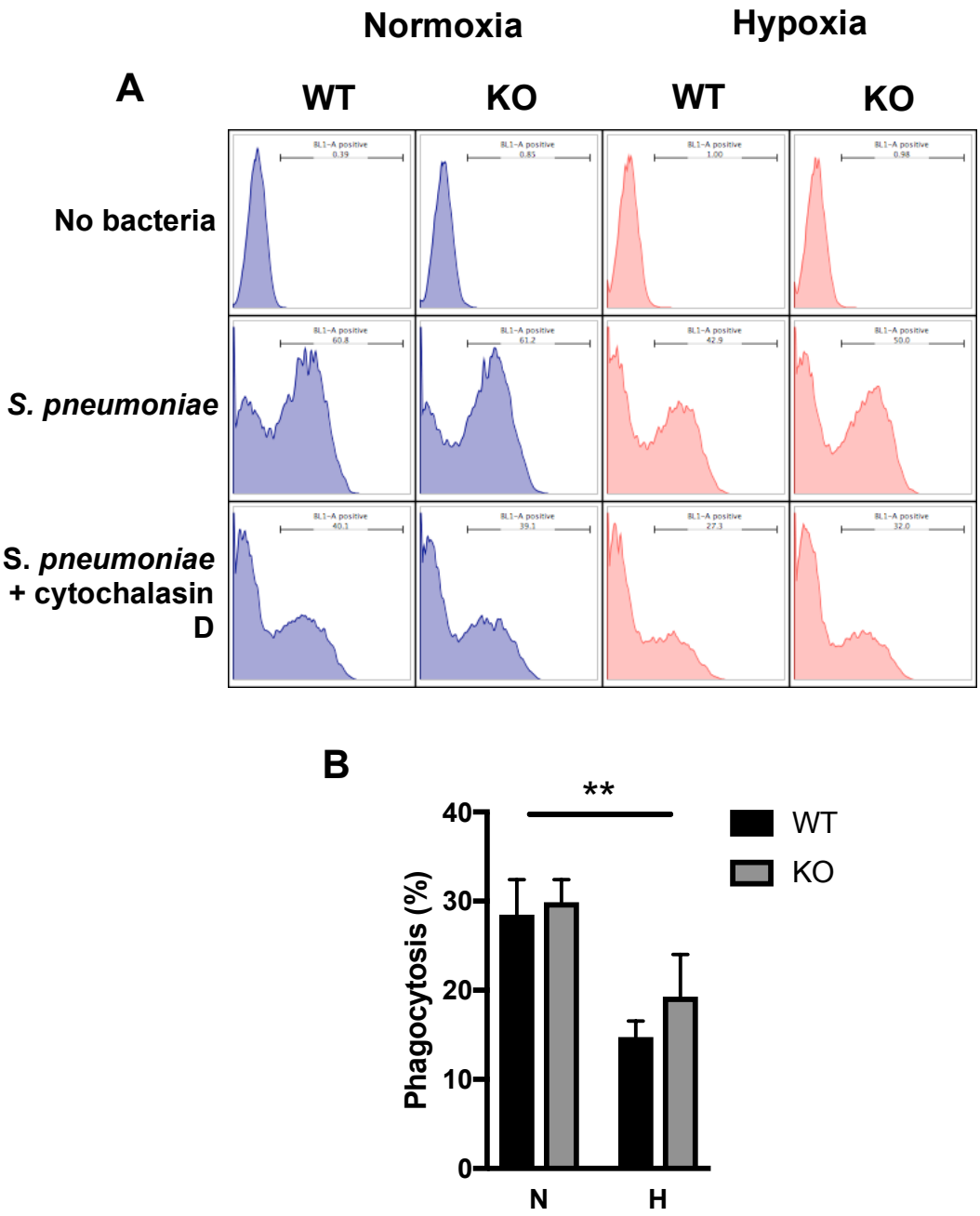

Figure 4.2.6-2: PHD3 knockout neutrophils have equivalent capacity for phagocytosis of heat-killed, CFSE-labelled D39 *Streptococcus pneumoniae*. Neutrophils were cultured for 1 hour with CFSE-labelled heat-killed *S. pneumonia* with and without cytochalasin D and fluorescence measured via flow cytometry. Phagocytosis (%) = % CFSE-positive neutrophils – % CFSE-positive cytochalasin D-treated neutrophils. Data expressed as mean±SEM and analysed with two-way ANOVA with Tukey's multiple comparisons, p**<0.01, n = 3. WT = wildtype (*PHD3*$^{fl/fl}$ LysMCre$^{-/-}$), KO = knockout (*PHD3*$^{fl/fl}$ LysMCre$^{+/-}$).

4.2.7. PHD3-deficient neutrophils have equivalent ROS production and respiratory burst activity

To understand why bacterial clearance and killing are enhanced in PHD3-deficient mice, we studied the capacity of neutrophils to mount a respiratory burst.

In parallel with our human studies (see Chapter 3), we measured the capacity of the neutrophils to regulate the pentose phosphate pathway. PHD3 deletion has been implicated in the upregulation of G6PD in clear cell Renal cell carcinoma cells (Miikkulainen *et al.*, 2017). Therefore, we examined expression of pentose phosphate pathway enzyme transcripts and looked at metabolic flux through these pathways.

Transcription of *G6pdx*, the rate-limiting enzyme of the pentose phosphate pathway involved in converting the glycolytic intermediate glucose 6-phosphate into ribulose 5-phosphate, is significantly upregulated in PHD3-deficient neutrophils compared to wildtype controls (mean (±SEM), WT = 1.09 (0.0609), KO= 2.55 (0.434), n = 4, p*<0.05)(Figure 4.2.7-1, A). Other enzymes studied are not significantly increased, although transcription of *RpiA* and *Rpe* appear higher (Figure 4.2.7-1, B-D). Despite enhanced transcription of *G6pdx*, flux through the pentose phosphate pathway is not significantly altered by the loss of PHD3 (mean (±SEM), WT ribose 5-phosphate/ribulose 5-phosphate = $3.20x10^4$ ($17.2x10^4$), KO ribose 5-phosphate/ribulose 5-phosphate = $2.45x10^4$ ($7.81x10^3$), WT sedoheptulose 7-phosphate = $1.01x10^5$ ($3.75x10^4$), KO sedoheptulose 7-phosphate = $1.51x10^5$ ($6.12x10^4$), erythrose 4-phosphate = 0 (0), erythrose 4-phosphate = 0 (0), n = 5)(Figure 4.2.7-2, B) with no change in $NADP^+$/NADPH ratio (mean (±SEM), WT = 1.13 (0.144), KO = 0.915 (0.0849), n = 5)(Figure 4.2.6-2, C) or GSH/GSSG ratio (mean (±SEM), WT = 234.9 (45.5), KO = 181 (15.9), n = 5)(Figure 4.2.7-2, D).

Furthermore, generation of reactive oxygen species is unaffected by loss of PHD3. Unstimulated cells baseline ROS production was unchanged by loss of PHD3 in both normoxic (21% O_2) and hypoxic (1% O_2) culture (mean (±SEM), WT N = $3.65x10^3$ (926), KO N = $4.54x10^3$ ($1.92x10^3$), WT H = $4.32x10^3$ ($1.19x10^3$), KO H = $5.57x10^3$), n = 5)(Figure 4.2.6-3, A). There was no difference between cells stimulated by fMLP (mean (±SEM), WT N = $5.64x10^3$ ($1.36x10^3$), KO N = $5.34x10^3$

($1.54x10^3$), WT H = $5.31x10^3$ ($1.36x10^3$), KO H = $6.71x10^3$ ($2.37x10^3$), n = 5)(Figure 4.2.7-3, B). The capacity for cells to undergo respiratory burst was also unchanged by loss of PHD3 (mean (±SEM), WT N = 1.57 (0.0897), KO N = 1.41 (0.160), WT H = 1.28 (0.0635), KO H = 1.23 (0.0538), n = 5, $p^*<0.05$)(Figure 4.2.7-3, C). These data show that PHD3 expression does not alter pentose phosphate pathway activity or the ability of the cells to undergo a respiratory burst, and this does not account for the enhanced efficiency of bacterial clearance in *PHD3*$^{fl/fl}$ LysMCre$^{+/-}$ animals.

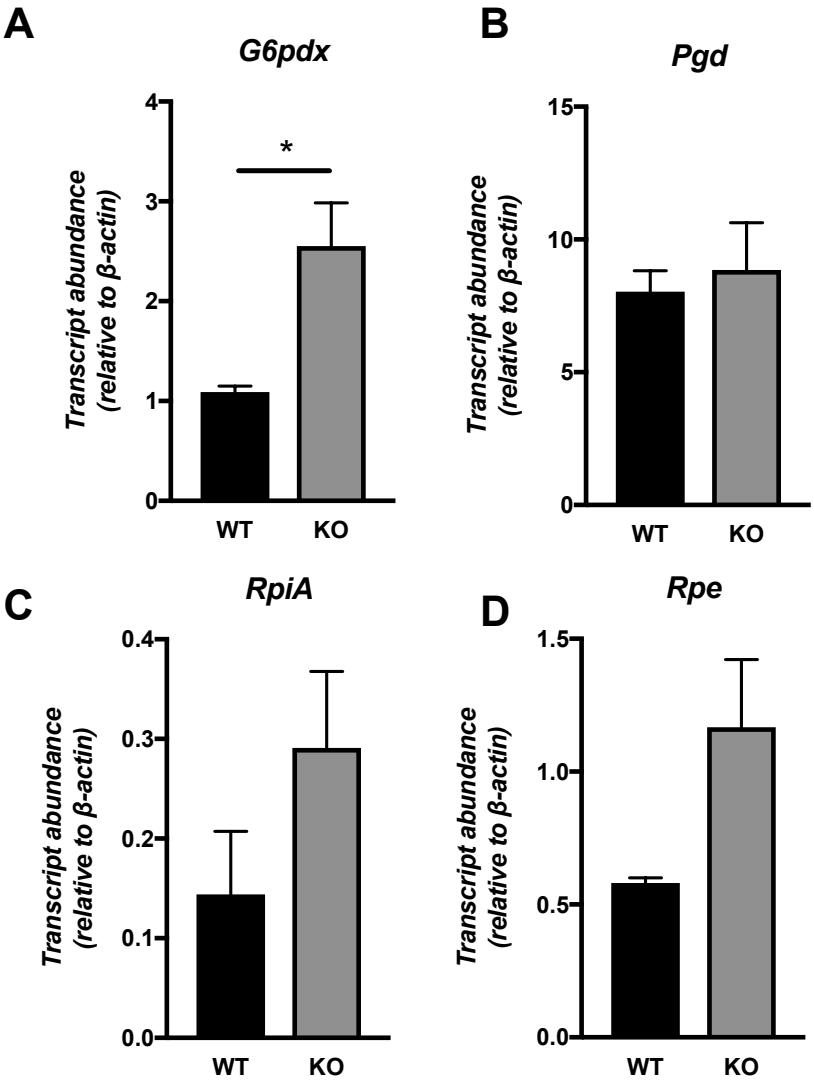

Figure 4.2.7-1: PHD3 deficient neutrophils have significantly greater expression of pentose phosphate pathway enzyme transcripts in normoxia. Mice nebulised with 1mg/ml LPS were housed in normoxia (21% O_2) and culled after 24 hours and BAL taken. Neutrophils isolated from mouse BAL were lysed and transcript level analysed via Taqman (A, B, C, D). Data expressed as mean±SEM and analysed with unpaired Student's two-tailed T test, p*<0.05, n = 4. WT = wildtype (*PHD3*$^{fl/fl}$ LysMCre$^{-/-}$), KO = knockout (*PHD3*$^{fl/fl}$ LysMCre$^{+/-}$).

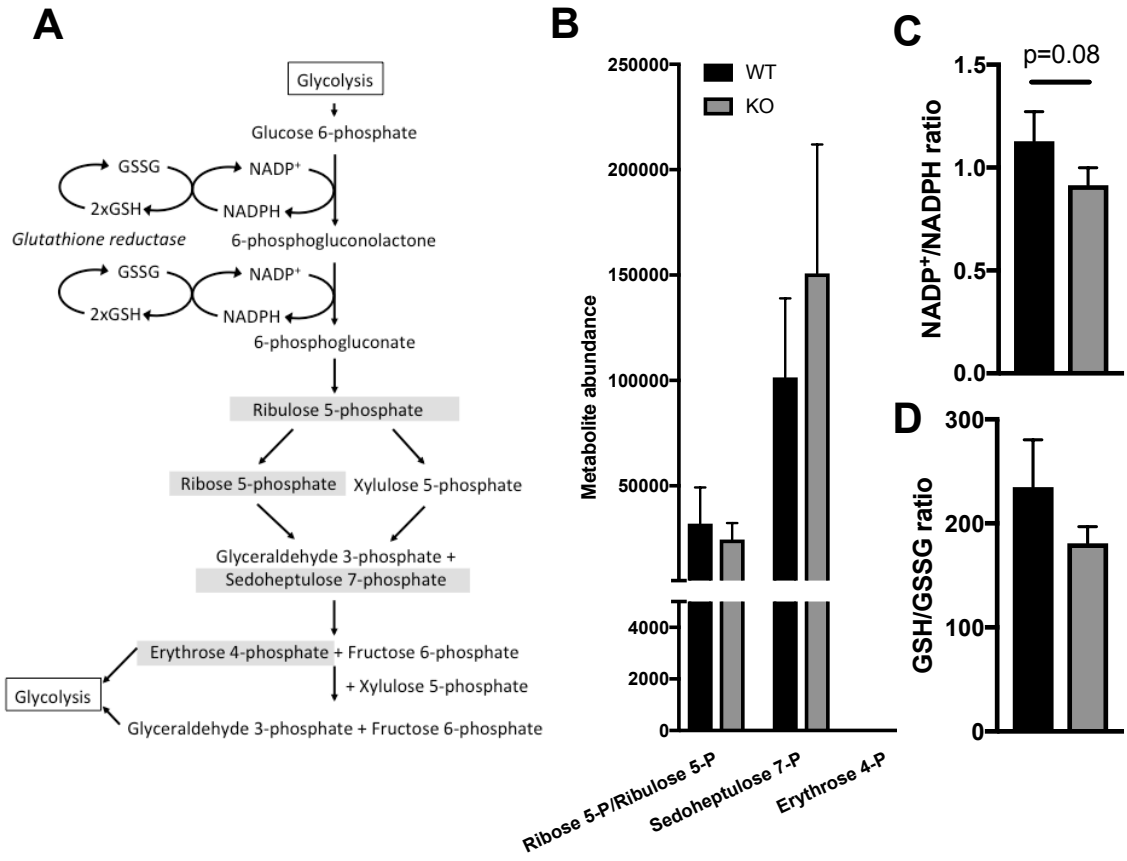

Figure 4.2.7-2: PHD3 deficient neutrophils do not have significantly increased pentose phosphate flux or a more oxidised NADP$^+$/NADPH pool. Mice nebulised with 1mg/ml LPS were housed in normoxia (N)(21% O_2) and culled after 24 hours and BAL taken. Neutrophils isolated from mouse BAL were further purified by percoll density centrifugation and metabolite abundance measured via LC-MS. (A, B, C, D). Data expressed as mean±SEM and analysed with 2-way ANOVA (B) or paired two-tailed Student's T tests (C,D), n = 5. WT = wildtype (*PHD3*$^{fl/fl}$ LysMCre$^{-/-}$), KO = knockout (*PHD3*$^{fl/fl}$ LysMCre$^{+/-}$).

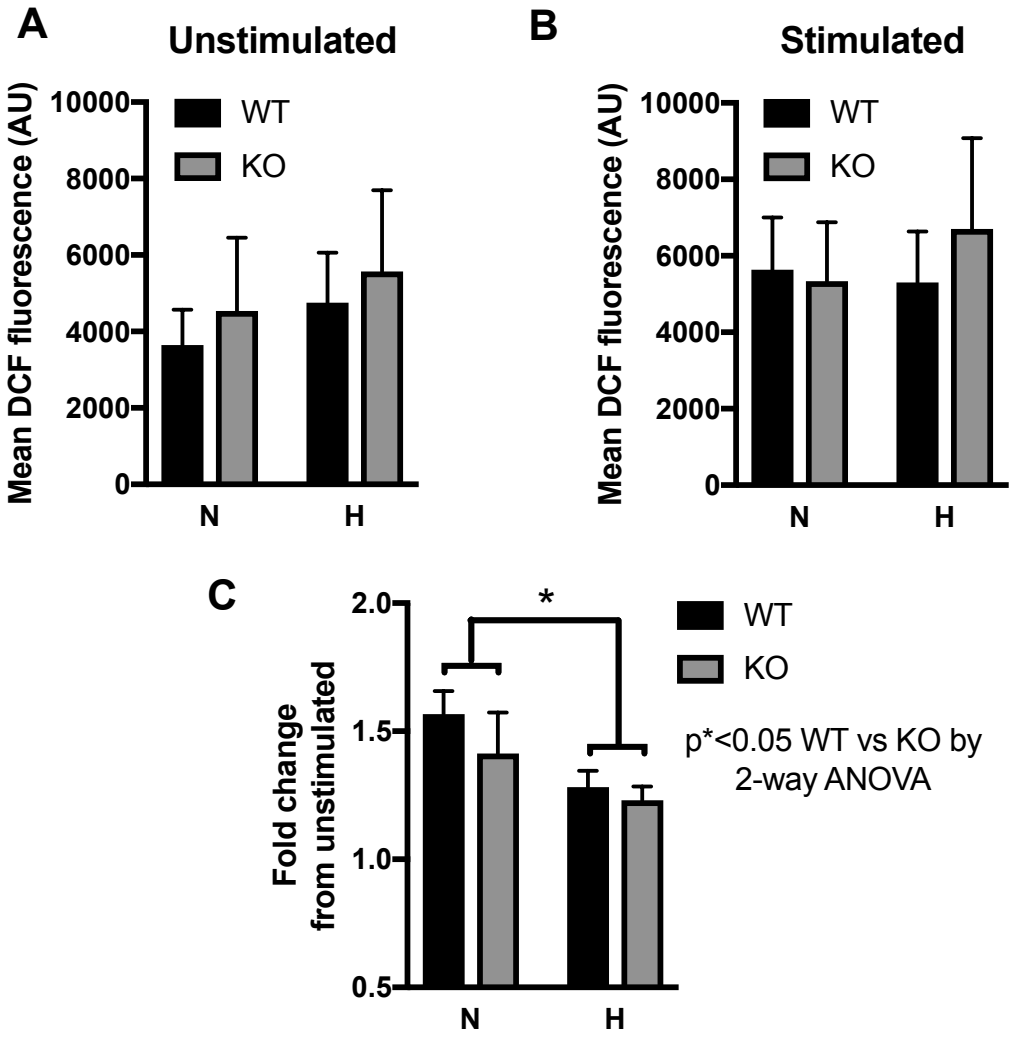

Figure 4.2.7-3: PHD3 deficient neutrophils have equivalent ROS production and capacity to undergo respiratory burst compared to wildtype controls. Mice nebulised with 1mg/ml LPS were housed in normoxia and culled after 24 hours and BAL taken. BAL neutrophils were cultured in normoxia (21%) or hypoxia (1%) either unstimulated (A) or cultured with 100nM fMLP (B) and ROS production measured through DCF staining and flow cytometry (A, B, C). Respiratory burst capacity was calculated as fold change in DCF fluorescence of fMLP stimulated cells from untreated control (C). Data expressed as mean±SEM and analysed with 2-way ANOVA, p*<0.05, n = 5. WT = wildtype (*PHD3*$^{fl/fl}$ LysMCre$^{-/-}$), KO = knockout (*PHD3*$^{fl/fl}$ LysMCre$^{+/-}$).

4.2.8. Loss of PHD3 does not influence glucose metabolism in normoxic conditions

To understand whether loss of PHD3 alone may affect metabolism as hypoxia does in human cells, we measured metabolic flux in neutrophils cultured in normoxia.

Loss of PHD3 does not affect energy production in the cell in normoxia as measured by ATP (mean (±SEM), WT = $3.33x10^5$ ($1.71x10^5$), KO = $3.35x10^5$ ($1.16x10^5$), n = 5, ns)(Figure 4.2.8-1, A), ADP (mean (±SEM), WT = $1.94x10^5$ ($1.15x10^5$), KO = $1.72x10^5$ ($6.03x10^4$), n = 5, ns)(Figure 4.2.8-1, B), AMP (mean (±SEM), WT = $1.21x10^5$ ($4.00x10^4$), KO = $1.26x10^5$ ($4.62x10^4$), n = 5, ns)(Figure 4.2.7-1, C) and energy status (mean (±SEM), WT = 1.77 (0.0738), KO = 2.00 (0.247), n = 5, ns)(Figure 4.2.8-1, D) and energy charge (mean (±SEM), WT = 0.630 (0.0466), KO = 0.655 (0.0792), n = 5, ns)(Figure 4.2.8-1, E).

Neutrophils from mice with myeloid-specific PHD3 deficiency also have equivalent levels of glycolytic intermediates compared to wildtype mice in normoxia (mean (±SEM), WT G-6P/F-6P = $3.39x10^5$ ($1.41x10^5$), KO G-6P/F-6P = $6.00x10^5$ ($2.93x10^5$), WT F-1,6 = $1.79x10^4$ ($1.09x10^4$), KO F-1, = $2.87x10^4$ ($1.37x10^4$), WT GAP = $2.00x10^4$ ($8.13x10^3$), KO GAP = $3.22x10^4$ ($1.56x10^4$), WT 2,3-PG = $1.62x10^4$ ($1.04x10^4$), KO 2,3-PG = $1.69x10^4$ ($6.64x10^3$), WT PEP = $1.47x10^4$ ($6.36x10^3$), KO PEP = $2.05x10^4$ ($8.24x10^3$), WT Lactate = $4.99x10^5$ ($1.39x10^5$), KO Lactate = $6.50x10^5$ ($2.141x10^5$), n = 5, ns)(Figure 4.2.8-2), indicating loss of PHD3 does not significantly influence glycolytic flux or energy production in inflammatory neutrophils.

Neutrophils isolated from mice with myeloid-specific PHD3 deletion have equivalent Krebs cycle flux compared to wildtype mice (mean (±SEM), WT citrate = $4.43x10^6$ ($1.47x10^6$), KO citrate = $4.74x10^6$ ($1.93x10^6$), WT α-KG = $9.10x10^4$ ($2.48x10^4$), KO α-KG = $9.87x10^4$ ($3.22x10^4$), WT succinate = $7.48x10^4$ ($2.92x10^4$), KO succinate = $9.12x10^4$ ($3.25x10^4$), WT malate = $9.68x10^5$ ($3.65x10^5$), KO malate = $1.31x10^6$ ($5.44x10^5$), WT fumarate = $1.84x10^5$ ($7.33x10^4$), KO fumarate = $2.29x10^5$ ($9.07x10^4$), n = 5, ns)(Figure 4.2.8-3). Likewise, neutrophils from myeloid-specific PHD3 deficient mice have equivalent free amino acids compared to

wildtype mice (mean (±SEM), WT glutamine = $4.29x10^4$ ($5.86x10^3$), KO glutamine = $1.05x10^5$ ($5.49x10^4$), WT glutamic acid = $1.42x10^6$ ($3.84x10^5$), KO glutamic acid = $1.91x10^6$ ($7.50x10^5$), WT serine = $8.46x10^4$ ($1.63x10^4$), KO serine = $1.42x10^5$ ($6.13x10^4$), WT aspartic acid= $6.16x10^5$ ($1.52x10^5$), KO aspartic acid = $7.52x10^5$ ($3.00x10^5$), WT asparagine = $9.86x10^4$ ($2.33x10^4$), KO asparagine = $1.56x10^5$ ($6.74x10^4$), WT glycine = $4.09x10^4$ ($1.29x10^4$), KO glycine = $6.29x10^4$ ($2.76x10^4$), WT alanine = $2.15x10^5$ ($6.58x10^4$), KO alanine = $2.77x10^5$ ($1.10x10^5$), WT valine = $2.87x10^4$ ($1.18x10^4$), KO valine = $3.07x10^4$ ($1.20x10^4$), WT leucine = $1.20x10^5$ ($5.03x10^4$), KO leucine = $1.30x10^5$ ($4.92x10^4$), WT arginine = $9.64x10^4$ ($4.31x10^4$), KO arginine = $1.00x10^5$ ($3.97x10^4$), WT proline = $6.12x10^4$ ($1.98x10^4$), KO proline = $7.81x10^4$ ($3.25x10^4$), n = 5, ns)(Figure 4.2.8-4).

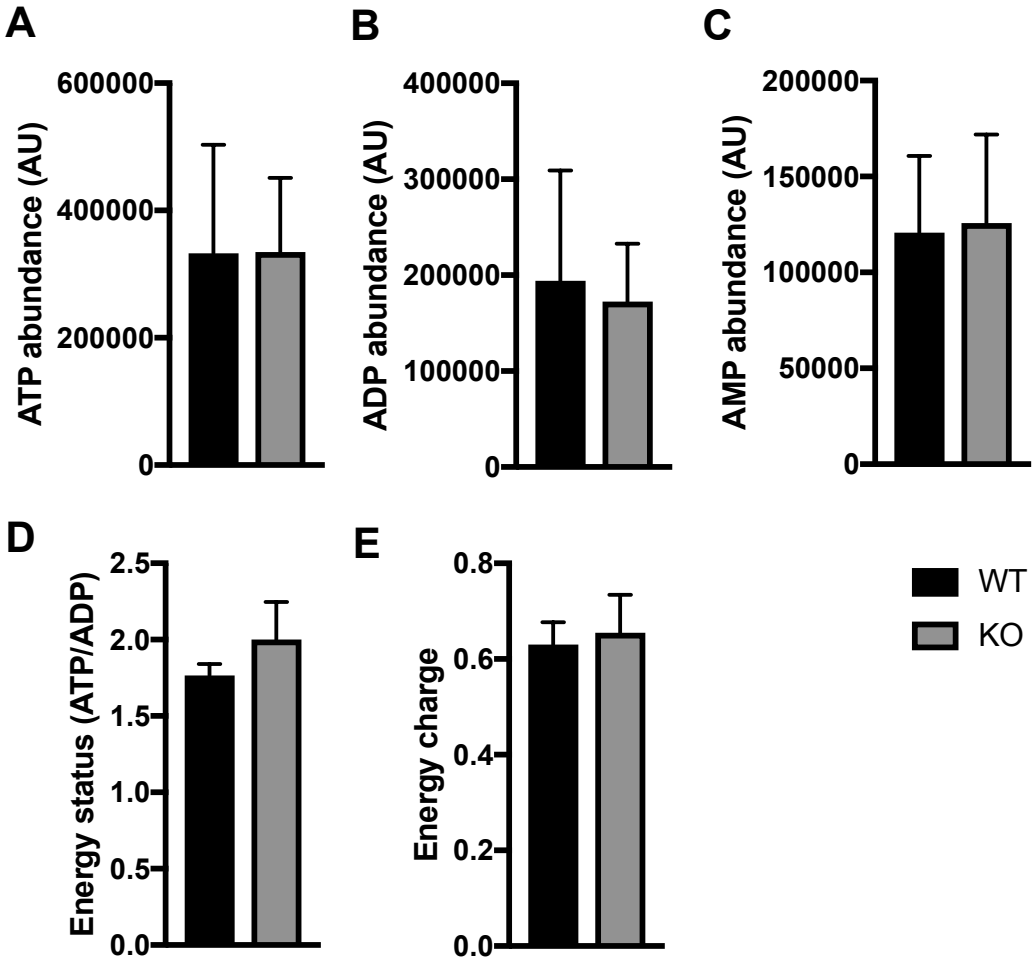

Figure 4.2.8-1: Loss of PHD3 does not affect neutrophil energy metabolism in normoxia. Mice nebulised with 1mg/ml LPS were housed in normoxia (21% O_2) and culled after 24 hours and BAL taken. Neutrophils isolated from mouse BAL were further purified by percoll density centrifugation and metabolite abundance measured via LC-MS. (A, B, C). D: Energy status was calculated as ATP/ADP. E: Energy charge was calculated as (ATP+0.5ADP)(AMP+ADP+ATP). Data expressed as mean±SEM and analysed with unpaired two-tailed Student's T tests, ns, n = 5. WT = wildtype (*PHD3*$^{fl/fl}$ LysMCre$^{-/-}$), KO = knockout (*PHD3*$^{fl/fl}$ LysMCre$^{+/-}$).

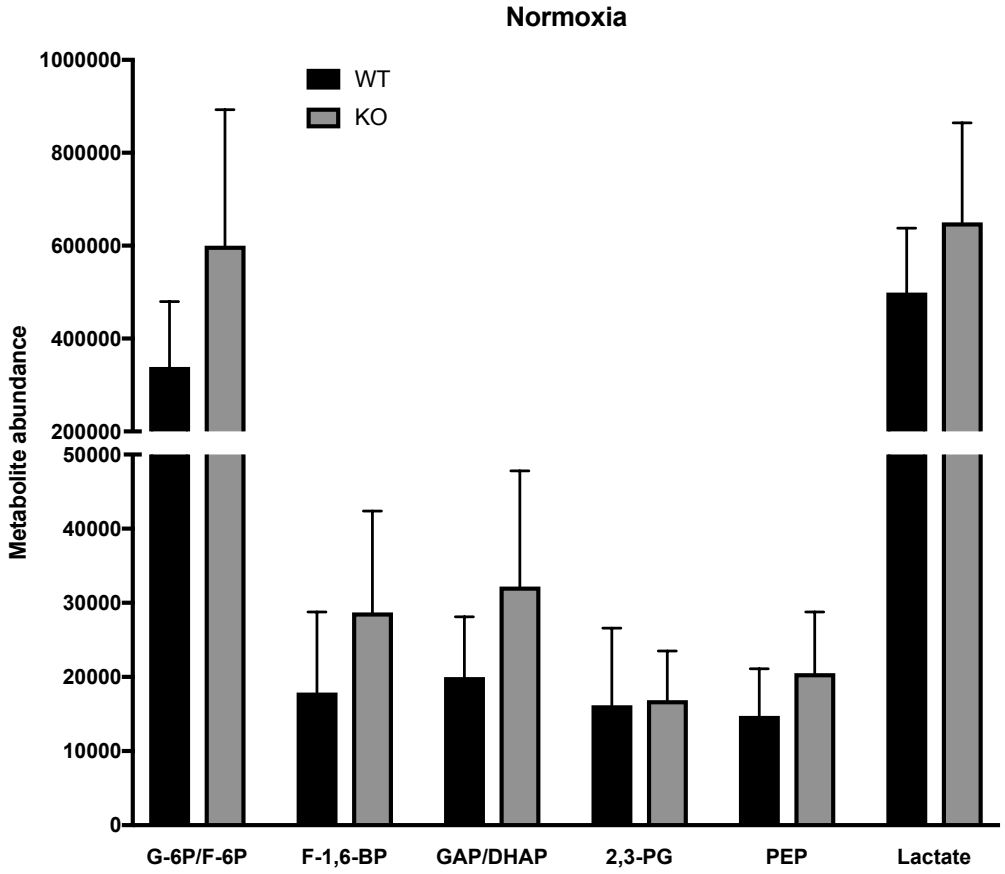

Figure 4.2.8-2: PHD3-deficient neutrophils have equivalent glycolytic flux compared to wildtype controls. Mice nebulised with 1mg/ml LPS were housed in normoxia and culled after 24 hours and BAL taken. Neutrophils isolated from mouse BAL were further purified by percoll density centrifugation and metabolite abundance measured via LC-MS. Data expressed as mean±SEM and analysed with 2-way ANOVA, n = 5, ns. WT = wildtype (*PHD3*$^{fl/fl}$ LysMCre$^{-/-}$), KO = knockout (*PHD3*$^{fl/fl}$ LysMCre$^{+/-}$).

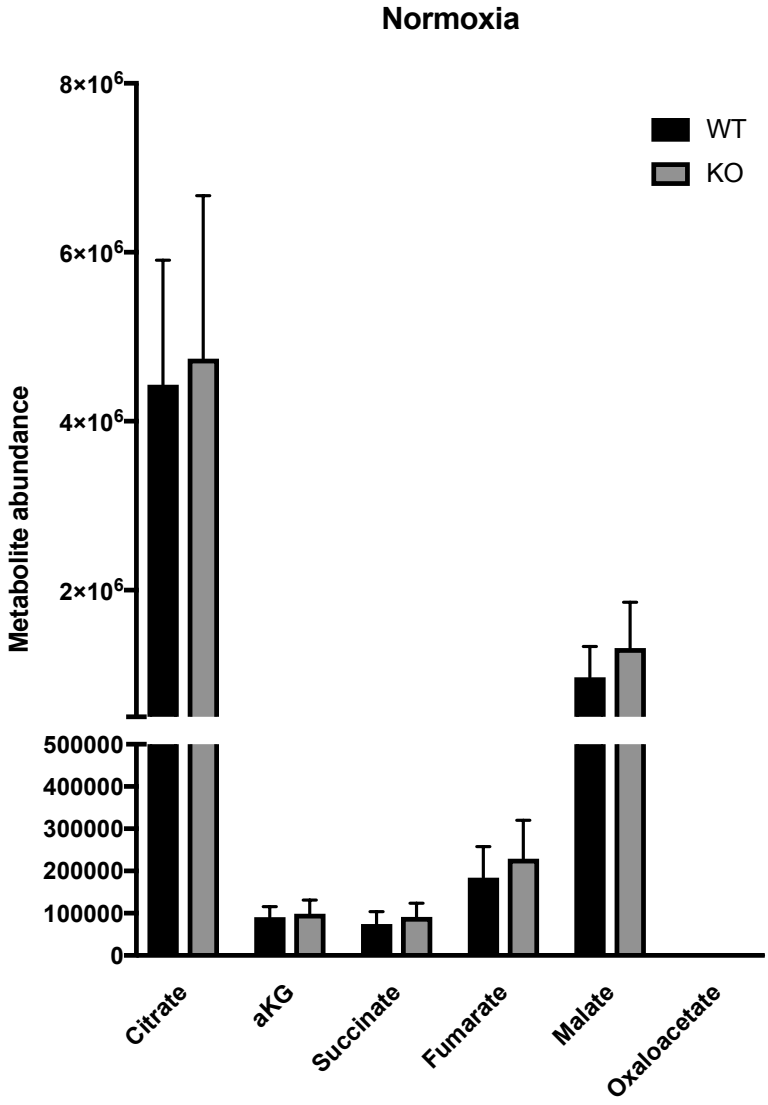

Figure 4.2.8-3: PHD3-deficient neutrophils have equivalent Krebs cycle flux compared to wildtype controls. Mice nebulised with 1mg/ml LPS were housed in normoxia and culled after 24 hours and BAL taken. Neutrophils isolated from mouse BAL were further purified by percoll density centrifugation and metabolite abundance measured via LC-MS. Data expressed as mean±SEM and analysed with 2-way ANOVA, n = 5, ns. WT = wildtype (*PHD3*$^{fl/fl}$ LysMCre$^{-/-}$), KO = knockout (*PHD3*$^{fl/fl}$ LysMCre$^{+/-}$).

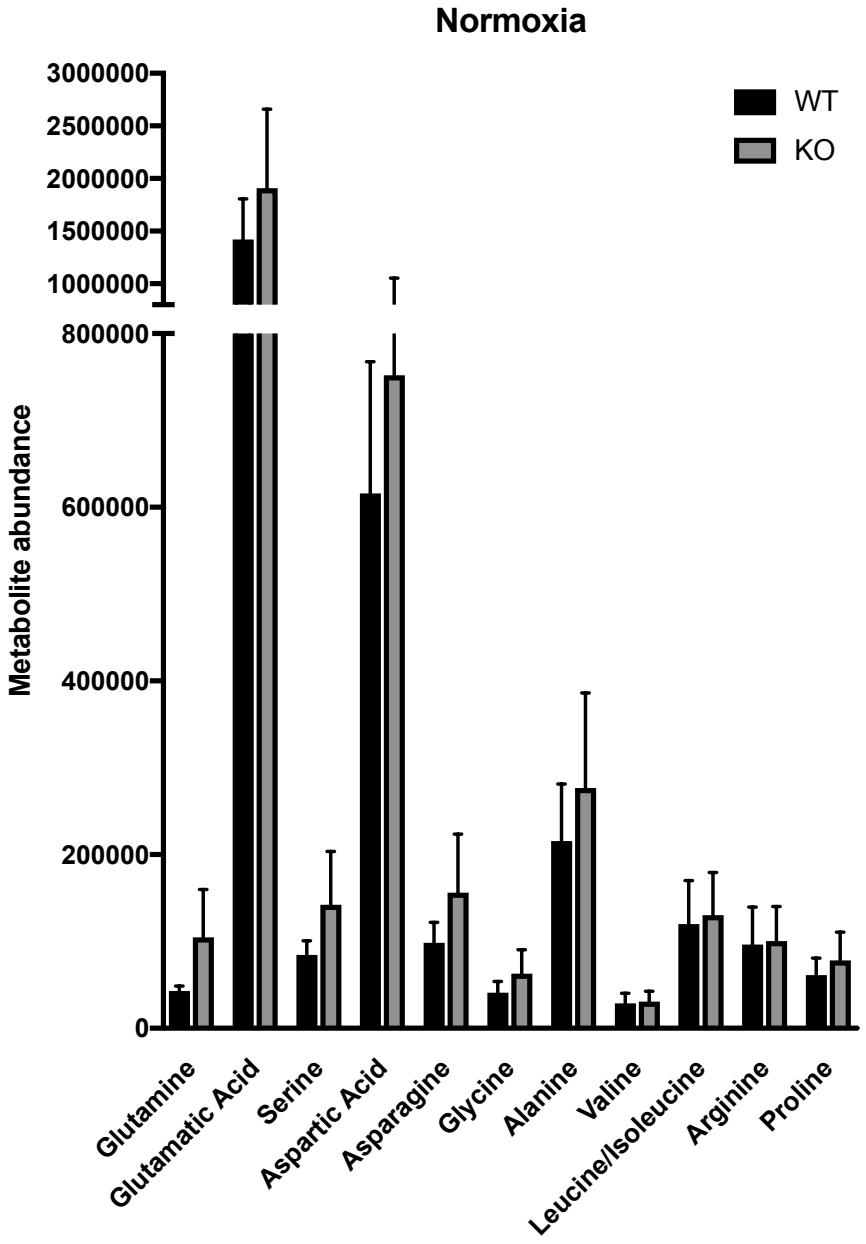

Figure 4.2.8-4: PHD3-deficient neutrophils have equivalent free amino acids compared to wildtype controls. Mice nebulised with 1mg/ml LPS were housed in normoxia and culled after 24 hours and BAL taken. Neutrophils isolated from mouse BAL were further purified by percoll density centrifugation and metabolite abundance measured via LC-MS. Data expressed as mean±SEM and analysed with 2-way ANOVA, n = 5, ns. WT = wildtype (*PHD3*$^{fl/fl}$ LysMCre$^{-/-}$), KO = knockout (*PHD3*$^{fl/fl}$ LysMCre$^{+/-}$).

4.2.9. Loss of PHD3 in hypoxia significantly reduces glycolytic flux

Although PHD3 requires oxygen to hydroxylase target proteins, *PHD3* transcription is profoundly upregulated in hypoxia (mean (±SEM), N = 0.0754 (0.0200), H = 2.45 (0.478), n = 4, p**<0.01)(Figure 4.2.9-1). Therefore, examining the metabolic effects of PHD3 deletion is important in determining how PHD3 regulates metabolic regulation in inflammation

Neutrophils isolated from myeloid-specific PHD3 knockouts have significantly lower levels of glycolytic metabolites after culture in hypoxia (mean (±SEM), WT G-6P/F-6P = $2.82x10^5$ ($7.44x10^4$), KO G-6P/F-6P = $2.36x10^5$ ($7.00x10^4$), WT F-1,6 = $1.87x10^4$ ($5.74x10^3$), KO F-1,6 = $7.08x10^3$ ($2.44x10^3$), WT GAP = $1.55x10^4$ ($4.57x10^3$), KO GAP = $1.25x10^4$ ($3.29x10^3$), WT 2,3-PG = $1.21x10^4$ ($3.08x10^3$), KO 2,3-PG = $4.67x10^3$ ($2.25x10^3$), WT PEP = $1.62x10^4$ ($3.72x10^3$), KO PEP = $1.12x10^4$ ($3.05x10^3$), WT Lactate = $7.33x10^5$ ($1.93x10^5$), KO Lactate = $3.89x10^5$ ($7.31x10^4$), n = 5, p*<0.05)(Figure 4.2.9-2). This reduced flux in glycolysis is paralleled by a reduction in flux through the Krebs cycle. Neutrophils isolated from myeloid-specific PHD3 knockouts have significantly lower flux through the Krebs cycle following hypoxic culture (mean (±SEM), WT citrate = $5.64x10^6$ ($1.01x10^6$), KO citrate = $2.95x10^6$, ($9.97x10^5$), WT α-KG = $8.69x10^4$ ($1.87x10^4$), KO α-KG = $6.65x10^4$ ($1.14x10^4$), WT succinate = $6.78x10^4$ ($1.47x10^4$), KO succinate = $3.84x10^4$ ($1.38x10^4$), WT malate = $1.25x10^6$ ($2.58x10^5$), KO = $7.43x10^5$ ($1.77x10^5$), WT oxaloacetate = 0 (0), KO oxaloacetate = 0 (0), n = 5, p*<0.05)(Figure 4.2.9-3).

Although PHD3-deficient neutrophils have a significant and profound drop in glycolytic and Krebs cycle flux, levels of ATP and energy charge are unchanged (mean (±SEM), WT = 2.80x105 ($5.49x10^4$), KO = 1.69x105 ($5.28x10^4$), n = 5, ns)(Figure 4.2.9-4, A), ADP (mean (±SEM), WT = 1.88x105 ($3.04x10^4$), KO = $1.02x10^5$ ($3.77x10^4$), n = 5, ns)(Figure 4.2.9-4, B), AMP (mean (±SEM), WT = $1.58x10^5$ ($5.94x10^4$), KO = $1.26x10^5$ ($6.54x10^4$), n = 5, ns)(Figure 4.2.9-4, C), and energy status (mean (±SEM), WT = 1.50 (0.129), KO = 1.70 (0.140), n = 5, ns)(Figure 4.2.9-4, D) and energy charge (mean (±SEM), WT = 0.596 (0.0338), KO = 0.576 (0.0441), n = 5, ns)(Figure 4.2.9-4, E).

PHD3-deficient neutrophils from mice housed in hypoxia also have significantly less free amino acids than wildtype mice (mean (±SEM), WT glutamine = $6.13x10^4$ ($2.38x10^4$), KO glutamine = $2.37x10^4$ ($4.28x10^3$), WT glutamic acid = $1.46x10^6$ ($3.81x10^5$), KO glutamic acid = $8.71x10^5$ ($1.77x10^5$), WT serine = $1.17x10^5$ ($3.44x10^4$), KO serine = $5.51x10^4$ ($1.17x10^4$), WT aspartic acid = $6.18x10^5$ ($1.43x10^5$), KO aspartic acid = $3.86x10^5$ ($7.77x10^4$), WT asparagine = $1.24x10^5$ ($3.18x10^4$), KO asparagine = $6.63x10^4$ ($1.77x10^4$), WT glycine = $4.68x10^4$ ($1.16x10^4$), KO glycine = $2.21x10^4$ ($6.13x10^3$), WT alanine = $2.32x10^5$ ($4.16x10^4$), KO alanine = $1.39x10^5$ ($3.89x10^4$), WT valine = $2.60x10^4$ ($5.84x10^3$), KO valine = $1.54x10^4$ ($4.25x10^3$), WT leucine = $1.09x10^5$ ($2.67x10^4$), KO leucine = $6.38x10^4$ ($2.00x10^4$), WT arginine = $8.24x10^4$ ($1.56x10^4$), KO arginine = $4.51x10^4$ ($1.25x10^4$), WT proline = $6.50x10^4$ ($1.48x10^4$), KO proline = $2.89x10^4$ ($7.17x10^3$), n = 5, p*0.05)(Figure 4.2.9-5). These data indicate PHD3-deficient neutrophils are metabolically compromised, with globally reduced metabolic flux.

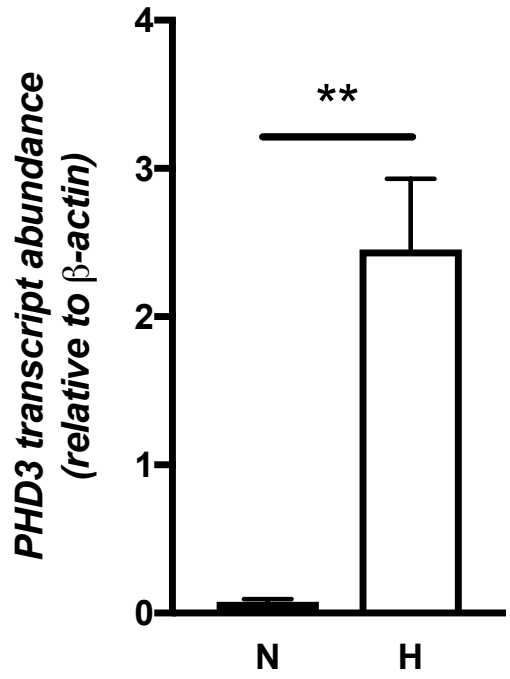

Figure 4.2.9-1. Neutrophil *PHD3* expression is significantly upregulated in hypoxia. Wild-type *PHD3*$^{fl/fl}$ LysMCre$^{+/-}$ mice were nebulised with 1mg/ml LPS, housed for 24 hours and then neutrophils isolated via bronchoalveolar lavage. Isolated neutrophils were cultured in normoxia (N) and hypoxia (H) for 4 hours, RNA extracted and *PHD3* transcript levels measured via quantitative PCR and normalised to *β-actin* transcript levels. Data expressed as mean±SEM and analysed with paired two-tailed Student's T tests, p**<0.01, n = 5.

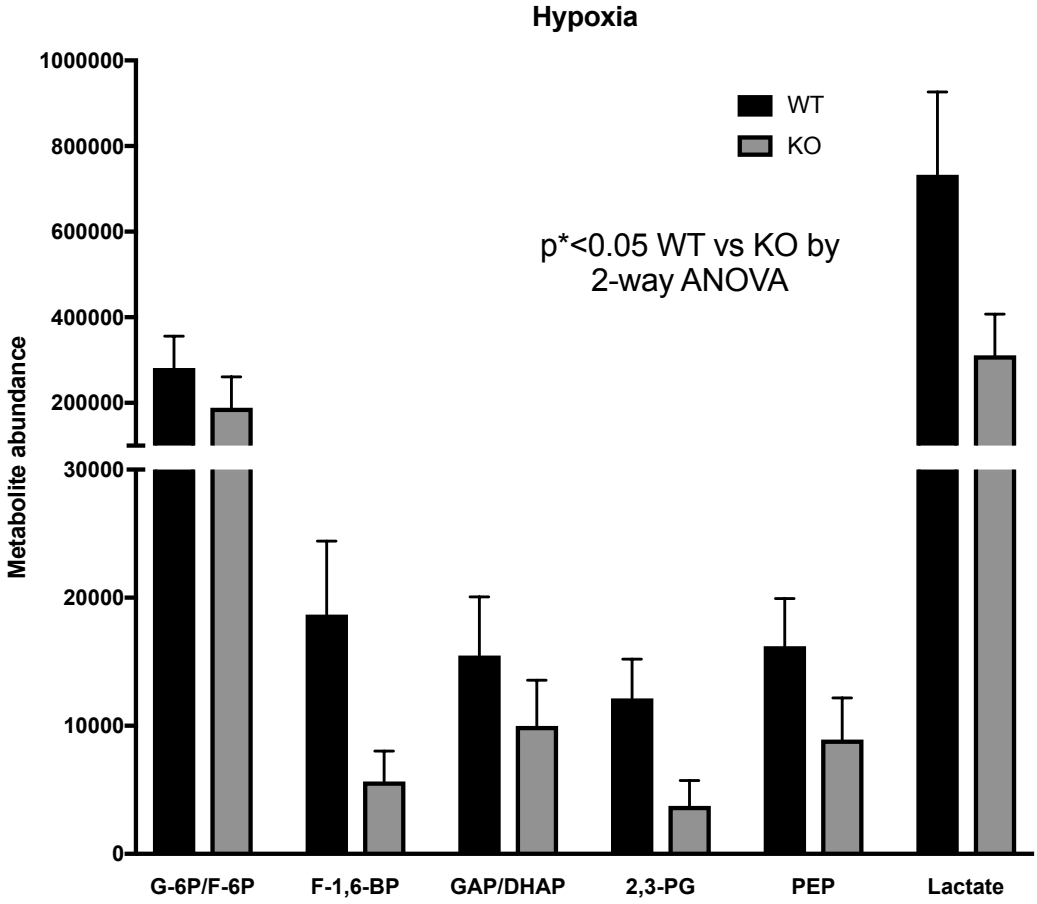

Figure 4.2.9-2: Neutrophils isolated from mice with myeloid-specific PHD3 knockout cultured in hypoxia have diminished glycolytic flux. Mice nebulised with 1mg/ml LPS were housed in hypoxia (10% O_2) and culled after 24 hours and BAL taken. Neutrophils isolated from mouse BAL were further purified by percoll density centrifugation and metabolite abundance measured via LC-MS. Data expressed as mean±SEM and analysed with 2-way ANOVA, p*<0.05, n =5 . WT = wildtype (*PHD3*$^{fl/fl}$ LysMCre$^{-/-}$), KO = knockout (*PHD3*$^{fl/fl}$ LysMCre$^{+/-}$).

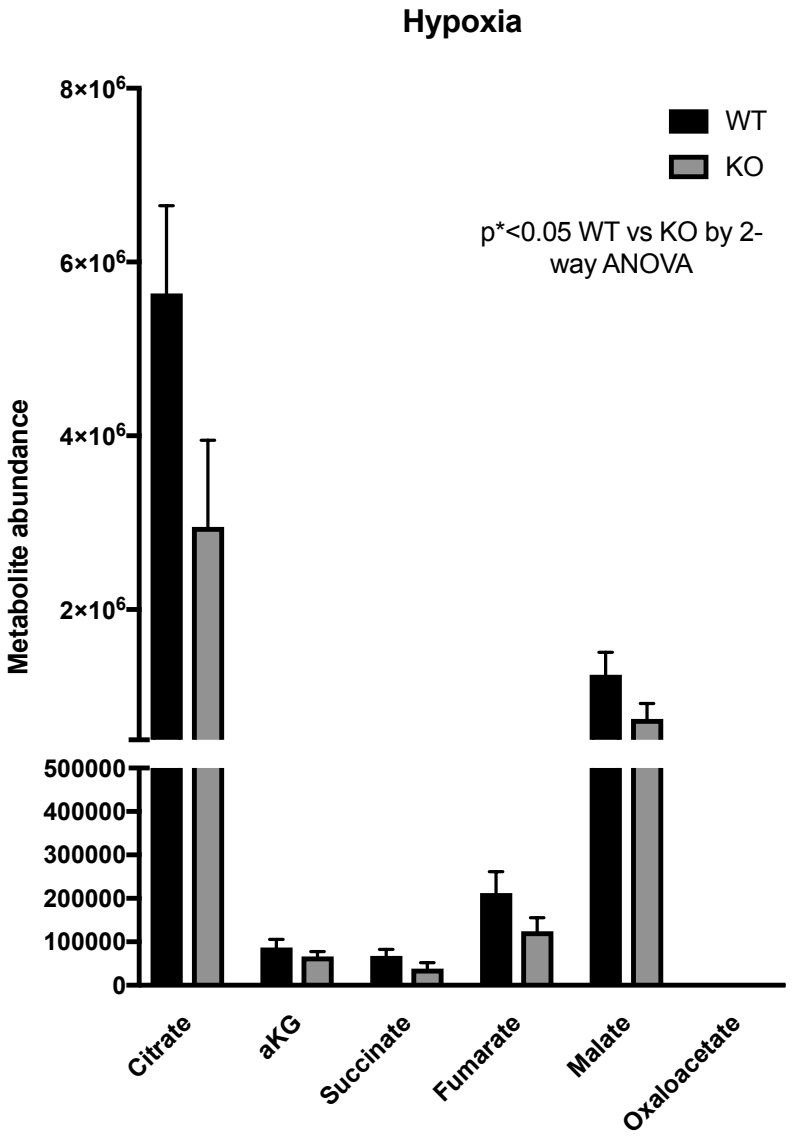

Figure 4.2.9-3: Neutrophils isolated from mice with myeloid-specific PHD3 knockout cultured in hypoxia have diminished krebs cycle activity. Mice nebulised with 1mg/ml LPS were housed in hypoxia (10% O_2) and culled after 24 hours and BAL taken. Neutrophils isolated from mouse BAL were further purified by percoll density centrifugation and metabolite abundance measured via LC-MS. (A, B). Data expressed as mean±SEM and analysed with 2-way ANOVA, p*<0.05, n=5. WT = wildtype (*PHD3*$^{fl/fl}$ LysMCre$^{-/-}$), KO = knockout (*PHD3*$^{fl/fl}$ LysMCre$^{+/-}$).

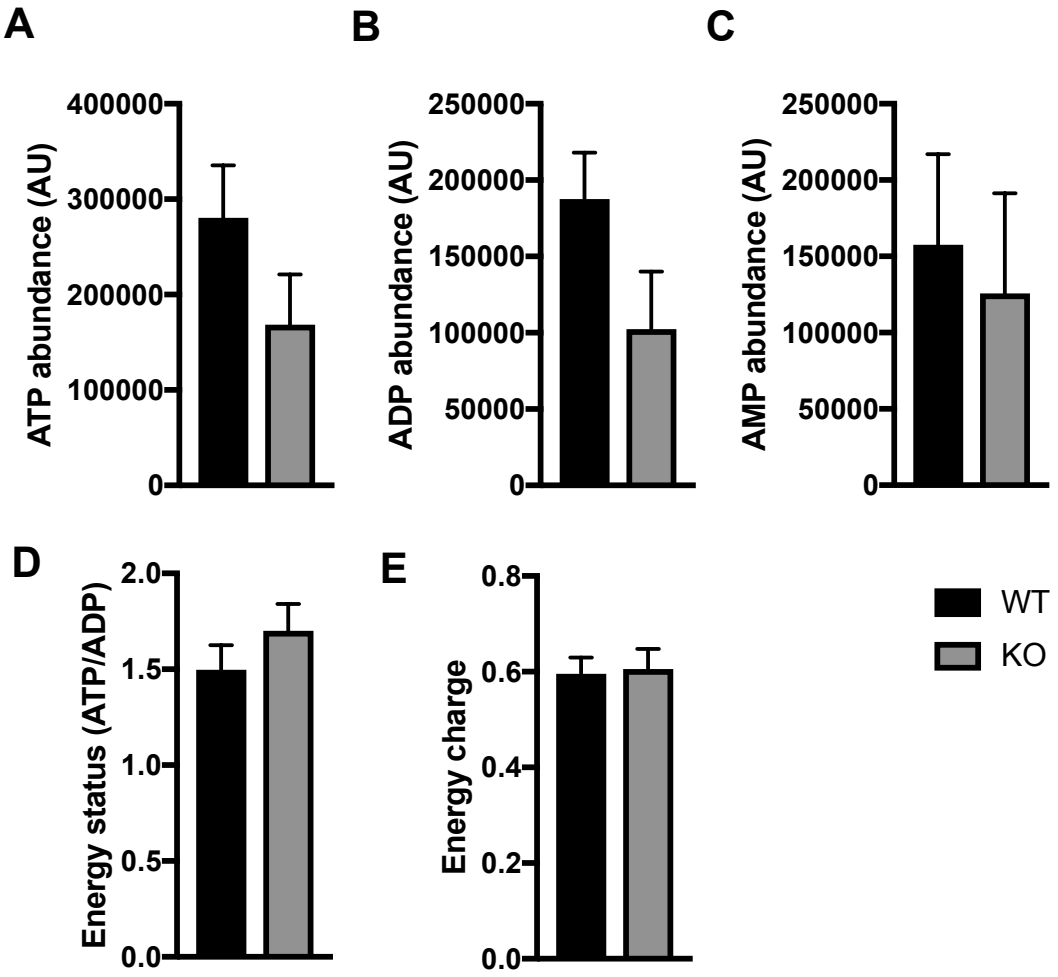

Figure 4.2.9-4: Loss of PHD3 does not influence energy status or availability of ATP in neutrophils from hypoxic mice. Mice nebulised with 1mg/ml LPS were housed in hypoxia (10% O_2) and culled after 24 hours and BAL taken. Neutrophils isolated from mouse BAL were further purified by percoll density centrifugation and metabolite abundance measured via LC-MS. (A-C). Energy status and charge were calculated from metabolite abundance (D, E). Data expressed as mean±SEM and analysed with paired two-tailed Student's T tests, n=5. WT = wildtype (*PHD3*$^{fl/fl}$ LysMCre$^{-/-}$), KO = knockout (*PHD3*$^{fl/fl}$ LysMCre$^{+/-}$).

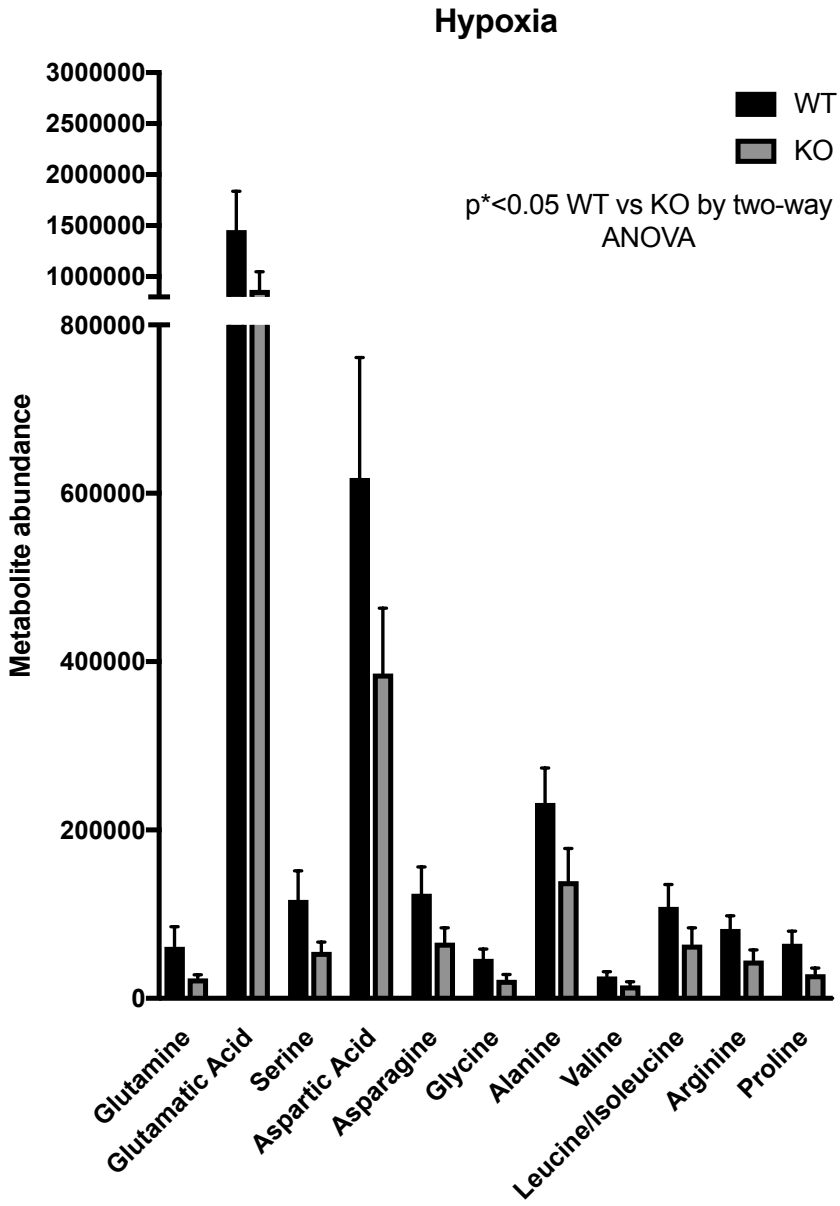

Figure 4.2.9-5: Neutrophils isolated from mice with myeloid specific PHD3 knockout cultured in hypoxia have diminished levels of free amino acids. Mice nebulised with 1mg/ml LPS were housed in hypoxia (10% O_2) and culled after 24 hours and BAL taken. Neutrophils isolated from mouse BAL were further purified by percoll density centrifugation and metabolite abundance measured via LC-MS. Data expressed as mean±SEM and analysed with 2-way ANOVA, p*<0.05, n=5. WT = wildtype (*PHD3*$^{fl/fl}$ LysMCre$^{-/-}$), KO = knockout (*PHD3*$^{fl/fl}$ LysMCre$^{+/-}$).

4.3. Discussion

4.3.1. Deletion of PHD3 activity in myeloid cells is associated with reduced inflammation and enhanced bacterial clearance

Deletion of *PHD3* has been shown to be beneficial for inflammation resolution in models of ischaemic injury (Rishi *et al.*, 2015)(Beneke *et al.*, 2017), acute lung injury and colitis (Walmsley *et al.*, 2011)., implicating PHD3 as a potential therapeutic target for combatting injury caused by chronic or acute inflammatory conditions. These studies use models of sterile inflammation induced by hypoxic ischaemic injury and immunomodulatory complexes, respectively. The role of PHD3 in mediating the immune response to invading pathogens, therefore, is unknown.

Our study is the first to show that PHD3 deletion in myeloid cells is beneficial for the resolution of a pathogen-mediated inflammatory response. *PHD3*$^{fl/fl}$ LysMCre$^{+/-}$ mice are more capable of bacterial control and resolution of infection in models of both *S. aureus* skin infection and a fulminant model of streptococcal pneumonia. In a *S. aureus* infection, knockout mice have significantly less localised inflammation and tissue damage over the course of 7 days of infection, as typified by smaller lesions (Figure 4.2.2-3, A-B) and less compromised tissue ultrastructure in the skin (Figure 4.2.2-6, A-B). Knockout mice have significantly diminished bacterial burden as measured 1 or 2 days after the induction of infection compared to wildtype littermate controls (Figure 4.2.2-4, A). Smaller abscesses correlate with lower bacterial burden in the tissue (Figure 4.2.2-4, B), suggesting smaller abscesses in *PHD3*$^{fl/fl}$ LysMCre$^{+/-}$ animals are therefore due to more effective control of bacterial infection. Moreover, from 4 to 7 days following infection, all abscesses from *PHD3*$^{fl/fl}$ LysMCre$^{+/-}$ animals begin to resolve, whereas abscesses in wildtype animals either resolve or are still developing by the end of the experiment, indicating animals with PHD3 deletion, from controlling the infection early on, are able to prevent bacteria proliferating in the skin and resolve the infection more efficiently. In a model of *S. pneumonia* infection, after 14 hours *PHD3*$^{fl/fl}$ LysMCre$^{+/-}$ mice have lower bacterial burden (Figure 4.2.3-1, A-B). In this model of infection, there is no change to total cell counts, neutrophil counts or signs of damage in the lung (Figure 4.2.3-1, C-E), suggesting that functional changes to the inflammatory cells

themselves account for enhanced bacterial clearance, rather than differences in cell number or recruitment efficiency, or efficiency of apoptosis as described in other studies (Walmsley *et al.*, 2011).

Myeloid-specific loss of PHD3 has no affect on animal health in a non-inflammatory context. As PHD3 is highly induced in inflammation and hypoxia (Walmsley *et al.*, 2011), it is not surprising that loss of PHD3 itself is not detrimental to the mice. Mice with myeloid-specific knockout of PHD3 are phenotypically normal and have equivalent weight and temperatures to littermate wild-type *PHD3*$^{fl/fl}$ LysMCre$^{-/-}$ mice (Figure 4.2.1-2, A, B). Interestingly, in the inflammatory context, throughout the development of a *S. aureus* abscess, neither *PHD3*$^{fl/fl}$ LysMCre$^{+/-}$ nor wildtype littermate control mice experienced any visible signs of sickness (Figure 4.2.2-1, A-C)(Figure 4.2.2-2, A-D). Even in subtle measurements of systemic illness such as rectal temperature change and weight loss, myeloid-specific PHD3 deficiency was not shown to exacerbate systemic symptoms of inflammation. To examine whether loss of PHD3 influenced the capability of hypoxic animals to respond to infection, we repeated the *S. aureus* skin infection model in mice housed in hypoxia (10% O_2). Consistent with previous studies in this model, we found hypoxia significantly induced sickness in the mice (Thompson *et al.*, 2017)(Figure 4.2.4-1). The degree of systemic sickness is equivalent between wildtype and knockout mice, with equivalent levels of hypoxia-induced hypothermia (Figure 4.2.4-1, C) and weight loss (Figure 4.2.4-1, D) following infection, as well as comparable signs of visible sickness (Figure 4.2.4-1, A, B), indicating that even in an inflammatory and hypoxic environment where PHD3 expression is the highest, myeloid-specific PHD3 expression is not essential in protecting the host from systemic symptoms of infection, although due to the degree of sickness experienced by the hypoxic mice, the experiment could not be extended to later time-points. Previous studies in this model by Thompson *et al* show that suppression of HIF-1α through preconditioning mice to hypoxia can prevent illness in hypoxic mice in this *S. aureus* abscess model through suppression of neutrophil glucose metabolism (Thompson *et al.*, 2017). That PHD3 deletion does not exacerbate symptoms in hypoxic mice therefore indicates that in this model, HIF-1α stability in neutrophils may not be controlled by PHD3 expression. Moreover, stabilization of HIF-1α has been shown to prolong

inflammation, whereas our model shows a profound pro-resolving effect of PHD3 inhibition (Elks *et al.*, 2011). PHD3 overexpression in adipose tissue is capable of suppressing HIF-1α activity (Kim *et al.*, 2014), although regulation of HIF-1α by PHD3 may be cell-type specific and dependent on the oxygen tension of the tissue and inflammatory context. Moreover, in hypoxia we see a reduction in glycolytic flux that is at odds with a HIF-1α activation phenotype. This could suggest that the benefit in our model occurs through a HIF-1α-independent mechanism, although further work is needed to confirm this.

4.3.2. Enhanced control of bacteria is not due to enhanced phagocytosis, respiratory burst or capacity for degranulation

To try and understand how knockout mice manage bacterial infection more efficiently, we looked at the capacity for these neutrophils to internalise bacteria through phagocytosis. PHD3-deficient neutrophils isolated from mouse BAL were not more efficient at phagocytosing *S. aureus* bioparticles (Figure 4.2.6-1, A, B), or *S. pneumonia* bacteria (Figure 4.2.6-2, A, B) in either normoxia or hypoxia. Interestingly, hypoxic cells are less effective at taking up both *S. aureus* and *S. pneumonia* (Figure 4.2.6-1, A, B)(Figure 4.2.6-2, A, B). In contrast, previous work has indicated that hypoxia does not influence the capacity for unstimulated human neutrophils to phagocytose *S. pneumonia* (McGovern *et al.*, 2011). Our experimental conditions differ as the neutrophils are derived from an inflammatory environment and exposed to hypoxia *in vivo*. The cells are isolated following 24 hours of inflammation; therefore, it is possible this level of acute hypoxia compromises the ability of the neutrophils to phagocytose bacteria. These airway neutrophils will also have translocated to the airway that will affect exposure to cytokines, expression of surface markers etc.

As wildtype and knockout neutrophils have equivalent phagocytic capacity (Figure 4.2.6-1, A, B)(Figure 4.2.6-2, A, B), we looked at whether at the capacity for neutrophils to undergo respiratory burst activity was altered by PHD3 knockout and whether this accounted for enhanced resolution of infection in knockout animals. Studies in clear cell renal cell carcinoma cells (ccRRCs), cells with an extensive literature regarding hypoxia response element expression, have implicated PHD3 as

a regulator of glucose metabolism, with loss of PHD3 suppressing the transcription of a number of carbohydrate metabolism genes in hypoxia including GLUT1, PFKP and LDHA, but enhancing the expression of G6PD, the rate limiting enzyme of the pentose phosphate pathway (Miikkulainen *et al.*, 2017). Moreover, killing of *S. aureus* is known to be mediated by the production of reactive oxygen species following activation of NADPH oxidase (Lekstrom-Himes and Gallin, 2000). From our data, it is clear that loss of PHD3 does not change the capacity for neutrophils to undergo a respiratory burst in normoxia or hypoxia. Baseline oxidant production was unchanged by loss of PHD3 (Figure 4.2.7-3, A). Neutrophils stimulated with fMLP upregulate ROS production, and the maximum threshold of ROS production in fMLP-treated cells was equivalent between wildtype and knockout mice (Figure 4.2.7-3, B). Moreover, this capacity to undergo respiratory burst is unchanged between wildtype and knockout mice as measured by fold change in DCF fluorescence between unstimulated and stimulated cells (Figure 4.2.7-3, C). We examined the capacity for neutrophils to regulate the OxPPP pathway as we did with human peripheral neutrophils in the previous chapter. Mass spectrometry analysis also showed no change in OxPPP flux (Figure 4.2.7-2, A, B) or $NADP^+$/NADPH ratio (Figure 4.2.7-2, C). There is no difference in GSH/GSSG ratio (Figure 4.2.7-3, D) and no change in ATP, ADP or AMP abundance or energy status (ATP/ADP) or energy charge (ATP/ADP/AMP)(Figure 4.2.8-1, C). Interestingly, despite no clear signs that the cells are regulating their ROS production, transcription of *G6pdx*, the rate-limiting enzyme for the pentose phosphate pathway, is significantly upregulated in neutrophils lacking PHD3 (Figure 4.2.7-1, A, B) consistent with studies in ccRCC cells, indicating in these cells that PHD3 may regulate *G6pdx* expression, but in cells from the inflammatory environment these processes are not regulated in a biologically relevant way that contributes to bacterial killing. That PHD3 knockout is also advantageous for killing of *S. pneumoniae,* which is known to be dependent on serine proteases rather than NADPH oxidase activity, it is clear regulation of oxidants by PHD3 does not account for the phenotype of enhanced bacterial clearance in these models (Standish and Weiser, 2009).

As it does not seem that oxidant production is being regulated by PHD3 knockout, and *S. pneumoniae* killing is enhanced by knockout of PHD3, we looked at the

capacity for PHD3 knockout neutrophils to produce neutrophil elastase and MPO in an inflammatory environment. Other components of the hypoxic response pathway are closely linked to granule protease production; HIF-1α expression correlates with neutrophil elastase activity in murine neutrophils (Peyssonnaux *et al.*, 2005). Hypoxia can also regulate the expression of Cathepsin G in macrophages (Fang *et al.*, 2009). In inflammatory BAL, elastase and MPO levels are slightly lower in PHD3 knockout animals, although this is likely due to a lower number of bacteria in the airways (Figure 4.2.5, B, D). When normalized to neutrophil number, MPO levels do appear slightly elevated (Figure 4.2.5, C). In a *S. aureus* infection, MPO levels in the abscess at 2 days after infection also appear higher in the knockout mice, although this is not significant (Figure 4.2.2-5, A). Measurement of MPO levels earlier in the course of infection may shed more light on the early regulation of degranulation in this model. Therefore, we cannot discount regulation of degranulation or granule protein production in mediating the enhanced bacterial clearance we see in $PHD3^{fl/fl}$ $LysMCre^{+/-}$ animals.

4.3.3. PHD3 differentially modulates neutrophil metabolism in normoxic and hypoxic conditions

PHD3 knockdown is known to regulate glucose metabolism in cancer cells (Miikkulainen *et al.*, 2017). Therefore, we investigated whether neutrophil metabolism was regulated by loss of PHD3. Carbohydrate metabolism is closely linked to neutrophil function and lifespan; high energy products such as ATP (Vaughan *et al.*, 2007) and Krebs cycle metabolites (Jones *et al.*, 2016) play key roles in modulating apoptosis. Of BAL neutrophils isolated from mice housed in normoxia, $PHD3^{fl/fl}$ $LysMCre^{+/-}$ neutrophils show no significant difference in energy and ATP availability (Figure 4.2.8-1, A) or levels of glycolytic metabolites (Figure 4.2.8-2, A), Krebs cycle metabolites (Figure 4.2.8-3, A) and free amino acids (Figure 4.2.8-4, A) compared to wildtype littermate controls. Although not significant, levels of all amino acids and glycolytic and Krebs cycle metabolites measured do appear subtly elevated in knockout neutrophils. It is possible this is because PHD3 is expressed in extremely low levels in normoxic cells. By contrast, in hypoxia, where PHD3 is usually highly expressed and hydroxylation activity is inhibited, $PHD3^{fl/fl}$ $LysMCre^{+/-}$ neutrophils have markedly and significantly lower levels of glycolytic

metabolites (Figure 4.2.9-2, A), Krebs cycle metabolites (Figure 4.2.9-3, A) and free amino acids (Figure 4.2.9-5, A). ATP levels in knockout neutrophils also appear diminished, but not significantly (Figure 4.2.9-4, A). It is possible that in normoxic conditions, PHD3 expression is low but activity is high, and PHD3 may hydroxylate HIF-1α and HIF-2α, targeting them for degradation and suppressing glycolytic flux. Conversely, in hypoxia, PHD3 is highly upregulated in hypoxia (Figure 4.2.9-1), and upregulates glycolysis through non-hydroxylase enzymatic activity. This would account for why knockout of PHD3 slightly enhances glycolytic flux in normoxia, and strongly suppresses glycolytic flux in hypoxia (Figure 4.2.8-1, Figure 4.2.9-1). This phenotype is supported by studies in cancer cells which show in hypoxia, loss of PHD3 downregulates the transcription of a number of glycolytic genes and the glucose transporter GLUT1 (Chen *et al.*, 2011)(Miikkulainen *et al.*, 2017). Interestingly, knockout of PHD3 has been shown to have no effect on lactate or ATP levels in BMDMs (Guentsch *et al.*, 2017).

The consequences of this metabolic modulation is unclear. Diminished glycolytic flux has been associated with advanced apoptosis (Pradelli *et al.*, 2014), which is mirrored in apoptosis data from knockout BAL neutrophils (Figure 4.2.5-1, D), and correlates with enhanced apoptosis in PHD3-deficient neutrophils in previous studies (Walmsley *et al.*, 2011). It is possible this reduction in glycolytic metabolite abundance precedes apoptosis, or that cells isolated from knockout BAL do not show more outward signs of apoptosis in their morphology, but are more advanced in the process of apoptosis than wildtype cells. Metabolic effects of PHD3 knockdown and inhibition are likely to be context and cell-specific due to the degree of interaction of PHD3 with HIF-1α and HIF-2α, balanced against non-hydroxylase activities of PHD3 on metabolic enzymes such as pyruvate kinase (Chen *et al.*, 2011).

4.3.4. Future of PHD3 inhibition

A major limitation of studying PHD3 is the absence of specific inhibitors for PHD3 activity. There are a number of available pan-hydroxylase inhibitors (Kim and Yang, 2015). The most often used is DMOG, an analogue of α-KG (Cunliffe *et al.*, 1992) . The overriding phenotype of pan-hydroxylase inhibition is of PHD2 inhibition and HIF-1α accumulation. However, DMOG also inhibits other 2-OG dependent

hydroxylases such as JHDM histone demethylases JMJD2A, 2C and 2D(Hamada *et al.*, 2009). Since then, a number of new compounds have been synthesised which have variable specificity for 2OG-dependent oxygenases, but higher specificity and less capable of inhibiting JDHM histone demethylases such as JARID1A-D and JMJD3 (Yeh *et al.*, 2017).

Most PHD inhibitors are pan-PHD inhibitors, and the phenotype of inhibition is predominantly due to PHD2 inhibition. Few efficient PHD3 inhibitors have been described in the literature. The Na group describe Pyrithione Zn (PZ) as an inhibitor which favours the inhibition of PHD3 over PHD2; however, they do not explore the activity of the molecule on other 2-OG dependent oxygenases (Na *et al.*, 2016). Zhang *et al* describe salidroside, an active ingredient of the Chinese herb *Rhodiola*, as a PHD3, but not PHD1 and 2, specific inhibitor which could enhance endothelial and smooth muscle cell migration (Zhang *et al.*, 2017).

Our data show that inhibition of PHD3 can have profound beneficial effects on bacterial clearance and inflammation resolution. However, inhibition of PHD2 can cause aberrant neutrophil inflammation. Molidustat, a 2OG-dependent high oxygenase inhibitor with a specificity to PHD2, exacerbated the inflammatory response to nebulised LPS (Sadiku *et al.*, 2017). Moreover, a range of PHD inhibitors including DMOG, L-mimosine, FG0041 and Roxadustat have been shown to have off target effects and are capable of suppressing C1q secretion by human macrophages, which could have deleterious effects in the context of inflammation resolution as C1q limits inflammasome activity following ingestion of apoptotic cells (Benoit *et al.*, 2012)(Kiriakidis *et al.*, 2017).

4.3.5. Summary

Myeloid specific PHD3 deletion is beneficial for bacterial control in models of both *S. pneumoniae* lung infection and *S. aureus* skin infection. Phenotyping of PHD3 deficient neutrophils shows no differences in capacity for phagocytosis, respiratory burst, degranulation or cytokine production. However, metabolism is globally regulated by PHD3 knockout in a way dependent on oxygen concentration, although how this may modulate bacterial clearance or neutrophilic inflammation is unknown.

5. Discussion

5.1. Summary of findings

My work on examining the role of neutrophil mitochondrial function leads on from two distinct branches of recent literature. The first describes the involvement of mitochondrial metabolism in regulating macrophage polarisation (Tannahill *et al.*, 2013) (Kelly and O'Neill, 2015). Although there have recently been numerous studies investigating M1, M2 and T cell metabolism, there have been very few studies investigating how neutrophil metabolism can modulate the inflammatory functions of this very abundant and metabolically active cell, largely due to the idea that neutrophils are predominantly glycolytic cells and therefore have limited capacity for metabolic regulation. The second was describing roles for the neutrophil mitochondria in a number of processes such as phagocytosis, apoptosis, chemotaxis, respiratory burst activation and autocrine purinergic signalling (Fossati *et al.*, 2003)(Bao *et al.*, 2014). These studies predominantly investigated metabolism in the context of ATP production, and not modulation of mROS or active immunomodulatory metabolites themselves.

I investigated the metabolic profile of the neutrophils in both hypoxia and in PHD3 knockouts. I found in unstimulated neutrophils, hypoxia enhances mROS release, which augments HIF-1α stability and neutrophil survival. Mitochondria-targeted antioxidants can induce neutrophil apoptosis, showing mROS are a pro-survival stimulus in the neutrophil. Acute hypoxia also increases flux through glycolysis and the pentose phosphate pathway. This metabolic switch is essential for maintaining hypoxic survival of the neutrophils, as treatment with the glycolytic inhibitor 2-DG or 6AN, or removal of glucose from the culture media, blocks neutrophil hypoxic survival (Figure 3.2.7-3, Figure 3.2.8-3). Increase in pentose phosphate pathway flux was shown to be important for maintaining hypoxic survival, potentially through the production of antioxidants including glutathione. In neutrophils cultured in hypoxia completely lacking glucose where neutrophil apoptosis is markedly accelerated, addition of antioxidants can completely prevent glucose-starvation-induced apoptosis. Therefore, our data show an important role for carbohydrate metabolism

aside from ATP production in maintaining neutrophil survival through the pentose phosphate pathway.

In contrast to studies in macrophages, pro-inflammatory stimuli, in this case hypoxia, do not change Krebs cycle activity and flux. Unpublished data from our group has also indicated LPS does not regulate neutrophil Krebs cycle flux or cause accumulation of succinate and citrate as it does in macrophages. This indicates neutrophils do not use their cycle to modulate their function. However, our data does show regulation of glycolytic capacity and pentose phosphate pathway flux are key determinants of neutrophil survival and function. Therefore, a parallel between mitochondrial metabolism and pro-inflammatory activity, as has been described in macrophages, is not present in neutrophils. It is clear non-mitochondrial metabolism is key in regulating neutrophil function and lifespan, with little regulation of mitochondrial metabolism.

In my data, I have shown that the regulation of metabolism by PHD3 has opposing effects depending on oxygen tension. Hypoxia appears to globally inhibit neutrophil metabolism in PHD3-deficient neutrophils, whereas in normoxic conditions, metabolism is increased globally. This may account for the divergent effects of PHD3 knockout in varying conditions. In highly oxidative environments, for example in the vasculature in models of sepsis, PHD3 deletion may be detrimental to resolving inflammation (Kiss *et al.*, 2012). However, in potentially hypoxic environments such as an ischaemic limb or *S. aureus* abscess, PHD3 deletion could be advantageous. Inflammation and hypoxia are extremely closely related, with inflamed sites often experiencing profound hypoxia, and hypoxia exacerbating inflammation (Bartels, Grenz and Eltzschig, 2013).

The metabolic signature of PHD3 knockout is totally distinct from PHD2 or HIF-1α knockout. HIF-1α regulation is known to switch cellular metabolism from mitochondrial metabolism to glycolysis through induction of glycolytic enzymes and PDK1, which suppresses pyruvate dehydrogenase and blocks entry of metabolites into the Krebs cycle (Semenza, 2007). In neutrophils, knockout of PHD2 profoundly induces glycolysis in both normoxic and hypoxic conditions due to enhanced stabilisation of HIF-1α, which leads to an exaggerated and detrimental neutrophilic

response in a model of inflammation (Sadiku *et al.*, 2017). Knockout of PHD3 in this case is beneficial for the resolution of infection and has suppressive effects on glycolysis and glucose metabolism. Regulation and inhibition of PHD3 therefore may be a novel therapeutic target in the treatment of chronic inflammatory diseases.

5.2. Therapeutic implications of this work

HIF-1α has been identified as a potent regulator of inflammation and has been linked to both acute and chronic inflammation. It is therefore a candidate as a therapeutic target. Directly modulating HIF-1α activity is a risky therapeutic strategy. HIF-1α inhibitors have been administered in the context of hypoxic tumours, and some compounds have shown success in suppressing tumour growth and metastasis in *in vivo* murine models (Dikmen *et al.*, 2008)(Jacoby *et al.*, 2010). In the context of infection, loss of HIF-1α can be disastrous, with suppression of HIF-1α limiting bactericidal activity and exacerbating systemic and localised measures of infection (Peyssonnaux *et al.*, 2005), and enhanced stabilization of HIF-1α through knockout of PHD2 can cause an exaggerated immune response (Sadiku *et al.*, 2017). One aspect of the therapeutic challenge in these pathways, therefore, is suppressing inappropriate HIF-1α expression in inflammation without compromising the normal function of the immune system. Our data show mROS can stabilise HIF-1α in hypoxia and are capable of subtly positively modulating neutrophil survival in hypoxia, specifically. Although this work is at an early stage, our data support the idea that mROS can modulate neutrophil survival, which could in turn modulate inflammation and may be a potential route for therapeutic intervention against chronic inflammation. Targeting neutrophil mROS has already shown some success in murine inflammatory models, as administration of complex III inhibitors can aid the resolution of an acute lung injury (Zmijewski *et al.*, 2008). Understanding the mechanism of how this occurs in neutrophils may therefore lead to a novel, targetable pathway which could be inhibited to limit, but not abrogate, HIF-1α stabilisation and neutrophil function in chronically inflamed sites where neutrophil activity is detrimental.

Our work also links neutrophil PHD3 expression with delayed bacterial clearance and a greater degree of inflammation in murine models of infection. Other studies

have shown inhibition of PHD3 is beneficial for the resolution of a sterile inflammation in hind limb ischaemia and LPS-induced lung injury (Walmsley *et al.*, 2011)(Swain *et al.*, 2014). This is the first study to show that in a bacterial infection, PHD3 knockout is beneficial. Often in chronic inflammatory diseases, patients present with frequent bacterial infections; therefore, the therapeutic challenge is to suppress the overactive immune response in these patients without compromising bactericidal activities of these immune cells. PHD3 could therefore offer an attractive target in these diseases.

5.3. Limitations

It is an important point that the work so far has used murine models of infection; the relevance of using mice to model the human immune system is controversial. The primary mechanism for *S. aureus* sensing neutrophils is through alpha defensin 1 (HNP-1) released by neutrophils triggering the activation of the saeR/S machinery; however, murine neutrophils do not produce HNP-1, indicating there may be differences in the *S. aureus* response against murine neutrophils (Guerra *et al.*, 2017). Moreover, the murine cytokine profile is markedly different to human neutrophils (Tecchio, Micheletti and Cassatella, 2014). The activity of *S. aureus* toxins such as HlgA, HlgC and LukF-PVL is limited against murine cells compared to human cells. One method for circumventing this could be to use a humanised murine model where profoundly immunodeficient NOD/SCID/IL2ry^{null} mice are seeded with human CD34^{+} umbilical cord blood, replacing components of the murine immune system with human immune cells (Shultz, Ishikawa and Greiner, 2007). These mice are more susceptible to *S. aureus* infection and may be a better model of human *S. aureus* infection that mouse models (Tseng *et al.*, 2015). Whether the progression of a *S. aureus* infection in a human would be modulated by PHD3 inhibition has yet to be elucidated.

A further limitation is associated with this work is use of the LysMCre mouse knockout model. LysM is expressed in all granulocytes subtypes and in mature macrophages (Clausen *et al.*, 1999). This is important as knockout of PHD3 is known to modulate macrophage function and apoptosis (Swain *et al.*, 2014), although we do not see differences in macrophage number in our model of sterile

inflammation (Figure 4.2.5-1, C). To confirm our phenotype is caused by neutrophils specifically, another model of knockout may need to be used. To address this limitation, we have derived a PHD3$^{fl/fl}$ Mrp8Cre$^{+/-}$ mouse line. Mrp8Cre restricts Cre expression to neutrophils and a small fraction of granulocyte/macrophage progenitor cells in the bone marrow (Passegué, Wagner and Weissman, 2004).

A limitation of the *in vitro* model we use is that we use a binary model of hypoxia where "hypoxia" is defined at 1% oxygen and "normoxia" is 21% oxygen. This model is used in wide range of *in vitro* cell culture models in both immune and non-immune cells (Hannah *et al.*, 1995)(Hoenderdos *et al.*, 2016)(Sadiku *et al.*, 2017). This model allows us to clearly differentiate phenotypic differences between hypoxic and normoxic cells. More involved models of oxygen regulation, for example the use of multiple oxygen tensions or cycling of arterial/venous/tissue oxygen tensions, may give a more accurate representation of the oxygen tensions experienced by a neutrophil in the body, although this is outside the scope of this study.

5.4. Future work

The mechanism for enhanced mitochondrial ROS production in hypoxia is currently unknown. The glycerol 3-phosphate is a possible candidate for this regulation. Unpublished data from our group suggests neutrophil modulate expression of cytoplasmic GPD1 protein expression, and addition of the mitochondrial glycerol 3-phosphate dehydrogenase inhibitor iGP-1 can inhibitor mitochondrial membrane hyperpolarization in hypoxia in a dose dependent way, although further studies are needed to ascertain whether this pathway accounts for the increase in mitochondrial ROS production we see in hypoxia.

Although inhibiting electron transport chain activity would likely modulate neutrophil reactive oxygen species production, these inhibitors tend to be profoundly toxic. Therefore, identification of a novel mitochondrial ROS-mediating pathway in neutrophils could offer a potential therapeutic target for limiting neutrophil inflammation in disease without side effects associated with inhibition of oxidative phosphorylation itself. The advent of novel GPD2 inhibitors will allow us to interrogate this pathway *in vitro* and *in vivo* (Orr *et al.*, 2014). Indeed, knockout of

GPD2 is non-lethal in mice, suggesting this pathway may be targetable *in vivo* without lethal consequences (Mracek, Drahota and Hou, 2013).

The mechanism behind improved bacterial clearance in PHD3$^{fl/fl}$ LysMCre$^{+/-}$ mice has not fully been elucidated either. There are some indications in the data that myeloperoxidase activity in inflamed tissue in both infective and sterile models of inflammation may be slightly elevated (Figure 4.2.2-5, Figure 4.2.2-6, Figure 4.2.5-2, D); whether or not this accounts for enhanced bacterial control in the absence of changes to phagocytic capacity or ROS generation is unclear. It is surprising that metabolism is highly regulated in the PHD3 knockouts, yet serine protease and MPO expression seems unaffected at the timepoints we have measured in these models. Future work will investigate whether MPO capacity is affected at earlier timepoints in this model. We do not know conclusively whether global regulation of metabolism in PHD3-deficient neutrophils contributes to the phenotype of enhanced bacterial control or apoptosis. Moreover, it is unclear whether the divergent effects of PHD3 knockout attribute to the enhancement of inflammation resolution. It follows that a reduction of global metabolism in hypoxic conditions may be due to either enhanced apoptosis in hypoxia as demonstrated in previous papers (Walmsley *et al.*, 2011). Indeed, we have shown inhibition of glycolysis through addition of inhibitors or withdrawal of glucose from the culture medium can induce apoptosis (Figure 3.2.7-3). It is possible that PHD3 knockout therefore prevents neutrophils from upregulated glucose metabolism in hypoxia and prevents them generating antioxidants and ATP that causes them to apoptose more rapidly. This may account for the enhanced resolution of inflammation but does not account for more effective bacterial clearance in infection models. Therefore, further work is needed to ascertain how regulation of metabolism by PHD3 modulates neutrophil function and apoptosis, and also how neutrophils clear bacteria more effective from the site of infection. Regulation of HIF-1α or HIF-2α may account for modulation of metabolism by PHD3, although as PHD3 is a negative regulator of HIF-1α, knockout should enhance HIF-1α activity and glycolytic flux.

6. Bibliography

Agani, F. H., Pichiule, P., Chavez, J. C. and LaManna, J. C. (2000) 'The role of mitochondria in the regulation of hypoxia-inducible factor 1 expression during hypoxia', *Journal of Biological Chemistry*, 275(46), pp. 35863–35867.

Akgul, C., Moulding, D. A. and Edwards, S. W. (2001) 'Molecular control of neutrophil apoptosis', *FEBS Lett*, 487(3), pp. 318–322.

Ambrosio, G., Zweier, J. L., Duilio, C., Kuppusamy, P., Santoro, G., Elia, P. P., Tritto, I., Cirillo, P., Condorelli, M., Chiariello, M. and Flaherty, J. T. (1993) 'Evidence that mitochondrial respiration is a source of potentially toxic oxygen free radicals in intact rabbit hearts subjected to ischemia and reflow', *Journal of Biological Chemistry*, 268(25), pp. 18532–18541.

Appelhoff, R. J., Tian, Y. M., Raval, R. R., Turley, H., Harris, A. L., Pugh, C. W., Ratcliffe, P. J. and Gleadle, J. M. (2004) 'Differential function of the prolyl hydroxylases PHD1, PHD2, and PHD3 in the regulation of hypoxia-inducible factor', *Journal of Biological Chemistry*, 279(37), pp. 38458–38465.

Aprelikova, O., Chandramouli, G. V. R., Wood, M., Vasselli, J. R., Riss, J., Maranchie, J. K., Linehan, W. M. and Barrett, J. C. (2004) 'Regulation of HIF prolyl hydroxylases by hypoxia-inducible factors', *Journal of Cellular Biochemistry*, 92(3), pp. 491–501.

Aprelikova, O., Pandolfi, S., Tackett, S., Ferreira, M., Salnikow, K., Ward, Y., Risinger, J. I., Barrett, J. C. and Niederhuber, J. (2009) 'Melanoma antigen-11 inhibits the hypoxia-inducible factor prolyl hydroxylase 2 and activates hypoxic response', *Cancer Research*, 69(2), pp. 616–624.

Aragonés, J., Schneider, M., Van Geyte, K., Fraisl, P., Dresselaers, T., Mazzone, M., Dirkx, R., Zacchigna, S., Lemieux, H., Jeoung, N. H., Lambrechts, D., Bishop, T., Lafuste, P., Diez-Juan, A., Harten, S. K., Van Noten, P., De Bock, K., Willam, C., Tjwa, M., Grosfeld, A., Navet, R., Moons, L., Vandendriessche, T., Deroose, C., Wijeyekoon, B., Nuyts, J., Jordan, B., Silasi-Mansat, R., Lupu, F., Dewerchin, M., Pugh, C., Salmon, P., Mortelmans, L., Gallez, B., Gorus, F., Buyse, J., Sluse, F.,

Harris, R. A., Gnaiger, E., Hespel, P., Van Hecke, P., Schuit, F., Van Veldhoven, P., Ratcliffe, P., Baes, M., Maxwell, P. and Carmeliet, P. (2008) 'Deficiency or inhibition of oxygen sensor Phd1 induces hypoxia tolerance by reprogramming basal metabolism', *Nature Genetics*, 40(2), pp. 170–180.

Baek, J. H., Mahon, P. C., Oh, J., Kelly, B., Krishnamachary, B., Pearson, M., Chan, D. A., Giaccia, A. J. and Semenza, G. L. (2005) 'OS-9 interacts with hypoxia-inducible factor 1α and prolyl hydroxylases to promote oxygen-dependent degradation of HIF-1α', *Molecular Cell*, 17(4), pp. 503–512.

Ballinger, C. a, Mendis-Handagama, C., Kalmar, J. R., Arnold, R. R. and Kinkade, J. M. (1994) 'Changes in the localization of catalase during differentiation of neutrophilic granulocytes.', *Blood*, 83(9), pp. 2654–68.

Banerjee, S., Zmijewski, J. W., Lorne, E., Liu, G., Sha, Y. and Abraham, E. (2010) 'Modulation of SCFβ-TrCP-dependent IκBα ubiquitination by hydrogen peroxide', *Journal of Biological Chemistry*, 285(4), pp. 2665–2675.

Bao, Y., Ledderose, C., Seier, T., Graf, A. F., Brix, B., Chong, E. and Junger, W. G. (2014) 'Mitochondria regulate neutrophil activation by generating ATP for autocrine purinergic signaling', *Journal of Biological Chemistry*, 289(39), pp. 26794–26803.

Barry, P. W. and Pollard, A. J. (2003) 'Altitude illness', *British Medical Journal*, 326(April), pp. 915–919.

Bartels, K., Grenz, A. and Eltzschig, H. K. (2013) 'Hypoxia and inflammation are two sides of the same coin', *Proceedings of the National Academy of Sciences*, 110(46), pp. 18351–18352.

Beerman, I., Luis, T. C., Singbrant, S., Lo Celso, C. and Méndez-Ferrer, S. (2017) 'The evolving view of the hematopoietic stem cell niche', *Experimental Hematology*, 50, pp. 22–26.

Bell, E. L., Klimova, T. A., Eisenbart, J., Moraes, C. T., Murphy, M. P., Budinger, G. R. S. and Chandel, N. S. (2007) 'The Qo site of the mitochondrial complex III is required for the transduction of hypoxic signaling via reactive oxygen species

production', *The Journal of Cell Biology*, 177(6), pp. 1029–1036.

Beneke, A., Guentsch, A., Hillemann, A., Zieseniss, A., Swain, L. and Katschinski, D. M. (2017) 'Loss of PHD3 in myeloid cells dampens the inflammatory response and fibrosis after hind-limb ischemia', *Cell Death and Disease*, 8(8), p. e2976.

Benita, Y., Kikuchi, H., Smith, A. D., Zhang, M. Q., Chung, D. C. and Xavier, R. J. (2009) 'An integrative genomics approach identifies Hypoxia Inducible Factor-1 (HIF-1)-target genes that form the core response to hypoxia', *Nucleic Acids Research*, 37(14), pp. 4587–4602.

Benoit, M. E., Clarke, E. V., Morgado, P., Fraser, D. A. and Tenner, A. J. (2012) 'Complement protein C1q directs macrophage polarization and limits inflammasome activity during the uptake of apoptotic cells', *The Journal of Immunology*, 188(11), pp. 5682–5693.

Berra, E., Benizri, E., Ginouvès, A., Volmat, V., Roux, D. and Pouysségur, J. (2003) 'HIF prolyl-hydroxylase 2 is the key oxygen sensor setting low steady-state levels of HIF-1α in normoxia', *EMBO Journal*, 22(16), pp. 4082–4090.

Boettcher, S., Gerosa, R. C., Radpour, R., Bauer, J., Ampenberger, F., Heikenwalder, M., Kopf, M. and Manz, M. G. (2014) 'Endothelial cells translate pathogen signals into G-CSF-driven emergency granulopoiesis', *Blood*, 124(9), pp. 1393–1403.

Bonello, S., Zähringer, C., BelAiba, R. S., Djordjevic, T., Hess, J., Michiels, C., Kietzmann, T. and Görlach, A. (2007) 'Reactive oxygen species activate the HIF-1α promoter via a functional NFκB site', *Arteriosclerosis, Thrombosis, and Vascular Biology*, 27(4), pp. 755–761.

Borregaard, N. (2010) 'Neutrophils, from Marrow to Microbes', *Immunity*, 33(5), pp. 657–670.

Branitzki-Heinemann, K., Mollerherm, H., Vollger, L., Husein, D. M., de Buhr, N., Blodkamp, S., Reuner, F., Brogden, G., Naim, H. Y. and Von Kockritz-Blickwede, M. (2016) 'Formation of neutrophil extracellular traps under low oxygen level',

Frontiers in Immunology, 7(November), pp. 1–9.

Briston, T., Yang, J. and Ashcroft, M. (2011) 'HIF-1α localization with mitochondria: A new role for an old favorite?', *Cell Cycle*, pp. 4170–4171.

Brown, S. T. and Nurse, C. A. (2008) 'Induction of HIF-2α is dependent on mitochondrial O2 consumption in an O2-sensitive adrenomedullary chromaffin cell line', *AJP: Cell Physiology*, 294(6), pp. C1305–C1312.

Brunelle, J. K., Bell, E. L., Quesada, N. M., Vercauteren, K., Tiranti, V., Zeviani, M., Scarpulla, R. C. and Chandel, N. S. (2005) 'Oxygen sensing requires mitochondrial ROS but not oxidative phosphorylation', *Cell Metabolism*, 1(6), pp. 409–414.

Campbell, E. L., Bruyninckx, W. J., Kelly, C. J., Glover, L. E., McNamee, E. N., Bowers, B. E., Bayless, A. J., Scully, M., Saeedi, B. J., Golden-Mason, L., Ehrentraut, S. F., Curtis, V. F., Burgess, A., Garvey, J. F., Sorensen, A., Nemenoff, R., Jedlicka, P., Taylor, C. T., Kominsky, D. J. and Colgan, S. P. (2014) 'Transmigrating neutrophils shape the mucosal microenvironment through localized oxygen depletion to influence resolution of inflammation', *Immunity*, 40(1), pp. 66–77.

Campbell, E. L., Kao, D. J. and Colgan, S. P. (2016) 'Neutrophils and the inflammatory tissue microenvironment in the mucosa', *Immunol Review*, 273(1), pp. 112–120.

Carrière, A., Carmona, M. C., Fernandez, Y., Rigoulet, M., Wenger, R. H., Pénicaud, L. and Casteilla, L. (2004) 'Mitochondrial reactive oxygen species control the transcription factor CHOP-10/GADD153 and adipocyte differentiation: A mechanism for hypoxia-dependent effect', *Journal of Biological Chemistry*, 279(39), pp. 40462–40469.

Chambers, J. W. and LoGrasso, P. V. (2011) 'Mitochondrial c-Jun N-terminal Kinase (JNK) signaling initiates physiological changes resulting in amplification of reactive oxygen species generation', *Journal of Biological Chemistry*, 286(18), pp. 16052–16062.

Chance, B. and Hollunger, G. (1961) ‘The interaction of energy and electron transfer reactions in mitochondria’, *Journal of Biological Chemistry*, 236(5), pp. 1577–1584.

Chandel, N. S., Maltepe, E., Goldwasser, E., Mathieu, C. E., Simon, M. C. and Schumacker, P. T. (1998) ‘Mitochondrial reactive oxygen species trigger hypoxia-induced transcription.’, *Proceedings of the National Academy of Sciences of the United States of America*, 95(20), pp. 11715–20.

Chandel, N. S., McClintock, D. S., Feliciano, C. E., Wood, T. M., Melendez, J. a, Rodriguez, a M. and Schumacker, P. T. (2000) ‘Reactive oxygen species generated at mitochondrial Complex III stabilize hypoxia-inducible factor-1α during hypoxia: A mechanism of O_2 sensing’, *Journal of Biological Chemistry*, 275(33), pp. 25130–25138.

Chang, S. C. and Yang, W. C. V. (2016) ‘Hyperglycemia, tumorigenesis, and chronic inflammation’, *Critical Reviews in Oncology/Hematology*, 108, pp. 146–153.

Chen, N., Rinner, O., Czernik, D., Nytko, K. J., Zheng, D., Stiehl, D. P., Zamboni, N., Gstaiger, M. and Frei, C. (2011) ‘The oxygen sensor PHD3 limits glycolysis under hypoxia via direct binding to pyruvate kinase’, *Cell Research*, 21(6), pp. 983–986.

Chipuk, J. E., Moldoveanu, T., Llambi, F., Parsons, M. J. and Green, D. R. (2010) ‘The BCL-2 Family Reunion’, *Molecular Cell*, 37(3), pp. 299–310.

Chou, R. C., Kim, N. D., Sadik, C. D., Seung, E., Lan, Y., Byrne, M. H., Haribabu, B., Iwakura, Y. and Luster, A. D. (2010) ‘Lipid-cytokine-chemokine cascade drives neutrophil recruitment in a murine model of inflammatory arthritis’, *Immunity*, 33(2), pp. 266–278.

Christensen, J. S., Jensen, T. G., Kolmos, H. J., Pedersen, C. and Lassen, A. (2012) ‘Bacteremia with Streptococcus pneumoniae: Sepsis and other risk factors for 30-day mortality - a hospital-based cohort study’, *European Journal of Clinical Microbiology and Infectious Diseases*, 31(10), pp. 2719–2725.

Clanton, T. L. (2007) 'Hypoxia-induced reactive oxygen species formation in skeletal muscle', *Journal of applied physiology*, 102, pp. 2379–2388.

Clausen, B. E., Burkhardt, C., Reith, W., Renkawitz, R. and Förster, I. (1999) 'Conditional gene targeting in macrophages and granulocytes using LysMcre mice', *Transgenic Research*, 8(4), pp. 265–277.

Codolo, G., Bossi, F., Durigutto, P., Bella, C. Della, Fischetti, F., Amedei, A., Tedesco, F., D'Elios, S., Cimmino, M., Micheletti, A., Cassatella, M. A., D'Elios, M. M. and De Bernard, M. (2013) 'Orchestration of inflammation and adaptive immunity in *Borrelia burgdorferi*-induced arthritis by neutrophil-activating protein A', *Arthritis and Rheumatism*, 65(5), pp. 1232–1242.

Colgan, S. P. and Taylor, C. T. (2010) 'Hypoxia: An alarm signal during intestinal inflammation', *Nature Reviews Gastroenterology and Hepatology*, 7(5), pp. 281–287.

Colotta, B. F., Re, F., Polentarutti, N., Sozzani, S. and Mantovani, A. (1992) 'Modulation of Granulocyte Survival and Programmed Cell Death by Cytokines and Bacterial Products', *Blood*, 80(8), pp. 2012–2020.

Cramer, T., Yamanishi, Y., Clausen, B. E., Förster, I., Pawlinski, R., Mackman, N., Haase, V. H., Jaenisch, R., Corr, M., Nizet, V., Firestein, G. S., Gerber, H. P., Ferrara, N. and Johnson, R. S. (2003) 'HIF-1α is essential for myeloid cell-mediated inflammation', *Cell*, 112(5), pp. 645–657.

Cunliffe, C. J., Franklin, T. J., Hales, N. J. and Hill, G. B. (1992) 'Novel inhibitors of Prolyl 4-Hydroxylase. 3. Inhibition by the substrate analogue *N*-oxaloglycine and its derivatives', *Journal of Medicinal Chemistry*, 35(14), pp. 2652–2658.

Dada, L. A., Chandel, N. S., Ridge, K. M., Pedemonte, C., Bertorello, A. M. and Sznajder, J. I. (2003) 'Hypoxia-induced endocytosis of Na,K-ATPase in alveolar epithelial cells is mediated by mitochondrial reactive oxygen species and PKC-ζ', *Cell*, 111(7), pp. 1057–1064.

Dancey, J. T., Deubelbeiss, K. A., Harker, L. A. and Finch, C. A. (1976) 'Neutrophil

Kinetics in Man', *The journal of clinical investigation*, 58(September), pp. 705–715.

Dengler, V. L., Galbraith, M. D. and Espinosa, J. M. (2014) 'Transcriptional regulation by hypoxia inducible factors', *Critical Reviews in Biochemistry and Molecular Biology*, 49(1), pp. 1–15.

Dickerhof, N., Pearson, J. F., Hoskin, T. S., Berry, L. J., Turner, R., Sly, P. D. and Kettle, A. J. (2017) 'Oxidative stress in early cystic fibrosis lung disease is exacerbated by airway glutathione deficiency', *Free Radical Biology and Medicine*. Elsevier B.V., 113(August), pp. 236–243.

Dikmen, Z. G., Gellert, G. C., Dogan, P., Yoon, H., Young, B. L., Chang, H. A. and Shay, J. W. (2008) 'In vivo and in vitro effects of a HIF-1α inhibitor, RX-0047', *Journal of Cellular Biochemistry*, 104(3), pp. 985–994.

Douda, D. N., Khan, M. A., Grasemann, H. and Palaniyar, N. (2015) 'SK3 channel and mitochondrial ROS mediate NADPH oxidase-independent NETosis induced by calcium influx', *Proceedings of the National Academy of Sciences*, 112(9), pp. 2817–2822.

Dröse, S., Hanley, P. J. and Brandt, U. (2009) 'Ambivalent effects of diazoxide on mitochondrial ROS production at respiratory chain complexes I and III', *Biochimica et Biophysica Acta - General Subjects*. Elsevier B.V., 1790(6), pp. 558–565.

Du, J., Xu, R., Hu, Z., Tian, Y., Zhu, Y., Gu, L. and Zhou, L. (2011) 'PI3K and ERK-induced Rac1 activation mediates hypoxia-induced HIF-1α expression in MCF-7 breast cancer cells', *PLoS ONE*, 6(9), pp. 1–9.

Dunwoodie, S. L. (2009) 'The role of hypoxia in development of the mammalian embryo', *Developmental Cell*, 17(6), pp. 755–773.

Duranteau, J., Chandel, N. S., Kulisz, A., Shao, Z. and Schumacker, P. T. (1998) 'Intracellular Signaling by Reactive Oxygen Species during Hypoxia in Cardiomyocytes', *Journal of Biological Chemistry*, 273(19), pp. 11619–11624.

Dyugovskaya, L., Polyakov, A., Cohen-Kaplan, V., Lavie, P. and Lavie, L. (2012) 'Bax/Mcl-1 balance affects neutrophil survival in intermittent hypoxia and

obstructive sleep apnea: Effects of p38MAPK and ERK1/2 signaling', *Journal of Translational Medicine*, 10(1), p. 211.

Dzhagalov, I., St. John, A. and He, Y. W. (2007) 'The antiapoptotic protein Mcl-1 is essential for the survival of neutrophils but not macrophages', *Blood*, 109(4), pp. 1620–1626.

Elks, P. M., Van Eeden, F. J., Dixon, G., Wang, X., Reyes-Aldasoro, C. C., Ingham, P. W., Whyte, M. K. B., Walmsley, S. R. and Renshaw, S. A. (2011) 'Activation of hypoxia-inducible factor-1α (hif-1α) delays inflammation resolution by reducing neutrophil apoptosis and reverse migration in a zebrafish inflammation model', *Blood*, 118(3), pp. 712–722.

Epaulard, O., Adam, L., Poux, C., Zurawski, G., Salabert, N., Rosenbaum, P., Dereuddre-Bosquet, N., Zurawski, S., Flamar, A.-L., Oh, S., Romain, G., Chapon, C., Banchereau, J., Lévy, Y., Le Grand, R. and Martinon, F. (2014) 'Macrophage- and neutrophil-derived TNF-α instructs skin langerhans cells to prime antiviral immune responses', *The Journal of Immunology*, 193(5), pp. 2416–2426.

Escribese, M. M., Sierra-Filardi, E., Nieto, C., Samaniego, R., Sanchez-Torres, C., Matsuyama, T., Calderon-Gomez, E., Vega, M. A., Salas, A., Sanchez-Mateos, P. and Corbi, A. L. (2012) 'The Prolyl Hydroxylase PHD3 identifies proinflammatory macrophages and its expression is regulated by Activin A', *The Journal of Immunology*, 189(4), pp. 1946–1954.

Fadeel, B. B., Åhlin, A., Henter, J., Orrenius, S. and Hampton, M. B. (1998) 'Involvement of Caspases in Neutrophil Apoptosis: Regulation by Reactive Oxygen Species', *Blood*, 92(12), pp. 4808–4818.

Fadok, V. A., Bratton, D. L., Konowal, A., Freed, P. W., Westcott, J. Y. and Henson, P. M. (1998) 'Macrophages that have ingested apoptotic cells in vitro inhibit proinflammatory cytokine production through autocrine/paracrine mechanisms involving TGF-β, PGE2, and PAF', *Journal of Clinical Investigation*, 101(4), pp. 890–898.

Fang, H., Hughes, R., Murdoch, C., Coffelt, S. B., Biswas, S. K., Harris, A. L.,

Johnson, R. S., Imityaz, H. Z., Simon, M. C., Fredlund, E., Greten, F. R. and Lewis, C. E. (2009) 'Hypoxia inducible factors 1 and 2 are important transcriptional effectors in primary macrophages experiencing hypoxia', *Hematology*, 114(4), pp. 844–860.

Fang, S., Qiu, J., Yu, H., Fan, H., Wu, X., Fang, Z., Shen, Q. and Chen, S. (2017) 'Associated of *EGLN1* and *EGLN3* single-nucleotide polymorphisms with chronic obstructive pulmonary disease risk in a Chinese population', *Int J Clin Exp Med*, 10(7), pp. 10866–10873.

Finsterbusch, M., Voisin, M.-B., Beyrau, M., Williams, T. J. and Nourshargh, S. (2014) 'Neutrophils recruited by chemoattractants in vivo induce microvascular plasma protein leakage through secretion of TNF', *The Journal of Experimental Medicine*, 211(7), pp. 1307–1314.

Fossati, G., Moulding, D., Spiller, D. G., Moots, R. J., White, M. R. H. and Edwards, S. W. (2003) 'The Mitochondrial Network of Human Neutrophils: Role in Chemotaxis, Phagocytosis, Respiratory Burst Activation, and Commitment to Apoptosis', *The Journal of Immunology*, 170(4), pp. 1964–1972.

Fox, S., Leitch, A. E., Duffin, R., Haslett, C. and Rossi, A. G. (2010) 'Neutrophil apoptosis: Relevance to the innate immune response and inflammatory disease', *Journal of Innate Immunity*, 2(3), pp. 216–227.

Fu, J. and Taubman, M. B. (2010) 'Prolyl hydroxylase EGLN3 regulates skeletal myoblast differentiation through an NF-κB-dependent pathway', *Journal of Biological Chemistry*, 285(12), pp. 8927–8935.

Fu, J. and Taubman, M. B. (2013) 'EGLN3 inhibition of NF-κB is mediated by Prolyl Hydroxylase-independent inhibition of IκB Kinase γ ubiquitination', *Molecular and Cellular Biology*, 33(15), pp. 3050–3061.

Fukuda, R., Zhang, H., Kim, J. whan, Shimoda, L., Dang, C. V. and Semenza, G. L. L. (2007) 'HIF-1 regulates cytochrome oxidase subunits to optimize efficiency of respiration in hypoxic cells', *Cell*, 129(1), pp. 111–122.

Furlow, P. W., Percy, M. J., Sutherland, S., Bierl, C., Mcmullin, M. F., Master, S. R., Lappin, T. R. J. and Lee, F. S. (2009) 'Erythrocytosis-associated HIF-2α Mutations Demonstrate a Critical Role for Residues C-terminal to the Hydroxylacceptor Proline', *Journal of Biological Chemistry*, 284(14), pp. 9050–9058.

Gasior, M., Rogawski, M. A. and Hartman, A. L. (2006) 'Neuroprotective and disease-modifying effects of the ketogenic diet', *Behavioural Pharmacology*, 17(5–6), pp. 431–439.

Gerald, D., Berra, E., Frapart, Y. M., Chan, D. A., Giaccia, A. J., Mansuy, D., Pouysségur, J., Yaniv, M. and Mechta-Grigoriou, F. (2004) 'JunD reduces tumor angiogenesis by protecting cells from oxidative stress', *Cell*, 118(6), pp. 781–794.

German, N., Cimermancic, P., Weinkam, P., Rettenmaier, T. J., Bichmann, L., Keedy, D. A., Woldeyes, R. A., Schneidman-duhovny, D., Omar, N., Mitchell, J. C., Wells, J. A., Fraser, J. S., Sali, A., Sciences, T., Francisco, S., Francisco, S., Francisco, S., Francisco, S., Francisco, S., Francisco, S., Francisco, S. and Francisco, S. (2017) 'PHD3 loss in cancer enables metabolic reliance on fatty acid oxidation via deactivation of ACC2', *Molecular Cell*, 428(4), pp. 709–719.

Le Goffe, C., Vallette, G., Charrier, L., Candelon, T., Bou-Hanna, C., Bouhours, J. F. and Laboisse, C. L. (2002) 'Metabolic control of resistance of human epithelial cells to H2O2 and NO stresses', *Biochem J*, 364, pp. 349–359.

Gottwald, E. M., Duss, M., Bugarski, M., Haenni, D., Schuh, C. D., Landau, E. M. and Hall, A. M. (2018) 'The targeted anti-oxidant MitoQ causes mitochondrial swelling and depolarization in kidney tissue', *Physiological Reports*, 6(7), pp. 1–9.

Gresham, H. D., Lowrance, J. H., Caver, T. E., Wilson, B. S., Cheung, A. L. and Lindberg, F. P. (2000) 'Survival of *Staphylococcus aureus* inside neutrophils contributes to infection', *The Journal of Immunology*, 164(7), pp. 3713–3722.

Guentsch, A., Beneke, A., Swain, L., Farhat, K., Nagarajan, S., Wielockx, B., Raithatha, K., Dudek, J., Rehling, P., Zieseniss, A., Jatho, A., Chong, M., Santos, C. X. C., Shah, A. M. and Katschinski, D. M. (2017) 'PHD2 Is a Regulator for

Glycolytic Reprogramming in Macrophages', *Molecular and Cellular Biology*, 37(1), pp. e00236-16.

Guerra, F. E., Borgogna, T. R., Patel, D. M., Sward, E. W. and Voyich, J. M. (2017) 'Epic immune battles of history: Neutrophils vs. *Staphylococcus aureus*', *Frontiers in Cellular and Infection Microbiology*, 7(June), pp. 1–19.

Guzy, R. D., Hoyos, B., Robin, E., Chen, H., Liu, L., Mansfield, K. D., Simon, M. C., Hammerling, U. and Schumacker, P. T. (2005) 'Mitochondrial complex III is required for hypoxia-induced ROS production and cellular oxygen sensing', *Cell Metabolism*, 1(6), pp. 401–408.

Guzy, R. D. and Schumacker, P. T. (2006) 'Oxygen sensing by mitochondria at complex III: The paradox of increased reactive oxygen species during hypoxia', in *Experimental Physiology*, pp. 807–819.

Guzy, R. D., Sharma, B., Bell, E., Chandel, N. S. and Schumacker, P. T. (2008) 'Loss of the SdhB, but not the SdhA, subunit of Complex II triggers reactive oxygen species-dependent Hypoxia-Inducible Factor activation and tumorigenesis', *Molecular and Cellular Biology*, 28(2), pp. 718–731.

Haider, L., Fischer, M. T., Frischer, J. M., Bauer, J., Höftberger, R., Botond, G., Esterbauer, H., Binder, C. J., Witztum, J. L. and Lassmann, H. (2011) 'Oxidative damage in multiple sclerosis lesions', *Brain*, 134(7), pp. 1914–1924.

Hall, C. J., Sanderson, L. E., Lawrence, L. M., Pool, B., Van Der Kroef, M., Ashimbayeva, E., Britto, D., Harper, J. L., Lieschke, G. J., Astin, J. W., Crosier, K. E., Dalbeth, N. and Crosier, P. S. (2018) 'Blocking fatty acid-fueled mROS production within macrophages alleviates acute gouty inflammation', *Journal of Clinical Investigation*, 128(5), pp. 1752–1771.

Hamada, S., Kim, T. D., Suzuki, T., Itoh, Y., Tsumoto, H., Nakagawa, H., Janknecht, R. and Miyata, N. (2009) 'Synthesis and activity of N-oxalylglycine and its derivatives as Jumonji C-domain-containing histone lysine demethylase inhibitors', *Bioorganic and Medicinal Chemistry Letters*, 19(10), pp. 2852–2855.

Hannah, S., Mecklenburgh, K., Rahman, I., Bellingan, G. J., Greening, A., Haslett, C. and Chilvers, E. R. (1995) 'Hypoxia prolongs neutrophil survival in vitro', *FEBS Letters*, 372, pp. 233–237.

Hara, S., Hamada, J., Kobayashi, C., Kondo, Y. and Imura, N. (2001) 'Expression and characterization of hypoxia-inducible factor (HIF)-3α in human kidney: Suppression of HIF-mediated gene expression by HIF-3α', *Biochemical and Biophysical Research Communications*, 287(4), pp. 808–813.

Harding, H. P., Zhang, Y., Zeng, H., Novoa, I., Lu, P. D., Calfon, M., Sadri, N., Yun, C., Popko, B., Paules, R., Stojdl, D. F., Bell, J. C., Hettmann, T., Leiden, J. M. and Ron, D. (2003) 'An integrated stress response regulates amino acid metabolism and resistance to oxidative stress', *Molecular Cell*, 11(3), pp. 619–633.

Haschemi, A., Kosma, P., Gille, L., Evans, C. R., Burant, C. F., Starkl, P., Knapp, B., Haas, R., Schmid, J. A., Jandl, C., Amir, S., Lubec, G., Park, J., Esterbauer, H., Bilban, M., Brizuela, L., Pospisilik, J. A., Otterbein, L. E. and Wagner, O. (2012) 'The sedoheptulose kinase CARKL directs macrophage polarization through control of glucose metabolism', *Cell Metabolism*, 15(6), pp. 813–826.

Haslett, C., Guthrie, L. A., Kopaniak, M. M., Johnston, R. B. and Henson, P. M. (1985) 'Modulation of multiple neutrophil functions by preparative methods or trace concentrations of bacterial lipopolysaccharide.', *The American journal of pathology*, 119(1), pp. 101–10.

Heerlein, K., Schulze, A., Hotz, L., Bärtsch, P. and Mairbäurl, H. (2005) 'Hypoxia decreases cellular ATP demand and inhibits mitochondrial respiration of A549 cells', *American Journal of Respiratory Cell and Molecular Biology*, 32(1), pp. 44–51.

Henze, A. T., Garvalov, B. K., Seidel, S., Cuesta, A. M., Ritter, M., Filatova, A., Foss, F., Dopeso, H., Essmann, C. L., Maxwell, P. H., Reifenberger, G., Carmeliet, P., Acker-Palmer, A. and Acker, T. (2014) 'Loss of PHD3 allows tumours to overcome hypoxic growth inhibition and sustain proliferation through EGFR', *Nature Communications*, 5, pp. 1–12.

Hernandez-Mijares, A., Rocha, M., Rovira-Llopis, S., Bañuls, C., Bellod, L., De Pablo, C., Alvarez, A., Roldan-Torres, I., Sola-Izquierdo, E. and Victor, V. M. (2013) 'Human leukocyte/endothelial cell interactions and mitochondrial dysfunction in type 2 diabetic patients and their association with silent myocardial ischemia', *Diabetes Care*, 36(6), pp. 1695–1702.

Hinke, S. A., Martens, G. A., Cai, Y., Finsi, J., Heimberg, H., Pipeleers, D. and Van De Casteele, M. (2007) 'Methyl succinate antagonises biguanide-induced AMPK-activation and death of pancreatic β-cells through restoration of mitochondrial electron transfer', *British Journal of Pharmacology*, 150(8), pp. 1031–1043.

Hirsch, J. G. and Fedorko, M. E. (1968) 'Ultrastructure of human leukocytes after simultaneous fixation with glutaraldehyde and osmium tetroxide and "postfixation" in uranyl acetate.', *The Journal of cell biology*, 38(3), pp. 615–627.

Hoenderdos, K. and Condliffe, A. (2013) 'The neutrophil in chronic obstructive pulmonary disease: Too little, too late or too much, too soon?', *American Journal of Respiratory Cell and Molecular Biology*, pp. 531–539.

Hoenderdos, K., Lodge, K. M., Hirst, R. A., Chen, C., Palazzo, S. G. C., Emerenciana, A., Summers, C., Angyal, A., Porter, L., Juss, J. K., O'Callaghan, C., Chilvers, E. R. and Condliffe, A. M. (2016) 'Hypoxia upregulates neutrophil degranulation and potential for tissue injury', *Thorax*, 71(11), pp. 1030–1038.

Hoffman, D. L., Salter, J. D. and Brookes, P. S. (2007) 'Response of mitochondrial reactive oxygen species generation to steady-state oxygen tension: implications for hypoxic cell signaling.', *American journal of physiology. Heart and circulatory physiology*, 292(1), pp. H101-108.

Hopfer, U., Hopfer, H., Jablonski, K., Stahl, R. A. K. and Wolf, G. (2006) 'The novel WD-repeat protein Morg1 acts as a molecular scaffold for hypoxia-inducible factor prolyl hydroxylase 3 (PHD3)', *Journal of Biological Chemistry*, 281(13), pp. 8645–8655.

Hu, C., Wang, L., Chodosh, L. a, Keith, B. and Simon, M. C. (2003) 'Differential roles of Hypoxia-Inducible Factor 1α (HIF-1α) and HIF-2α in hypoxic gene

regulation.', *Molecular and Cellular Biology*, 23(24), pp. 9361–9374.

Hu, Q., Ren, J., Li, G., Wu, J., Wu, X., Wang, G., Gu, G., Ren, H., Hong, Z. and Li, J. (2018) 'The mitochondrially targeted antioxidant MitoQ protects the intestinal barrier by ameliorating mitochondrial DNA damage via the Nrf2/ARE signaling pathway', *Cell Death and Disease*, 9(3).

Huang, J., Xiao, Y., Xu, A. and Zhou, Z. (2016) 'Neutrophils in type 1 diabetes', *Journal of Diabetes Investigation*, 7(5), pp. 652–663.

Hudasek, K., Brown, S. T. and Fearon, I. M. (2004) 'H_2O_2 regulates recombinant Ca^{2+} channel α_{1C} subunits but does not mediate their sensitivity to acute hypoxia', *Biochemical and Biophysical Research Communications*, 318(1), pp. 135–141.

Hui, A., Bauer, A., Striet, J., Schnell, P. and Czyzyk-Krzeska, M. (2006) 'Calcium signaling stimulates translation of HIF-α during hypoxia', *The FASEB Journal*, 20(3), pp. 466–475.

Intlekofer, A. M., DeMatteo, R. G., Venneti, S., Finley, L. W. S., Lu, C., Judkins, A. R., Rustenburg, A. S., Grinaway, P. B., Chodera, J. D., Cross, J. R. and Thompson, C. B. (2015) 'Hypoxia Induces Production of L-2-Hydroxyglutarate', *Cell Metabolism*, 22(2), pp. 304–311.

Ishihara, H., Nakazaki, M., Kanegae, Y., Inukai, K., Asano, T., Katagiri, H., Yazaki, Y., Kikuchi, M., Miyazaki, J., Saito, I. and Oka, Y. (1996) 'Effect of mitochondrial and/or cytosolic Glycerol 3-Phosphate Dehydrogenase overexpression on glucose-stimulated insulin secretion from MIN6 and HIT Cells', *Diabetes*, 45(September), pp. 1238–1244.

Jacoby, J. J., Erez, B., Korshunova, M. V, Williams, R. R., Furutani, K., Takahashi, O., Kirkpatrick, L., Lippman, S. M., Powis, G., O'Reilly, M. S. and Herbst, R. S. (2010) 'Treatment with HIF-1α antagonist PX-478 inhibits progression and spread of orthotopic human small cell lung cancer and lung adenocarcinoma in mice', *J Thorac Oncol*, 5(7), pp. 940–949.

Jones, R., McDonald, K. E., Willson, J. A., Ghesquiere, B., Sammut, D., Daniel, E.,

Harris, A. J., Lewis, A., Thompson, A. A. R., Dickson, R. S., Plant, T., Murphy, F., Sadiku, P., Keevil, B. G., Carmeliet, P., Whyte, M. K. B., Newell-Price, J. and Walmsley, S. R. (2016) 'Mutations in succinate dehydrogenase B (*SDHB*) enhance neutrophil survival independent of HIF-1α expression', *Blood*, 127(21), pp. 2638–2641.

Jung, S.-N., Yang, W. K., Kim, J., Kim, H. S., Kim, E. J., Yun, H., Park, H., Kim, S. S., Choe, W., Kang, I. and Ha, J. (2008) 'Reactive oxygen species stabilize hypoxia-inducible factor-1α protein and stimulate transcriptional activity via AMP-activated protein kinase in DU145 human prostate cancer cells', *Carcinogenesis*, 29(4), pp. 713–721.

Kasahara, Y., Iwai, K., Yachie, A., Ohta, K., Konno, A., Seki, H., Miyawaki, T. and Taniguchi, N. (1997) 'Involvement of reactive oxygen intermediates in spontaneous and CD95 (Fas/APO-1)-mediated apoptosis of neutrophils.', *Blood*, 89(5), pp. 1748–53.

Kelly, B. and O'Neill, L. A. J. (2015) 'Metabolic reprogramming in macrophages and dendritic cells in innate immunity', *Cell Research*, 25(7), pp. 771–784.

Kennedy, A. D. and Deleo, F. R. (2009) 'Neutrophil apoptosis and the resolution of infection', *Immunol Res*, 43(1–3), pp. 25–61.

Kent, B. D., Mitchell, P. D. and McNicholas, W. T. (2011) 'Hypoxemia in patients with COPD: cause, effects, and disease progression.', *International journal of chronic obstructive pulmonary disease*, 6, pp. 199–208.

Kim, M., Neinast, M. D., Frank, A. P., Sun, K., Park, J., Zehr, J. A., Vishvanath, L., Morselli, E., Amelotte, M., Palmer, B. F., Gupta, R. K., Scherer, P. E. and Clegg, D. J. (2014) 'ERα upregulates *Phd3* to ameliorate HIF-1 induced fibrosis and inflammation in adipose tissue', *Molecular Metabolism*, 3(6), pp. 642–651.

Kim, S., Choe, J. H., Lee, G. J., Kim, Y. S., Kim, S. Y., Lee, H.-M., Jin, H. S., Kim, T. S., Kim, J.-M., Cho, M.-J., Shin, E.-C., Jo, E.-K. and Kim, J.-S. (2017) 'Ionizing radiation induces innate immune responses in macrophages by generation of mitochondrial reactive oxygen species', *Radiation Research*, 187(1), pp. 32–41.

Kim, S. Y. and Yang, E. G. (2015) ‘Recent advances in developing inhibitors for hypoxia-inducible factor prolyl hydroxylases and their therapeutic implications’, *Molecules*, 20(11), pp. 20551–20568.

Kioka, H., Kato, H., Fujikawa, M., Tsukamoto, O., Suzuki, T., Imamura, H., Nakano, A., Higo, S., Yamazaki, S., Matsuzaki, T., Takafuji, K., Asanuma, H., Asakura, M., Minamino, T., Shintani, Y., Yoshida, M., Noji, H., Kitakaze, M., Komuro, I., Asano, Y. and Takashima, S. (2014) ‘Evaluation of intramitochondrial ATP levels identifies G0/G1 switch gene 2 as a positive regulator of oxidative phosphorylation’, *Proceedings of the National Academy of Sciences*, 111(1), pp. 273–278.

Kiriakidis, S., Hoer, S. S., Burrows, N., Biddlecome, G., Khan, M. N., Thinnes, C. C., Schofield, C. J., Rogers, N., Botto, M., Paleolog, E. and Maxwell, P. H. (2017) ‘Complement C1q is hydroxylated by collagen prolyl 4 hydroxylase and is sensitive to off-target inhibition by prolyl hydroxylase domain inhibitors that stabilize hypoxia-inducible factor’, *Kidney International*, 92(4), pp. 900–908.

Kiss, J., Mollenhauer, M., Walmsley, S. R., Kirchberg, J., Radhakrishnan, P., Niemietz, T., Dudda, J., Steinert, G., Whyte, M. K. B., Carmeliet, P., Mazzone, M., Weitz, J. and Schneider, M. (2012) ‘Loss of the oxygen sensor PHD3 enhances the innate immune response to abdominal sepsis’, *The Journal of Immunology*, 189(4), pp. 1955–1965.

Klevens, R. M., Morrison, M. M. A. M., Nadle, J., et al, Petit, S., Gershman, K., Ray, S., Harrison, L. H., Lynfield, R., Craig, A. S., Zell, E. R., Fosheim, G. E., Mcdougal, L. K., Carey, R. B. and Fridkin, S. K. (2007) ‘Invasive Methicillin-resistant Staphylococcus aureus infections in the United States’, *JAMA*, 298(15), pp. 1763–1771.

Knighton, D. R., Halliday, B. and Hunt, T. K. (1984) ‘Oxygen as an antibiotic’, *Archives of Surgery*, 119(2), p. 199.

Köditz, J., Nesper, J., Wottawa, M., Stiehl, D. P., Camenisch, G., Franke, C., Myllyharju, J., Wenger, R. H. and Katschinski, D. M. (2007) ‘Oxygen-dependent

ATF-4 stability is mediated by the PHD3 oxygen sensor', *Blood*, 110(10), pp. 3610–3617.

Kominsky, D. J., Campbell, E. L. and Colgan, S. P. (2010) 'Metabolic Shifts in Immunity and Inflammation', *The Journal of Immunology*, 184(8), pp. 4062–4068.

Kramer, P. A., Ravi, S., Chacko, B., Johnson, M. S. and Darley-Usmar, V. M. (2014) 'A review of the mitochondrial and glycolytic metabolism in human platelets and leukocytes: Implications for their use as bioenergetic biomarkers', *Redox Biology*. Elsevier, pp. 206–210.

Krawczyk, C. M., Holowka, T., Sun, J., Blagih, J., Amiel, E., DeBerardinis, R. J., Cross, J. R., Jung, E., Thompson, C. B., Jones, R. G. and Pearce, E. J. (2010) 'Toll-like receptor-induced changes in glycolytic metabolism regulate dendritic cell activation', *Blood*, 115(23), pp. 4742–4749.

Kröller-Schön, S., Steven, S., Kossmann, S., Scholz, A., Daub, S., Oelze, M., Xia, N., Hausding, M., Mikhed, Y., Zinßius, E., Mader, M., Stamm, P., Treiber, N., Scharffetter-Kochanek, K., Li, H., Schulz, E., Wenzel, P., Münzel, T. and Daiber, A. (2014) 'Molecular mechanisms of the crosstalk between mitochondria and NADPH Oxidase through reactive oxygen species - studies in white blood cells and in animal models', *Antioxidants & Redox Signaling*, 20(2), pp. 247–266.

Kulisz, A., Chen, N., Chandel, N. S., Shao, Z. and Schumacker, P. T. (2002) 'Mitochondrial ROS initiate phosphorylation of p38 MAP kinase during hypoxia in cardiomyocytes', *American Journal of Physiology - Lung Cellular and Molecular Physiology*, 282(6), pp. L1324–L1329.

Kussmaul, L. and Hirst, J. (2006) 'The mechanism of superoxide production by NADH : ubiquinone oxidoreductase (complex I) from bovine heart mitochondria', 103(20).

Lakshman, R. and Finn, A. (2001) 'Neutrophil disorders and their management', *Journal of Clinical Pathology*, 54, pp. 7–19.

Lawrence, T. (2009) 'The nuclear factor NF-κB pathway in inflammation.', *Cold*

Spring Harb Perspect Biol, 1(6), pp. 1–10.

Lazzerini, M., Sonego, M. and Pellegrin, M. C. (2015) 'Hypoxaemia as a mortality risk factor in acute lower respiratory infections in children in low and middle-income countries: Systematic review and meta-analysis', *PLoS ONE*, 10(9), pp. 1–17.

Lee, J., Bruce-Keller, A. J., Kruman, Y., Chan, S. L. and Mattson, M. P. (1999) '2-Deoxy-D-glucose protects hippocampal neurons against excitotoxic and oxidative injury: Evidence for the involvement of stress proteins', *Journal of Neuroscience Research*, 57(1), pp. 48–61.

Lee, S.-R., Kwon, K.-S., Kim, S.-R. and Rhee, S. G. (1998) 'Reversible inactivation of Protein-tyrosine Phosphatase 1B in A431 cells stimulated with epidermal growth factor', *J Biol Chem*, 273(25), pp. 15366–15372.

Lekstrom-Himes, J. A. and Gallin, J. I. (2000) 'Immunodeficiency diseases caused by defects in phagocytes', *Advances in Immunology*, 343(23), pp. 1703–1714.

Lévy, P., Pépin, J. L., Arnaud, C., Tamisier, R., Borel, J. C., Dematteis, M., Godin-Ribuot, D. and Ribuot, C. (2008) 'Intermittent hypoxia and sleep-disordered breathing: Current concepts and perspectives', *European Respiratory Journal*, 32(4), pp. 1082–1095.

Li, X., Wang, X., Zheng, M. and Luan, Q. X. (2016) 'Mitochondrial reactive oxygen species mediate the lipopolysaccharide-induced pro-inflammatory response in human gingival fibroblasts', *Experimental Cell Research*, 347(1), pp. 212–221.

Liemburg-Apers, D. C., Willems, P. H. G. M., Koopman, W. J. H. and Grefte, S. (2015) 'Interactions between mitochondrial reactive oxygen species and cellular glucose metabolism', *Archives of Toxicology*, 89(8), pp. 1209–1226.

Lin, E. W., Karakasheva, T. A., Hicks, P. D., Bass, A. J. and Rustgi, A. K. (2016) 'The tumor microenvironment in esophageal cancer', *Oncogene*, 35(41), pp. 5337–5349.

Lindberg, F. P., Bullard, D. C., Caver, T. E., Gresham, H. D., Beaudet, A. L. and Brown, E. J. (1996) 'Decreased resistance to bacterial infection and granulocyte

defects in lAP-deficient mice', *Science*, 274((5288)), pp. 795–798.

Liu, H., Savaraj, N., Priebe, W. and Lampidis, T. J. (2002) 'Hypoxia increases tumor cell sensitivity to glycolytic inhibitors: A strategy for solid tumor therapy (Model C)', *Biochemical Pharmacology*, 64(12), pp. 1745–1751.

Liu, W., Shen, S. M., Zhao, X. Y. and Chen Dr., G. Q. (2012) 'Targeted genes and interacting proteins of hypoxia inducible factor-1', *International Journal of Biochemistry and Molecular Biology*, pp. 165–178.

Liu, X.-H., Yu, E. Z., Li, Y.-Y. and Kagan, E. (2006) 'HIF-1α has an anti-apoptotic effect in human airway epithelium that is mediated via Mcl-1 gene expression.', *Journal of cellular biochemistry*, 97(4), pp. 755–65.

Liu, Y., Huo, Z., Yan, B., Lin, X., Zhou, Z. N., Liang, X., Zhu, W., Liang, D., Li, L., Liu, Y., Zhao, H., Sun, Y. and Chen, Y. H. (2010) 'Prolyl hydroxylase 3 interacts with Bcl-2 to regulate doxorubicin-induced apoptosis in H9c2 cells', *Biochemical and Biophysical Research Communications*, 401(2), pp. 231–237.

Liu, Y., Wang, Y., Ding, W. and Wang, Y. (2018) 'Mito-TEMPO alleviates renal fibrosis by reducing inflammation, mitochondrial dysfunction, and endoplasmic reticulum stress', *Oxidative Medicine and Cellular Longevity*, pp. 1–13.

Lluis, J. M., Buricchi, F., Chiarugi, P., Morales, A. and Fernandez-Checa, J. C. (2007) 'Dual role of mitochondrial reactive oxygen species in hypoxia signaling: Activation of Nuclear Factor-κB via c-SRC- and oxidant-dependent cell death', *Cancer Research*, 67(15), pp. 7368–7377.

Lood, C., Blanco, L. P., Purmalek, M. M., Carmona-Rivera, C., De Ravin, S. S., Smith, C. K., Malech, H. L., Ledbetter, J. A., Elkon, K. B. and Kaplan, M. J. (2016) 'Neutrophil extracellular traps enriched in oxidized mitochondrial DNA are interferogenic and contribute to lupus-like disease', *Nature Medicine*, 22(2), pp. 146–153.

Lu, H., Forbes, R. A. and Verma, A. (2002) 'Hypoxia-inducible factor 1 activation by aerobic glycolysis implicates the Warburg effect in carcinogenesis', *Journal of*

Biological Chemistry, 277(26), pp. 23111–23115.

Luo, H. R. and Loison, F. (2008) 'Constitutive neutrophil apoptosis: Mechanisms and regulation', *American Journal of Hematology*, pp. 288–295.

Luo, W., Hu, H., Chang, R., Zhong, J., Knabel, M., O'Meally, R., Cole, R. N., Pandey, A. and Semenza, G. L. (2011) 'Pyruvate kinase M2 is a PHD3-stimulated coactivator for hypoxia-inducible factor 1', *Cell*. Elsevier Inc., 145(5), pp. 732–744.

Lyczak, J. B., Cannon, C. L. and Pier, G. B. (2002) 'Lung infections associated with cystic fibrosis', *Clinical microbiology reviews*, 15(2), pp. 194–222.

Mackay, I. R. and Rosen, F. S. (2000) 'Immunodeficiency diseases caused by defects in phagocytes', *New England Journal of Medicine*, 343(23), pp. 1703–1714.

Maianski, N. A., Geissler, J., Srinivasula, S. M., Alnemri, E. S., Roos, D. and Kuijpers, T. W. (2004) 'Functional characterization of mitochondria in neutrophils: A role restricted to apoptosis', *Cell Death and Differentiation*, 11(2), pp. 143–153.

Majmundar, A. J., Wong, W. J. and Simon, M. C. (2010) 'Hypoxia-Inducible Factors and the response to hypoxic stress', *Molecular Cell*, 40(2), pp. 294–309.

Majumdar, S. R., Eurich, D. T., Gamble, J. M., Senthilselvan, A. and Marrie, T. J. (2011) 'Oxygen saturations less than 92% are associated with major adverse events in outpatients with pneumonia: A population-based cohort study', *Clinical Infectious Diseases*, 52(3), pp. 325–331.

Makino, Y., Cao, R., Svensson, K., Bertilsson, G., Asman, M., Tanaka, H., Cao, Y., Berkenstam, A. and Poellinger, L. (2001) 'Inhibitory PAS domain protein is a negative regulator of hypoxia-inducible gene expression', *Nature*, 414(6863), p. 550–554.

Mansfield, K. D., Guzy, R. D., Pan, Y., Young, R. M., Cash, T. P., Schumacker, P. T. and Simon, M. C. (2005) 'Mitochondrial dysfunction resulting from loss of cytochrome c impairs cellular oxygen sensing and hypoxic HIF-α activation', *Cell Metabolism*, 1(6), pp. 393–399.

Marriott, H. M., Jackson, L. E., Wilkinson, T. S., Simpson, A. J., Mitchell, T. J., Buttle, D. J., Cross, S. S., Ince, P. G., Hellewell, P. G., Whyte, M. K. B. and Dockrell, D. H. (2008) 'Reactive oxygen species regulate neutrophil recruitment and survival in pneumococcal pneumonia', *American Journal of Respiratory and Critical Care Medicine*, 177(8), pp. 887–895.

Martínez-Cayuela, M. (1995) 'Oxygen free radicals and human disease', *Biochimie*, 77(3), pp. 147–161.

Martínez-reyes, I., Diebold, L. P., Kong, H., Schieber, M., Hensley, C. T., Mehta, M. M., Wang, T., Santos, J. H., Woychik, R., Dufour, E., Spelbrink, J. N., Weinberg, S. E., Deberardinis, R. J. and Chandel, N. S. (2016) 'TCA cycle and mitochondrial membrane potential are necessary for diverse biological functions', *Mol Cell*, 61(2), pp. 199–209.

Masson, N., Appelhoff, R. J., Tuckerman, J. R., Tian, Y. M., Demol, H., Puype, M., Vandekerckhove, J., Ratcliffe, P. J. and Pugh, C. W. (2004) 'The HIF prolyl hydroxylase PHD3 is a potential substrate of the TRiC chaperonin', *FEBS Letters*, 570(1–3), pp. 166–170.

Masson, N., Singleton, R. S., Sekirnik, R., Trudgian, D. C., Ambrose, L. J., Miranda, M. X., Tian, Y. M., Kessler, B. M., Schofield, C. J. and Ratcliffe, P. J. (2012) 'The FIH hydroxylase is a cellular peroxide sensor that modulates HIF transcriptional activity', *EMBO Reports*, 13(3), pp. 251–257.

Maxwell, P. H., Wlesener, M. S., Chang, G. W., Clifford, S. C., Vaux, E. C., Cockman, M. E., Wykoff, C. C., Pugh, C. W., Maher, E. R. and Ratcliffe, P. J. (1999) 'The tumour suppressor protein VHL targets hypoxia-inducible factors for oxygen-dependent proteolysis', *Nature*, 399(6733), pp. 271–275.

McGovern, N. N., Cowburn, A. S., Porter, L., Walmsley, S. R., Summers, C., Thompson, A. A. R., Anwar, S., Willcocks, L. C., Whyte, M. K. B., Condliffe, A. M. and Chilvers, E. R. (2011) 'Hypoxia selectively inhibits respiratory burst activity and killing of *Staphylococcus Aureus* in human neutrophils', *J Immunol*, 186(1), pp. 453–463.

McGuinness, W., Kobayashi, S. and DeLeo, F. (2016) ‘Evasion of neutrophil killing by *Staphylococcus aureus*’, *Pathogens*, 5(1), p. 32.

Metzen, E., Zhou, J., Jelkmann, W., Fandrey, J. and Brune, B. (2003) ‘Nitric oxide impairs normoxic degradation of HIF-1α by inhibition of Prolyl Hydroxylases’, *Molecular Biology of the Cell*, 14(August), pp. 3470–3481.

Michiels, C. (2004) ‘Physiological and pathological responses to hypoxia’, *American Journal of Pathology*, 164(6), pp. 1875–1882.

Miikkulainen, P., Högel, H., Rantanen, K., Suomi, T., Kouvonen, P., Elo, L. L. and Jaakkola, P. M. (2017) ‘HIF prolyl hydroxylase PHD3 regulates translational machinery and glucose metabolism in clear cell renal cell carcinoma’, *Cancer & Metabolism*, 5(1), p. 5.

Mills, E. L., Kelly, B., Logan, A., Frezza, C., Murphy, M. P., Neill, L. A. O., Mills, E. L., Kelly, B., Logan, A., Costa, A. S. H., Varma, M. and Bryant, C. E. (2016) ‘Succinate Dehydrogenase supports metabolic repurposing of mitochondria to drive inflammatory macrophages’, *Cell*, 167, pp. 457–470.

Milot, E. and Filep, J. G. (2011) ‘Regulation of neutrophil survival/apoptosis by Mcl-1’, *TheScientificWorldJournal*, 11, pp. 1948–1962.

Mishalian, I., Bayuh, R., Eruslanov, E., Michaeli, J., Levy, L., Zolotarov, L., Singhal, S., Albelda, S. M., Granot, Z. and Fridlender, Z. G. (2014) ‘Neutrophils recruit regulatory T-cells into tumors via secretion of CCL17 - A new mechanism of impaired antitumor immunity’, *International Journal of Cancer*, 135(5), pp. 1178–1186.

Moniaga, C. S., Watanabe, S., Honda, T., Nielsen, S. and Hara-Chikuma, M. (2015) ‘Aquaporin-9-expressing neutrophils are required for the establishment of contact hypersensitivity’, *Scientific Reports*, 5(October), pp. 1–13.

Moulding, D. A., Quayle, J. A., Hart, C. A. and Edwards, S. W. (1998) ‘Mcl-1 expression in human neutrophils: regulation by cytokines and correlation with cell survival.’, *Blood*, 92(7), pp. 2495–2502.

Mracek, T., Drahota, Z. and Hou, J. (2013) 'The function and the role of the mitochondrial glycerol-3-phosphate dehydrogenase in mammalian tissues', *Biochimica et Biophysica Acta*, 1827, pp. 401–410.

Mugabo, Y., Zhao, S., Seifried, A., Gezzar, S., Al-Mass, A., Zhang, D., Lamontagne, J., Attane, C., Poursharifi, P., Iglesias, J., Joly, E., Peyot, M.-L., Gohla, A., Madiraju, S. R. M. and Prentki, M. (2016) 'Identification of a mammalian glycerol-3-phosphate phosphatase: Role in metabolism and signaling in pancreatic β-cells and hepatocytes', *Proceedings of the National Academy of Sciences*, 113(4), pp. E430–E439.

Na, Y. R., Woo, D. J., Kim, S. Y. and Yang, E. G. (2016) 'Pyrithione Zn selectively inhibits hypoxia-inducible factor prolyl hydroxylase PHD3', *Biochemical and Biophysical Research Communications*, 472(2), pp. 313–318.

Nakayama, K., Gazdoiu, S., Abraham, R., Pan, Z.-Q. and Ronai, Z. (2007) 'Hypoxia-induced assembly of prolyl hydroxylase PHD3 into complexes: implications for its activity and susceptibility for degradation by the E3 ligase Siah2', *Biochemical Journal*, 401(1), pp. 217–226.

Napoli, C., Martin-Padura, I., de Nigris, F., Giorgio, M., Mansueto, G., Somma, P., Condorelli, M., Sica, G., De Rosa, G. and Pelicci, P. (2003) 'Deletion of the p66Shc longevity gene reduces systemic and tissue oxidative stress, vascular cell apoptosis, and early atherogenesis in mice fed a high-fat diet', *Proceedings of the National Academy of Sciences*, 100(4), pp. 2112–2116.

Ng, C. T., Biniecka, M., Kennedy, A., McCormick, J., FitzGerald, O., Bresnihan, B., Buggy, D., Taylor, C. T., O'Sullivan, J., Fearon, U. and Veale, D. J. (2010) 'Synovial tissue hypoxia and inflammation *in vivo*', *Annals of the Rheumatic Diseases*, 69(7), pp. 1389–1395.

Ni, R., Cao, T., Xiong, S., Fan, G., Lacefield, J. C., Lu, Y., Tissier, S. Le, Peng, T., Sciences, M., Health, L., Centre, S. and Biophysics, M. (2016) 'Therapeutic inhibition of mitochondrial reactive oxygen species with Mito-TEMPO reduces diabetic cardiomyopathy', *Free Radical Biology and Medicine*, 90, pp. 12–23.

Ogino, T., Packer, L. and Maguire, J. J. (1997) 'Neutrophil antioxidant capacity during the respiratory burst: Loss of glutathione induced by chloramines', *Free Radical Biology and Medicine*, 23(3), pp. 445–452.

Orr, A. L., Ashok, D., Sarantos, M. R., Ng, R., Shi, T., Gerencser, A. A., Hughes, R. E. and Brand, M. D. (2014) 'Novel inhibitors of mitochondrial sn-glycerol 3-phosphate dehydrogenase', *PLoS ONE*, 9(2), p. e89938.

Palacios-Callender, M., Quintero, M., Hollis, V. S., Springett, R. J. and Moncada, S. (2004) 'Endogenous NO regulates superoxide production at low oxygen concentrations by modifying the redox state of cytochrome c oxidase.', *Proceedings of the National Academy of Sciences of the United States of America*, 101(20), pp. 7630–5.

Papayannopoulos, V. (2018) 'Neutrophil extracellular traps in immunity and disease', *Nature Reviews Immunology*, 18(2), pp. 134–147.

Papayannopoulos, V., Metzler, K. D., Hakkim, A. and Zychlinsky, A. (2010) 'Neutrophil elastase and myeloperoxidase regulate the formation of neutrophil extracellular traps', *Journal of Cell Biology*, 191(3), pp. 677–691.

Passegué, E., Wagner, E. F. and Weissman, I. L. (2004) 'JunB deficiency leads to a myeloproliferative disorder arising from hematopoietic stem cells', *Cell*, 119(3), pp. 431–443.

Pearlstein, D. P., Ali, M. H., Mungai, P. T., Hynes, K. L., Gewertz, B. L. and Schumacker, P. T. (2002) 'Role of mitochondrial oxidant generation in endothelial cell responses to hypoxia', *Arteriosclerosis, Thrombosis, and Vascular Biology*, 22(4), pp. 566–573.

Pektas, S. and Knapp, M. J. (2013) 'Substrate preference of the HIF-prolyl hydroxylase-2 (PHD2) and substrate-induced conformational change', *Journal of Inorganic Biochemistry*, 126, pp. 55–60.

Peng, Y. J., Yuan, G., Ramakrishnan, D., Sharma, S. D., Bosch-Marce, M., Kumar, G. K., Semenza, G. L. and Prabhakar, N. R. (2006) 'Heterozygous HIF-1α

deficiency impairs carotid body-mediated systemic responses and reactive oxygen species generation in mice exposed to intermittent hypoxia', *Journal of Physiology*, 577(2), pp. 705–716.

Perretti, M., Soehnlein, O. and Ortega-Gómez, A. (2013) 'Resolution of inflammation : an integrated view', *EMBO Molecular Medicine*, 5, pp. 661–674.

Peyssonnaux, C., Datta, V., Cramer, T., Doedens, A., Theodarakis, E. A., Gallo, R. L., Hurtado-Ziola, N., Nizet, V. and Johnson, R. S. (2005) 'HIF-1α expression regulates the bacterial capacity of phagocytes.', *J. Clin. Invest.*, 115(7), pp. 1806–1815.

Pham, C. T. N. (2006) 'Neutrophil serine proteases: Specific regulators of inflammation', *Nature Reviews Immunology*, 6(7), pp. 541–550.

Pietarinen-Runtti, P., Lakari, E., Raivio, K. O. and Kinnula, V. L. (2000) 'Expression of antioxidant enzymes in human inflammatory cells', *American journal of physiology - Cell physiology*, 278(1), pp. C118-25.

Pillay, J., Braber, I. Den, Vrisekoop, N., Kwast, L. M., Boer, R. J. De, Borghans, A. M., Tesselaar, K. and Koenderman, L. (2010) 'Brief report In vivo labeling with $^{2}H_2O$ reveals a human neutrophil lifespan of 5.4 days', *Blood*, 116(4), pp. 625–628.

Place, T. L. and Domann, F. E. (2013) 'Prolyl-hydroxylase 3: Evolving Roles for an Ancient Signaling Protein.', *Hypoxia*, 2013(1), pp. 13–17.

Pradelli, L. A., Villa, E., Zunino, B., Marchetti, S. and Ricci, J. E. (2014) 'Glucose metabolism is inhibited by caspases upon the induction of apoptosis', *Cell Death and Disease*, 5(9), pp. e1406-7.

Quinlan, C. L., Orr, A. L., Perevoshchikova, I. V., Treberg, J. R., Ackrell, B. A. and Brand, M. D. (2012) 'Mitochondrial complex II can generate reactive oxygen species at high rates in both the forward and reverse reactions', *Journal of Biological Chemistry*, 287(32), pp. 27255–27264.

van Raam, B. J., Sluiter, W., de Wit, E., Roos, D., Verhoeven, A. J. and Kuijpers, T. W. (2008) 'Mitochondrial membrane potential in human neutrophils is maintained

by complex III activity in the absence of supercomplex organisation', *PLoS ONE*, 3(4).

Rankin, E. B., Rha, J., Selak, M. A., Unger, T. L., Keith, B., Liu, Q. and Haase, V. H. (2009) 'Hypoxia-Inducible Factor 2 regulates hepatic lipid metabolism', *Molecular and Cellular Biology*, 29(16), pp. 4527–4538.

Rantanen, K., Pursiheimo, J.-P., Hogel, H., Miikkulainen, P., Sundstrom, J. and Jaakkola, P. M. (2013) 'p62/SQSTM1 regulates cellular oxygen sensing by attenuating PHD3 activity through aggregate sequestration and enhanced degradation', *Journal of Cell Science*, 126(5), pp. 1144–1154.

Rantanen, K., Pursiheimo, J., Hogel, H., Himanen, V., Metzen, E. and Jaakola, P. M. (2007) 'Prolyl Hydroxylase PHD3 activates oxygen-dependent protein aggregation', *Molecular Biology of the Cell*, 19(1), pp. 2231–2240.

Ren, Y., Xie, Y., Jiang, G., Fan, J., Yeung, J., Li, W., Tam, P. K. H. and Savill, J. (2008) 'Apoptotic cells protect mice against Lipopolysaccharide-induced shock', *The Journal of Immunology*, 180(7), pp. 4978–4985.

Renshaw, S. A., Parmar, J. S., Singleton, V., Rowe, S. J., Dockrell, D. H., Dower, S. K., Bingle, D., Chilvers, E. R., Whyte, M. K. B., Dockrell, D. H., Dower, S. K., Bingle, C. D. and Chilvers, E. R. (2003) 'Acceleration of Human Neutrophil Apoptosis by TRAIL', *The Journal of Immunology*, 170, pp. 1027–1033.

Rhee, S. G., Bae, Y. S., Lee, S.-R. and Kwon, J. (2000) 'Hydrogen peroxide: A key messenger that modulates protein phosphorylation through cysteine oxidation', *Science Signaling*, 2000(53), p. pe1.

Rhee, S. G., Kang, S. W., Tekle, E., Baines, I. C., Seo, M. S., Chock, P. B. and Bae, Y. S. (1997) 'Epidermal Growth Factor (EGF)-induced generation of hydrogen peroxide', *Journal of Biological Chemistry*, 272(1), pp. 217–221.

Rishi, M. T., Selvaraju, V., Thirunavukkarasu, M., Shaikh, I. A., Takeda, K., Fong, G. H., Palesty, J. A., Sanchez, J. A. and Maulik, N. (2015) 'Deletion of prolyl hydroxylase domain proteins (PHD1, PHD3) stabilizes hypoxia inducible factor-1α,

promotes neovascularization, and improves perfusion in a murine model of hind-limb ischemia', *Microvascular Research*, 97, pp. 181–188.

Rodriguez-Prados, J.-C., Traves, P. G., Cuenca, J., Rico, D., Aragones, J., Martin-Sanz, P., Cascante, M. and Bosca, L. (2010) 'Substrate Fate in Activated Macrophages: A Comparison between Innate, Classic, and Alternative Activation', *The Journal of Immunology*, 185(1), pp. 605–614.

Rodriguez, J., Herrero, A., Li, S., Rauch, N., Quintanilla, A., Wynne, K., Krstic, A., Acosta, J. C., Taylor, C., Schlisio, S. and von Kriegsheim, A. (2018) 'PHD3 regulates p53 protein stability by hydroxylating Proline 359', *Cell Reports*, 24(5), pp. 1316–1329.

Rodriguez, J., Pilkington, R., Garcia Munoz, A., Nguyen, L. K., Rauch, N., Kennedy, S., Monsefi, N., Herrero, A., Taylor, C. T. and von Kriegsheim, A. (2016) 'Substrate-trapped interactors of PHD3 and FIH cluster in distinct signaling pathways', *Cell Reports*. The Authors, 14(11), pp. 2745–2760.

Sadiku, P., Willson, J. A., Dickinson, R. S., Murphy, F., Harris, A. J., Lewis, A., Sammut, D., Mirchandani, A. S., Ryan, E., Watts, E. R., Thompson, A. A. R., Marriott, H. M., Dockrell, D. H., Taylor, C. T., Schneider, M., Maxwell, P. H., Chilvers, E. R., Mazzone, M., Moral, V., Pugh, C. W., Ratcliffe, P. J., Schofield, C. J., Ghesquiere, B., Carmeliet, P., Whyte, M. K. B. and Walmsley, S. R. (2017) 'Prolyl hydroxylase 2 inactivation enhances glycogen storage and promotes excessive neutrophilic responses', *Journal of Clinical Investigation*, 127(9), pp. 3407–3420.

Santore, M. T., McClintock, D. S., Lee, V. Y., Budinger, G. R. S. and Chandel, N. S. (2002) 'Anoxia-induced apoptosis occurs through a mitochondria-dependent pathway in lung epithelial cells.', *American journal of physiology - Lung cellular and molecular physiology*, 282(4), pp. L727–L734.

Sato, M., Sakota, M. and Nakayama, K. (2010) 'Human PRP19 interacts with prolyl-hydroxylase PHD3 and inhibits cell death in hypoxia', *Experimental Cell Research*, 316(17), pp. 2871–2882.

Sawa, K., Uematsu, T., Korenaga, Y., Hirasawa, R., Kikuchi, M., Murata, K., Zhang, J., Gai, X., Sakamoto, K., Koyama, T. and Satoh, T. (2017) 'Krebs cycle intermediates protective against oxidative stress by modulating the level of reactive oxygen species in neuronal HT22 cells', *Antioxidants*, 6(1), p. 21.

Scapini, P., Lapinet-Vera, J. A., Gasperini, S., Calzetti, F., Bazzoni, F. and Cassatella, M. A. (2000) 'The neutrophil as a cellular source of chemokines', *Immunological Reviews*, 177(4), pp. 195–203.

Scheel-Toellner, D., Wang, K., Craddock, R., Webb, P. R., McGettrick, H. M., Assi, L. K., Parkes, N., Clough, L. E., Gulbins, E., Salmon, M. and Lord, J. M. (2004) 'Reactive oxygen species limit neutrophil life span by activating death receptor signaling', *Blood*, 104(8), pp. 2557–2564.

Schoepflin, Z. R., Silagi, E. S., Shapiro, I. M. and Risbud, M. V. (2017) 'PHD3 is a transcriptional coactivator of HIF-1a in nucleus pulposus cells independent of the PKM2-JMJD5 axis', *FASEB Journal*, 31(9), pp. 3831–3847.

Schofield, C. J. and Ratcliffe, P. J. (2004) 'Oxygen sensing by HIF hydroxylases', *Nature Reviews Molecular Cell Biology*, 5(5), pp. 343–354.

Selak, M. A., Armour, S. M., MacKenzie, E. D., Boulahbel, H., Watson, D. G., Mansfield, K. D., Pan, Y., Simon, M. C., Thompson, C. B. and Gottlieb, E. (2005) 'Succinate links TCA cycle dysfunction to oncogenesis by inhibiting HIF-α prolyl hydroxylase', *Cancer Cell*, 7(1), pp. 77–85.

Semenza, G. L. (1998) 'Hypoxia-inducible factor 1: master regulator of O_2 homeostasis', *Current Opinion in Genetics & Development*, 8, pp. 588–594.

Semenza, G. L. (2002) 'HIF-1 and tumor progression: Pathophysiology and therapeutics', *Trends in Molecular Medicine*, 8(4), pp. 62–67.

Semenza, G. L. (2007) 'HIF-1 mediates the Warburg effect in clear cell renal carcinoma', *Journal of Bioenergetics and Biomembranes*, 39(3), pp. 231–234.

Shultz, L. D., Ishikawa, F. and Greiner, D. L. (2007) 'Humanized mice in translational biomedical research', *Nature Reviews Immunology*, 7(2), pp. 118–130.

Sim, S., Yong, T.-S., Park, S.-J., Im, K. -i., Kong, Y., Ryu, J.-S., Min, D.-Y. and Shin, M. H. (2005) 'NADPH oxidase-derived reactive oxygen species-mediated activation of ERK1/2 is required for apoptosis of human neutrophils induced by Entamoeba histolytica', *The Journal of Immunology*, 174(7), pp. 4279–4288.

Singh, G. (2014) 'Mitochondrial FAD-linked glycerol-3-phosphate dehydrogenase: A target for cancer therapeutics', *Pharmaceuticals*, 7(2), pp. 192–206.

Snow, B. J., Rolfe, F. L., Lockhart, M. M., Frampton, C. M., O'Sullivan, J. D., Fung, V., Smith, R. A. J., Murphy, M. P. and Taylor, K. M. (2010) 'A double-blind, placebo-controlled study to assess the mitochondria- targeted antioxidant MitoQ as a disease-modifying therapy in Parkinson's disease', *Movement Disorders*, 25(11), pp. 1670–1674.

Srinivas, V., Leshchinsky, I., Sang, N., King, M. P., Minchenko, A. and Caro, J. (2001) 'Oxygen sensing and HIF-1 activation does not require an active mitochondrial respiratory chain electron-transfer pathway', *Journal of Biological Chemistry*, 276(25), pp. 21995–21998.

Stacey, M. A., Marsden, M., Pham N, T. A., Clare, S., Dolton, G., Stack, G., Jones, E., Klenerman, P., Gallimore, A. M., Taylor, P. R., Snelgrove, R. J., Lawley, T. D., Dougan, G., Benedict, C. A., Jones, S. A., Wilkinson, G. W. G. and Humphreys, I. R. (2014) 'Neutrophils recruited by IL-22 in peripheral tissues function as TRAIL-dependent antiviral effectors against MCMV', *Cell Host and Microbe*, 15(4), pp. 471–483.

Standish, A. J. and Weiser, J. N. (2009) 'Human neutrophils kill *Streptococcus pneumoniae* via serine proteases', *The Journal of Immunology*, 183(4), pp. 2602–2609.

Stănescu, D., Sanna, A., Veriter, C., Kostianev, S., Calcagni, P. G., Fabbri, L. M. and Maestrelli, P. (1996) 'Airways obstruction, chronic expectoration, and rapid decline of FEV1 in smokers are associated with increased levels of sputum neutrophils', *Thorax*, 51(3), pp. 267–271.

Stark, M. A., Huo, Y., Burcin, T. L., Morris, M. A., Olson, T. S. and Ley, K. (2005)

‘Phagocytosis of apoptotic neutrophils regulates granulopoiesis via IL-23 and IL-17’, *Immunity*, 22(3), pp. 285–294.

Steinwede, K., Henken, S., Bohling, J., Maus, R., Ueberberg, B., Brumshagen, C., Brincks, E. L., Griffith, T. S., Welte, T. and Maus, U. A. (2012) ‘TNF-related apoptosis-inducing ligand (TRAIL) exerts therapeutic efficacy for the treatment of pneumococcal pneumonia in mice’, *The Journal of Experimental Medicine*, 209(11), pp. 1937–1952.

Stiehl, D. P., Wirthner, R., Köditz, J., Spielmann, P., Camenisch, G. and Wenger, R. H. (2006) ‘Increased prolyl 4-hydroxylase domain proteins compensate for decreased oxygen levels: Evidence for an autoregulatory oxygen-sensing system’, *Journal of Biological Chemistry*, 281(33), pp. 23482–23491.

Sullivan, L. B. and Chandel, N. S. (2014) ‘Mitochondrial reactive oxygen species and cancer’, *Cancer & Metabolism*, 2(1), p. 17.

Sundaresan, M., Yu, Z.-X., Ferrans, V. J., Irani, K. and Finkel, T. (1995) ‘Requirement for generation of H_2O_2 for platelet-derived growth factor signal transduction’, *Science*, 270, pp. 296–299.

Sureda, A., Batle, J. M., Tauler, P., Cases, N., Aguiló, A., Tur, J. A. and Pons, A. (2004) ‘Neutrophil tolerance to oxidative stress induced by hypoxia/reoxygeneration’, *Free Radical Research*, 38(9), pp. 1003–1009.

Suzuki, Y. J., Forman, H. J. and Sevanian, A. (1996) ‘Oxidants as stimulators of signal transduction’, *Free Radical Biology and Medicine*, 22(1–2), pp. 269–285.

Swain, L., Wottawa, M., Hillemann, A., Beneke, A., Odagiri, H., Terada, K., Endo, M., Oike, Y., Farhat, K. and Katschinski, D. M. (2014) ‘Prolyl-4-hydroxylase domain 3 (PHD3) is a critical terminator for cell survival of macrophages under stress conditions’, *Journal of Leukocyte Biology*, 96(3), pp. 365–375.

Takeda, K., Ho, V. C., Takeda, H., Duan, L.-J., Nagy, A. and Fong, G.-H. (2006) ‘Placental but not heart defects are associated with elevated hypoxia-inducible factor α levels in mice lacking Prolyl Hydroxylase Domain protein 2’, *Molecular and*

Cellular Biology, 26(22), pp. 8336–8346.

Tal, M. C., Sasai, M., Lee, H. K., Yordy, B., Shadel, G. S. and Iwasaki, A. (2009) 'Absence of autophagy results in reactive oxygen species-dependent amplification of RLR signaling', *Proceedings of the National Academy of Sciences*, 106(8), pp. 2770–2775.

Taniguchi, C. M., Finger, E. C., Krieg, A. J., Wu, C., Diep, A. N., Lagory, E. L., Wei, K., McGinnis, L. M., Yuan, J., Kuo, C. J. and Giaccia, A. J. (2013) 'Cross-talk between hypoxia and insulin signaling through Phd3 regulates hepatic glucose and lipid metabolism and ameliorates diabetes', *Nature Medicine*, 19(10), pp. 1325–1330.

Tannahill, G. M., Curtis, A. M., Adamik, J., Palsson-Mcdermott, E. M., McGettrick, A. F., Goel, G., Frezza, C., Bernard, N. J., Kelly, B., Foley, N. H., Zheng, L., Gardet, A., Tong, Z., Jany, S. S., Corr, S. C., Haneklaus, M., Caffrey, B. E., Pierce, K., Walmsley, S., Beasley, F. C., Cummins, E., Nizet, V., Whyte, M., Taylor, C. T., Lin, H., Masters, S. L., Gottlieb, E., Kelly, V. P., Clish, C., Auron, P. E., Xavier, R. J. and O'Neill, L. A. J. (2013) 'Succinate is an inflammatory signal that induces IL-1β through HIF-1α', *Nature*, 496(7444), pp. 238–242.

Taylor, C. T. and Colgan, S. P. (2017) 'Regulation of immunity and inflammation by hypoxia in immunological niches', *Nature Reviews Immunology*, 17(12), pp. 774–785.

Tecchio, C., Micheletti, A. and Cassatella, M. A. (2014) 'Neutrophil-derived cytokines: Facts beyond expression', *Frontiers in Immunology*, 5(Oct), pp. 1–7.

Thomas, M. P., Whangbo, J., McCrossan, G., Deutsch, A., Martinod, K., Walch, M. and Lieberman, J. (2014) 'Leukocyte protease binding to nucleic acids promotes nuclear localisation and cleavage of nucleic acid binding proteins', *J Immunol*, 192(11), pp. 5390–5397.

Thompson, A. A. R., Dickinson, R. S., Murphy, F., Thomson, J. P., Marriott, H. M., Tavares, A., Willson, J., Williams, L., Lewis, A., Mirchandani, A., Dos Santos Coelho, P., Doherty, C., Ryan, E., Watts, E., Morton, N. M., Forbes, S., Stimson, R.

H., Hameed, A. G., Arnold, N., Preston, J. A., Lawrie, A., Finisguerra, V., Mazzone, M., Sadiku, P., Goveia, J., Taverna, F., Carmeliet, P., Foster, S. J., Chilvers, E. R., Cowburn, A. S., Dockrell, D. S., Johnson, R. S., Meehand, R. R., Whyte, M. K. B. and Walmsley, S. R. (2017) 'Hypoxia determines survival outcomes of bacterial infection through HIF-1α dependent re-programming of leukocyte metabolism', *Sci Immunol*, 2(8).

Thompson, A. A. R., Elks, P. M., Marriott, H. M., Eamsamarng, S., Higgins, K. R., Lewis, A., Williams, L., Parmar, S., Shaw, G., McGrath, E. E., Formenti, F., Van Eeden, F. J., Kinnula, V. L., Pugh, C. W., Sabroe, I., Dockrell, D. H., Chilvers, E. R., Robbins, P. A., Percy, M. J., Simon, M. C., Johnson, R. S., Renshaw, S. A., Whyte, M. K. B. and Walmsley, S. R. (2014) 'Hypoxia-inducible factor 2α regulates key neutrophil functions in humans, mice and zebrafish', *Blood*, 123(3), pp. 366–376.

Thompson, R., Binham, J., Plant, T., Whyte, M. K. B. and Walmsley, S. R. (2013) 'Hypoxia, the HIF pathway and neutrophilic inflammatory responses', *Biological Chemistry*, pp. 471–477.

Tishler, R. B., Calderwood, S. K., Coleman, C. N. and Price, B. D. (1993) 'Increases in sequence specific DNA binding by p53 following treatment with chemotherapeutic and DNA damaging agents.', *Cancer research*, 53, pp. 2212–2216.

Tschopp, J. and Schroder, K. (2010) 'NLRP3 inflammasome activation: The convergence of multiple signalling pathways on ROS production?', *Nature Reviews Immunology*, 10(3), pp. 210–215.

Tseng, C. W., Biancotti, J. C., Berg, B. L., Gate, D., Kolar, S. L., Müller, S., Rodriguez, M. D., Rezai-Zadeh, K., Fan, X., Beenhouwer, D. O., Town, T. and Liu, G. Y. (2015) 'Increased susceptibility of humanized NSG mice to Panton-Valentine leukocidin and *Staphylococcus aureus* skin infection', *PLoS Pathogens*, 11(11), pp. 1–17.

Uttara, B., Singh, A. V, Zamboni, P. and Mahajan, R. T. (2009) 'Oxidative stress

and neurodegenerative diseases: a review of upstream and downstream antioxidant therapeutic options.', *Current neuropharmacology*, 7(1), pp. 65–74.

Vaughan, K. R., Stokes, L., Prince, L. R., Meis, S., Matthias, U., Bingle, C. D., Sabroe, I., Surprenant, A. and Whyte, M. K. B. (2007) 'Inhibition of neutrophil apoptosis by ATP is mediated by the P2Y11 receptor', *J Immunol*, 179(12), pp. 8544–8553.

Vaux, E. C., Metzen, E., Yeates, K. M. and Ratcliffe, P. J. (2001) 'Regulation of hypoxia-inducible factor is preserved in the absence of a functioning mitochondrial respiratory chain Regulation of hypoxia-inducible factor is preserved in the absence of a functioning mitochondrial respiratory chain', *Regulation*, 98(2), pp. 296–302.

Victor, V. M., Rovira-Llopis, S., Saiz-Alarcon, V., Sangüesa, M. C., Rojo-Bofill, L., Bañuls, C., Falcón, R., Castelló, R., Rojo, L., Rocha, M. and Hernández-Mijares, A. (2014) 'Altered mitochondrial function and oxidative stress in leukocytes of anorexia nervosa patients', *PLoS ONE*, 9(9).

Vorobjeva, N., Prikhodko, A., Galkin, I., Pletjushkina, O., Zinovkin, R., Sud'ina, G., Chernyak, B. and Pinegin, B. (2017) 'Mitochondrial reactive oxygen species are involved in chemoattractant-induced oxidative burst and degranulation of human neutrophils in vitro', *European Journal of Cell Biology*, 96(3), pp. 254–265.

Vrbacký, M., Drahota, Z., Mráček, T., Vojtíšková, A., Ješina, P., Stopka, P. and Houštěk, J. (2007) 'Respiratory chain components involved in the glycerophosphate dehydrogenase-dependent ROS production by brown adipose tissue mitochondria', *Biochimica et Biophysica Acta - Bioenergetics*, 1767(7), pp. 989–997.

Walmsley, S. R., Chilvers, E. R., Thompson, A. a, Vaughan, K., Marriott, H. M., Parker, L. C., Shaw, G., Parmar, S., Schneider, M., Sabroe, I., Dockrell, D. H., Milo, M., Taylor, C. T., Johnson, R. S., Pugh, C. W., Ratcliffe, P. J., Maxwell, P. H., Carmeliet, P. and Whyte, M. K. B. (2011) 'Prolyl hydroxylase 3 (PHD3) is essential for hypoxic regulation of neutrophilic inflammation in humans and mice', *Journal of Clinical Investigation*, 121(3), pp. 1053–1063.

Walmsley, S. R., Print, C., Farahi, N., Peyssonnaux, C., Johnson, R. S., Cramer, T.,

Sobolewski, A., Condliffe, A. M., Cowburn, A. S., Johnson, N. and Chilvers, E. R. (2005) 'Hypoxia-induced neutrophil survival is mediated by HIF-1α–dependent NF-κB activity', *The Journal of Experimental Medicine*, 201(1), pp. 105–115.

Walmsley, S. R., Print, C., Farahi, N., Peyssonnaux, C., Johnson, R. S., Cramer, T., Sobolewski, A., Condliffe, A. M., Cowburn, A. S., Johnson, N. and Chilvers, E. R. (2005) 'Hypoxia-induced neutrophil survival is mediated by HIF-1α–dependent NF-κB activity', *The Journal of Experimental Medicine*, 201(1), pp. 105–115.

Wang, A., Huen, S. C., Luan, H. H., Yu, S., Zhang, C., Gallezot, J. D., Booth, C. J. and Medzhitov, R. (2016) 'Opposing effects of fasting metabolism on tissue tolerance in bacterial and viral inflammation', *Cell*, 166(6), pp. 1512–1525.

Wang, T., Liu, H., Lian, G., Zhang, S. Y., Wang, X. and Jiang, C. (2017) 'HIF1α-induced glycolysis metabolism is essential to the activation of inflammatory macrophages', *Mediators of Inflammation*. Hindawi, p. Article ID 9029327.

West, A. P., Shadel, G. S. and Ghosh, S. (2011) 'Mitochondria in innate immune responses', *Nat Rev Immunol*, 11(6), pp. 389–402.

Woerlee, G. M. (1988) 'Blood Gases - Arterial and Venous', in *Common Perioperative Problems and the Anaesthetist*, pp. 150–153.

Wood, J. G., Johnson, J. S., Mattioli, L. F. and Gonzalez, N. C. (2000) 'Systemic hypoxia increases leukocyte emigration and vascular permeability in conscious rats.', *Journal of Applied Physiology*, 89(4), pp. 1561–8.

Wu, S. B. and Wei, Y. H. (2012) 'AMPK-mediated increase of glycolysis as an adaptive response to oxidative stress in human cells: Implication of the cell survival in mitochondrial diseases', *Biochimica et Biophysica Acta - Molecular Basis of Disease*, 1822(2), pp. 233–247.

Wulf, D. (2002) 'Free radicals in the physiological control of cell function', *Physiological Reviews*, 88, pp. 47–95.

Xie, L., Pi, X., Mishra, A., Fong, G., Peng, J. and Patterson, C. (2012) 'PHD3-dependent hydroxylation of HCLK2 promotes the DNA damage response', *Journal*

of Clinical Investigation, 122(8), pp. 2827–2836.

Xie, L., Xiao, K., Whalen, E. J., Forrester, M. T., Freeman, R. S., Fong, G., Gygi, S. P., Lefkowitz, R. J. and Stamler, J. S. (2009) 'Oxygen-regulated β_2-adrenergic receptor hydroxylation by EGLN3 and ubiquitinylation by pVHL', *Science Signaling*, 2(78), pp. 1–21.

Xintaropoulou, C., Ward, C., Wise, A., Marston, H., Turnbull, A. and Langdon, S. P. (2015) 'A comparative analysis of inhibitors of the glycolysis pathway in breast and ovarian cancer cell line models', *Oncotarget*, 6(28), pp. 25677–25695.

Xu, W., Chi, L., Row, B. W., Xu, R., Ke, Y., Xu, B., Luo, C., Kheirandish, L., Gozal, D. and Liu, R. (2004) 'Increased oxidative stress is associated with chronic intermittent hypoxia-mediated brain cortical neuronal cell apoptosis in a mouse model of sleep apnea', *Neuroscience*, 126(2), pp. 313–323.

Xu, W., Yang, H., Liu, Y., Yang, Y., Wang, P., Kim, S.-H., Ito, S., Yang, C., Wang, P., Xiao, M.-T., Liu, L.-X., Jiang, W., Liu, J., Zhang, J., Wang, B., Frye, S., Zhang, Y., Xu, Y., Lei, Q., Guan, K.-L., Zhao, S. and Xiong, Y. (2011) 'Oncometabolite 2-Hydroxyglutarate is a competitive inhibitor of α-ketoglutarate-dependent dioxygenases', *Cancer Cell*, 19(1), pp. 17–30.

Xue, J., Li, X., Jiao, S., Wei, Y., Wu, G. and Fang, J. (2010) 'Prolyl Hydroxylase-3 is down-regulated in colorectal cancer cells and inhibits IKKβ independent of hydroxylase activity', *Gastroenterology*, 138(2), pp. 606–615.

Yamamoto, A., Taniuchi, S., Tsuji, S., Hasui, M. and Kobayashi, Y. (2002) 'Role of reactive oxygen species in neutrophil apoptosis following ingestion of heat-killed *Staphylococcus aureus*', *Clinical and Experimental Immunology*, 129(3), pp. 479–484.

Yeh, T.-L., Leissing, T. M., Abboud, M. I., Thinnes, C. C., Atasoylu, O., Holt-Martyn, J. P., Zhang, D., Tumber, A., Lippl, K., Lohans, C. T., Leung, I. K. H., Morcrette, H., Clifton, I. J., Claridge, T. D. W., Kawamura, A., Flashman, E., Lu, X., Ratcliffe, P. J., Chowdhury, R., Pugh, C. W. and Schofield, C. J. (2017) 'Molecular and cellular mechanisms of HIF prolyl hydroxylase inhibitors in clinical trials',

Chem. Sci., 8, pp. 7651–7668.

Yoo, S., Go, E., Kim, Y., Lee, S. and Kwon, J. (2016) 'Roles of reactive oxygen species in rheumatoid arthritis pathogenesis', *Journal of Rheumatic Diseases*, 23(6), pp. 340–347.

Yost, C. C., Cody, M. J., Harris, E. S., Thornton, N. L., Mcinturff, A. M., Martinez, M. L., Chandler, N. B., Rodesch, C. K., Albertine, K. H., Petti, C. A., Weyrich, A. S. and Zimmerman, G. A. (2009) 'Impaired neutrophil extracellular trap (NET) formation: A novel innate immune deficiency of human neonates', *Blood*, 113(25), pp. 6419–6428.

Zeidler, C., Germeshausen, M., Klein, C. and Welte, K. (2009) 'Clinical implications of *ELA2-, HAX1-,* and G-CSF-receptor *(CSF3R)* mutations in severe congenital neutropenia', *British Journal of Haematology*, 144(4), pp. 459–467.

Zhang, J., Kasim, V., Xie, Y. D., Huang, C., Sisjayawan, J., Dwi Ariyanti, A., Yan, X. S., Wu, X. Y., Liu, C. P., Yang, L., Miyagishi, M. and Wu, S. R. (2017) 'Inhibition of PHD3 by salidroside promotes neovascularization through cell-cell communications mediated by muscle-secreted angiogenic factors', *Scientific Reports*, 7(March), pp. 1–18.

Zhou, R., Yazdi, A. S., Menu, P. and Tschopp, J. (2011) 'A role for mitochondria in NLRP3 inflammasome activation', *Nature*, 469(7329), pp. 221–226.

Zlotnik, A. and Yoshie, O. (2012) 'The chemokine superfamily revisited', *Immunity*, 36(5), pp. 705–712.

Zmijewski, J. W., Lorne, E., Zhao, X., Tsuruta, Y., Sha, Y., Liu, G., Siegal, G. P. and Abraham, E. (2008) 'Mitochondrial respiratory complex I regulates neutrophil activation and severity of lung injury', *American Journal of Respiratory and Critical Care Medicine*, 178(2), pp. 168–179.

7. Appendices

7.1. 8% SDS gel composition

The following solutions were prepared in separate 50ml Falcon tubes. Volumes are per gel.

	Stacking Gel	**Resolving Gel**
dH_2O.	3ml	8ml
40% Acrylamide	620µl	3ml
1.5M Tris-HCl pH 8 (BioRad®)	-	3.8ml
0.5M Tris-HCl pH 6.8 (BioRad®)	1260µl	-
20% SDS	25µl	75µl
20% APS	50µl	150µl
TEMED (Sigma-Aldrich)	5µl	6µl

7.2. Western blotting solutions

10x Running Buffer stock

190g Glycine, 30.3g Tris Base, 50ml 20% SDS (BioRad®), made up to 1L with dH_2O.

1x Running Buffer

100ml 10x Running Buffer, 900ml dH_2O

10x Transfer Buffer stock

145g Glycine, 29g Tris Base, made up to 800ml with dH_2O.

1x Transfer Buffer.

Make immediately before use. 150ml 10x Transfer Buffer, 300ml Methanol, 1050ml dH_2O.

10x TBS stock

100ml Tris-HCl 1M pH8.0 (BioRad®), 97.3g NaCl, made up to 1000ml with dH_2O.

1x TBS

100ml 10x TBS, 900ml dH_2O.

10x TBS-Tween stock

100ml Tris-HCl 1M pH8.0 (BioRad®), 97.3g NaCl, 5ml Tween-20, made up to 1000ml with dH_2O

1x TBS-Tween

100ml 10x TBS-Tween, 900ml d dH_2O.

Blocking buffer

5g skimmed milk powder, 100ml 1x TBS

7.3. Primers used to genotype transgenic murine colonies

Target	Sequence (5'-> 3')	Product sizes
LysMCre recombinase	F- TGCAAGTTGAATAACCGGAAA R- CTAGAGCCTGTTTTGCACGTTC	250bp

7.4. Mouse sickness Score

7.4.1. Sickness score 1

A single score was applied to each animal as follows:

A normal and unremarkable condition	=0
Slight illness, defined as lethargy and ruffled fur	=1
Mild illness, defined as severe lethargy, ruffled fur and hunched back	=2
Moderate illness, with the above signs plus exudative accumulation around partially closed eyes	=3
Severe illness	=4
Death	=5

7.4.2. Sickness score 2

Mice were assessed by 5 criteria: Coat, activity, breathing, dehydration and movement. A total score was calculated from individual scores for these criteria.

	0	**1**	**2**	**3**
Coat	Normal	Rough/Lack of grooming	Unkempt, thin, wounds, staring coat	Loss of fur
Activity	Normal	Isolated, abnormal posture	Huddled/inactive or overactive	Moribund or fitting
Breathing	Normal	Rapid, shallow	Rapid, abdominal	Laboured, blue
Dehydration	Nil	Skin less elastic	Skin tents	Skin tents, eyes sunken
Movement	Normal	Slight incoordination/abnormality	Uncoordinated, reluctant to move	Staggering, paralysis, limb dragging

7.5. Murine BAL MPO assay buffers

HTAB buffer

5mg/ml hexadecyltrimethylammonium bromide in 50mM potassium phosphate buffer pH 6.0

O-dianisidine

0.167mg/ml O-dianisidine hydrochloride (Cayman Chemicals, UK).

0.0005% H2O2 in 50mM potassium phosphate buffer pH 6.0

50mM potassium phosphate buffer pH 6.0

6.392g potassium phosphate monobasic (KH_2PO_4)

0.522g potassium phosphate dibasic (K_2HPO_4)

1 litre deionised water

7.6. Murine qPCR

7.6.1. Real time polymerase chain reaction

1ul of cDNA was added to 19ul of the following RT qPCR mastermix:

2x mastermix	10ul
Water	8ul
Primer/probe mix	1ul

7.6.2. Murine primers for real time polymerase chain reactions

Commercially available primer-probe pairs all from Thermofisher Scientific, UK.

Target gene	**Taqman ID**
Glucose-6-phosphate dehydrogenase (*G6pdx)*	Mm04260097_m1
Phosphogluconate dehydrogenase *(Pgd)*	Mm00503037_m1
Ribose 5-phosphate isomerase A *(RpiA)*	Mm00485790_m1
Ribulose-phosphate 3-epimerase *(Rpe)*	Mm01256463_m1

7.7. Western blots

HIF-1α

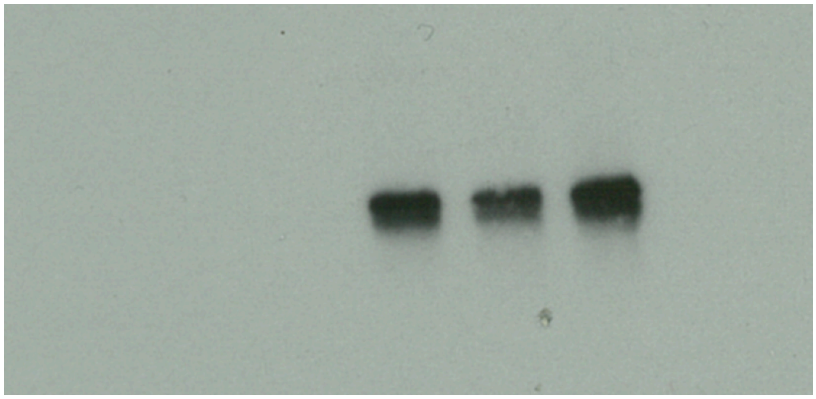

p38 MAPK

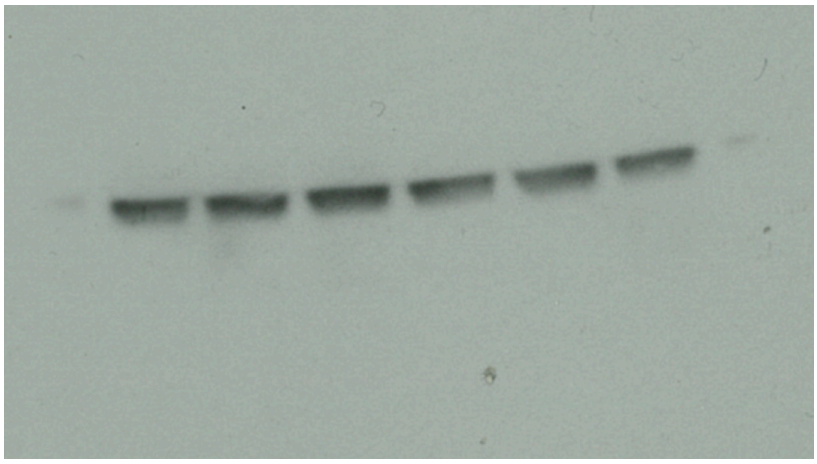

7.8. Western blot antibodies

Antibody	Supplier	Dilution
HIF-1a	Cell Signalling	1:500
P38 MAP kinase	Cell Signalling	1:2000
Goat anti-rabbit HRP	Mako	1:2000